



Title	Synthesis, Magnetic Properties and Reactions of Chromium (III) and Cobalt (III) Dinuclear Complexes
Author(s)	藤原, 隆司
Citation	大阪大学, 1994, 博士論文
Version Type	VoR
URL	https://doi.org/10.11501/3079350
rights	
Note	

The University of Osaka Institutional Knowledge Archive : OUKA

<https://ir.library.osaka-u.ac.jp/>

The University of Osaka

Synthesis, Magnetic Properties and Reactions of
Chromium(III) and Cobalt(III) Dinuclear Complexes

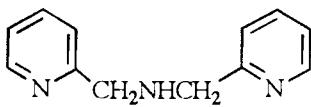
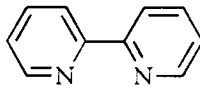
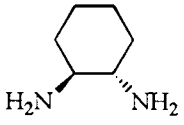
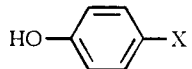
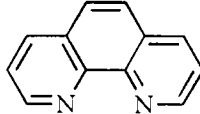
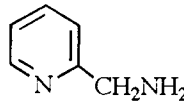
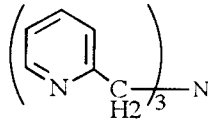
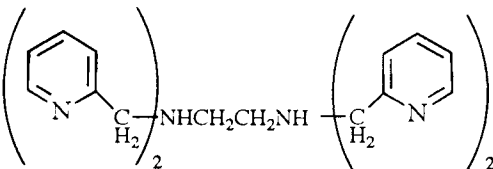
Takashi Fujihara

Faculty of Science
Osaka University
1994

Contents

	page
Abbreviations of the ligands	
1. General Introduction 1
2. Systematic Synthesis of the Chromium(III)-Cobalt(III) and Chromium(III)-Chromium(III) Dinuclear Complexes 5
3. Characterization and Structures of the Chromium(III)-Cobalt(III) and Chromium(III)-Chromium(III) Dinuclear Complexes 15
4. Stereochemistry and Paramagnetic Influence on the Multinuclear NMR Spectra of the Chromium(III)-Cobalt(III) and Chromium(III)- Cobalt(III) Dinuclear Complexes 58
5. Magnetic Exchange Interaction in Chromium(III)-Chromium(III) Dinuclear Complexes 91
6. Base Hydrolysis Reaction in Chromium(III)-Chromium(III) Dinuclear Complexes 106
7. Concluding Remarks 136
References 138
Appendixes 143
Acknowledgement 161

Abbreviations of the ligands

acacH	$\text{CH}_3\text{COCH}_2\text{COCH}_3$
γ -amb	$\text{NH}_2\text{CH}_2\text{CH}_2\text{CH}_2\text{CCOOH}$ (γ -ambH)
α -ala	$\text{CH}_3\text{CH}(\text{NH}_2)\text{COOH}$ (α -alaH)
β -ala	$\text{NH}_2\text{CH}_2\text{CH}_2\text{COOH}$ (β -alaH)
bispicam	
bpy	
<i>R,R</i> -chxn	
en	$\text{NH}_2\text{CH}_2\text{CH}_2\text{NH}_2$
gly	$\text{NH}_2\text{CH}_2\text{COOH}$ (glyH)
nta	$\text{N}(\text{CH}_2\text{COOH})_3$ (H_3nta)
L-phe	$\text{C}_6\text{H}_5\text{CH}_2\text{CH}(\text{NH}_2)\text{COOH}$ (L-pheH)
X-PhO	 (X-PhOH)
phen	
picam	
L-ser	$\text{HOCH}_2(\text{NH}_2)\text{COOH}$ (L-serH)
tmpa	
tn	$\text{NH}_2\text{CH}_2\text{CH}_2\text{CH}_2\text{NH}_2$
tpe	
trien	$\text{NH}_2\text{CH}_2\text{CH}_2\text{NHCH}_2\text{CH}_2\text{NHCH}_2\text{CH}_2\text{NH}_2$

1. General Introduction

Dinuclear complexes are the simplest assembled system in the polynuclear one. In the dinuclear complex, two coordination polyhedrons are connected by the bridging ligand(s). As shown in Figure 1-1, there are several bridging types; a point-sharing, an edge-sharing and a face-sharing form and so on. There are also long-range bridged complexes which are connected by the long chain bridging ligand(s). The bridging ligands are often monoatomic ions as halogeno anions X^- , O^{2-} and S^{2-} , or polyatomic anions as OH^- , NH_2^- and H_2O . In these cases a ligating atom is bound to the two metal ions. Polydentate ligands as $RCOO^-$, SO_4^{2-} , PO_4^{3-} , etc., act as a bidentate bridging ligand.

The chromium(III) dinuclear complexes with hydroxide ion as bridging ligands together with cobalt(III) dinuclear ones have been widely studied about the synthesis, structures, reactivities and magnetic properties since the pioneering works of S. M. Jørgensen and A. Werner.¹⁻¹⁰ Springborg recently reviewed the development of researches about the hydroxo-bridged complexes of chromium(III), cobalt(III), rhodium(III) and iridium(III).¹¹ Though many researches of the relation between magnetic properties and structures have carried out in the chromium(III) dinuclear complexes because of the interest in magnetic interaction between the metal ions,¹¹⁻²⁵ there are few studies of the relation among magnetic properties, reactivities, structures and coordinate bond character of the bridging states.^{13, 26-28} The relation between the coordinate bond characters of the ligands and the physical and chemical properties of the chromium(III) dinuclear complexes has not been clear yet.

Taking into account the situation at present, systematic and basic studies about the relation between the coordinate bond characters of the ligands and the physical and chemical properties of the dinuclear complexes are required. In order to accomplish such study, it is necessary to design and to synthesize new chromium(III)-cobalt(III) and chromium(III)-chromium(III) dinuclear complexes which have various kinds of bridging and/or non-bridging ligand, and to examine the influences by the coordinate bond characters of the ligands on the structures, the magnetic properties and the reactivities of

these complexes.

In this work, synthesis, structures, magnetic properties and base hydrolysis reactions of the chromium(III)-cobalt(III) and chromium(III)-chromium(III) dinuclear complexes in the various fashion with μ -OH and/or μ -RCOO bridging ligands, as shown in Figure 1-2, were studied by means of the UV/VIS absorption and infrared(IR) spectra, circular dichroism(CD) spectra, acid dissociation constants, multinuclear NMR, magnetic susceptibility measurements, kinetics of base hydrolysis and single X-ray crystal structure analysis.

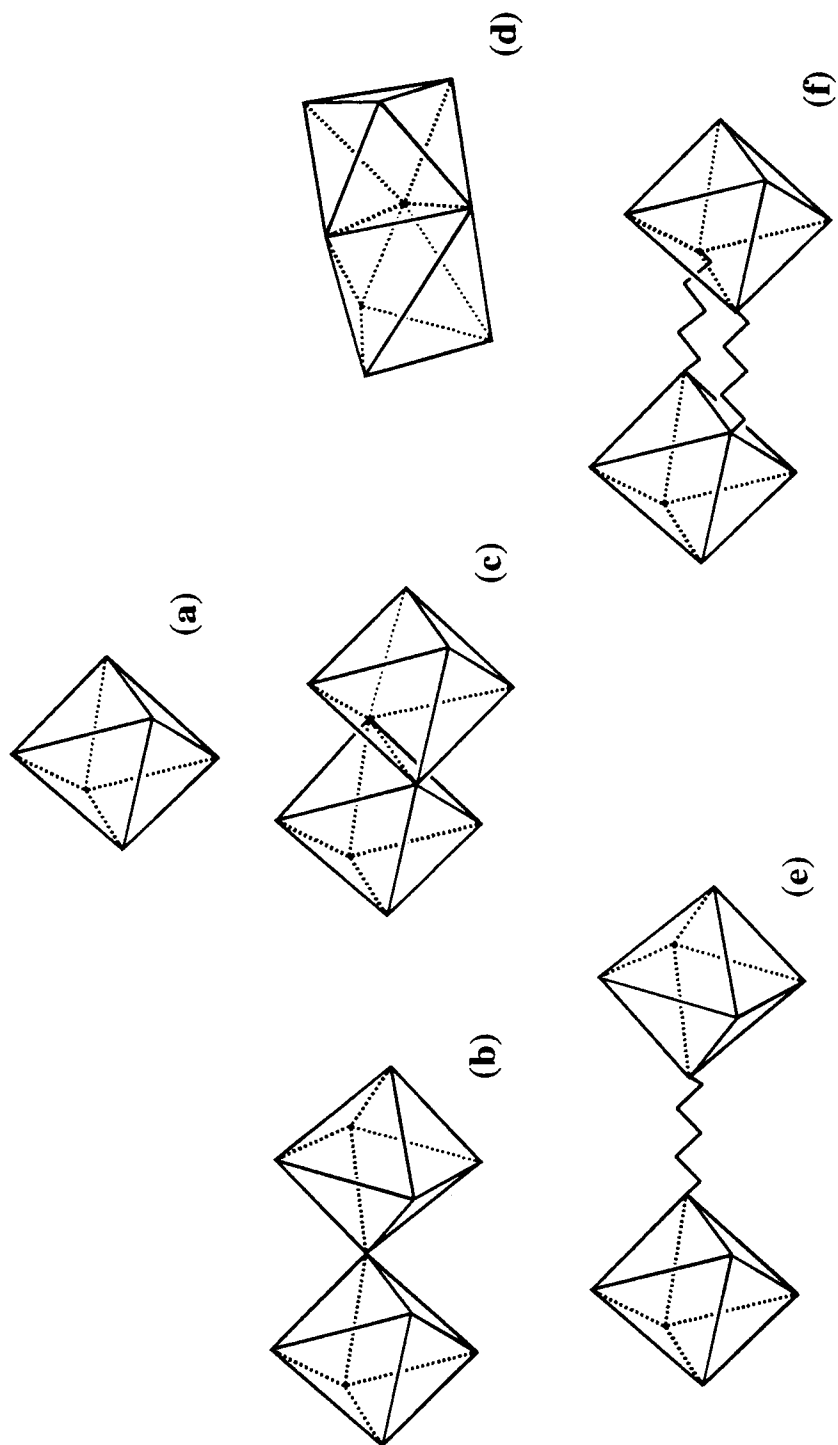


Figure 1-1. The fashion of the bridging structures: (a) original mononuclear unit, (b) a point-sharing, (c) an edge-sharing, (d) a face-sharing, (e) and (f) bridged complexes with long chain bridging ligand(s).

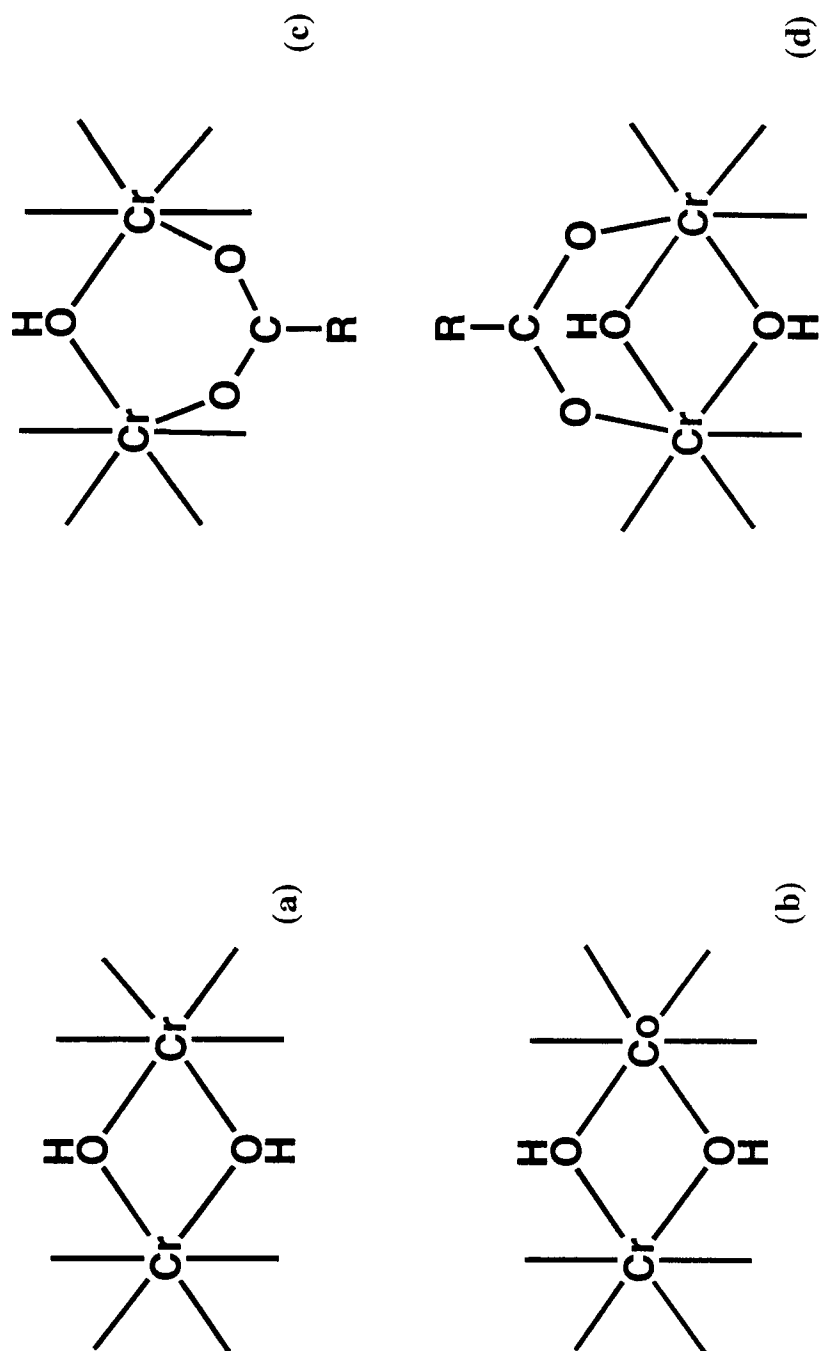


Figure 1-2. Various bridging structures of chromium(III)-chromium(III) and chromium(III)-cobalt(III) dinuclear complexes with $\mu\text{-OH}$ and/or $\mu\text{-RCOO}$ ligands: (a) $[\text{Cr}(\mu\text{-OH})_2\text{Cr}]$, (b) $[\text{Cr}(\mu\text{-OH})(\mu\text{-RCOO})\text{Cr}]$, (c) $[\text{Cr}(\mu\text{-OH})_2(\mu\text{-RCOO})\text{Cr}]$ and (d) $[\text{Cr}(\mu\text{-OH})_2(\mu\text{-RCOO})_2\text{Cr}]$.

To clarify the non-bridging ligands are not shown.

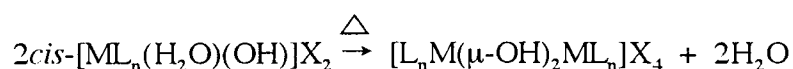
2. Systematic Synthesis of the Chromium(III)-Cobalt(III) and Chromium(III)-Chromium(III) Dinuclear Complexes

2.1 Introduction

The well-known chromium(III) and cobalt(III) dinuclear complexes with general formula in $[L_nM(\mu-OH)_2ML_n]^{n+/n-}$ have been synthesized from the corresponding mononuclear complexes by aqueous hydrolysis reaction as follows:



where L_n is monodentates, bidentates or tetradentate ligand(s). Since the aqueous hydrolysis reaction often forms some higher polynuclear complexes and gives the different isomers as byproducts, the expected yields are relatively low. On the other hand, $[L_nM(\mu-OH)_2ML_n]^{n+}$ type dinuclear complexes which coordinate NH_3 , en and tn ligands can also be obtained by the solid-state thermal reaction as the following equation:



where X is an anionic counterion. In contrast to aqueous hydrolysis reaction, the solid-state reaction often gives the dinuclear complexes in quantitative yield. In the crystals of $cis-[ML_n(H_2O)(OH)]X_2$, the two cations can form an intermolecular hydrogen bonded ion pair as shown in Figure 2-1. Therefore the water ligands would be lost easily and the yields are very high.

Recently, the synthesis via the air-oxydation step of the chromium(II) compounds with various amine ligands in aqueous or in methanolic solution under the open air was reported.^{18,28,29,30} The starting material are adopted as $[Cr^{II}_2(CH_3COO)_4(H_2O)_2]$, $Cr^{II}SO_4 \cdot 6H_2O$ and $Cr^{II}C_4O_4 \cdot 2H_2O$. It is noted that the CH_3COO^- , SO_4^{2-} and $C_4O_4^{2-}$ ions remained and coordinated to chromium(III) ion as a bridging ligand. This method is expected to be versatile to obtain of the carboxylato bridged chromium(III) dinuclear complexes.

In this chapter, it will be described that synthesis of the chromium(III)-cobalt(III) and chromium(III)-chromium(III) dinuclear complexes with various bridging ligands by the

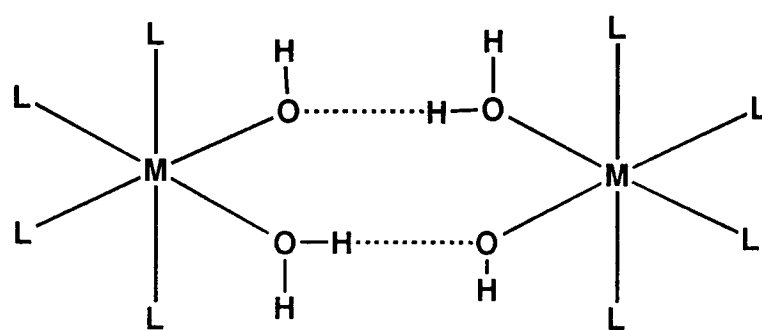


Figure 2-1. The intermolecular hydrogen-bonded ion pair of $cis-[ML_4(OH)(H_2O)]X_2$ which is often found in the solid state.

methods of the aqueous hydrolysis and of the oxidation of the Cr(II) compounds.

2.2 Materials

The precursor complexes: $K_2[Cr_2(nta)_2(OH)_2] \cdot 4H_2O$,³¹
cis-[Co(NH₃)₄(H₂O)₂]₂(SO₄)₃ · 3H₂O,³² [Co(CO₃)(en)₂]Cl,³³ [Co(CO₃)(tn)₂]Cl,³⁴
cis-[CoCl₂{(R,R)chxn}₂]Cl,³⁵ *cis*-α-[Co(trien)(H₂O)₂](ClO₄)₃,³⁶
cis-α-[CoCl₂(picam)₂]Cl · H₂O,³⁷ [Co(CO₃)(bpy)₂]Cl · 2H₂O,³⁸
[Co(CO₃)(phen)₂]Cl · 4.5H₂O,³⁸ *cis*-[CrCl(H₂O)(NH₃)₄]SO₄,³⁹
cis-[CrCl₂(en)₂]Cl · H₂O,⁴⁰ *cis*-[CrCl(dmsO){(R,R)chxn}₂]Cl₂,⁴⁰
cis-[Cr(tn)₂(H₂O)₂](NO₃)₃,⁴¹ *cis*-α-[CrCl₂(trien)]Cl · H₂O,⁴²
cis-α-[CrCl₂(picam)₂]Cl,⁴³ *cis*-[Cr(OH)(H₂O)(bpy)₂](ClO₄)₂⁴⁴ and
cis-[Cr(phen)₂(H₂O)₂](NO₃)₃ · 2H₂O⁴⁴ were synthesized by the reported methods and identified by elemental analysis and UV/VIS absorption spectra. Deuteriated acetic acid with 99 atom % ²H was purchased from Merck. EtOH-d₆ was purchased from Aldrich. Deuteriated acetic acid CH₃COOD was prepared from the reaction of acetic acid anhydrous with D₂O. All other materials were commercially available.

2.3 Preparation of the heterometal [(nta)Cr(μ-OH)₂M(N)₄]⁺ Complexes (**A-1** to **8**)

i) [(nta)Cr(OH)₂Co(NH₃)₄]Cl · 3H₂O (**A-1**). *cis*-[Co(NH₃)₄(H₂O)₂]₂(SO₄)₃ · 3H₂O (1.68 g, 2.5mmol) was dissolved with stirring in 25 cm³ of H₂O for 20 min. at 40 °C. To this solution, the solid K₂[Cr₂(nta)₂(OH)₂] · 4H₂O (0.84 g, 1.25 mmol) was added with stirring. This mixture was adjusted to pH 7 by adding 2 M (1 M = 1 mol dm⁻³) NaOH solution and stirred for 30 min. at 40 °C. The reaction solution was cooled to room temperature and loaded on a column (SP-Sephadex C-25 cation exchanger, 3 x 40 cm). The column was washed with water and eluted by 0.2 M NaCl solution. After washing with water the column gave only one band. This band was collected. The eluate was evaporated and desalted by adding methanol and ethanol. Finally, the crude complex was precipitated by adding ethanol and acetone. This was purified by dissolving in a minimum amount of water and reprecipitated with ethanol and acetone. The obtained crystals were washed with acetone

and ether and air dried. Yield 0.56g.

ii) $[(\text{nta})\text{Cr}(\text{OH})_2\text{Co}(\text{en})_2]\text{Cl} \cdot 2.5\text{H}_2\text{O}$ (**A-2**). $[\text{Co}(\text{CO}_3)(\text{en})_2]\text{Cl}$ (0.68 g, 2.5mmol) was dissolved in 20 cm³ of 1 M HClO_4 . The CO_2 gas was evolved. The solution was heated at 60°C. When the evolution of CO_2 ceased, the solid $\text{K}_2[\text{Cr}_2(\text{nta})_2(\text{OH})_2] \cdot 4\text{H}_2\text{O}$ (0.86 g, 1.25 mmol) was added. The following synthetic procedure is the same with that for complex **A-1** except for the reaction conditions(60 °C, 30 min). Yield 0.35g.

iii) $[(\text{nta})\text{Cr}(\text{OH})_2\text{Co}(\text{tn})_2]\text{Cl} \cdot 1.5\text{H}_2\text{O}$ (**A-3**). The compound was prepared as complex **A-2**, with $[\text{Co}(\text{CO}_3)(\text{tn})_2]\text{Cl}$ (0.78g, 2.5mmol). Yield 0.38g.

iv) $[(\text{nta})\text{Cr}(\text{OH})_2\text{Co}\{(R,R)\text{chxn}\}_2]\text{Cl} \cdot 3\text{H}_2\text{O}$ (**A-4**). *cis*- $[\text{CoCl}_2\{(R,R)\text{chxn}\}_2]\text{Cl}$ (0.98g, 2.5 mmol) was added to a three fold equimolar amount of freshly prepared moist Ag_2O . The mixture were stirred at room temperature and filtered to remove AgCl . The violet filtrate was cooled on an ice bath and acidified with concentrated hydrochloric acid. From this solution, the **A-4** was prepared as complex **A-2**. Yield 0.47g.

v) $[(\text{nta})\text{Cr}(\text{OH})_2\text{Co}(\text{trien})]\text{Cl} \cdot 2.5\text{H}_2\text{O}$ (**A-5**). The compound was prepared as complex **A-1** with *cis*- α - $[\text{Co}(\text{trien})(\text{H}_2\text{O})_2](\text{ClO}_4)_3$ (1.35g, 2.5 mmol) except for the reaction conditions(60 °C, 30 min). Yield 0.37g.

vi) $[(\text{nta})\text{Cr}(\text{OH})_2\text{Co}(\text{picam})_2]\text{Cl} \cdot 2\text{H}_2\text{O}$ (**A-6**). The compound was prepared as complex **A-4** with *cis*- α -*trans*(py)- $[\text{CoCl}_2(\text{picam})_2]\text{Cl} \cdot \text{H}_2\text{O}$ (1.0 g, 2.5mmol). Yield 0.51g.

vii) $[(\text{nta})\text{Cr}(\text{OH})_2\text{Co}(\text{bpy})_2]\text{Cl} \cdot 3\text{H}_2\text{O}$ (**A-7**). The compound was prepared as complex **A-2** with $[\text{Co}(\text{CO}_3)(\text{bpy})_2]\text{Cl} \cdot 2\text{H}_2\text{O}$ (1.26g, 2.5mmol). Yield 0.50g.

viii) $[(\text{nta})\text{Cr}(\text{OH})_2\text{Co}(\text{phen})_2]\text{Cl} \cdot 2\text{H}_2\text{O}$ (**A-8**). The compound was prepared as complex **A-2** with $[\text{Co}(\text{CO}_3)(\text{phen})_2]\text{Cl} \cdot 4.5\text{H}_2\text{O}$ (1.4 g, 2.5 mmol). Yield 0.48g.

2.4 Preparation of the homometal $[(\text{nta})\text{Cr}(\mu\text{-OH})_2\text{M}(\text{N})_4]^+$ Complexes (**B-1 to 8**)

i) $[(\text{nta})\text{Cr}(\text{OH})_2\text{Cr}(\text{NH}_3)_4]\text{Cl} \cdot 2.5\text{H}_2\text{O}$ (**B-1**). The compound was prepared as complex **A-1** with *cis*- $[\text{CrCl}(\text{H}_2\text{O})(\text{NH}_3)_4]\text{SO}_4$ (0.68 g, 2.5 mmol). Yield 0.33g.

ii) $[(\text{nta})\text{Cr}(\text{OH})_2\text{Cr}(\text{en})_2]\text{Cl} \cdot 3.5\text{H}_2\text{O}$ (**B-2**). The compound was prepared as complex **A-1** with *cis*- $[\text{CrCl}_2(\text{en})_2]\text{Cl} \cdot \text{H}_2\text{O}$ (0.75 g, 2.5 mmol) except for the reaction conditions(60°C, 30 min). Yield 0.57g.

- iii) $[(\text{nta})\text{Cr}(\text{OH})_2\text{Cr}(\text{tn})_2]\text{Cl} \cdot 1.5\text{H}_2\text{O}$ (**B-3**). This compound was prepared as complex **A-2** with $\text{cis}-[\text{Cr}(\text{tn})_2(\text{H}_2\text{O})_2](\text{NO}_3)_3$ (1.03 g, 2.5 mmol). Yield 0.60g.
- iv) $[(\text{nta})\text{Cr}(\text{OH})_2\text{Cr}\{(R,R)\text{chxn}\}_2]\text{Cl} \cdot 3.5\text{H}_2\text{O}$ (**B-4**). The compound was prepared as complex **B-2** with $\text{cis}-[\text{CrCl}(\text{dmsO})\{(R,R)\text{chxn}\}_2]\text{Cl}_2$ (1.16 g, 2.5 mmol) Yield 0.57 g.
- v) $[(\text{nta})\text{Cr}(\text{OH})_2\text{Cr}(\text{trien})]\text{Cl} \cdot 2\text{H}_2\text{O}$ (**B-5**). This compound was prepared as complex **A-2** with $\text{cis}-\alpha-[\text{CrCl}_2(\text{trien})]\text{Cl} \cdot \text{H}_2\text{O}$ (0.81 g, 2.5mmol). Yield 0.51g.
- vi) $[(\text{nta})\text{Cr}(\text{OH})_2\text{Cr}(\text{picam})_2]\text{Cl} \cdot 2.5\text{H}_2\text{O}$ (**B-6**). This compound was prepared as complex **A-3** with $\text{cis}-\alpha-[\text{CrCl}_2(\text{picam})_2]\text{Cl}$ (0.96 g, 2.5 mmol). Yield 0.38g.
- vii) $[(\text{nta})\text{Cr}(\text{OH})_2\text{Cr}(\text{bpy})_2]\text{Cl} \cdot 5.5\text{H}_2\text{O}$ (**B-7**). $\text{cis}-[\text{Cr}(\text{bpy})_2(\text{OH})(\text{H}_2\text{O})](\text{ClO}_4)_2$ (1.66 g, 2.5mmol) was dissolved in $25 \text{ cm}^3 \text{ H}_2\text{O}$ at 60°C and acidified with $1 \text{ dm}^3 \text{ mol HCl}$ solution (pH 4). The compound was prepared as complex **A-2**. Yield 0.60 g.
- viii) $[(\text{nta})\text{Cr}(\text{OH})_2\text{Cr}(\text{phen})_2]\text{Cl} \cdot 7\text{H}_2\text{O}$ (**B-8**). This compound was prepared as complex **A-2** with $\text{cis}-[\text{Cr}(\text{phen})_2(\text{H}_2\text{O})_2](\text{NO}_3)_3 \cdot 2\text{H}_2\text{O}$ (1.68 g, 2.5 mmol). Yield 0.57g.

2.5 Preparation of $[\text{Cr}_2(\mu\text{-OH})(\mu\text{-RCOO})(\text{en})_4](\text{ClO}_4)_4$ (en complexes) (**C-1a** to **7a**)

The reported ($\text{R} = \text{H}$ and CH_3) and the new ($\text{R} = \text{CH}_2\text{Cl}$, CH_3OCH_2 , C_2H_5 , $\text{n-C}_3\text{H}_7$ and CH_2ClCH_2) complexes were prepared from $[\text{Cr}_2(\text{OH})_2(\text{en})_4]^{4+}$ by the method of Springborg and Toftlund.⁴⁵

2.6 Preparation of $[(\text{nta})\text{Cr}(\mu\text{-OH})(\mu\text{-RCOO})\text{Cr}(\text{en})_2]\text{Cl}$ (nta complexes) (**C-1b** to **8b**)

All the complexes of this type ($\text{R} = \text{H}$, CH_3 , CH_2Cl , CH_3OCH_2 , C_2H_5 , $\text{n-C}_3\text{H}_7$, CH_2ClCH_2 , and C_6H_5) were synthesized by the following method. $\text{cis}-[\text{CrCl}_2(\text{en})_2]\text{Cl} \cdot \text{H}_2\text{O}$ (0.74g, 2.5 mmol) was dissolved in H_2O (20 cm^3) at 60°C with stirring. To the resultant red solution was added 0.84g (1.25 mmol) of $\text{K}_2[\text{Cr}_2(\text{nta})_2(\text{OH})_2] \cdot 4\text{H}_2\text{O}$. The mixture was stirred for 10 min to become a clear solution. After this was neutralized with 2 M NaOH solution, stirring was allowed to continue for 30 min at 60°C to form the violet complex, $[(\text{nta})\text{Cr}(\text{OH})_2\text{Cr}(\text{en})_2]^+$ which was described in Section 2.2. To the violet solution was added 10 mmol of RCOOH . The mixture was stirred at 45°C for 20 min. The color of the solution changed violet to reddish violet. After this solution was cooled to room

temperature, the pH was adjusted to pH 7 with 2 M NaOH solution. The filtered solution was poured onto a 3.5 x 60 cm column of a SP-Sephadex (C-25, Na⁺) cation exchanger. After washing the column with water, the charged complex was eluted with 0.1 M NaCl solution. The column gave two bands. The second violet band (E2) was confirmed to be unreacted [(nta)Cr(OH)₂Cr(en)₂]⁺ by the UV/VIS absorption spectra. The first reddish violet band (E1) was condensed with a vacuum rotary evaporator to as small a volume as possible at 25 °C. A white precipitate of NaCl was filtered off. After the repeated removal of NaCl for a few times in the same manner, ethanol and acetone were added to the condensed E1 eluate. The solution was allowed to stand in a refrigerator. Reddish violet crystals were obtained. Recrystallization was carried out by addition of ethanol and acetone to the concentrated aqueous solution, followed by standing in a refrigerator. Yield 46% to 58% (based on Cr). The deuteriated complexes were synthesized by the similar method with use of the deuteriated nta ligand³¹ or CD₃COOD.

2.7 Preparation of [Cr₂(μ-OH)₂(μ-RCOO)(bispicam)₂]^{3+ or 4+} complexes

- i) Bis(2-pyridylmethyl)amine (bispicam). Bis(2-pyridylmethyl)amine trihydrochloride monohydrate (bispicam·3HCl·H₂O) was prepared by the literature method.²⁸ Free bispicam ligand was extracted with ether from aqueous solution of the trihydrochloride by adding excess of solid NaOH and obtained by removing ether before preparing complexes.
- ii) Deuteriated bispicam(bispicam-d₁). Deuteriated bispicam-d₁ was prepared by the reaction of pyridine-2-aldehyde and deuteriated 2-picolylamine-d₁ by the same method of non-deuteriated bispicam·3HCl·H₂O.²⁸ The 2-picolylamine-d₁ with a formula C₅H₄N-CHDNH₂ was prepared by the literature method to synthesize 2-picolylamine⁴⁶ as follows. A sample of 2-pyridinealdoxime (5 g, 0.041 mol) was dissolved in 25 cm³ of EtOH-d₆ and 20 cm³ of acetone. This solution was stirred and added Zn powder (40 g) and CH₃COOD (40 g) during 3 h. This mixture was stirred over night. The Zn powder and Zn(CH₃COO)₂ were removed by filtration. The filtrate was evaporated. To the residue was added excess of solid KOH. The free amine layer was extracted with ether. The extract was dried with sodium sulfate and ether was removed on a rotary evaporator. Yield 2.15g (48

%). The extent of deuteration of 2-picolyamine-d₁ was estimated to be 92% on the basis of the ¹H NMR spectrum, which was measured on a sample containing a known amount of *t*-BuOH as a standard. The obtained 2-picolyamine-d₁ was used for preparing bispicam-d₁ without further purification.

iii) Preparation of [Cr₂^{III}(RCOO)₄(H₂O)₂] (R = H, CH₃, CH₃CH₂, CH₂Cl, and CH₂ClCH₂). They were prepared by the reported methods.⁴⁷ All these complexes were synthesized and stored under N₂ atmosphere.

iv) Preparation of [Cr₂^{III}(RCOO)₄Cl₂]Cl (R = -CH₂NH₃⁺, -CH₂CH₂NH₃⁺, -CH₂CH₂CH₂NH₃⁺, -CH(CH₃)NH₃⁺, and -CH(OH)NH₃⁺). These complexes were synthesized by slightly modified reported method.⁴⁷ All these complexes were also synthesized and stored under N₂ atmosphere.

v) Preparation of [Cr₂(OH)₂(RCOO)(bispicam)₂]X₃·nH₂O (R = H, CH₃, CH₃CH₂, CH₂Cl, CH₂ClCH₂, CH₂NH₃, CH₂CH₂NH₃, CH₂CH₂CH₂NH₃, CH(CH₃)NH₃, and CH(OH)NH₃) (**D-1** to **18**). The free bispicam (0.6 g, 3mmol) was dissolved in 15 cm³ of H₂O in N₂ atmosphere. To this solution, 1.5 mmol of [Cr₂^{III}(RCOO)₄(H₂O)₂] or [Cr₂^{III}(RCOO)₄Cl₂]Cl was added and dissolved with stirring. This solution was vigorously stirred in the air for 3 h. The color of the solution gradually changed from blue to red. The solution was filtered and added saturated NaClO₄ aqueous solution. Red precipitates were obtained. This precipitates were collected and washed with ethanol and ether. The recrystallization was carried out from minimum amount of 1 mM HClO₄ at 90 °C. Yield 27 - 35% (based on Cr).

The bromide salts were obtained as follows. The aqueous solution of perchlorates were through the QAE-Sephadex column (Br⁻ form). The eluate was collected and evaporated to dryness. The crude bromides were recrystallized from aqueous solution added with EtOH. The other salts were obtained from concentrated aqueous solution of the bromide salt by adding corresponding sodium salt (NaI, NaBF₄ and NaPF₆). They were recrystallized from hot water (90 °C).

Analytical data were summarized in Tables 2-1, 2 and 3.

Table 2-1. Analytical data and colors of the $[(\text{nta})\text{Cr}(\text{OH})_2\text{M}(\text{N})_4]\text{Cl}\cdot n\text{H}_2\text{O}$ complexes.

Complex	No.	Color	Analysis (%)		
			C	H	N
$[(\text{nta})\text{Cr}(\text{OH})_2\text{Co}(\text{NH}_3)_4]\text{Cl}\cdot 3\text{H}_2\text{O}$	A-1	Violet	Found(Calcd)	Found(Calcd)	Found(Calcd)
			14.69(14.63)	5.34(5.11)	14.27(13.99)
$[(\text{nta})\text{Cr}(\text{OH})_2\text{Co}(\text{en})_2]\text{Cl}\cdot 2.5\text{H}_2\text{O}$	A-2	Violet	22.50(23.01)	5.48(5.40)	13.12(13.06)
$[(\text{nta})\text{Cr}(\text{OH})_2\text{Co}(\text{tn})_2]\text{Cl}\cdot 1.5\text{H}_2\text{O}$	A-3	Violet	26.51(27.32)	5.75(5.61)	12.88(13.16)
$[(\text{nta})\text{Cr}(\text{OH})_2\text{Co}\{(R,R)\text{chxn}\}_2]\text{Cl}\cdot 3\text{H}_2\text{O}$	A-4	Violet	33.42(33.50)	5.92(5.83)	10.83(10.90)
$[(\text{nta})\text{Cr}(\text{OH})_2\text{Co}(\text{trien})]\text{Cl}\cdot 2.5\text{H}_2\text{O}$	A-5	Violet	25.75(25.70)	5.58(5.49)	12.51(12.41)
$[(\text{nta})\text{Cr}(\text{OH})_2\text{Co}(\text{picam})_2]\text{Cl}\cdot 2\text{H}_2\text{O}$	A-6	Violet	34.82(34.71)	4.55(4.45)	11.28(11.20)
$[(\text{nta})\text{Cr}(\text{OH})_2\text{Co}(\text{bpy})_2]\text{Cl}\cdot 3\text{H}_2\text{O}$	A-7	Brown	42.49(42.31)	4.11(4.08)	9.53(9.42)
$[(\text{nta})\text{Cr}(\text{OH})_2\text{Co}(\text{phen})_2]\text{Cl}\cdot 2\text{H}_2\text{O}$	A-8	Brown	47.10(47.10)	3.69(3.65)	9.16(9.13)
$[(\text{nta})\text{Cr}(\text{OH})_2\text{Cr}(\text{NH}_3)_4]\text{Cl}\cdot 2.5\text{H}_2\text{O}$	B-1	Violet	15.18(15.38)	5.31(5.21)	14.36(14.75)
$[(\text{nta})\text{Cr}(\text{OH})_2\text{Cr}(\text{en})_2]\text{Cl}\cdot 3.5\text{H}_2\text{O}$	B-2	Violet	22.05(21.99)	5.73(5.83)	12.85(12.63)
$[(\text{nta})\text{Cr}(\text{OH})_2\text{Cr}(\text{tn})_2]\text{Cl}\cdot 1.5\text{H}_2\text{O}$	B-3	Violet	26.85(26.92)	5.82(5.84)	13.05(13.05)
$[(\text{nta})\text{Cr}(\text{OH})_2\text{Cr}\{(R,R)\text{chxn}\}_2]\text{Cl}\cdot 3.5\text{H}_2\text{O}$	B-4	Violet	33.11(33.06)	6.64(6.63)	10.72(10.62)
$[(\text{nta})\text{Cr}(\text{OH})_2\text{Cr}(\text{trien})]\text{Cl}\cdot 2\text{H}_2\text{O}$	B-5	Violet	26.50(26.48)	5.56(5.50)	12.88(12.90)
$[(\text{nta})\text{Cr}(\text{OH})_2\text{Cr}(\text{picam})_2]\text{Cl}\cdot 2.5\text{H}_2\text{O}$	B-6	Violet	34.71(33.82)	4.69(4.58)	11.24(10.93)
$[(\text{nta})\text{Cr}(\text{OH})_2\text{Cr}(\text{bpy})_2]\text{Cl}\cdot 5.5\text{H}_2\text{O}$	B-7	Green	39.80(40.40)	4.56(5.42)	9.06(8.93)
$[(\text{nta})\text{Cr}(\text{OH})_2\text{Cr}(\text{phen})_2]\text{Cl}\cdot 7\text{H}_2\text{O}$	B-8	Green	42.49(42.32)	4.52(4.46)	8.26(8.12)

Table 2-3 . Analytical data of $[\text{Cr}_2(\text{OH})_2(\text{RCOO})_2]^{3+ \text{ or } 4+}$ complexes.

Complex	No.	Analysis (%)		
		C	H	N
		Found(Calcd)	Found(Calcd)	Found(Calcd)
$[\text{Cr}_2(\text{OH})_2(\text{HCOO})(\text{bispicam})_2](\text{ClO}_4)_3 \cdot 0.5\text{H}_2\text{O}$	D-1	34.06(33.78)	3.45(3.40)	9.52(9.45)
$[\text{Cr}_2(\text{OH})_2(\text{HCOO})(\text{bispicam})_2]\text{I}_3 \cdot 5\text{H}_2\text{O}$	D-2	28.52(28.53)	3.62(3.74)	7.94(7.99)
$[\text{Cr}_2(\text{OH})_2(\text{HCOO})(\text{bispicam})_2]\text{Br}_3 \cdot 5\text{H}_2\text{O}$	D-3	32.21(32.95)	4.21(4.31)	9.10(9.22)
$[\text{Cr}_2(\text{OH})_2(\text{HCOO})(\text{bispicam})_2](\text{BF}_4)_3 \cdot 0.5\text{H}_2\text{O}$	D-4	34.91(35.29)	3.54(3.55)	9.87(9.88)
$[\text{Cr}_2(\text{OH})_2(\text{HCOO})(\text{bispicam})_2](\text{PF}_6)_3 \cdot 1.5\text{H}_2\text{O}$	D-5	28.65(28.78)	3.11(3.09)	8.08(8.05)
$[\text{Cr}_2(\text{OH})_2(\text{CH}_3\text{COO})(\text{bispicam})_2](\text{ClO}_4)_3 \cdot 2.5\text{H}_2\text{O}$	D-6	33.17(33.26)	3.77(3.86)	9.00(8.95)
$[\text{Cr}_2(\text{OH})_2(\text{CH}_3\text{COO})(\text{bispicam})_2]\text{I}_3 \cdot 3\text{H}_2\text{O}$	D-7	30.27(30.31)	3.66(3.62)	8.19(8.16)
$[\text{Cr}_2(\text{OH})_2(\text{CH}_3\text{COO})(\text{bispicam})_2](\text{BF}_4)_3 \cdot \text{H}_2\text{O}$	D-8	35.81(35.73)	3.77(3.81)	9.61(9.62)
$[\text{Cr}_2(\text{OH})_2(\text{CH}_3\text{CH}_2\text{COO})(\text{bispicam})_2](\text{ClO}_4)_3 \cdot 0.5\text{H}_2\text{O}$	D-9	35.27(35.37)	3.76(3.74)	9.22(9.17)
$[\text{Cr}_2(\text{OH})_2(\text{CH}_2\text{ClCOO})(\text{bispicam})_2](\text{ClO}_4)_3 \cdot \text{H}_2\text{O}$	D-10	33.37(33.00)	3.49(3.41)	8.88(8.88)
$[\text{Cr}_2(\text{OH})_2(\text{CH}_2\text{ClCOO})(\text{bispicam})_2]\text{I}_3 \cdot 3\text{H}_2\text{O}$	D-11	29.86(29.33)	3.49(3.41)	7.95(7.89)
$[\text{Cr}_2(\text{OH})_2(\text{CH}_2\text{ClCH}_2\text{COO})(\text{bispicam})_2](\text{ClO}_4)_3 \cdot 0.5\text{H}_2\text{O}$	D-12	31.32(31.37)	3.15(3.22)	8.06(8.13)
$[\text{Cr}_2(\text{OH})_2(\text{CH}_2\text{ClCH}_2\text{COO})(\text{bispicam})_2]\text{I}_3 \cdot 0.5\text{H}_2\text{O}$	D-13	34.73(34.09)	3.59(3.50)	9.02(8.83)
$[\text{Cr}_2(\text{OH})_2(\text{H}_3\text{NCH}_2\text{COO})(\text{bispicam})_2](\text{ClO}_4)_3 \cdot 3\text{H}_2\text{O}$	D-14	29.79(29.37)	3.67(3.70)	9.15(9.22)
$[\text{Cr}_2(\text{OH})_2(\text{H}_3\text{NCH}_2\text{CH}_2\text{COO})(\text{bispicam})_2](\text{ClO}_4)_3 \cdot 3\text{H}_2\text{O}$	D-15	30.15(30.10)	3.75(3.84)	9.02(9.10)
$[\text{Cr}_2(\text{OH})_2(\text{H}_3\text{NCH}_2\text{CH}_2\text{CH}_2\text{COO})(\text{bispicam})_2](\text{ClO}_4)_3$	D-16	31.16(31.10)	3.75(3.84)	9.34(9.10)
$[\text{Cr}_2(\text{OH})_2(\text{I}_3\text{NCH}(\text{CH}_3)\text{COO})(\text{bispicam})_2](\text{ClO}_4)_3 \cdot 3\text{H}_2\text{O}$	D-17	29.33(29.66)	3.75(3.78)	8.55(8.97)
$[\text{Cr}_2(\text{OH})_2(\text{H}_3\text{NCH}(\text{OH})\text{COO})(\text{bispicam})_2](\text{ClO}_4)_3 \cdot 3\text{H}_2\text{O}$	D-18	32.21(32.42)	3.70(3.59)	9.42(9.45)

Table 2-2. Analytical data for newly obtained $[\text{Cr}_2(\text{OH})(\text{RCOO})(\text{en})_4](\text{ClO}_4)_4 \cdot n\text{H}_2\text{O}$ and $[(\text{nta})\text{Cr}(\text{OH})(\text{RCOO})\text{Cr}(\text{en})_2]\text{Cl} \cdot n\text{H}_2\text{O}$ complexes

Compounds	No.	found (calcd) / %		
		C	H	N
$[\text{Cr}_2(\text{OH})(\text{CH}_3\text{CH}_2\text{COO})(\text{en})_4](\text{ClO}_4)_4 \cdot 2\text{H}_2\text{O}$	C-3a	15.45(15.22)	4.94(4.88)	13.06(12.90)
$[\text{Cr}_2(\text{OH})(\text{CH}_3\text{CH}_2\text{CH}_2\text{COO})(\text{en})_4](\text{ClO}_4)_4 \cdot 0.5\text{H}_2\text{O}$	C-4a	16.66(16.85)	4.71(4.83)	12.88(13.10)
$[\text{Cr}_2(\text{OH})(\text{CH}_2\text{ClCOO})(\text{en})_4](\text{ClO}_4)_4$	C-5a	13.99(14.09)	4.28(4.14)	12.89(13.14)
$[\text{Cr}_2(\text{OH})(\text{CH}_2\text{ClCH}_2\text{COO})(\text{en})_4](\text{ClO}_4)_4 \cdot 2\text{H}_2\text{O}$	C-6a	14.67(14.64)	4.59(4.58)	12.46(12.41)
$[\text{Cr}_2(\text{OH})(\text{CH}_3\text{OCH}_2\text{COO})(\text{en})_4](\text{ClO}_4)_4 \cdot 4\text{H}_2\text{O}$	C-7a	15.07(15.25)	4.60(4.65)	12.73(12.94)
$[(\text{nta})\text{Cr}(\text{OH})(\text{HCOO})\text{Cr}(\text{en})_2]\text{Cl} \cdot 4.5\text{H}_2\text{O}$	C-1b	22.08(22.36)	5.46(5.63)	11.35(11.85)
$[(\text{nta})\text{Cr}(\text{OH})(\text{CH}_3\text{COO})\text{Cr}(\text{en})_2]\text{Cl} \cdot 3\text{H}_2\text{O}$	C-2b	25.14(24.94)	5.68(5.58)	11.93(12.12)
$[(\text{nta})\text{Cr}(\text{OH})(\text{CH}_3\text{CH}_2\text{COO})\text{Cr}(\text{en})_2]\text{Cl} \cdot 2.5\text{H}_2\text{O}$	C-3b	26.79(27.00)	5.71(5.58)	12.02(11.92)
$[(\text{nta})\text{Cr}(\text{OH})(\text{CH}_3\text{CH}_2\text{CH}_2\text{COO})\text{Cr}(\text{en})_2]\text{Cl} \cdot \text{H}_2\text{O}$	C-4b	29.40(29.51)	5.70(5.66)	12.10(12.29)
$[(\text{nta})\text{Cr}(\text{OH})(\text{CH}_2\text{ClCOO})\text{Cr}(\text{en})_2]\text{Cl} \cdot 1.5\text{H}_2\text{O}$	C-5b	24.27(24.63)	4.70(4.82)	11.47(11.97)
$[(\text{nta})\text{Cr}(\text{OH})(\text{CH}_2\text{ClCH}_2\text{COO})\text{Cr}(\text{en})_2]\text{Cl} \cdot 2\text{H}_2\text{O}$	C-6b	25.55(25.67)	5.18(5.14)	11.60(11.51)
$[(\text{nta})\text{Cr}(\text{OH})(\text{CH}_3\text{OCH}_2\text{COO})\text{Cr}(\text{en})_2]\text{Cl} \cdot 2\text{H}_2\text{O}$	C-7b	26.01(26.47)	5.39(5.47)	11.66(11.87)
$[(\text{nta})\text{Cr}(\text{OH})(\text{C}_6\text{H}_5\text{COO})\text{Cr}(\text{en})_2]\text{Cl} \cdot 2.5\text{H}_2\text{O}$	C-8b	32.43(32.36)	5.27(5.27)	11.08(11.10)

3. Characterization and Structures of the Chromium(III)-Cobalt(III) and Chromium(III)-Chromium(III) Dinuclear Complexes

3.1 Introduction

In Chapter 2, the synthesis of the chromium(III) and cobalt(III) dinuclear complexes was described. In this chapter, the characterization and structural study of the obtained dinuclear complexes were examined by means of UV/VIS, CD and IR spectra, acid dissociation constant and single crystal X-ray crystal structure analysis.

3.2 Experimental

3.2.1 Measurements

Absorption and CD spectra were recorded on a HITACHI 330 spectrophotometer and a JASCO J-500 spectropolarimeter, respectively at room temperature. Infrared spectra were measured on a Shimadzu IR-135 on KBr pellets.

The pH measurements were carried out by using a Horiba F-7SS pH meter with a #6028 coupling electrode at 25 °C. The acid dissociation constants were estimated by the method of Mønsted and Mønsted⁴⁸ using pH measurements and absorption spectra.

3.2.2 X-Ray Crystal Structure Determination

All measurements were made on a Rigaku AFC5R diffractometer with graphite monochromated MoK α radiation and the calculations were performed using TEXSAN⁴⁹ crystallographic software package of Molecular Structure Corporation.

The crystals suitable for the X-ray crystal structure determination, [(nta)Cr(OH)₂Co(tn)₂]Cl·1.5H₂O (**A-3**), [(nta)Cr(OH)₂Cr(tn)₂]Cl·1.5H₂O (**B-3**) and [(nta)Cr(OH)₂Cr(phen)₂]Cl·7H₂O (**B-8**) were obtained by slowly evaporation of the corresponding concentrated aqueous solutions. Suitable crystal of [Cr₂(OH)₂(HCOO)(bispicam)₂](ClO₄)₃·0.5H₂O (**D-1**) for X-ray study was obtained by cooling hot aqueous solution.

The data collection was carried out 23 ± 1 °C using ω -2 θ scan method. The direct

Table 3-1. Crystallographic data for [(nta)Cr(OH)₂Co(tn)₂]Cl · 1.5H₂O (**A-3**), [(nta)Cr(OH)₂Cr(tn)₂]Cl · 1.5H₂O (**B-3**) and [(nta)Cr(OH)₂Cr(phen)₂]Cl · 7H₂O (**B-8**).

	(A-3)	(B-3)	(B-8)
Formula	C ₁₂ H ₃₁ O _{9.5} N ₅ CrCoCl	C ₁₂ H ₃₁ O _{9.5} N ₅ Cr ₂ Cl	C ₃₀ H ₃₈ O ₁₅ N ₅ Cr ₂ Cl
Formula Weight	543.79	536.85	848.10
Crystal System	monoclinic	monoclinic	triclinic
Space Group	C2/c(No. 15)	C2/c(No. 15)	P $\bar{1}$ (No. 2)
a, Å	16.384(2)	16.465(3)	15.79(1)
b, Å	14.660(2)	14.727(2)	18.04(1)
c, Å	18.874(2)	19.057(2)	12.77(1)
α , deg			96.39(8)
β , deg	110.77(1)	110.277(9)	102.23(7)
γ , deg			102.83(7)
V, Å ³	4239(1)	4334.5(9)	3418(5)
Z value	8	8	4
D _{calcd} , g cm ⁻³	1.676	1.645	1.648
μ (Mo K α), cm ⁻¹	14.60	11.56	7.76
No. of unique refl.	6438	6604	10803
No. of obsd. refl.	6646	6818	11251
F ₀₀₀	2216	2232	1752
R ^a	0.038	0.042	0.077
R _w ^b	0.048	0.049	0.100

^a $R = \sum ||F_o| - |F_c|| / \sum |F_o|$. ^b $R_w = [(\sum_w (|F_o| - |F_c|)^2 / \sum_w F_o^2)]^{1/2}$.

Table 3-2. Crystallographic data for $[\text{Cr}_2(\text{OH})(\text{HCOO})(\text{bispicam})_2](\text{ClO}_4)_3 \cdot 0.5\text{H}_2\text{O}(\mathbf{D-1})$.

Formula	$\text{C}_{25}\text{H}_{31}\text{O}_{16.5}\text{N}_6\text{Cr}_2\text{Cl}_3$
Formula Weight	897.89
Crystal System	orthorhombic
Space Group	Pnma(No. 62)
a, Å	14.771(3)
b, Å	12.346(6)
c, Å	19.054(4)
V, Å ³	3475(3)
Z value	4
D _{calcd} , g cm ⁻³	1.699
$\mu(\text{Mo K}\alpha)$, cm ⁻¹	9.21
No. of unique refl.	5475
No. of obsd. refl.	5657
F ₀₀₀	1812
R ^a	0.053
R _w ^b	0.059

$$^a R = \sum ||F_o| - |F_c|| / \sum |F_o| \quad ^b R_w = [(\sum_w (|F_o| - |F_c|)^2 / \sum_w F_o^2)]^{1/2}.$$

methods followed by normal heavy-atom procedures were used for structure analysis. The positional and thermal parameters were refined by the full-matrix least-squares refinement. All hydrogen atoms except for those of the complex (**B-8**) were found in the difference-Fourier map and refined isotropically. Non-hydrogen atoms were refined with anisotropic thermal parameters except for the seven oxygen atoms of crystalline waters (O(101) - O(107)) and Cl(2) in complex (**B-8**) which were refined isotropically.

Crystallographic data for three complexes are listed in Table 3-1 and 2. The Tables of the fractional coordinates and anisotropic thermal parameters are listed in Appendixes.

3.3 Results and Discussion

3.3.1 Characterization of $[(\text{nta})\text{Cr}(\text{OH})_2\text{M}(\text{N})_4]^+$ complexes

i) Synthetic method of the $[(\text{nta})\text{Cr}(\text{OH})_2\text{M}(\text{N})_4]^+$ complexes. The analytical data as shown in Table 2-1 do not exclude a possibility of hydrogen bonded aggregates with $[\text{Cr}(\text{nta})(\text{OH})(\text{H}_2\text{O})]^-$ and $[\text{M}(\text{N})_4(\text{OH})(\text{H}_2\text{O})]^{2+}$ as found in $[\text{Cr}(\text{bpy})_2(\text{OH})(\text{H}_2\text{O})]_2^{4+}$.⁵⁰ Since they did not separate out on SP-Sephadex column chromatography, it is apparent that they are not aggregates, but have a $\text{di}(\mu\text{-OH})$ structure.

When the reaction solution was separated by the column chromatography, only one band ($[(\text{nta})\text{Cr}(\text{OH})_2\text{M}(\text{N})_4]^+$) was eluted by 0.2 M NaCl aqueous solution. No formation of the symmetrical dinuclear complexes like $[\text{Cr}_2(\mu\text{-OH})_2(\text{N})_4]^{++}$ and $[\text{Cr}_2(\text{nta})_2(\mu\text{-OH})_2]^{2-}$ were detected in the column chromatography. It is found to be a specific formation of the unsymmetrical $[(\text{nta})\text{Cr}(\text{OH})_2\text{M}(\text{N})_4]^+$ type dinuclear complexes in this reaction. These obtained dinuclear complexes except for complex **A-1** are stable and there is no change in UV/VIS spectra for several days in aqueous solution. The complex **A-1** decomposes relatively fast to the monomeric species in aqueous solutions.

The synthesis of $\text{di}(\mu\text{-OH})$ $[\text{Cr}(\text{III})\text{-Co}(\text{III})]$ heterometal dinuclear complexes $[(\text{en})_2\text{Cr}(\mu\text{-OH})_2\text{Co}(\text{en})_2]^{++}$ was firstly reported by Josephsen and Schäffer.⁵¹ They obtained the crude product by the solid state reaction using a syncrystallized mixture of $\Lambda\text{-cis-}[\text{Cr}(\text{en})_2(\text{OH})(\text{H}_2\text{O})]^{2+}$ and $\Delta\text{-cis-}[\text{Co}(\text{en})_2(\text{OH})(\text{H}_2\text{O})]^{2+}$ as dithionate. The pure product was obtained from impurities successfully utilized differences in the rate of the

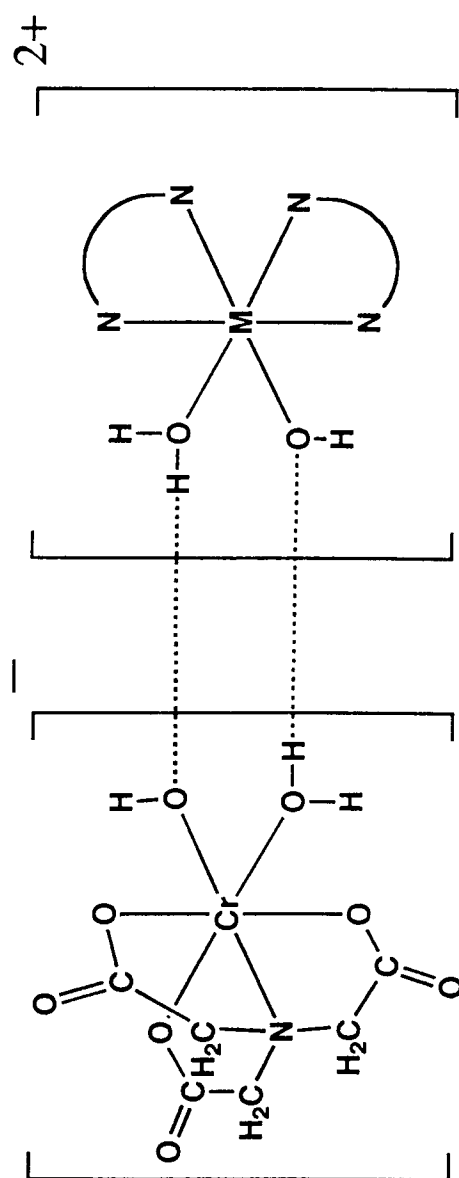


Figure 3-1. Proposed structure of an ion pair with $[(\text{nta})\text{Cr}(\text{OH})(\text{H}_2\text{O})]^-$ and $[\text{M}(\text{N})_4(\text{OH})(\text{H}_2\text{O})]^{2+}$.

diol-monool equilibrium. On the other hand, the heterometal $[(\text{nta})\text{Cr}(\text{OH})_2\text{Co}(\text{N})_4]^+$ complexes are synthesized in aqueous solutions and obtained pure product easier in this study. They have a rigid $[\text{Cr}(\text{OH})_2\text{Co}]$ bridging structure without monool-diol equilibrium in the aqueous solution because of no spectral change in time except for complex **A-1**.

Similar types of unsymmetrical $\text{di}(\mu\text{-OH})$ $[\text{Co(III)-Co(III)}]$ complexes $[\text{LCo}(\mu\text{-OH})_2\text{Co}(\text{L}')(\text{L}'')]^{n+}$ ($\text{L} = \text{edda}^{2-}$; ethylenediaminediacetato or nta^{3-} , and L' and $\text{L}'' = \text{NH}_3$, en , gly^-) were synthesized by Ama *et al.*^{52,53} Such unsymmetrical $\text{di}(\mu\text{-OH})$ dinuclear complexes seem to be easily formed in the neutral or slightly basic aqueous solutions in the range of pH 7 to 9. In such reaction conditions, the deprotonation of the coordinated waters of the mononuclear diaqua complex occurs and an aquahydroxo $[\text{LM}(\text{OH})(\text{H}_2\text{O})]^{n+}$ complex is formed. The aquahydroxo complexes often form the aggregates by the intermolecular hydrogen bonds in aqueous solution. The resultant ion pair changes to $\text{di}(\mu\text{-OH})$ dinuclear complex through aqueous hydrolysis reaction.¹¹ In our experiments, the precursor mononuclear diaqua complexes change into $[\text{Cr}(\text{nta})(\text{OH})(\text{H}_2\text{O})]^-$ and $[\text{M}(\text{N})_4(\text{OH})(\text{H}_2\text{O})]^{2+}$ by deprotonation of the coordinated water. The resulting aquahydroxo complexes would be assembled and form the ion pair as an intermediate of the dinuclear complex, owing to not only the intermolecular hydrogen bond between aqua and hydroxo ligands but also the electrostatic attractive force between a cation ($[\text{M}(\text{N})_4(\text{OH})(\text{H}_2\text{O})]^{2+}$) and an anion ($[\text{Cr}(\text{nta})(\text{OH})(\text{H}_2\text{O})]^-$) as shown in Figure 2-1. Though Ama *et al.* claimed that the important factor to form such unsymmetrical dinuclear complexes is the intramolecular hydrogen bonds between non-bridging ligands,^{52,53} $[(\text{nta})\text{Cr}(\text{OH})_2\text{M}(\text{picam}, \text{bpy} \text{ or } \text{phen})_2]^+$ complexes which have no hydrogen atom to form the intramolecular hydrogen bond between amine proton and carboxylato ligating oxygen ($\text{N-H} \cdots \text{O}$) are found to be formed in this study. The above facts suggest that the electrostatic attractive force also plays an important role to form $[(\text{nta})\text{Cr}(\text{OH})_2\text{M}(\text{N})_4]^+$ type dinuclear complexes analogously to the hydrogen bonds between non-bridging ligands.

According to the structures of the precursor complexes, the geometrical and absolute configurations for $\text{M}(\text{N})_4$ moieties are retained in the corresponding dinuclear complexes as follows : the bis(picam) complexes (**A-6** and **B-6**) are *trans*-(py) type, the trien ones (**A-5**

and **B-5**) are *cis*- α type, and bis{(R,R)chxn} ones (**A-4** and **B-4**) are Δ absolute configuration.

ii) The crystal structure of [(nta)Cr(OH)₂Co(tn)₂]Cl·1.5H₂O (**A-3**). The selected bond lengths and bond angles are listed in Table 3-3. A perspective view of this dinuclear complex cation is shown in Figure 3-2. The chromium(III) and cobalt(III) ions are in an approximately octahedral environment. The [Cr(OH)₂Co] bridging unit is almost flat.

The Co-N(tn) bond lengths fall in the range of 1.956(3)Å to 1.994(3)Å (average 1.969Å). These are almost the same values for the reported Co-tn complexes.⁵⁴ The Cr-N(nta) and Cr-O(nta) bond lengths are 2.060(3)Å and 1.975Å(average), respectively. The bond lengths and angles in the Cr(nta) moiety are almost the same values for those of K₂[Cr₂(nta)(μ -OH)(μ -CH₃COO)]·4H₂O⁵⁵ and Cs₂[Cr₂(nta)₂(μ -OH)₂]·4H₂O.⁵⁶

The (nta)Cr-O(8)H distance *trans* to the nta amine nitrogen atom is 1.913(2)Å and significantly shorter by 0.054Å than the (nta)Cr-O(7)H distance (1.967(2)Å) *cis* to one as shown in Table 3-3. This difference is not obviously found in the symmetrical type di(μ -OH) bridged Cs₂[Cr₂(nta)₂(OH)₂]·4H₂O.⁵⁶ The similar differences in Cr-N bonds between *cis* and *trans* positions of tertiary amine nitrogen atoms are found in analogous nta type monomeric complexes [Cr((S)-LDA or (S)-PDA)(im)₂] ((S)-LDA = *l*-leucine-*N,N*-diacetato, (S)-PDA = *l*-phenylalanine-*N,N*-diacetato and im = imidazolato) by Bocarsly *et al.*⁵⁷ The (tn)₂Co-OH bond lengths showed little difference (Co-O(7)H: 1.935(2) Å and Co-O(8)H: 1.921(2) Å), while the Co-OH bond length in [Co₂(μ -OH)₂(en)₄](NO₃)₄ is 1.93 Å.⁵⁸

The definition of the chelate ring 1, 2A and 2B in the propane-1,3-diamine ligand is shown in Figure 3-2. The chelate ring 1 has a chair conformation. Following the definition of the propane-1,3-diamine rings by Jurnak and Raymond,⁵⁹ the chair ring conformer folds the central carbon atom in the chelate ring 1 which defines a rotation direction antiparallel to the direction defined by the metal ion configuration. Therefore the chelate ring 1 is "a" conformation. The chelate ring 2, three carbon atoms are disordered. The chelate ring 2A takes a skewboat conformation and the "δ" chelate configuration in which a line between the

Table 3-3. Selected bond lengths(Å) and bond angles(deg) for
[(nta)Cr(OH)₂Co(tn)₂]Cl·1.5H₂O (**A-3**).

Co-N(2)	1.965(3)	Co-N(3)	1.956(3)
Co-N(4)	1.961(3)	Co-N(5)	1.994(3)
Co-O(7)	1.935(2)	Co-O(8)	1.921(2)
Cr-N(1)	2.060(3)	Cr-O(1)	1.960(2)
Cr-O(3)	1.995(3)	Cr-O(5)	1.971(2)
Cr-O(7)	1.967(2)	Cr-O(8)	1.913(2)
O(7)CoO(8)	80.69(9)	O(7)CoN(2)	88.1(1)
O(7)CoN(3)	96.3(1)	O(7)CoN(4)	170.9(1)
O(7)CoN(5)	87.2(1)	O(8)CoN(2)	86.2(1)
O(8)CoN(3)	174.7(1)	O(8)CoN(4)	90.6(1)
O(8)CoN(5)	92.3(1)	N(2)CoN(3)	89.4(1)
N(2)CoN(4)	88.6(1)	N(2)CoN(5)	175.2(1)
N(3)CoN(4)	92.2(1)	N(3)CoN(5)	91.9(1)
N(4)CoN(5)	95.9(1)	O(7)CrO(8)	80.07(8)
O(1)CrO(7)	174.97(9)	O(1)CrO(8)	94.97(9)
O(1)CrN(1)	84.8(1)	O(1)CrO(3)	91.4(1)
O(1)CrO(5)	89.3(1)	O(3)CrO(5)	163.52(9)
O(3)CrO(7)	88.52(9)	O(3)CrO(8)	97.46(9)
O(3)CrN(1)	80.8(1)	O(5)CrO(7)	92.23(9)
O(5)CrO(8)	98.9(1)	O(5)CrN(1)	82.9(1)
O(7)CrN(1)	100.11(9)	O(8)CrN(1)	178.2(1)
CoO(7)Cr	98.20(8)	CoO(8)Cr	100.61(8)

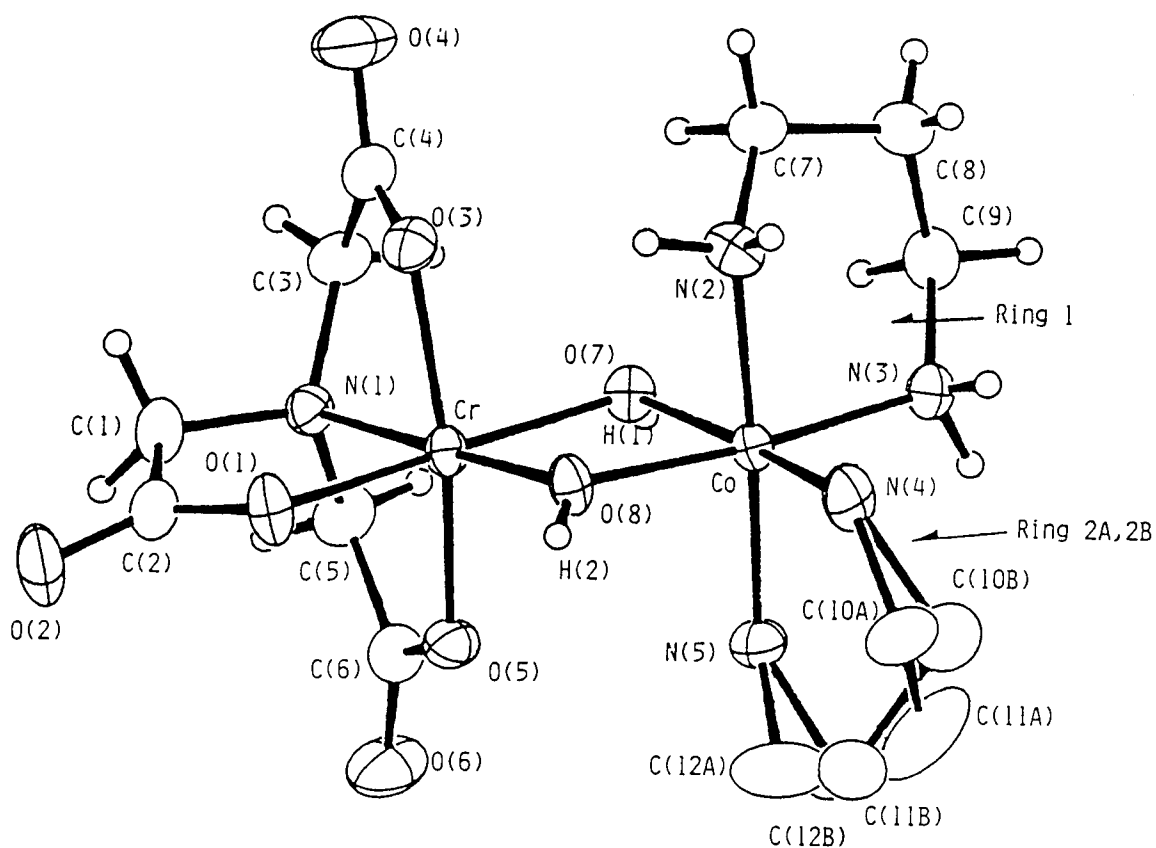


Figure 3-2. An ORTEP drawing of $[(nta)Cr(OH)_2Co(tn)_2]^+$ (**A-3**) with thermal ellipsoids drawn at the 50 % probability level. Some hydrogen atoms in the tn chelate rings are omitted to clarify.

nitrogen atoms and a line between the carbon atoms bound to the nitrogen atoms shows a right-handed helix.⁵⁹ The chelate ring 2B takes a skewboat conformation and the "λ" chelate configuration in which that shows a left-handed helix. The total conformation of Cr(tn)₂ moiety in Figure 3-2 is then Δaλ(δ).⁵⁹

The intramolecular hydrogen bonds are expected between the amine protons of the propane-1,3-diamine ligands and coordinated oxygen atoms of the nta one as observed in the [(edda)Co(μ-OH)₂Co(en)(gly)]⁺⁵³ and [(H₂O)L₃Cr(μ-OH)₂CrL₃(H₂O)]⁴⁺⁶⁰ type complexes. The distances of N(2)···O(3) and N(5)···O(5) are 3.192(4) and 2.967(4)Å, respectively. Since the N···O distances are in the range of 2.57 to 3.24Å,⁶¹ there are two intramolecular hydrogen bonds between tn and nta ligands. The amine proton of the chelate ring 1 is found to be formed a hydrogen bond with the coordinated nta oxygen atom in the neighboring complex (N(3)···O'(2) 2.860Å). Since two hydrogen bonds(intra- and intermolecular) exist in the chelate ring 1, the conformation of ring 1 would be fixed. However, since such intramolecular hydrogen bond does not exist in the ring 2, its conformation would not be determined and the carbon atoms would be disordered. The hydrogen atoms of bridging OH proton bonds to the oxygen atom of crystalline water(O(9)) (O(8)···O(9) 2.723(3)Å) and to the Cl⁻ counter anion (O(8)···Cl 3.171(2)Å).

iii) The crystal structure of [(nta)Cr(OH)₂Cr(tn)₂]Cl·1.5H₂O (**B-3**). This dinuclear complex is isostructural with [(nta)Cr(OH)₂Co(tn)₂]Cl·1.5H₂O (**A-3**). The selected bond lengths and bond angles are listed in Table 3-4. A perspective view of this complex cation is shown in Figure 3-3. Each of the chromium(III) ions is in an approximately octahedral environment. The bridging plane is almost flat.

The average Cr-N(tn) bond length is 2.083 Å. This is the same value for the reported Cr-tn complexes.⁶² The Cr-N(nta) and Cr-O(nta) bond lengths are 2.052(3)Å and 1.971Å(average) respectively.

The difference in the (nta)Cr-OH bond lengths is the same as in the case of complex **A-3**. The (nta)Cr(2)-O(8)H and (nta)Cr(2)-O(7)H distances are 1.921(3)Å and 1.976(2)Å, respectively. There is also little difference in the (tn)₂Cr-OH bond lengths (Cr(1)-O(7)H:

Table 3-4. Selected bond lengths(Å) and bond angles(deg) for [(nta)Cr(OH)₂Cr(tn)₂]Cl · 1.5H₂O (**B-3**).

Cr(1)-N(2)	2.075(3)	Cr(1)-N(3)	2.077(3)
Cr(1)-N(4)	2.076(3)	Cr(1)-N(5)	2.102(3)
Cr(1)-O(7)	1.967(3)	Cr(1)-O(8)	1.951(2)
Cr(2)-N(1)	2.052(3)	Cr(2)-O(1)	1.951(2)
Cr(2)-O(3)	1.991(3)	Cr(2)-O(5)	1.970(3)
Cr(2)-O(7)	1.976(2)	Cr(2)-O(8)	1.921(3)
O(7)Cr(1)O(8)	80.63(9)	O(7)Cr(1)N(2)	88.8(1)
O(7)Cr(1)N(3)	97.3(1)	O(7)Cr(1)N(4)	171.4(1)
O(7)Cr(1)N(5)	88.0(1)	O(8)Cr(1)N(2)	87.7(1)
O(8)Cr(1)N(3)	174.5(1)	O(8)Cr(1)N(4)	91.4(1)
O(8)Cr(1)N(5)	93.2(1)	N(2)Cr(1)N(3)	87.4(1)
N(2)Cr(1)N(4)	90.0(1)	N(2)Cr(1)N(5)	176.4(1)
N(3)Cr(1)N(4)	91.1(1)	N(3)Cr(1)N(5)	91.6(1)
N(4)Cr(1)N(5)	93.4(1)	O(7)Cr(2)O(8)	80.1(1)
O(1)Cr(2)O(3)	91.3(1)	O(1)Cr(2)O(5)	89.6(1)
O(1)Cr(2)O(7)	175.7(1)	O(1)Cr(2)O(8)	95.1(1)
O(1)Cr(2)N(1)	84.9(1)	O(3)Cr(2)O(5)	163.8(1)
O(3)Cr(2)O(7)	88.7(1)	O(3)Cr(2)O(8)	97.6(1)
O(3)Cr(2)N(1)	80.9(1)	O(5)Cr(2)O(7)	91.6(1)
O(5)Cr(2)O(8)	98.4(1)	O(5)Cr(2)N(1)	83.2(1)
O(7)Cr(2)N(1)	99.3(1)	O(8)Cr(2)N(1)	178.4(1)
Cr(1)O(7)Cr(2)	98.27(9)	Cr(1)O(8)Cr(2)	100.72(9)

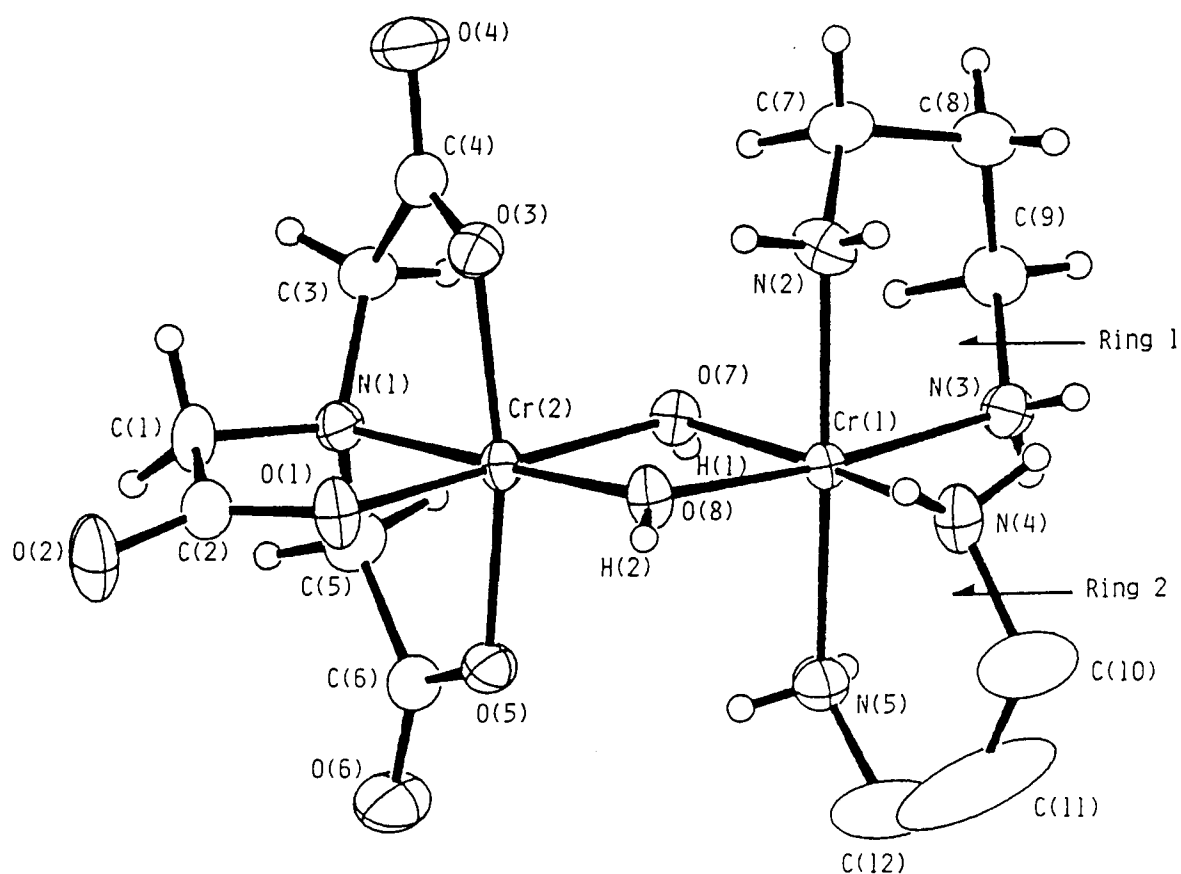


Figure 3-3. An ORTEP drawing of $[(nta)Cr(OH)_2Cr(tn)_2]^+$ (**B-3**) with thermal ellipsoids drawn at the 50 % probability level. Some hydrogen atoms in the tn chelate ring are omitted to clarify.

1.967(3)Å and Cr(1)-O(8)H: 1.951(2)Å).

In the Cr(tn)₂ moiety, the definition of the tn chelate rings 1 and 2 is shown in Figure 3-3. The chelate ring 1 has a chair conformation and "a" conformation as described in complex **A-3**. On the other hand, the chelate ring 2 has a skewboat conformation which is nearly planar and the "δ" chelate conformation.⁵⁹ The total conformation of Cr(tn)₂ moiety in Figure 3-3 is then Δaδ.⁵⁹

The intramolecular hydrogen bonds between the amine protons of the propane-1,3-diamine ligands and coordinated oxygen atoms of the nta one also exists. The distances of N(2)···O(3) and N(5)···O(5) are 3.241(4) and 3.055(5)Å, respectively. The intermolecular hydrogen bondings are the same as complex **A-3**.

iv) The crystal structures of [(nta)Cr(OH)₂Cr(phen)₂]Cl·7H₂O (**B-8**). The selected bond lengths and angles are listed in Table 3-5. Two crystallographically independent complex cations (molecules 1 and 2 in Table 3-5) are contained in an asymmetric unit. Figure 3-4 shows a perspective view of molecule 1. Each of the chromium(III) ions is in an approximately octahedral environment. The bridging units are almost flat.

The average Cr-N(phen) bond length is 2.06 Å. This is the same value of [Cr₂(μ-OH)₂(phen)₄]X₄ (X = Cl⁶³ and I⁶⁴) complexes. The average Cr-N(nta) and Cr-O(nta) bond lengths are 2.05Å and 1.96Å, respectively.

The difference in the (nta)Cr-OH bonds between *trans* and *cis* to the nta nitrogen atom is also observed in the complex **B-8** by 0.02Å (average value) similarly as shown in the complexes **A-3** and **B-3**.

Unlike the complexes **A-3** and **B-3**, there is no possibility to form the intramolecular hydrogen bond between the phen and nta ligand. The picam and bpy complexes also have no such intramolecular hydrogen bond. In the aqueous solutions, the picam, bpy and phen complexes are stable for several days. The Cr(N)₄-OH bond length of complex **B-8** is significantly shorter by 0.04Å than those of the complex (**B-3**). The average (N)₄Cr-OH bond lengths in [Cr₂(OH)₂(phen)₄]⁴⁺^{63,64} (1.92Å) is also shorter by 0.03Å than that in [Cr₂(OH)₂(en)₄]⁴⁺⁶⁵ (1.95Å). This is due to a π-bond interaction in the M-(N)₄ bond

Table 3-5. Selected Bond Lengths(Å) and Bond Angles(deg) for
 $[(\text{nta})\text{Cr}(\text{OH})_2\text{Cr}(\text{phen})_2]^+$ (**B-8**).

molecule 1		molecule 2	
Cr(1)-O(1)	1.94(1)	Cr(4)-O(11)	1.93(1)
Cr(1)-O(3)	1.979(8)	Cr(4)-O(13)	1.996(9)
Cr(1)-O(5)	1.969(8)	Cr(4)-O(15)	1.918(9)
Cr(1)-O(8)	1.95(1)	Cr(4)-O(18)	1.947(8)
Cr(1)-O(7)	1.970(9)	Cr(4)-O(17)	1.96(1)
Cr(1)-N(1)	2.05(1)	Cr(4)-N(11)	2.04(1)
Cr(2)-O(7)	1.92(1)	Cr(3)-O(17)	1.923(8)
Cr(2)-O(8)	1.92(1)	Cr(3)-O(18)	1.91(1)
Cr(2)-N(2)	2.05(1)	Cr(3)-N(12)	2.05(1)
Cr(2)-N(3)	2.07(1)	Cr(3)-N(13)	2.06(1)
Cr(2)-N(4)	2.08(1)	Cr(3)-N(14)	2.058(9)
Cr(2)-N(5)	2.07(1)	Cr(3)-N(15)	2.07(1)
N(1)-C(1)	1.49(2)	N(11)-C(51)	1.48(2)
N(1)-C(3)	1.47(2)	N(11)-C(53)	1.46(2)
N(1)-C(5)	1.45(1)	N(11)-C(55)	1.46(2)
C(1)-C(2)	1.52(2)	C(51)-C(52)	1.50(2)
C(3)-C(4)	1.51(2)	C(53)-C(54)	1.52(2)
C(5)-C(6)	1.54(2)	C(55)-C(56)	1.51(2)
O(1)Cr(1)O(7)		O(11)Cr(4)O(17)	169.3(4)
O(1)Cr(1)O(5)		O(11)Cr(4)N(15)	93.8(4)
O(1)Cr(1)O(8)		O(11)Cr(4)O(18)	95.3(4)
O(3)Cr(1)O(7)		O(13)Cr(4)O(17)	87.8(4)
O(3)Cr(1)N(1)		O(13)Cr(4)N(11)	80.8(4)
O(5)Cr(1)O(8)		O(15)Cr(4)O(18)	95.0(4)
O(7)Cr(1)O(8)		O(17)Cr(4)O(18)	77.6(4)
O(8)Cr(1)N(1)		O(18)Cr(4)N(11)	177.1(4)
O(1)Cr(1)O(3)		O(11)Cr(4)O(13)	85.9(4)
O(1)Cr(1)N(1)		O(11)Cr(4)N(11)	86.0(4)
O(3)Cr(1)O(5)		O(13)Cr(4)O(15)	163.1(4)
O(3)Cr(1)O(8)		O(13)Cr(4)O(18)	95.3(4)
O(5)Cr(1)O(7)		O(15)Cr(4)O(17)	94.7(4)
O(5)Cr(1)N(1)		O(15)Cr(4)N(11)	82.3(4)
O(7)Cr(1)N(1)		O(17)Cr(4)N(11)	101.5(4)

Table 3-5. continued.

O(7)Cr(2)N(2)	92.5(4)	O(17)Cr(3)N(12)	95.0(4)
O(7)Cr(2)N(4)	174.3(4)	O(17)Cr(3)N(14)	168.8(4)
O(8)Cr(2)N(2)	93.5(4)	O(18)Cr(3)N(12)	92.5(4)
O(8)Cr(2)N(4)	93.4(4)	O(18)Cr(3)N(14)	92.8(4)
N(2)Cr(2)N(3)	80.8(4)	N(12)Cr(3)N(13)	79.6(4)
N(2)Cr(2)N(5)	169.3(4)	N(12)Cr(3)N(15)	168.6(4)
N(3)Cr(2)N(5)	94.8(4)	N(13)Cr(3)N(15)	91.5(4)
O(7)Cr(2)O(8)	81.4(4)	O(17)Cr(3)O(18)	79.4(4)
O(7)Cr(2)N(3)	94.2(4)	O(17)Cr(3)N(13)	97.5(4)
O(7)Cr(2)N(5)	97.6(4)	O(17)Cr(3)N(15)	93.2(4)
O(8)Cr(2)N(3)	172.6(4)	O(18)Cr(3)N(13)	171.3(4)
O(8)Cr(2)N(5)	91.6(4)	O(18)Cr(3)N(15)	96.8(4)
N(2)Cr(2)N(3)	80.8(4)	N(12)Cr(3)N(14)	93.3(4)
N(2)Cr(2)N(5)	169.3(4)	N(13)Cr(4)N(14)	91.3(4)
N(3)Cr(2)N(5)	94.8(4)	N(14)Cr(3)N(15)	79.7(4)
Cr(1)O(7)Cr(2)	99.3(4)	Cr(3)O(17)Cr(4)	101.0(4)
Cr(1)O(8)Cr(2)	99.9(4)	Cr(3)O(18)Cr(4)	101.9(4)

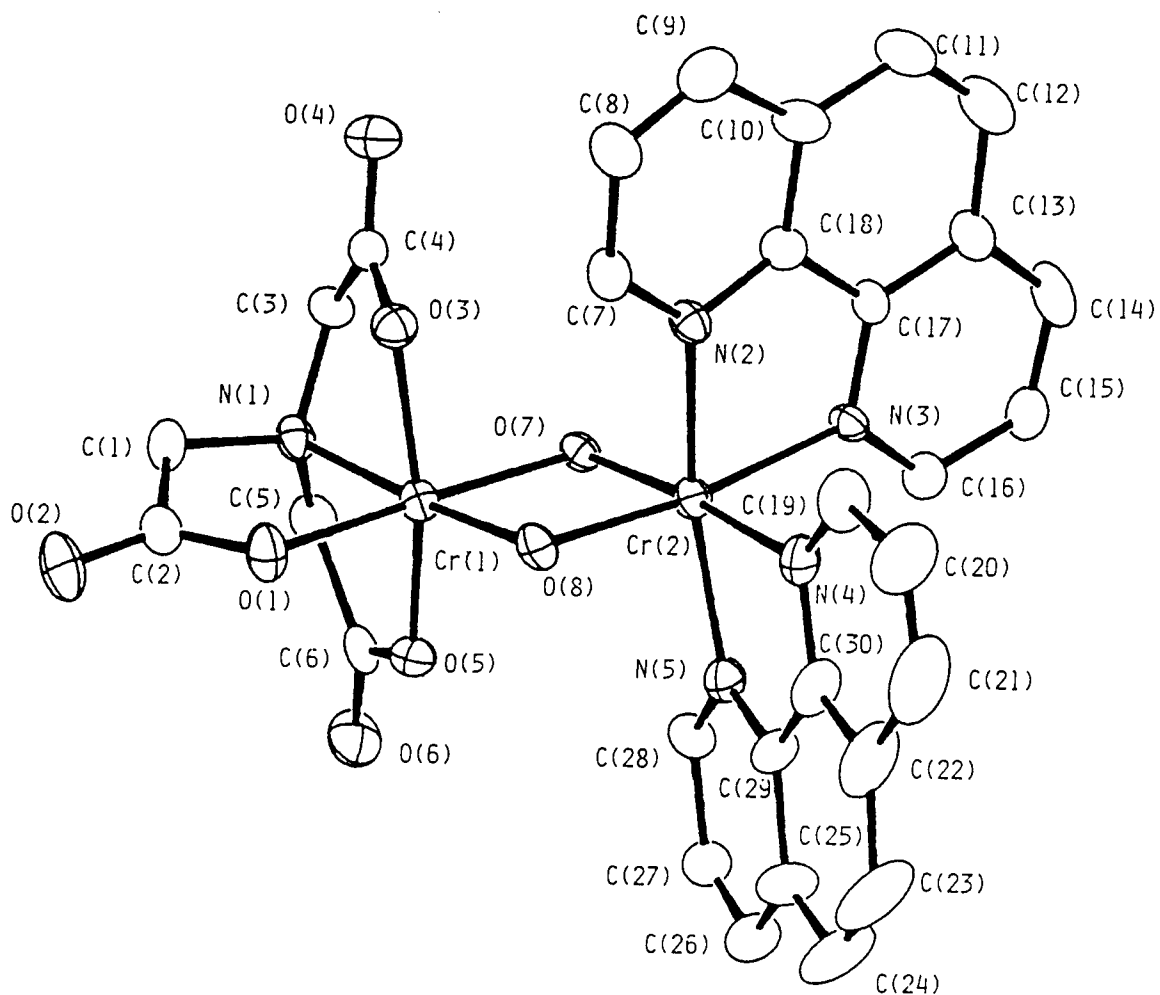


Figure 3-4. An ORTEP drawing of $[(nta)Cr(OH)_2Cr(phen)_2]^+$ (**B-8**) (molecule 1) with thermal ellipsoids drawn at the 50 % probability level. Hydrogen atoms are omitted to clarify.

stabilizes the $M(N)_4$ -OH bond. This result is consistent with the difference of the stability between $[Cr_2(OH)_2(en)_4]^{4+}$ and $[Cr_2(OH)_2(phen)_4]^{4+}$ in the aqueous solution. The $[Cr_2(OH)_2(en)_4]^{4+}$ comes easily into equilibrium between mono(μ -OH) and di(μ -OH) species.⁶⁶ It is considered that the strength of the Cr-OH bond would be also important for the stability of the di(μ -OH) dinuclear complexes in aqueous solution.

v) Comparison of the structures in the bridging units between the hetero- and homometal dinuclear complexes. Except for the bridging unit, structural parameters of Cr(nta), Cr(tn)₂, Co(tn)₂ and Cr(phen)₂ moieties are almost the same as those of the $[L_2M(\mu-OH)_2ML_2]$ type (L = bidentate) symmetrical dinuclear complexes. In Table 3-6, the selected bond lengths and angles for the dinuclear complexes are compared. The metal-metal distance in $[(nta)Cr(OH)_2Co(tn)_2]^+$ (**A-3**) is 2.9493(7) Å. It is expected that the Cr-Co distance in heterometal dinuclear complex would be an averaged value of the corresponding homometal dinuclear complexes since the bond lengths and angles in **A-3** are almost the same values of the corresponding homometal dinuclear ones, however, the Cr-Co distance is shorter than the expected average value (2.965 Å) of the metal-metal distances between $[Co_2(OH)_2(en)_4]^{4+}$ (2.951 Å)⁵⁸ and $[Cr_2(nta)_2(OH)_2]^{2-}$ (2.979 Å).⁵⁶ The same difference is also observed in $[(nta)Cr(OH)_2Cr(tn)_2]^+$ (**B-3**) (2.9816(9) Å), where the average value is 3.019 Å of the metal-metal distances between $[Cr_2(OH)_2(en)_4]^{4+}$ (3.059 Å)⁶⁵ and $[Cr_2(nta)_2(OH)_2]^{2-}$ (2.979 Å).⁵⁶ However, the average metal-metal distance in $[(nta)Cr(OH)_2Cr(phen)_2]^+$ (**B-8**) (2.981 Å) is almost equal to the average value (2.988 Å) of the metal-metal distances between $[Cr_2(OH)_2(phen)_4]^{4+}$ (2.997 Å)^{63,64} and $[Cr_2(nta)_2(OH)_2]^{2-}$ (2.979 Å).⁵⁶ The shorter metal-metal distances in complex **A-3** and **B-3** than the averaged values would be due to the intramolecular hydrogen bonds between the tn amine protons and nta carboxylato atoms as described above, since such difference is not obtained in the complex **B-8** which has no hydrogen atoms to form the intramolecular hydrogen bond between the phen and nta ligand.

The (nta)Cr-OH bonds *trans* to the nta nitrogen atom in the aliphatic diamine complexes **A-3** and **B-3** are significantly shorter by about 0.03 Å than those in the aromatic diimine

Table 3-6. Selected bond lengths(Å) and angles(deg) for the homo- and heterometal dinuclear complexes.

	M-N ^f	(nta)Cr-OH	(N) ₂ Co-OH	(N) ₂ Cr-OH	OCr(nta)O	OCr(N) ₂ O	OCr(N) ₂ O	M-O-N ^f
[(nta)Cr(OH) ₂ Co(tn) ₂][Cl·1.5H ₂ O(A-3)]	2.9493(7)	1.967(2) ^a 1.913(2) ^b	1.928		80.07(8)	80.69(9)		99.4
[(nta)Cr(OH) ₂ Cr(tn) ₂][Cl·1.5H ₂ O(B-3)]	2.9816(9)	1.976(2) ^a 1.921(3) ^b		1.959	80.1(1)		80.63(9)	99.5
[(nta)Cr(OH) ₂ Cr(phen) ₂][Cl·7H ₂ O(B-8)]	2.981	1.97 ^a 1.95 ^b		1.92	78.9		80.4	100.5
Cs ₂ [Cr ₂ (nta) ₂ (OH) ₂] ^c ·4H ₂ O ^e	2.979	1.985			82.7			97.3
[Co ₂ (OH) ₂ (en) ₄](NO ₃) ₄ ^d	2.951(1)		1.93			79.8(1)	100.1(1)	
[Cr ₂ (OH) ₂ (phen) ₄][Cl ₄ ·6H ₂ O ^e	3.008			1.927			77.3	102.7
[Cr ₂ (OH) ₂ (phen) ₄][₄ ·4H ₂ O ^f	2.986			1.920			77.9	102.0
[Cr ₂ (OH) ₂ (en) ₄](ClO ₄) ₂ Cl ₂ ·2H ₂ O ^g	3.059			1.949			76.58	103.42

^a O(7). ^b O(8). ^c reference 56. ^d reference 58. ^e reference 63. ^f reference 64. ^g reference 65.

complex **B-8**, while the (N)₄Cr-OH bonds in complexes **A-3** and **B-3** are longer by 0.04 Å than that in the complex **B-8**. It is considered that the differences of the (nta)Cr-OH bonds between complexes **A-3** or **B-3** and **B-8** are due to the extent of the π -bond interaction of (N)₄M-OH bond. It is noticeable that the (nta)Cr-OH bonds *trans* to the nta nitrogen atom vary with the extent of the π -bond interaction of M(N)₄-OH bond, but those *cis* to the nta one are almost unaltered.

vi) Acid strength of bridging hydroxide. The colors of aqueous solutions of the complexes **A-1** ~ **4** and **B-1** ~ **4** instantaneously change from red to blue by adding sodium hydroxide solution. The reaction is reversible and presumably due to the deprotonation of the hydroxo bridges giving μ -hydroxo- μ -oxo complexes. Similar spectral behavior in alkaline solution was reported for [Cr₂(OH)₂(NH₃)₈]⁴⁺,⁶⁷ [Cr₂(OH)₂(en)₄]⁴⁺,⁶⁸ [Cr₂(μ -OH)(μ -SO₄)(en)₂]³⁺,⁶⁹ and [Cr₂(μ -OH)(μ -CH₃COO)(en)₄]⁴⁺.⁴⁵ The pK_{a1} values of above complexes were reported to be about 12. The pK_{a1} values of the bridging hydroxo ligands for the [Cr(III)-Co(III)] and [Cr(III)-Cr(III)] complexes varied with the kinds of the coordinated diamines as shown in Table III-7. The pK_{a1} values are about 12 for the aliphatic amine complexes (NH₃, en, tn, (R,R)chxn and trien). The pK_{a1} values are 9.8 and 11 for the picam complexes. The pK_{a1} values are about 9 for the bpy and phen complexes. These results are the same as [Cr₂(μ -OH)₂(N)₈]⁴⁺ type dinuclear complexes¹¹ as shown in Table 3-7. This tendency of the acid strength would correspond to the π -acceptor interaction in the M-N((N)₄) bond. It is considered that the π -acceptor interaction in the M-N bond affects the M-OH bond. The M-N bond is strengthened by the π -acceptor interaction, the M-O bond is enhanced by the π -donor interaction simultaneously as a push-pull action. The pK_{a2} values were not estimated exactly because of the decomposition of the dinuclear complexes in the relatively strong alkaline aqueous solutions.

Since two bridging OH are not equivalent, it is necessary to clarify which hydrogen atom in the bridging hydroxide is dissociated. The stronger Cr-OH bond causes the weaker O-H bond and the proton would be easy to dissociate. Since the longer (N)₄M-OH bond causes the shorter (nta)Cr-OH bonds *trans* to the nta amine nitrogen as found in the crystal

Table 3-7. Acid Strength of bridging hydroxide for obtained dinuclear complexes^a and [LCr(OH)₂CrL]ⁿ⁺ type complexes^b.

Complex	No.	pK _{a1}	pK _{a2}
[(nta)Cr(OH) ₂ Co(NH ₃) ₄] ⁺	A-1	— ^c	— ^c
[(nta)Cr(OH) ₂ Co(en) ₂] ⁺	A-2	~ 12	— ^c
[(nta)Cr(OH) ₂ Co(tn) ₂] ⁺	A-3	~ 12	— ^c
[(nta)Cr(OH) ₂ Co{(R,R)chxn} ₂] ⁺	A-4	~ 12	— ^c
[(nta)Cr(OH) ₂ Co(trien) ₂] ⁺	A-5	~ 12	— ^c
[(nta)Cr(OH) ₂ Co(picam) ₂] ⁺	A-6	11	— ^c
[(nta)Cr(OH) ₂ Co(bpy) ₂] ⁺	A-7	9.3	— ^c
[(nta)Cr(OH) ₂ Co(phen) ₂] ⁺	A-8	9.4	— ^c
[(nta)Cr(OH) ₂ Cr(NH ₃) ₄] ⁺	B-1	~ 12	— ^c
[(nta)Cr(OH) ₂ Cr(en) ₂] ⁺	B-2	~ 12	— ^c
[(nta)Cr(OH) ₂ Cr(tn) ₂] ⁺	B-3	~ 12	— ^c
[(nta)Cr(OH) ₂ Cr{(R,R)chxn} ₂] ⁺	B-4	~ 12	— ^c
[(nta)Cr(OH) ₂ Cr(trien) ₂] ⁺	B-5	~ 12	— ^c
[(nta)Cr(OH) ₂ Cr(picam) ₂] ⁺	B-6	9.8	— ^c
[(nta)Cr(OH) ₂ Cr(bpy) ₂] ⁺	B-7	9.0	— ^c
[(nta)Cr(OH) ₂ Cr(phen) ₂] ⁺	B-8	9.2	— ^c
[(NH ₃) ₄ Cr(OH) ₂ Cr(NH ₃) ₄] ⁴⁺		~ 12	—
[(en) ₂ Cr(OH) ₂ Cr(en) ₂] ⁴⁺		~ 12	>14
[(tn) ₂ Cr(OH) ₂ Cr(tn) ₂] ⁴⁺		~ 12	—
[(mepic) ₂ Cr(OH) ₂ Cr(mepic) ₂] ⁴⁺ ^d		10.7	—
[(bpy) ₂ Cr(OH) ₂ Cr(bpy) ₂] ⁴⁺		7.60	11.9
[(phen) ₂ Cr(OH) ₂ Cr(phen) ₂] ⁴⁺		7.40	11.8
[(nta) ₂ Cr(OH) ₂ Cr(nta) ₂] ²⁻		8.7	9.8

^a at 25 °C and ionic strength *I* = 0.1 mol dm⁻³ adjusted with KCl. ^b Data from reference 11. ^c Not determined because of the decomposition.

^d mepic is 1-(2-pyridyl)ethylamine.

structures, the O-H bond strength *trans* to the nta amine nitrogen would not be changed. Therefore, the hydrogen atom bounds to the oxygen *cis* to the nta amine nitrogen of which the (nta)Cr-OH bond is not affected by the (N)₄M-OH one would be dissociated at first.

The [Cr(III)-Co(III)] complexes exhibit little larger pK_{a1} values than the [Cr(III)-Cr(III)] ones. Though there is no data of acid strengths in di(μ -OH) [Co(III)-Co(III)] complexes, the pK_a values of the coordinated water of *cis*-[Co(en)₂(H₂O)₂]³⁺ (pK_{a1} : 6.06 and pK_{a2} : 8.19) is larger than those of *cis*-[Cr(en)₂(H₂O)₂]³⁺ (pK_{a1} : 4.75 and pK_{a2} : 7.35).¹¹ This is consistent with the trends observed for the dinuclear complexes.

vii) Absorption and CD Spectra. The dinuclear complexes have broad absorption bands because of the two different chromophores ([CrNO₅] and [MN₄O₂] (M = Cr(III) and Co(III))) in the first spin allowed d-d absorption band region. The splitting spectral pattern in this region were observed in some complexes. The splitted absorption maxima are assigned to the [(nta)Cr(OH)₂] and [(OH)₂M(N)₄] chromophores from the longer wavelength, respectively as shown in Table 3-8. These spectral result is consistent with the unsymmetrical [(nta)Cr(OH)₂M(N)₄]⁺ structure. The UV/VIS absorption spectra of four complexes **A-2**, **7**, **B-2** and **7** are shown in Figure 3-5. The broad absorption band observed at 35000 cm⁻¹ (ca. 285 nm) for the [Cr(III)-Co(III)] aliphatic diamine complexes in Figure 3-5b as observed in the di(μ -OH) bridged [Co(III)-Co(III)] complexes.^{52,53,70} For the complexes **A-6**, **7** and **8** with the pyridine ligands, such an absorption band is not observed owing to overlapping with the $\pi \cdot \pi^*$ intraligand transition band. These absorption bands at 35000 cm⁻¹ are assigned to the charge transfer (CT) transition of Co-OH moiety for the [Co(μ -OH)₂Co] type complexes.⁷⁰ It is noted that this CT transition appears even in these [Cr(μ -OH)₂Co] complexes. The absorption intensities of these CT transitions for the [Cr(III)-Co(III)] complexes in this study are smaller by about one-fourth than those of the [Co(III)-Co(III)] ones.^{52,53}

The inflection at 35100 cm⁻¹ (285 nm) appears for the [Cr(III)-Cr(III)] aliphatic diamine complexes. The complex **B-4** exhibits the CD maxima at 35100 cm⁻¹ (285 nm). Such

Table 3-8. Absorption and CD spectral data for dinuclear complexes in aqueous solutions.

Complex	Absorption maxima		
	λ / nm ($\epsilon / \text{mol}^{-1} \text{dm}^3 \text{cm}^{-1}$)		
	σ_{I}	σ_{II}	
	$[(\text{nta})\text{Cr}(\text{OH})_2]^-$	$[(\text{N})_4\text{M}(\text{OH})_2]$	
$[(\text{nta})\text{Cr}(\text{OH})_2 \text{Co}(\text{NH}_3)_4]^+$		545(146)	380(223)
$[(\text{nta})\text{Cr}(\text{OH})_2 \text{Co}(\text{en})_2]^+$	600sh(100)	510(161)	380sh(210)
$[(\text{nta})\text{Cr}(\text{OH})_2 \text{Co}(\text{tn})_2]^+$		531(125)	390sh(170)
$[(\text{nta})\text{Cr}(\text{OH})_2 \text{Co}\{(R,R)\text{chxn}\}_2]^{+a}$		516(313)	380sh(380)
$[(\text{nta})\text{Cr}(\text{OH})_2 \text{Co}(\text{trien})_2]^+$		508(318)	380sh(360)
$[(\text{nta})\text{Cr}(\text{OH})_2 \text{Co}(\text{picam})_2]^+$		510(180)	370sh(360)
$[(\text{nta})\text{Cr}(\text{OH})_2 \text{Co}(\text{bpy})_2]^+$	580sh(90)	485(129)	
$[(\text{nta})\text{Cr}(\text{OH})_2 \text{Co}(\text{phen})_2]^+$		512(133)	
$[(\text{nta})\text{Cr}(\text{OH})_2 \text{Cr}(\text{NH}_3)_4]^+$		555(91)	401(118) 285(70) ^b
$[(\text{nta})\text{Cr}(\text{OH})_2 \text{Cr}(\text{en})_2]^+$	585sh(90)	520(111)	398(131) 285(70) ^b
$[(\text{nta})\text{Cr}(\text{OH})_2 \text{Cr}(\text{tn})_2]^+$	580(87)	522(93)	402(123) 285(75) ^b
$[(\text{nta})\text{Cr}(\text{OH})_2 \text{Cr}\{(R,R)\text{chxn}\}_2]^{+c}$	590sh(90)	520(119)	398(133) 285(75) ^b
$[(\text{nta})\text{Cr}(\text{OH})_2 \text{Cr}(\text{trien})_2]^+$		555(148)	400(140) 285(75) ^b
$[(\text{nta})\text{Cr}(\text{OH})_2 \text{Cr}(\text{picam})_2]^+$		540(128)	402(141)
$[(\text{nta})\text{Cr}(\text{OH})_2 \text{Cr}(\text{bpy})_2]^+$		565(96)	
$[(\text{nta})\text{Cr}(\text{OH})_2 \text{Cr}(\text{phen})_2]^+$		565(97)	

^a CD maxima (λ / nm ($\Delta\epsilon / \text{mol}^{-1} \text{dm}^3 \text{cm}^{-1}$)) 538(0.900) 496(-1.024) 370(0.696). ^b inflection.

^c CD maxima (λ / nm ($\Delta\epsilon / \text{mol}^{-1} \text{dm}^3 \text{cm}^{-1}$)) 698(0.058) 590(0.595) 489(-2.950) 370(0.320) 285(0.046)

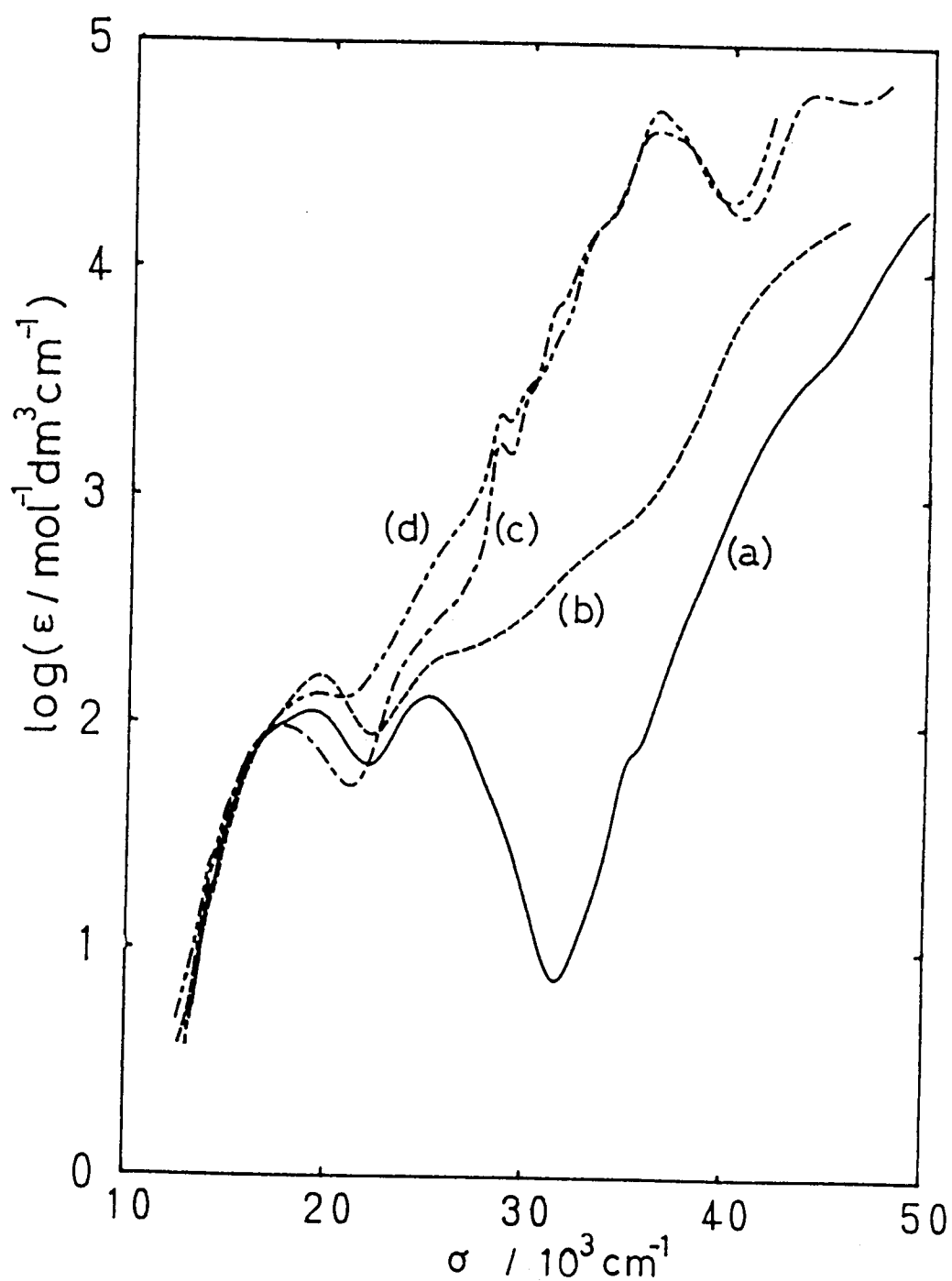


Figure 3-5. The UV/VIS absorption spectra of four $[(nta)Cr(OH)_2M(N)_4]^+$ complexes in aqueous solution. (a) $M = Cr^{III}$ and $(N)_4 = (en)_2$ (**A-2**), (b) $M = Co^{III}$ and $(N)_4 = (en)_2$ (**B-2**), (c) $M = Cr^{III}$ and $(N)_4 = (bpy)_2$ (**A-7**) and (d) $M = Co^{III}$ and $(N)_4 = (bpy)_2$ (**B-7**).

inflections of the complexes **B-6**, **7** and **8** with the pyridine ligands were not observed owing to overlapping with the $\pi\text{-}\pi^*$ intraligand transition band. These absorption bands are considered to be characteristic of the [Cr(III)-Cr(III)] complexes. But the assignment is not clear.

3.3.2 Characterization of $[\text{Cr}_2(\text{OH})(\text{RCOO})(\text{en})_4]^{4+}$ (en complexes) and $[(\text{nta})\text{Cr}(\text{OH})(\text{RCOO})\text{Cr}(\text{en})_2]^+$ complexes (nta complexes)

i) Synthetic method of $[\text{Cr}(\text{OH})(\text{RCOO})\text{Cr}]$ type dinuclear complexes. Since the analytical data (Table 2-2) gave satisfactory results, the en complexes are identified as $[\text{Cr}_2(\text{OH})(\text{RCOO})(\text{en})_4]^{4+}$. The UV/vis absorption spectra for newly prepared en complexes are identical with the literature ones (Table 3-9). The elemental analysis (Table 2-2) and column chromatographic behavior for the nta complexes indicate that the present complexes have the carboxylato bridging dinuclear structures, together with the observation of two absorption maxima or shoulder around 590 and 509 nm corresponding to $\text{Cr}(\text{nta})(\text{O})_2$ and *cis*- $\text{Cr}(\text{en})_2(\text{O})_2$ chromophores.

The infrared spectral behavior in difference between the asymmetric (ν_{as}) and symmetric (ν_{s}) stretching frequency for the carboxylates shows the existence of the carboxylate bridging ligand; $\Delta\nu(\text{COO}) = \nu_{\text{as}} - \nu_{\text{s}}$ for the bridging carboxylates are smaller than those for the corresponding sodium salts as shown in Table 3-10, and the linear correlation is found between the ν_{as} and the $\text{p}K_{\text{a}}$ values for the bridging carboxylates^{13,45,27} in Figure 3-6.

Two geometrical isomers are possible for $[(\text{nta})\text{Cr}(\text{OH})(\text{RCOO})\text{Cr}(\text{en})_2]^+$ as shown in Figure 3-7. Careful column chromatography gave only one band. The ^2H NMR spectra of deuteriated complex $[(\text{nta-d}_6)\text{Cr}(\text{OH})(\text{CD}_3\text{COO})\text{Cr}(\text{en})_2]^+$ gave only one set of the signal components; three (-11.0, -24.6 and -31.5 ppm) and one (47.4 ppm) signal for the nta-d₆ and CD_3COO^- ligand, respectively. These facts confirm the existence of only one geometrical isomer, but not of a mixture of two ones. The (a) structure in Figure 3-7 seems to be more favored than the (b) one in view of the release of the steric congestion between the glycinate ring chelate in the nta ligand and the en chelate, in accordance with the structures in $\text{K}_2[(\text{nta})\text{Cr}(\mu\text{-OH})(\mu\text{-CH}_3\text{COO})\text{Cr}(\text{nta})]\cdot 4\text{H}_2\text{O}$ ⁵⁵ and $[(\text{tren})\text{Cr}(\mu\text{-OH})(\mu\text{-$

Table 3-9. Visible absorption spectral data for $[\text{Cr}_2(\text{OH})(\text{RCOO})(\text{en})_4]^{4+}$ and $[(\text{nta})\text{Cr}(\text{OH})(\text{RCOO})\text{Cr}(\text{en})_2]^+$ complexes

Compounds	No.	$\lambda_{\text{max}} / \text{nm} (\epsilon / \text{mol}^{-1} \text{dm}^3 \text{cm}^{-1})$		
$[\text{Cr}_2(\text{OH})(\text{RCOO})(\text{en})_4]^{4+}$ ^a				
R = H	C-1a	504(202)	376(90)	
CH ₃	C-2a	505(210)	378(99)	
CH ₃ CH ₂	C-3a	505(208)	377(101)	
CH ₃ CH ₂ CH ₂	C-4a	505(207)	377(99)	
CH ₂ Cl	C-5a	504(200)	376(88)	
CH ₂ ClCH ₂	C-6a	505(201)	377(96)	
CH ₃ OCH ₂	C-7a	504(207)	376(94)	
$[(\text{nta})\text{Cr}(\text{OH})(\text{RCOO})\text{Cr}(\text{en})_2]^{+}$ ^b				
R = H	C-1b	590sh(90)	509(128)	403(128)
CH ₃	C-2b	590sh(90)	507(141)	404(133)
CH ₃ CH ₂	C-3b	590sh(90)	509(135)	404(132)
CH ₃ CH ₂ CH ₂	C-4b	590sh(90)	509(136)	404(131)
CH ₂ Cl	C-5b	590sh(90)	507(131)	405(128)
CH ₂ ClCH ₂	C-6b	590sh(90)	509(133)	404(128)
CH ₃ OCH ₂	C-7b	590sh(110)	506(144)	405(147)
C ₆ H ₅	C-8b	590sh(90)	509(128)	403(128)

^a in 0.01 mol dm⁻³ HCl. ^b in H₂O.

Table 3-10. Infra-red spectral data (cm^{-1}) for $[\text{Cr}_2(\text{OH})(\text{RCOO})(\text{en})_4]^{4+}$, $[(\text{nta})\text{Cr}(\text{OH})(\text{RCOO})\text{Cr}(\text{en})_2]^+$ and RCOONa in CO stretching region^a

compounds	No.	$\nu_{\text{as}}(\text{CO})$	$\nu_{\text{s}}(\text{CO})$	$\Delta\nu(\text{CO})$
$[\text{Cr}_2(\text{OH})(\text{RCOO})(\text{en})_4]^{4+}$				
R = H	C-1a	1572	1380	192
CH ₃	C-2a	1550	1422	128
CH ₃ CH ₂	C-3a	1540	1445	95
CH ₃ CH ₂ CH ₂	C-4a	1536	1455	81
CH ₂ Cl	C-5a	1598	1443	155
CH ₂ ClCH ₂	C-6a	1555	1455	100
CH ₃ OCH ₂	C-7a	1575	1460	115
$[(\text{nta})\text{Cr}(\text{OH})(\text{RCOO})\text{Cr}(\text{en})_2]^+$				
R = H	C-1b	1568	1380	188
CH ₃	C-2b	1555	1420	135
CH ₃ CH ₂	C-3b	1545	1438	107
CH ₃ CH ₂ CH ₂	C-4b	1540	1453	87
CH ₂ Cl	C-5b	1592	1445	145
CH ₂ ClCH ₂	C-6b	1554	1458	96
CH ₃ OCH ₂	C-7b	1568	1460	108
C ₆ H ₅	C-8b	1540	1425	115
RCOONa				
R = H		1590	1355	253
CH ₃		1578	1425	153
CH ₃ CH ₂		1553	1421	132
CH ₃ CH ₂ CH ₂		1558	1420	138
CH ₂ Cl		1610	1445	145
CH ₂ ClCH ₂		1560	1420	140
CH ₃ OCH ₂		1613	1422	191
C ₆ H ₅		1540	1425	115

^a KBr pellets.

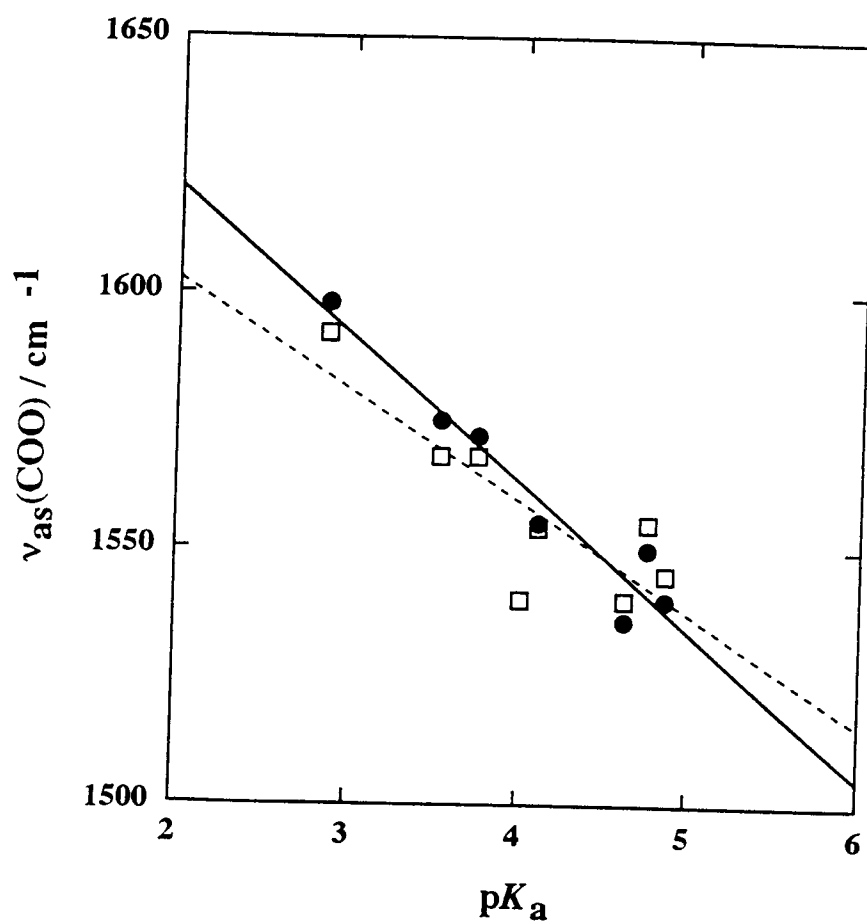
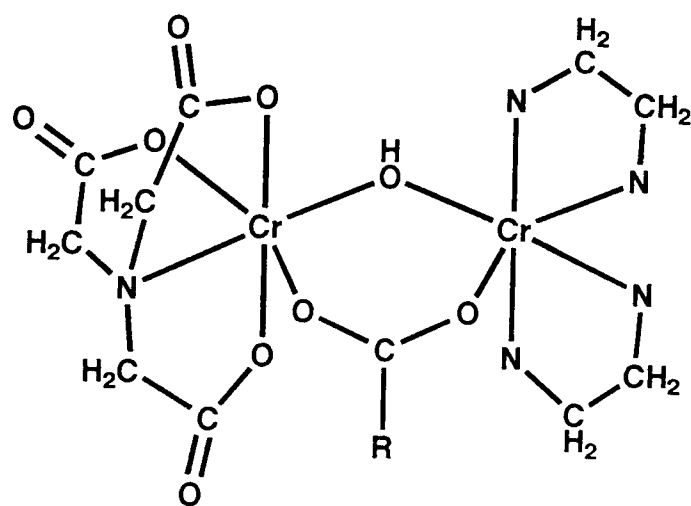
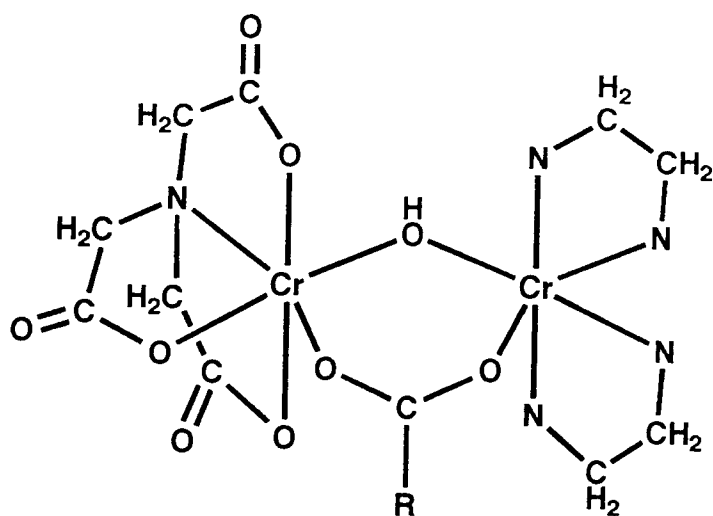


Figure 3-6. Correlations between $\nu_{as}(\text{COO})$ and pK_a values of $[\text{Cr}_2(\text{OH})(\text{RCOO})(\text{en})_4]^{4+}$ (●, —) and $[(\text{nta})\text{Cr}(\text{OH})(\text{RCOO})\text{Cr}(\text{en})_2]^+$ (□, - - -). Lines shown are least-squares fit.



(a)

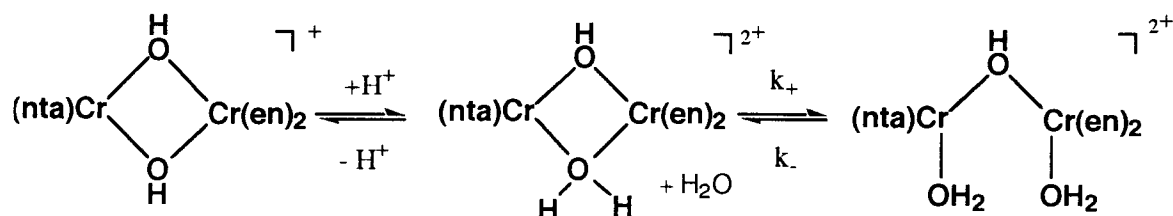


(b)

Figure 3-7. Possible geometrical structures of $[(\text{nta})\text{Cr}(\mu\text{-OH})(\mu\text{-RCOO})\text{Cr}(\text{en})_2]^+$.

$\text{CO}_3\text{Cr}(\text{tren})](\text{ClO}_4)_3 \cdot 4\text{H}_2\text{O}$,⁷¹ where the oxygen atom of the μ -carboxylato or μ -carbonato ligand is located at the *cis* position to the tertiary amine nitrogen in the nta or tren ligand. Moreover, the following kinetic and structural considerations also support the (a) structure. $[(\text{nta})\text{Cr}(\text{OH})(\text{RCOO})\text{Cr}(\text{en})_2]^+$ are formed by the reaction of $[(\text{nta})\text{Cr}(\text{OH})_2\text{Cr}(\text{en})_2]^+$ with free RCOOH . In the acidic condition, the hydroxo bridge cleavage of $[(\text{nta})\text{Cr}(\text{OH})_2\text{Cr}(\text{en})_2]^+$ occurs firstly to give $[(\text{nta})(\text{H}_2\text{O})\text{Cr}(\mu\text{-OH})\text{Cr}(\text{H}_2\text{O})(\text{en})_2]^{2+}$ before forming $[(\text{nta})\text{Cr}(\text{OH})(\text{RCOO})\text{Cr}(\text{en})_2]^+$.

Since there is no monool-diol equilibrium in the $[(\text{nta})\text{Cr}(\text{OH})_2\text{Cr}(\text{en})_2]^+$, the formation of $[(\text{nta})(\text{H}_2\text{O})\text{Cr}(\text{OH})\text{Cr}(\text{H}_2\text{O})(\text{en})_2]^{2+}$ would be anticipated as follows:



The bridging OH ligand is protonated in the acidic condition at first. Since the aqua bridged species which is very unstable and labile with respect to bridge cleavage,¹¹ $[(\text{nta})(\text{H}_2\text{O})\text{Cr}(\text{OH})\text{Cr}(\text{H}_2\text{O})(\text{en})_2]^{2+}$ is immediately formed. The protonation reaction of the bridging OH is affected $\text{Cr}(\text{N})_4$ bond as we seen in the deprotonation reaction of the bridging OH ligand in Section 3.3.1, because $[(\text{nta})\text{Cr}(\text{OH})_2\text{Cr}(\text{bpy} \text{ and } \text{phen})_2]^+$ did not react with RCOOH . Therefore, the hydroxo bridging ligand *cis* to the tertiary amine nitrogen in the nta which is affected $\text{Cr}(\text{N})_4$ bond is protonated in the acidic condition. Thus, it is plausible that the acid catalyzed cleavage could occur at the *cis* position to the tertiary amine nitrogen in the nta ligand to form the (a) structure rather than the (b) one in Figure 3-7. This coordination environment is apparently crowded by the steric interaction among the substituents in the bridging carboxylates, the en and nta's glycinato chelate rings. However, the bridging site seems to leave room for enough space to be unaffected even by the bulky R substitution groups, since there is little difference in formation yield of this type of complexes with carboxylates ($\text{R} = \text{H}$, 58; CH_3 , 56; C_2H_5 , 54; CH_3OCH_2 , 50; CH_2Cl , 50; $n\text{-C}_3\text{H}_7$, 47; CH_2ClCH_2 , 46; C_6H_5 , 48%).

3.3.3 Characterization of $[\text{Cr}_2(\text{OH})_2(\text{RCOO})(\text{bispicam})_2]^{3+ \text{ or } 4+}$ complexes

i) Synthetic method of $[\text{Cr}_2(\text{OH})_2(\text{RCOO})(\text{bispicam})_2]^{3+ \text{ or } 4+}$. Chromium(II) carboxylato complexes easily react with the tridentate ligand N,N-bis(2-pyridylmethyl)amine (bispicam) in water. Though the previous report was only concerned with $\mu\text{-CH}_3\text{COO}^-$ complexes,^{18,30} it is found that many μ -carboxylato chromium(III) dinuclear complexes can be prepared from chromium(II) carboxylato ones in this study. The crude products were easily obtained from the red reaction solution by adding saturated NaClO_4 aqueous solution without using column chromatographic separation and fractional recrystallization as performed in $[\text{Cr}_2(\mu\text{-OH})_2(\mu\text{-SO}_4)(\text{bispicam})_2]^{2+}$ ²⁸ and $[\text{Cr}_2(\mu\text{-OH})_2(\mu\text{-CH}_3\text{COO})(\text{tpen})]^{3+}$,¹⁸ respectively. The obtained crude perchlorates can be easily recrystallized from hot water and gave satisfactorily analytical results. These complexes are stable for several days in aqueous solution.

As shown in some μ -carboxylato chromium(III) dinuclear complexes,^{13,27,45} the infrared spectral behavior in difference between asymmetric (ν_{as}) and symmetric (ν_{s}) stretching frequencies for the carboxylates decreases in the following order: monodentate carboxylate, free carboxylate and bidentate or bridged carboxylate. In Table 3-11, the $\Delta\nu(\text{COO})$ values ($\Delta\nu = \nu_{\text{as}} - \nu_{\text{s}}$) for all the carboxylato complexes are lower than those for the corresponding free carboxylato ions. Though there is no corresponding data to compare for the amino acidato complexes, the $\Delta\nu(\text{COO})$ value of the $[\text{Cr}_2(\text{OH})_2(\text{H}_3\text{NCH}_2\text{COO})(\text{bispicam})_2]^{4+}$ (126 cm^{-1}) is comparable to that of $[\text{Cr}_2(\text{OH})(\text{H}_3\text{NCH}_2\text{COO})(\text{en})_4]^{5+}$ (185 cm^{-1}).⁴⁵ The $\Delta\nu(\text{COO})$ values of other amino acidato complexes are also comparable to that of $[\text{Cr}_2(\text{OH})_2(\text{H}_3\text{NCH}_2\text{COO})(\text{bispicam})_2]^{4+}$. The linear correlations between the $\text{p}K_{\text{a}}$ values of the free carboxylic acids and the frequencies $\nu_{\text{as}}(\text{COO})$ of the corresponding μ -carboxylato chromium(III) and cobalt(III) complexes were found.^{13,27,45} A similar relationship in the present carboxylato complexes are obtained as shown in Figure 3-8. This result supports that the obtained complexes have the μ -carboxylato structure.

There exists three geometrical isomers of the obtained complexes for $[\text{Cr}_2(\text{OH})_2(\text{SO}_4)(\text{bispicam})_2]^{2+}$ as Larsen, Michelsen and Pedersen considered (Figure

Table 3-11. Infra-red spectral data (cm^{-1}) of obtained dinuclear complexes (perchlorates) and carboxylate sodium salt in C-O stretching frequency region.^a

Compounds	$\nu_{\text{as}}(\text{CO})$	$\nu_{\text{s}}(\text{CO})$	$\Delta\nu$	$\text{pK}_{\text{a}}^{\text{b}}$
$[\text{Cr}_2(\text{OH})_2(\text{HCOO})(\text{bispicam})_2]^{3+}$ HCOONa	1555	1437	118	3.75
$[\text{Cr}_2(\text{OH})_2(\text{CH}_3\text{COO})(\text{bispicam})_2]^{3+}$ CH_3COONa	1590 1530	1355 1440	235 90	4.76
$[\text{Cr}_2(\text{OH})_2(\text{CH}_3\text{CH}_2\text{COO})(\text{bispicam})_2]^{3+}$ $\text{CH}_3\text{CH}_2\text{COONa}$	1578 1525	1425 1445	153 100	4.87
$[\text{Cr}_2(\text{OH})_2(\text{CH}_2\text{ClCOO})(\text{bispicam})_2]^{3+}$ $\text{CH}_2\text{ClCOONa}$	1553 1578	1421 1436	132 142	2.87
$[\text{Cr}_2(\text{OH})_2(\text{CH}_2\text{ClCH}_2\text{COO})(\text{bispicam})_2]^{3+}$ $\text{CH}_2\text{ClCH}_2\text{COONa}$	1610 1532	1420 1433	190 99	4.11
$[\text{Cr}_2(\text{OH})_2(\text{H}_3\text{NCH}_2\text{COO})(\text{bispicam})_2]^{3+}$	1560	1420	140	
$[\text{Cr}_2(\text{OH})_2(\text{H}_3\text{NCH}_2\text{CH}_2\text{COO})(\text{bispicam})_2]^{3+}$	1560	1436	126	
$[\text{Cr}_2(\text{OH})_2(\text{H}_3\text{NCH}_2\text{CH}_2\text{COO})(\text{bispicam})_2]^{3+}$	1545	1440	105	
$[\text{Cr}_2(\text{OH})_2(\text{H}_3\text{NCH}_2\text{CH}_2\text{CH}_2\text{COO})(\text{bispicam})_2]^{3+}$	1553	1444	109	
$[\text{Cr}_2(\text{OH})_2(\text{H}_3\text{NCH}(\text{CH}_3)\text{COO})(\text{bispicam})_2]^{3+}$	1555	1445	110	
$[\text{Cr}_2(\text{OH})_2(\text{H}_3\text{NCH}(\text{OH})\text{COO})(\text{bispicam})_2]^{3+}$	1560	1445	115	

^a KBr pellet. ^b Data from Stability constants.

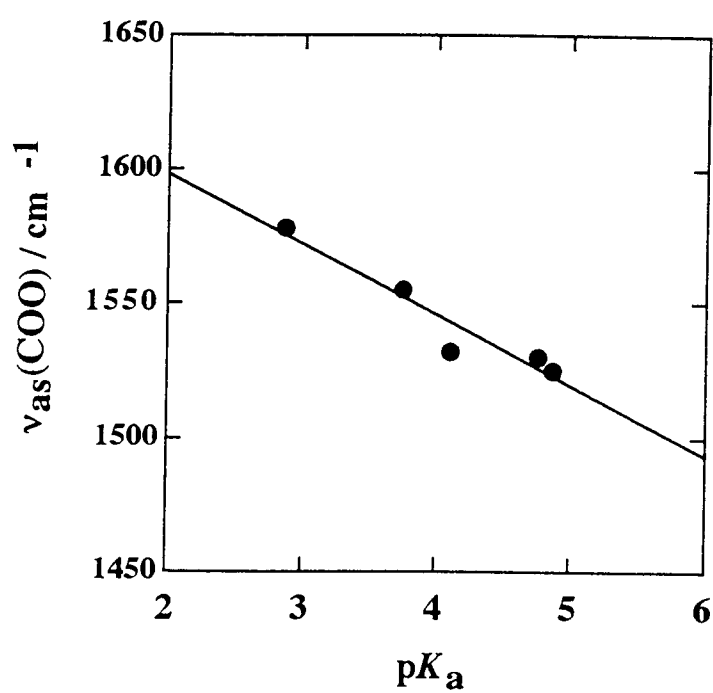
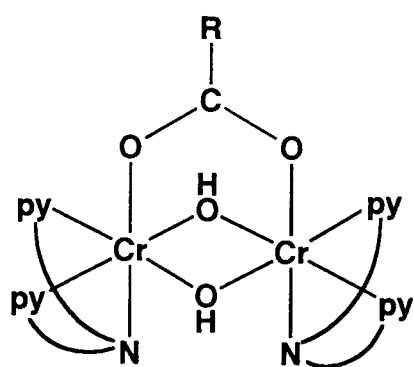
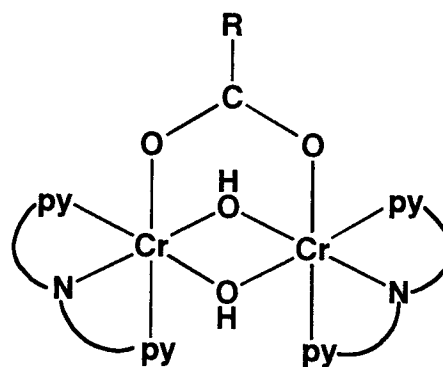


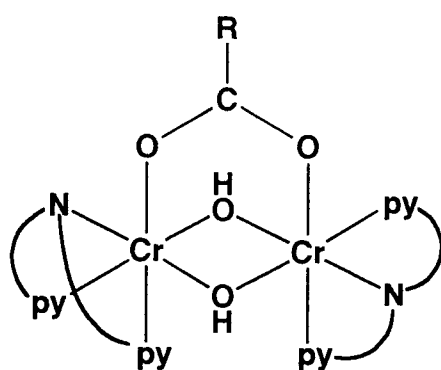
Figure 3-8. Correlation between $\nu_{as}(\text{COO})$ and pK_a values of $[\text{Cr}_2(\text{OH})_2(\text{RCOO})(\text{bispicam})_2]^{3+}$. Line shown is least-squares fit.



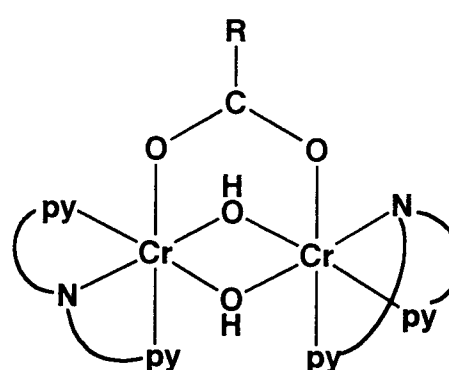
(a)



(b)



(c)



(d)

Figure 3-9. Possible geometrical structures of $[\text{Cr}_2(\text{OH})(\text{RCOO})(\text{bispicam})_2]^{3+}$:
 (a) meso- (C_{2v}) , (b) meso- (C_2) , (c) and (d) the enantiomeric pair.

Table 3-12. ^2H NMR spectral data for $[\text{Cr}_2(\text{OH})_2(\text{RCOO})(\text{bispicam-d}_1)_2]^{3+}$ in H_2O .

Complex	δ (intensity)		$\Delta\delta^a$
	δ_A	δ_B	
$[\text{Cr}_2(\text{OH})_2(\text{HCOO})(\text{bispicam-d}_1)_2]^{3+}$	22.1(4)	-14.3(4)	36.4
$[\text{Cr}_2(\text{OH})_2(\text{CH}_3\text{COO})(\text{bispicam-d}_1)_2]^{3+}$	13.2(4)	-10.1(4)	23.3
$[\text{Cr}_2(\text{OH})_2(\text{CH}_3\text{CH}_2\text{COO})(\text{bispicam-d}_1)_2]^{3+}$	15.5(4)	-12.4(4)	27.9
$[\text{Cr}_2(\text{OH})_2(\text{CH}_2\text{ClCOO})(\text{bispicam-d}_1)_2]^{3+}$	26.0(4)	-12.5(4)	38.5
$[\text{Cr}_2(\text{OH})_2(\text{CH}_2\text{ClCH}_2\text{COO})(\text{bispicam-d}_1)_2]^{3+}$	20.7(4)	-12.8(4)	33.5
$[\text{Cr}_2(\text{OH})_2(\text{H}_3\text{NCH}_2\text{COO})(\text{bispicam-d}_1)_2]^{3+}$	14.8(4)	-10.5(4)	25.3
$[\text{Cr}_2(\text{OH})_2(\text{H}_3\text{NCH}_2\text{CH}_2\text{COO})(\text{bispicam-d}_1)_2]^{3+}$	13.9(4)	-11.3(4)	25.2
$[\text{Cr}_2(\text{OH})_2(\text{H}_3\text{NCH}_2\text{CH}_2\text{CH}_2\text{COO})(\text{bispicam-d}_1)_2]^{3+}$	15.5(4)	-12.4(4)	27.9
$[\text{Cr}_2(\text{OH})_2(\text{H}_3\text{NCH}(\text{CH}_3)\text{COO})(\text{bispicam-d}_1)_2]^{3+}$	15.7(4)	-12.4(4)	27.5
$[\text{Cr}_2(\text{OH})_2(\text{H}_3\text{NCH}(\text{OH})\text{COO})(\text{bispicam-d}_1)_2]^{3+}$	14.8(4)	-12.3(4)	27.1

^a The shift difference. $\Delta\delta = \delta_A - \delta_B$.

3-9).²⁸ In order to establish the geometrical isomers of the present complexes, the deuterium NMR were employed. Since $[\text{Cr}_2(\text{OH})_2(\text{CD}_3\text{COO})(\text{bispicam})_2]^{3+}$ exhibited only one resonance at δ 44.0, it is found that only one isomer exists. When bispicam- d_1 coordinates to the chromium(III) ion as a tridentate, the deuterium atom equivalently exists in the four methylene proton sites in one bispicam ligand. According to Figure 3-9, the ^2H NMR spectra of $[\text{Cr}_2(\text{OH})_2(\text{RCOO})(\text{bispicam-}\text{d}_1)_2]^{3+}$ or $^{4+}$ expect to give two signals in the (a) isomer, four ones in the (b) isomer and four ones in the (c) and (d) isomers. As shown in Table 3-12, all the dinuclear complexes containing bispicam- d_1 gave two signals with the same intensities. This indicates that there is two kinds of unequivalent methylene deuterons. Seeing the whole structures of Figure 3-9, the meso- C_{2v} isomer (a) is only appropriate to the results in ^2H NMR spectra.

ii) Crystal Structure of $[\text{Cr}_2(\text{OH})_2(\text{HCOO})(\text{bispicam})_2](\text{ClO}_4)_3 \cdot 0.5\text{H}_2\text{O}$ (**D-1**). The complex consists of two octahedrally coordinated chromium atoms bridging by two hydroxo and one formate ligands as shown in Figure 3-10. The structure of the complex is the same as expected by the ^2H NMR spectra. The selected bond lengths and angles are listed in Table 3-13. The overall symmetry of the complex cation is close to C_2 and there is a crystallographic mirror plane through O(1), O(2) and C(1). The average Cr-OH bond length is 1.952 Å and falls in the range of the normal Cr-OH bond.^{4, 5, 18, 28, 72, 73} The Cr-N bonds are almost the similar magnitude to the related complexes.^{18, 28} The average CrO(H)Cr angle is 97.7° and slightly smaller than those of the di(μ -OH) chromium(III) dinuclear complexes,⁷² since the two polyhedrons are more attracted by the additional bridging ligand as $[\text{Cr}_2(\text{OH})_2(\text{SO}_4)(\text{bispicam})_2]^{2+}$ ²⁸ and $[\text{Cr}_2(\text{OH})_2(\text{CH}_3\text{COO})(\text{tpen})]^{3+}$.¹⁸ The interplanar angle between CrO_1O_2 and $\text{Cr}'\text{O}_1\text{O}_2$ plane is 27°.

Table 3-14 shows the comparison of selected the structural parameters of the related complexes. The Cr-O(formate) distance is 1.977(3) Å and little longer than that of $[\text{Cr}_2(\mu\text{-OH})(\mu\text{-HCOO})_2(\text{H}_2\text{O})_6]^{3+}$.⁷³ The C-O bond in the formate ligand is slightly shorter than that of $[\text{Cr}_2(\text{OH})_2(\text{CH}_3\text{COO})(\text{tpen})]^{3+}$ complexes.¹⁸ There is no peculiar structural parameters of $[\text{Cr}_2(\text{OH})_2(\text{HCOO})(\text{bispicam})_2]^{3+}$ in comparison with other complexes. The

Table 3-13. Selected bond lengths (Å) and bond angles (deg) for [Cr₂(OH)₂(HCOO)(bispicam)₂](ClO₄)₃·0.5H₂O (**D-1**).

Cr(1)-O(1)	1.957(3)	Cr(1)-O(2)	1.946(3)
Cr(1)-O(3)	1.977(3)	Cr(1)-N(1)	2.066(4)
Cr(1)-N(2)	2.042(4)	Cr(1)-N(3)	2.046(4)
O(3)-C(1)	1.255(4)		
O(1)Cr(1)O(2)	78.5(1)	O(1)Cr(1)O(3)	92.7(1)
O(1)Cr(1)N(1)	94.7(2)	O(1)Cr(1)N(2)	91.3(1)
O(1)Cr(1)N(3)	171.4(2)	O(2)Cr(1)O(3)	92.7(1)
O(2)Cr(1)N(1)	95.2(2)	O(2)Cr(1)N(2)	167.9(1)
O(2)Cr(1)N(3)	93.9(1)	O(3)Cr(1)N(1)	170.1(1)
O(3)Cr(1)N(2)	94.3(1)	O(3)Cr(1)N(3)	91.8(1)
N(1)Cr(1)N(2)	79.0(1)	N(1)Cr(1)N(3)	81.7(1)
N(1)Cr(1)N(3)	95.7(1)	Cr(1)O(1)Cr(1)	97.3(2)
Cr(1)O(2)Cr(1)	98.1(1)	Cr(1)O(3)C(1)	125.7(3)
O(3)C(1)O(3)	128.3(6)		

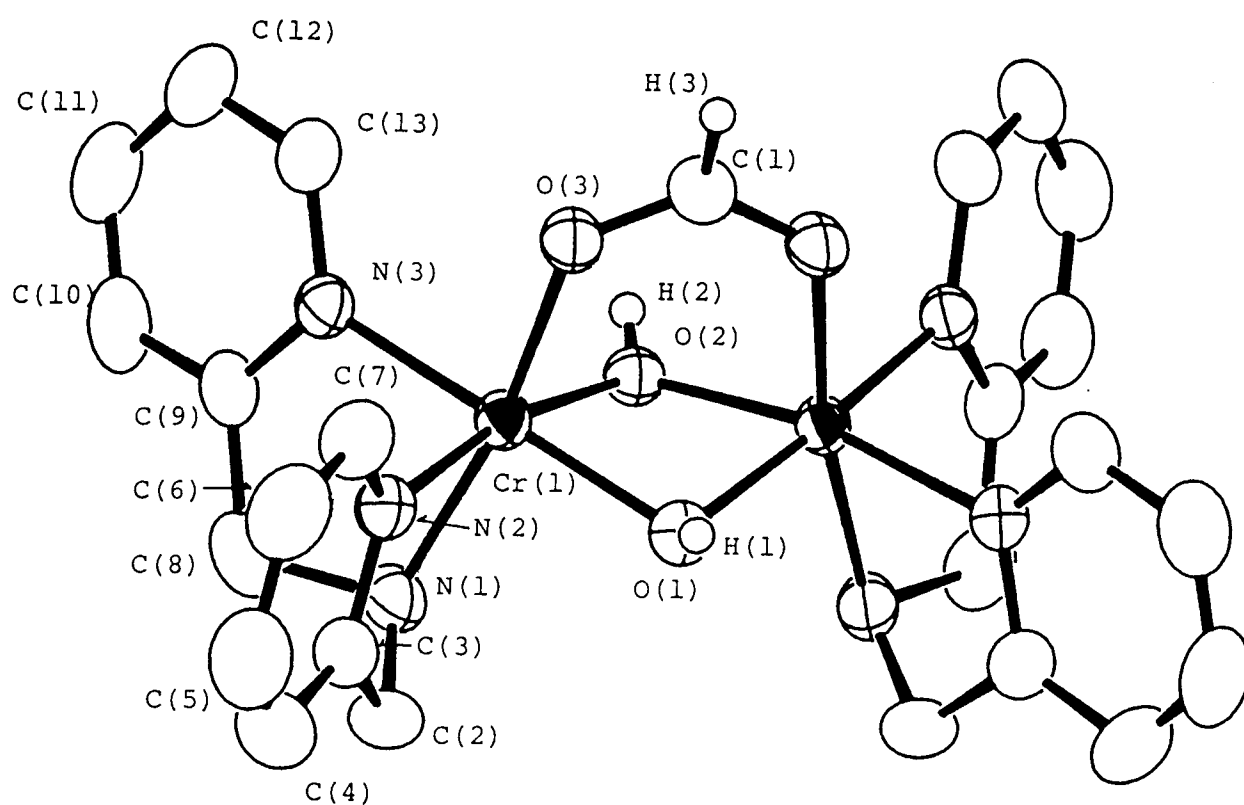


Figure 3-10. An ORTEP drawing of $[\text{Cr}_2(\text{OH})(\text{HCOO})(\text{bispicam})_2]^{3+}$ cation in the crystals of the perchlorate salt (**D-1**) with thermal ellipsoids drawn at the 50 % probability level. Some hydrogen atoms are omitted to clarify.

Table 3-14. Selected bond lengths and angles(deg) for carboxylato bridged complexes.

	Cr-OH	Cr-O	Cr-N(py)	Cr-N(NH)	CrOHCr	OCrO	Cr-Cr
$[\text{Cr}_2(\text{OH})_2(\text{HCOO})(\text{bispicam})_2](\text{ClO}_4)_3 \cdot 0.5\text{H}_2\text{O}^a$	1.952	1.977(3)	2.044	2.066(4)	97.7	78.5(1)	2.939(2)
$[\text{Cr}_2(\text{OH})_2(\text{CH}_3\text{COO})(\text{tpen})](\text{ClO}_4)_3^b$	1.942	1.958	2.030	2.084	93.1	84.6	2.818
$[\text{Cr}_2(\text{OH})_2(\text{SO}_4)(\text{bispicam})_2](\text{S}_2\text{O}_6) \cdot 3\text{H}_2\text{O}^c$	1.947	1.973	2.053	2.065	96.97	80.26	2.9157(6)
$[\text{Cr}_2(\text{OH})(\text{HCOO})_2(\text{H}_2\text{O})_6](\text{pts})_3 \cdot 2\text{H}_2\text{O}^{d,e}$	1.920	1.959	—	—	123.4(2)	—	3.381(1)

^a This work. ^b Reference 18. ^c Reference 28. ^d Reference 73. ^e pts means *p*-toruenesulfonate ion.

Cr-N(H) bond in the complex **D-1** is little shorter than that of $[\text{Cr}_2(\text{OH})_2(\text{CH}_3\text{COO})(\text{tpen})]^{3+}$.

Though the two methylene moieties are inequivalent in the crystal because of the torsion angles of $41.7(4)^\circ$ and $19.1(5)^\circ$ in the $\text{CrN}_1\text{C}_2\text{C}_3$ and $\text{CrN}_1\text{C}_8\text{C}_9$, respectively, the $[\text{Cr}_2(\text{OH})_2(\text{RCOO})(\text{bispicam-d}_1)_2]^{3+ \text{ or } 4+}$ exhibited two signals with equivalent intensities in ^2H NMR. This means the torsion angles of Cr-N-C-C are averaged and two methylene rings are equivalent in the bispicam ligand in solution.

The hydrogen atoms in the bridging hydroxo groups are involved in hydrogen bonds to two perchlorate ions. The O-O distances are $\text{O}(1)(\text{OH}) \cdots \text{O}(12)(\text{ClO}_4) = 2.877(7) \text{ \AA}$ and $\text{O}(2)(\text{OH}) \cdots \text{O}(31)(\text{ClO}_4) = 2.798(7) \text{ \AA}$. The average angle (θ) between O-O line of hydroxo bridged oxygen atoms and hydrogen atoms is 25.8° .

iii) Absorption Spectra. The absorption and CD spectral data in the visible region are summarized in Table 3-15. Figure 3-11 shows the absorption spectrum of $[\text{Cr}_2(\text{OH})_2(\text{HCOO})(\text{bispicam})_2]^{3+}$ in 1mM HClO_4 solution. The first-absorption band maxima of $[\text{Cr}_2(\text{OH})_2(\text{RCOO})(\text{bispicam})_2]^{3+ \text{ or } 4+}$ is at *ca.* 510 nm. This value is slightly red-shifted from that of the $[\text{Cr}_2(\text{OH})_2(\text{CH}_3\text{COO})(\text{tpen})]^{3+}$ (500 nm).¹⁸ Since the $[\text{Cr}_2(\text{OH})_2(\text{CH}_3\text{COO})(\text{tpen})]^{3+}$ is strained by the ethylene chain which connects the two bispicam ligand, the ligand field is changed slightly. Compared with the $[\text{Cr}_2(\text{OH})_2(\text{SO}_4)(\text{bispicam})]^{2+}$ (533 nm),²⁸ the first absorption band maxima of $[\text{Cr}_2(\text{OH})_2(\text{RCOO})(\text{bispicam})_2]^{3+ \text{ or } 4+}$ is blue shifted. This is due to the difference of the ligand field strength between the sulfato and carboxylato ligands.

iv) Acid strength of bridging aminoacid ligands. The acid dissociation constants of the μ -amino acid complexes were determined potentiometrically on 5 mM aqueous solutions in 0.1 M NaClO_4 at 25°C . In contrast to $[\text{Cr}_2(\text{OH})(\text{glyH})(\text{en})_4]^{5+}$ which occurs a carboxylato bridge cleavage reaction, the present μ -aminoacid complexes are so stable that a normal titration method can be employed. This relatively robustness of the present complexes in the slightly basic solution would be related to the bridging structures of $[\text{Cr}(\text{OH})_2(\text{RCOO})\text{Cr}]$

compared to that of $[\text{Cr}(\text{OH})(\text{RCOO})\text{Cr}]$. The obtained acid strengths are summarized in Table 3-16. The $\text{p}K_a$ value of $[\text{Cr}_2(\text{OH})_2(\text{glyH})(\text{bispicam})_2]^{4+}$ is comparable to that of $[\text{Cr}_2(\text{OH})(\text{glyH})(\text{en})_4]^{5+}$ ($\text{p}K_a = 7.5$). As Springborg and Toftlund claimed,⁴⁵ it is considered that these increased acid strength in the dinuclear complexes is due to the coordination to the two metal centers. The acid strengths for $-\text{NH}_3$ group in the β - and γ -amino acid are found to be weaker than that in the α -amino acid. This tendency is the same as acid strengths in the free amino acid $\text{NH}_2(\text{CH}_2)_n\text{COOH}$. The acid strength of the bridging amino acid in the dinuclear complexes is affected by the properties in the free amino acid.

Table 3-15. Visible absorption spectral data for $[\text{Cr}_2(\text{OH})_2(\text{RCOO})(\text{bispicam})_2]^{3+}$ in 1mM HClO_4 solution.

Complex	Absorption maxima			
	λ / nm	ϵ / $\text{mol}^{-1} \text{dm}^3 \text{cm}^{-1}$	λ / nm	ϵ / $\text{mol}^{-1} \text{dm}^3 \text{cm}^{-1}$
$[\text{Cr}_2(\text{OH})_2(\text{HCOO})(\text{bispicam})_2]^{3+}$	674(3.1)	512(71)	384(82)	345sh(55)
$[\text{Cr}_2(\text{OH})_2(\text{CH}_3\text{COO})(\text{bispicam})_2]^{3+}$	672(4.4)	510(83)	384(99)	345sh(55)
$[\text{Cr}_2(\text{OH})_2(\text{CH}_3\text{CH}_2\text{COO})(\text{bispicam})_2]^{3+}$	675(4.5)	510(82)	383(93)	345sh(65)
$[\text{Cr}_2(\text{OH})_2(\text{CH}_2\text{ClCOO})(\text{bispicam})_2]^{3+}$	675(4.3)	511(85)	384(97)	345sh(75)
$[\text{Cr}_2(\text{OH})_2(\text{CH}_2\text{ClCH}_2\text{COO})(\text{bispicam})_2]^{3+}$	675(3.5)	510(81)	384(89)	345sh(70)
$[\text{Cr}_2(\text{OH})_2(\text{H}_3\text{NCH}_2\text{COO})(\text{bispicam})_2]^{3+}$	673(3.2)	512(80)	384(80)	345sh(60)
$[\text{Cr}_2(\text{OH})_2(\text{H}_3\text{NCH}_2\text{CH}_2\text{COO})(\text{bispicam})_2]^{3+}$	676(4.5)	512(84)	384(91)	345sh(65)
$[\text{Cr}_2(\text{OH})_2(\text{H}_3\text{NCH}_2\text{CH}_2\text{CH}_2\text{COO})(\text{bispicam})_2]^{3+}$	675(3.3)	511(77)	384(84)	345sh(60)
$[\text{Cr}_2(\text{OH})_2(\text{H}_3\text{NCH}(\text{CH}_3)\text{COO})(\text{bispicam})_2]^{3+a}$	673(2.5)	512(83)	382(87)	345sh(70)
$[\text{Cr}_2(\text{OH})_2(\text{H}_3\text{NCH}(\text{OH})\text{COO})(\text{bispicam})_2]^{3+b}$	673(3.4)	513(80)	383(79)	345sh(60)

^a L-ala CD maxima (λ / nm ($\Delta\epsilon$ / $\text{mol}^{-1} \text{dm}^3 \text{cm}^{-1}$)) 512(-0.103).

^b L-ser CD maxima (λ / nm ($\Delta\epsilon$ / $\text{mol}^{-1} \text{dm}^3 \text{cm}^{-1}$)) 525(-0.211) 430(0.012).

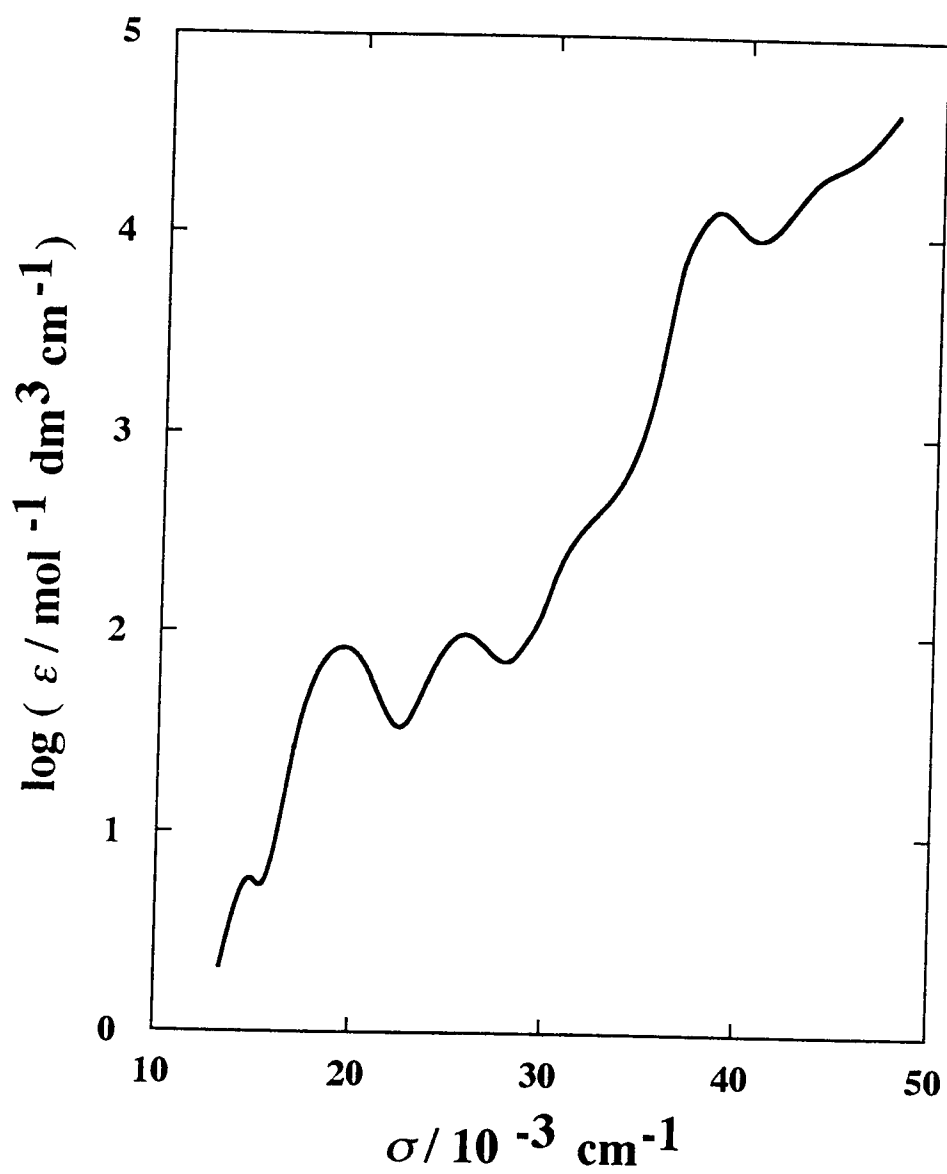


Figure 3-11. Absorption spectrum of $[\text{Cr}_2(\text{OH})_2(\text{HCOO})(\text{bispicam})_2]^{3+}$ in 1mM HClO_4 solution.

Table 3-16. Acid strengths of bridging amino acid for $[\text{Cr}_2(\text{OH})_2(\text{RCOO})(\text{bispicam})_2]^{3+ \text{ a}}$.

Complex	$\text{pK}_a^{\text{ b}}$
$[\text{Cr}_2(\text{OH})_2(\text{H}_3\text{NCH}_2\text{COO})(\text{bispicam})_2]^{3+}$	7.60
$[\text{Cr}_2(\text{OH})_2(\text{H}_3\text{NCH}_2\text{CH}_2\text{COO})(\text{bispicam})_2]^{3+}$	9.22
$[\text{Cr}_2(\text{OH})_2(\text{H}_3\text{NCH}_2\text{CH}_2\text{CH}_2\text{COO})(\text{bispicam})_2]^{3+}$	9.42
$[\text{Cr}_2(\text{OH})_2(\text{H}_3\text{NCH}(\text{CH}_3)\text{COO})(\text{bispicam})_2]^{3+}$	7.51
$[\text{Cr}_2(\text{OH})_2(\text{H}_3\text{NCH}(\text{OH})\text{COO})(\text{bispicam})_2]^{3+}$	7.49

^a At 25°C and ionic strength $I = 1.0$ (NaClO_4). ^b Uncertainty is estimated ± 0.05 pK_a unit.

4. Stereochemistry and Paramagnetic Influence on the Multinuclear NMR Spectra of the Chromium(III)-Cobalt(III) and Chromium(III)-Chromium(III) Dinuclear Complexes

4.1 Introduction

Although chromium(III) complexes with various organic ligands have attracted attention, their structural characterization in the solution has been hampered by the inability to employ NMR spectroscopy owing to their paramagnetic properties. Recently, the ^2H NMR spectra of paramagnetic chromium(III) complexes with various kinds of deuteriated ligands have been found to be useful in the study of stereochemistry and electronic properties.⁷⁴ However, there has been no systematic study about dinuclear complexes using ^2H NMR. It is expected that the application of ^2H NMR for the chromium(III) dinuclear complexes would make us to obtain the valuable information of characteristics of the dinuclear complexes. However, the ^2H NMR study often suffers from the tedious and expensive deuteriation of the ligands, since the natural abundance of ^2H is only $1.5 \times 10^{-2}\%$. Nitrogen-14 and cobalt-59 NMR of the chromium(III)-cobalt(III) ($[\text{Cr(III)-Co(III)}]$) and chromium(III)-chromium(III) ($[\text{Cr(III)-Cr(III)}]$) dinuclear complexes which were synthesized in this study is expected to give more straightforward and valuable information since the natural abundance of ^{14}N and ^{59}Co are 99.63% and 100%, respectively.

In this chapter, the applications of the multinuclear NMR to the above mentioned dinuclear complexes were described. The stereochemistry and coordinate bond character of the ligands in the dinuclear complexes were elucidated on the basis of the ^2H NMR spectra. At the same time, the influences of the paramagnetic unpaired electrons in the chromium(III) ion on the multinuclear NMR spectra for the $[(\text{nta})\text{Cr}(\text{OH})_2\text{M}(\text{N})_4]^+$ ($\text{M} = \text{Co}^{3+}$ and Cr^{3+}) were examined in comparison with those related diamagnetic compounds.

4.2 Experimental

4.2.1 Preparation of compounds

i) Deuteriated nitrilotriacetic acid ($\text{H}_3\text{nta-d}_6$). The deuteriation was carried out by the method

reported by Koine *et al.*.³¹

ii) Deuteriated bipyridine (bpy-d₈). The deuteration of bpy was carried out by slightly modified reported method.⁷⁵

iii) Preparation of other complexes. The complexes [Cr(nta)(H₂O)₂],⁵⁷ [Co₂(OH)₂(en)₄]Br₄·nH₂O,⁶⁷ [(nta)Co(OH)₂Co(en)₂]Cl·nH₂O⁵² and [(H₂O)₂M^{II}{(μ-OH)₂Co^{III}(en)₂}₂](ClO₄)₄ (M^{II} = Ni, Co and Zn)⁷⁶ were obtained by the literature methods. *cis*-[Co(N)₄(H₂O)₂]³⁺ and *cis*-[Co(N)₄(OH)₂]⁺ (N)₄ = (en)₂, (tn)₂, (bpy)₂ and (phen)₂ were obtained from decomposition of the corresponding carboxylato complexes by acid^{33,34,35} and adjusted to appropriate pH in the solution.

4.2.2 Measurements.

¹H, ²H, ⁵⁹Co NMR spectra were measured using a JEOL GSX-270 and/or EX-270 FT NMR spectrometer. Nitrogen-14 NMR spectra were recorded using a JEOL GX-500 FT NMR spectrometer. The external standards used were TSP[δ(¹H) = 0], C²HCl₃ [δ(²H) = 7.24], Na¹⁴NO₃ [δ(¹⁴N) = 0] and [Co(NH₃)₆]Cl₃ [δ(⁵⁹Co) = 8100], with the downfield shift defined as positive.

4.3 Results and Discussion

4.3.1 ¹H NMR Spectra

The ¹H NMR spectra of *cis*-[Co(bpy)₂(H₂O)₂]³⁺ in D₂O revealed coupled signals from δ 7.3 to 9.4. They are assigned to the bpy aromatic protons (Figure 4-1b). To this solution (concentration of the complex = 0.05 M) was added [Cr(nta)(H₂O)₂] with various concentrations (0.005, 0.01, 0.02 and 0.05 M). The linewidths of each signal increased and the coupled signals became simple with increasing concentration of [Cr(nta)(H₂O)₂] as shown in Figure 4-1b ~ e. Their chemical shifts, however, did not change. The similar NMR behavior was reported for the ¹H NMR spectra of the ion paired [Co^{III}(phen)₂Cl₂]₂[Co^{II}Cl₄]·2H₂O with ⁴A₂ ground state for Co²⁺ similar to Cr³⁺ ground state in dmso solution,⁴⁴ where pronounced line-broadening effect and small change of the chemical shifts was also observed on going from the more dilute to the more concentrated

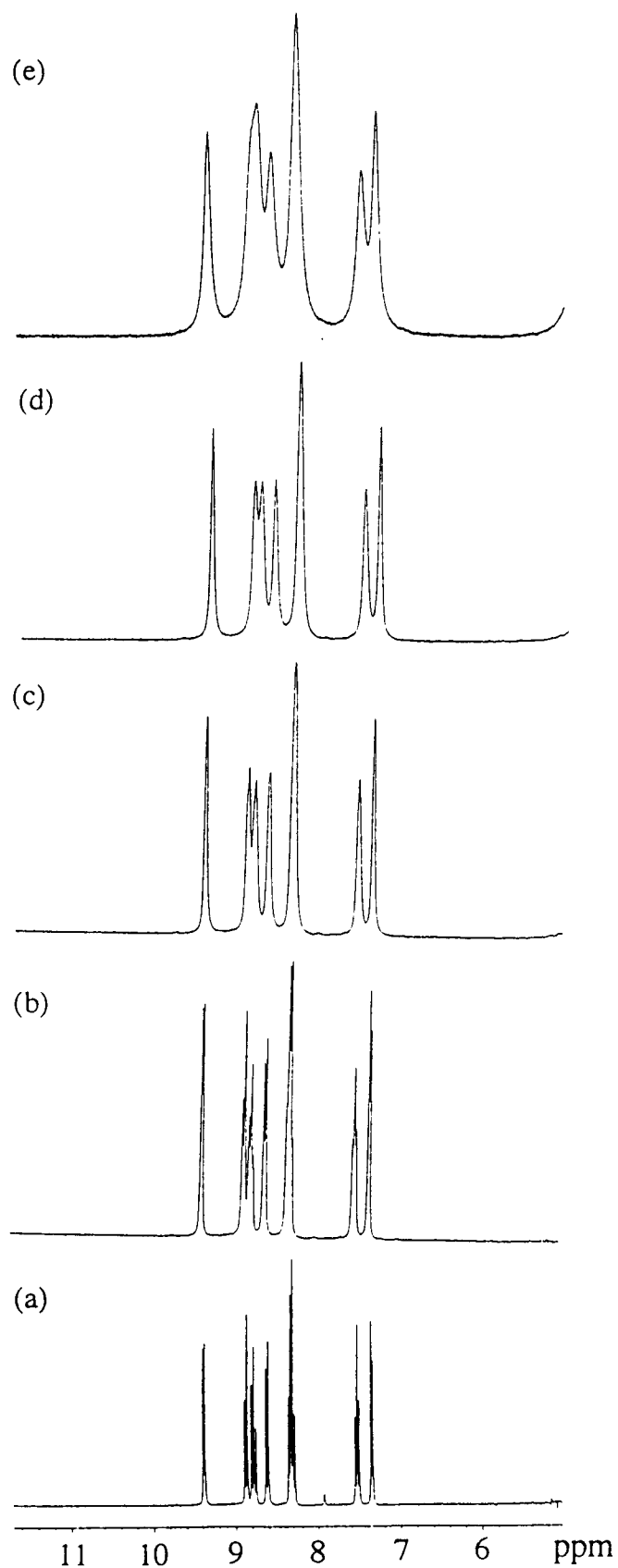


Figure 4-1. ^1H NMR spectra of $\text{cis-}[\text{Co}(\text{bpy})_2(\text{H}_2\text{O})_2]^{3+}$ in D_2O :
 (a) before adding $[\text{Cr}(\text{nta})(\text{H}_2\text{O})_2]$, after adding $[\text{Cr}(\text{nta})(\text{H}_2\text{O})_2]$ (b) 0.005 M,
 (c) 0.01 M, (d) 0.02 M and (e) 0.05 M.

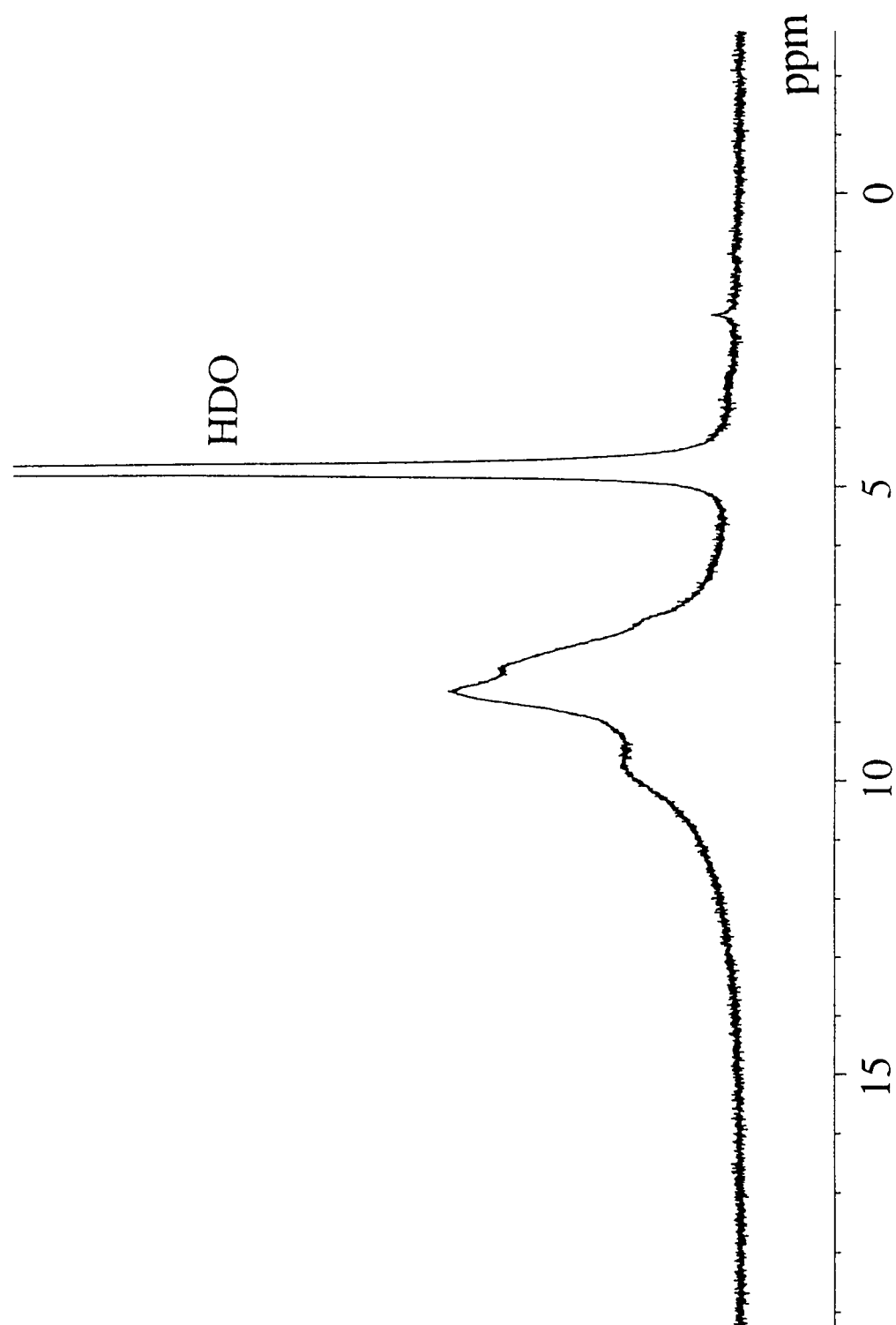


Figure 4-2. ^1H NMR spectra of $[(\text{nta})\text{Cr}(\text{OH})_2\text{Co}(\text{bpy})_2]^+$ in D_2O .

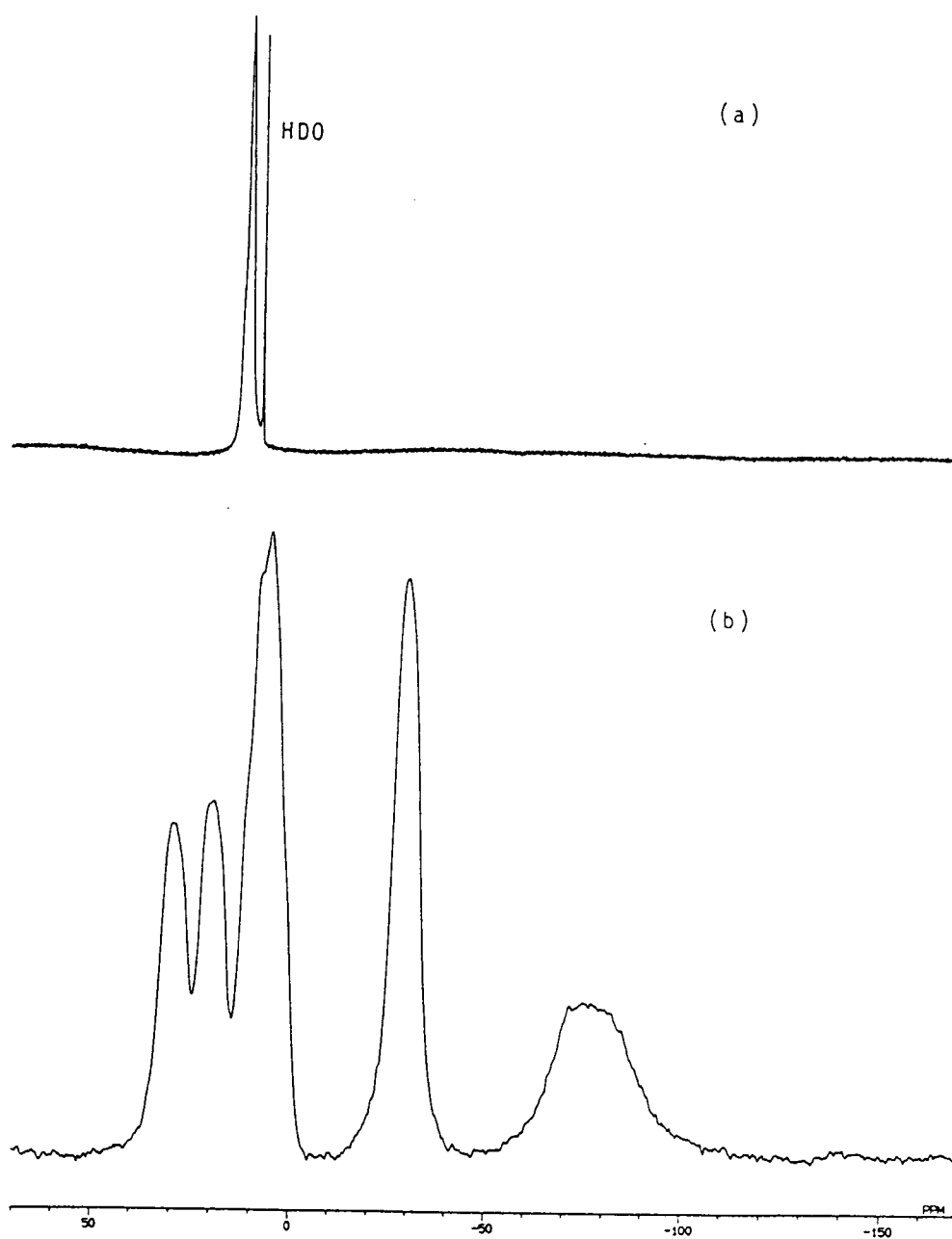


Figure 4-3. ^2H NMR spectra of $[(\text{nta})\text{Cr}(\text{OH})_2\text{Co}(\text{bpy}-\text{d}_8)_2]^+$ (a) and $[(\text{nta})\text{Cr}(\text{OH})_2\text{Cr}(\text{bpy}-\text{d}_8)_2]^+$ (b) in H_2O .

solution. In aqueous solution at the pH *ca.* 7, the coordinated H₂O ligand in *cis*-[Co(bpy)₂(H₂O)₂]³⁺ and [Cr(nta)(H₂O)₂] would deprotonate, and they become *cis*-[Co(bpy)₂(OH)(H₂O)]²⁺ and [Cr(nta)(OH)(H₂O)]⁻ as described in Chapter 3. They would assemble and form the ion pair by the electrostatic attractive force as shown in Fig 3-1. In such ion pairs, the isotropic hyperfine interaction constant (Fermi contact term) is small and the dipolar interaction with the unpaired electrons is effective.⁷⁸ The increased linewidths are due to the dipolar relaxation of unpaired electrons of [Cr(nta)(OH)(H₂O)]⁻ moiety. The unchanged chemical shifts would be due to the small dipolar interaction ($\delta^{\text{iso}} = \delta^{\text{con}} + \delta^{\text{dip}}$, δ^{con} and $\delta^{\text{dip}} \sim 0$, then $\delta^{\text{iso}} \sim 0$ where δ^{iso} , δ^{con} and δ^{dip} are the observed isotropic shift, contact interaction and dipolar interaction, respectively). The influence of the paramagnetic unpaired electrons through the hydrogen bond is relatively small in this ion pair, since the paramagnetic ion center is relatively far from Co³⁺ ion.

On the other hand, [(nta)Cr(OH)₂Co(bpy)₂]⁺ revealed very broad resonances different from those of *cis*-[Co(bpy)₂(H₂O)₂]³⁺ from δ 8 to 10 (Figure 4-2). The NMR spectra were independent in the concentration of complex (from 0.005 to 0.05 M, not shown here). Since the ²H NMR spectra of deuteriated [(nta)Cr(OH)₂Co(bpy-d₈)₂]⁺ exhibited the signals in the same range of ¹H NMR spectra as shown in Figure 4-3a, all the bpy protons would resonant in these region. Since this complex has a rigid dinuclear structure bridged by the hydroxo ions, the proton nuclei in [(nta)Cr(OH)₂Co(bpy)₂]⁺ were more affected by the unpaired electrons in (nta)Cr^{III} moiety through the bridging OH than those in the ion pair of *cis*-[Co(bpy)₂(OH)(H₂O)]²⁺ and [Cr(nta)(OH)(H₂O)]⁻ via the hydrogen bonds. The very broad resonances would be due to the dipolar and contact relaxation. The isotropic shifts, however, were relatively small in spite of the very broad resonance. ²H NMR spectra of [(nta)Cr(OH)₂Cr(bpy-d₈)₂]⁺ exhibited large contact shifts as shown in Figure 4-3b. It is found that the deuteron nuclei of the ligand which coordinates directly to the paramagnetic chromium(III) ion are more affected by the paramagnetic unpaired electrons than those which do not coordinate directly to the paramagnetic center. The influence of the paramagnetic unpaired electrons through the OH bridging ligands is not so large.

4.3.2 ^2H NMR spectra and stereochemistry

The ^2H NMR spectra of $[(\text{nta-d}_6)\text{Cr}(\text{OH})_2\text{M}(\text{N})_4]^+$ ($\text{M} = \text{Co}$ and Co) were measured and their data were summarized in Table 4-1. The ^2H NMR spectra of the $[\text{Cr}(\text{III})\text{-Co}(\text{III})]$ and $[\text{Cr}(\text{III})\text{-Cr}(\text{III})]$ complexes are observed with large contact shifts. On the basis of the signal assignment made as for the previously reported $\text{Cr-nta}^{31,55}$ and $[\text{Cr}(\text{edta})]^-$ type complexes,^{74b} it appears that the tetradentate nta^{3-} ligand has two acetate chelate rings (G-rings) with chemically inequivalent methylene deuterons and acetate chelate ring (R-ring) with the equivalent deuterons^{31,55} as shown in Figure 4-4. The signals from δ -4.4 to -10.6 and from δ -27.2 to -34.6 are assigned to the inequivalent methylene deuterons in the G-rings, and those from δ -9.1 to -23.6 to the equivalent methylene ones in the R-ring. Table 4-1 shows the spectral data with assignment. The complexes with the aliphatic diamines (**A-1, 2, 3, 4, 5, B-1, 2, 3, 4 and 5**) show the similar spectral patterns to each other and to the reported Cr-nta complexes.^{31,55} Since the $[\text{Cr}(\text{III})\text{-Cr}(\text{III})]$ complexes gave the similar spectral patterns to the corresponding $[\text{Cr}(\text{III})\text{-Co}(\text{III})]$ ones with variation of diamine ligands, the ^2H NMR spectra would be influenced by the $(\text{N})_4$ ligands and insignificantly by the metal ion M in the $\text{M}(\text{N})_4$ moieties. Figure 4-5 shows ^2H NMR spectra of three $[\text{Cr}(\text{III})\text{-Cr}(\text{III})]$ complexes.

The isotropic contact shifts for the deuteriated acetate methylenes in the edta-like hexadentate coordinated chromium(III) mononuclear complexes were related to the glycinate chelate ring conformation between the chemical shifts and the torsion angles in the Cr-N-C-C(O) fragment of the acetato(glycinato) rings according to a Karpuls-like or $\cos^2\theta$ relation^{74b} as shown in Figure 4-6. The $\cos^2\theta$ relation gives equations (1) and (2) for the A(axial) and B(equatorial) vicinal deuterons as shown in Figure 4-6. The difference between their NMR shifts is expressed as in equation (3), where the angles α are defined as shown in Figure 4-6 (taking positive sign for clockwise rotation) and C is a constant including the spin density.

$$\delta_A = C \cos^2\theta \quad (1)$$

$$\delta_B = C \cos^2(\theta + 120^\circ) \quad (2)$$

$$\Delta\delta_{A,B} = \delta_A - \delta_B = (-\sqrt{3}/2)C \sin(2\alpha) \quad (3)$$

Table 4-1. ^2H NMR chemical shifts for $[(\text{nta-d}_6)\text{Cr}(\text{OH})_2\text{M}(\text{N})_4]^{+}$ complexes in H_2O solutions.

Complex	No.	δ (degeneracy)		$\Delta\delta_{\text{A,B}}(\text{G-ring})^{\text{a}}$
		R-ring	G-ring	
$[(\text{nta-d}_6)\text{Cr}(\text{OH})_2\text{Co}(\text{NH}_3)_4]^{+}$	A-1	-10.6(2) ^b	-10.6(2) ^b	24.0
$[(\text{nta-d}_6)\text{Cr}(\text{OH})_2\text{Co}(\text{en})_2]^{+}$	A-2	-9.1(2) ^b	-9.1(2) ^b	24.6
$[(\text{nta-d}_6)\text{Cr}(\text{OH})_2\text{Co}(\text{tn})_2]^{+}$	A-3	-12.5(2)	-9.0(2)	24.5
$[(\text{nta-d}_6)\text{Cr}(\text{OH})_2\text{Co}\{(R,R)\text{chxn}\}_2]^{+}$	A-4	-12.5(2)	-5.6(2)	27.8
$[(\text{nta-d}_6)\text{Cr}(\text{OH})_2\text{Co}(\text{trien})_2]^{+}$	A-5	-10.4(2)	-4.4(2)	29.0
$[(\text{nta-d}_6)\text{Cr}(\text{OH})_2\text{Co}(\text{picam})_2]^{+}$	A-6	-15.6(2)	-4.0(1)	27.7
$[(\text{nta-d}_6)\text{Cr}(\text{OH})_2\text{Co}(\text{bpy})_2]^{+}$	A-7	-23.6(2)	-6.0(1)	22.1
$[(\text{nta-d}_6)\text{Cr}(\text{OH})_2\text{Co}(\text{phen})_2]^{+}$	A-8	-23.6(2)	-7.8(1)	18.5
$[(\text{nta-d}_6)\text{Cr}(\text{O})(\text{OH})\text{Co}(\text{phen})_2]$	A-8^c	-23.0(2)	-9.0(1)	17.0
$[(\text{nta-d}_6)\text{Cr}(\text{OH})_2\text{Cr}(\text{NH}_3)_4]^{+}$	B-1	-10.1(2) ^b	-10.1(2) ^b	18.7
$[(\text{nta-d}_6)\text{Cr}(\text{OH})_2\text{Cr}(\text{en})_2]^{+}$	B-2	-9.4(2)	-6.0(2)	21.2
$[(\text{nta-d}_6)\text{Cr}(\text{OH})_2\text{Cr}(\text{tn})_2]^{+}$	B-3	-10.3(2)	-7.0(2)	17.3
$[(\text{nta-d}_6)\text{Cr}(\text{OH})_2\text{Cr}\{(R,R)\text{chxn}\}_2]^{+}$	B-4	-12.7(2)	-7.7(2)	20.4
$[(\text{nta-d}_6)\text{Cr}(\text{OH})_2\text{Cr}(\text{trien})_2]^{+}$	B-5	-10.2(2) ^b	-10.2(2) ^b	21.7
$[(\text{nta-d}_6)\text{Cr}(\text{OH})_2\text{Cr}(\text{picam})_2]^{+}$	B-6	-14.0(2)	-4.0(1)	22.8
$[(\text{nta-d}_6)\text{Cr}(\text{OH})_2\text{Cr}(\text{bpy})_2]^{+}$	B-7	-17.9(2)	-5.2(1)	17.5
$[(\text{nta-d}_6)\text{Cr}(\text{OH})_2\text{Cr}(\text{phen})_2]^{+}$	B-8	-18.1(2)	-7.5(1)	16.5
$[(\text{nta-d}_6)\text{Cr}(\text{O})(\text{OH})\text{Cr}(\text{phen})_2]$	B-8^c	-18.0(1)	-8.1(1)	13.8

^a $\Delta\delta_{\text{A,B}} = \delta_{\text{A}} - \delta_{\text{B}}$; see text. ^b Degenerated signals. ^c In the $\text{NH}_4\text{Cl-NH}_3$ buffered solution.

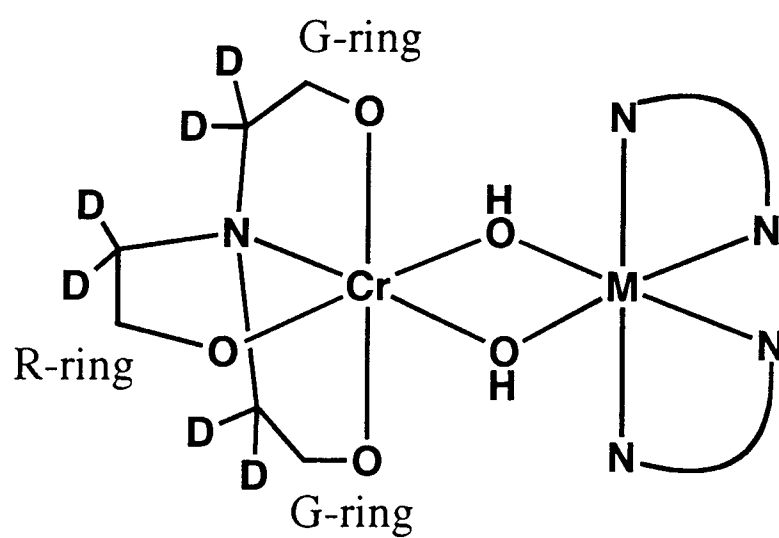


Figure 4-4. The description of the G- and R-ring in the tetradentate nta ligand in $[(\text{nta})\text{Cr}(\text{OH})_2\text{M}(\text{N})_4]^+$.

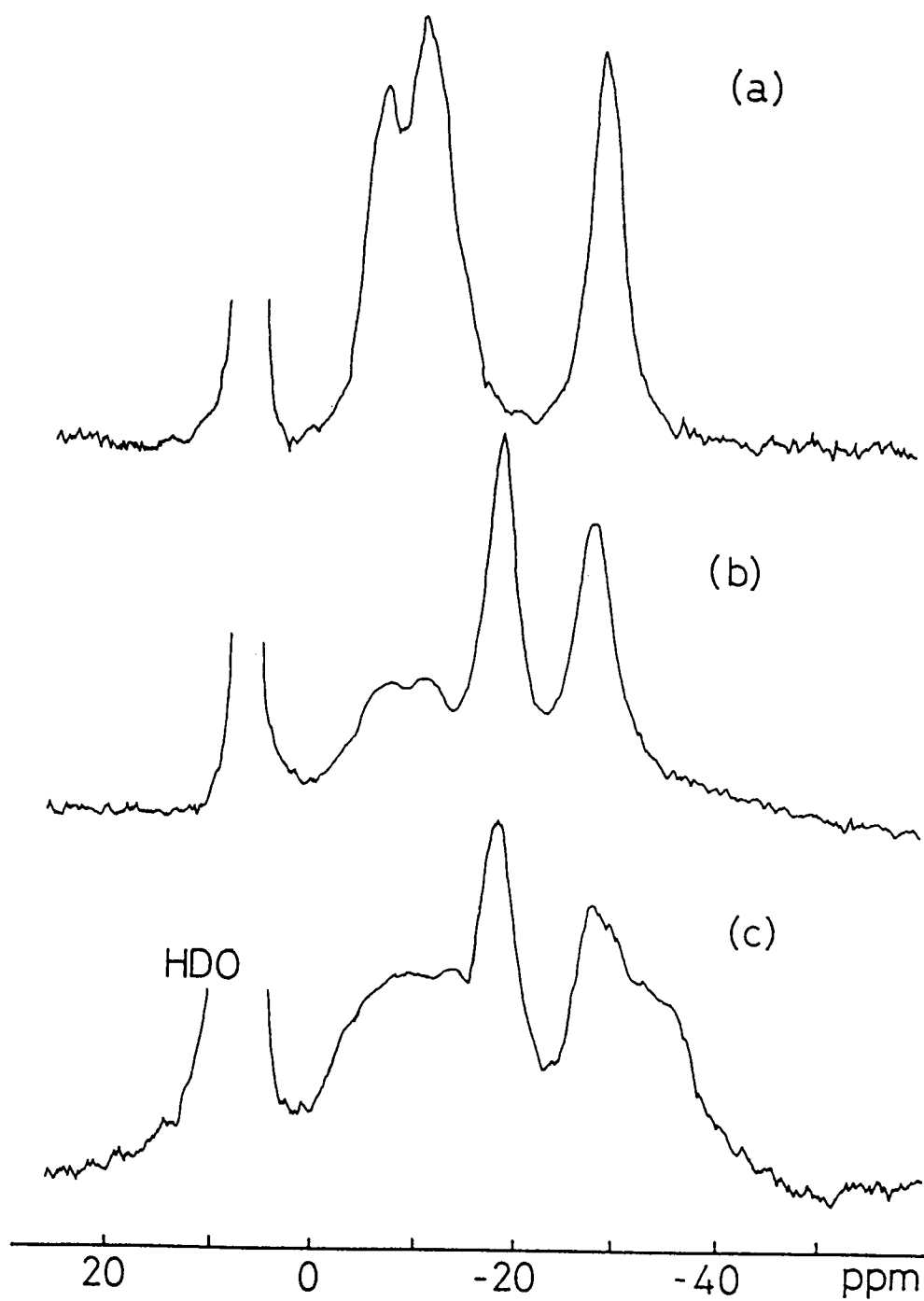


Figure 4-5. ^2H NMR spectra of $[(\text{nta-d}_6)\text{Cr}(\text{OH})_2\text{Cr}(\text{N})_4]^+$:
 (a) $(\text{N})_4 = (\text{en})_2$, (b) $(\text{N})_4 = (\text{phen})_2$ and (c) $[(\text{nta-d}_6)\text{Cr}(\text{O})(\text{OH})\text{Cr}(\text{phen})_2]$.

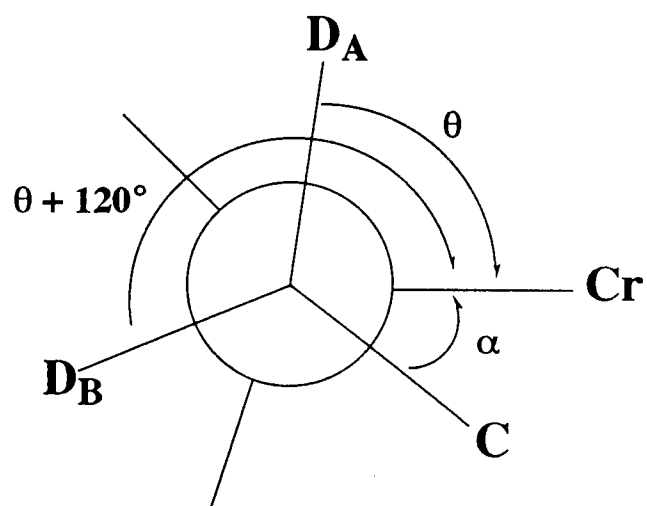


Figure 4-6. Dihedral angles for Cr-N-C-D_{A(axial)} (θ), Cr-N-C-D_{B(equatorial)} ($\theta+120^\circ$) and Cr-N-C-C(O) chains exemplifying the δ conformation with a negative α angle.

Table 4-2 shows the dihedral angles and sum of angles for the nta chelate rings for the dinuclear complexes **A-3**, **B-3** and **8**. Though the separation of the signals of the G-ring is expected for three complexes because of the inequivalent torsion angles α as described in the reference 74b, the signals of the G-rings for complexes **A-3** and **B-3** did not separate. It is likely that the nta chelate conformation of the G-rings are not frozen, but take an averaged conformation in the solution. The hydrogen bonds between the tn and nta ligands seem not to retain the nta chelate rings in solution.

On the other hand, the complexes with pyridine rings (**A-6**, **7**, **8**, **B-6**, **7** and **8**) show different spectral patterns. Figure 4-7 is a schematic representation of the ^2H NMR chemical shifts. At the lowest field, two signals due to the deuterons in the G-ring appeared with equivalent intensities from δ -4.0 to -14.0 (Figure 4-5b, 4-7c \sim e and 4-7i \sim k). This separation of the signals for the deuterons in the G-ring is caused by the inequivalency of two G-rings. This suggests that the G-ring chelate conformation is frozen in these complexes in solution. The frozen conformations in the solution is considered to result from the non-bonding interactions between the nta ligand and heteroaromatic rings. In the complex **B-8**, there are differences in the distances and angles between the oxygen atoms of the two G-rings and hydrogen atoms of phen ligands ($\text{C-H} \cdots \text{O}$) as shown in Table 4-3. These nonbonding interactions retain inequivalent G-rings in the solution. That is, implication of such nonbonding interactions between nonbridging ligands are claimed in the stereoselective formation of Δ, Δ - and Λ, Λ - $[\text{Cr}_2(\text{OH})_2(\text{phen or bpy})_4]^{4+}$ complexes.⁷⁸ Moreover, in the $[(\text{nta})\text{Cr}(\mu\text{-O})(\mu\text{-OH})\text{Cr}(\text{phen})_2]$ complexes of which the bridging unit is altered by deprotonated bridging oxo ligand as described in Chapter 3 (the Cr-O bond becomes shorter), since the nonbonding interaction would be more pronounced, the highest field signal is separated from δ -28.0 to -34.0 as shown in Figures 4-5c and 4-7l. The $[(\text{nta})\text{Cr}(\mu\text{-O})(\mu\text{-OH})\text{Co}(\text{phen})_2]$ complex also reveals the same spectral pattern as shown in Table 4-1.

The average torsion angles α of the two G-rings are 34.2° and 33.6° and $\sin(2\alpha)$ gives 0.929 and 0.922 for **A-3** and **B-3**, respectively. There is a small difference in the $\sin(2\alpha)$ values. Therefore the shift difference between **A-3** and **B-3** of the G-rings result from the

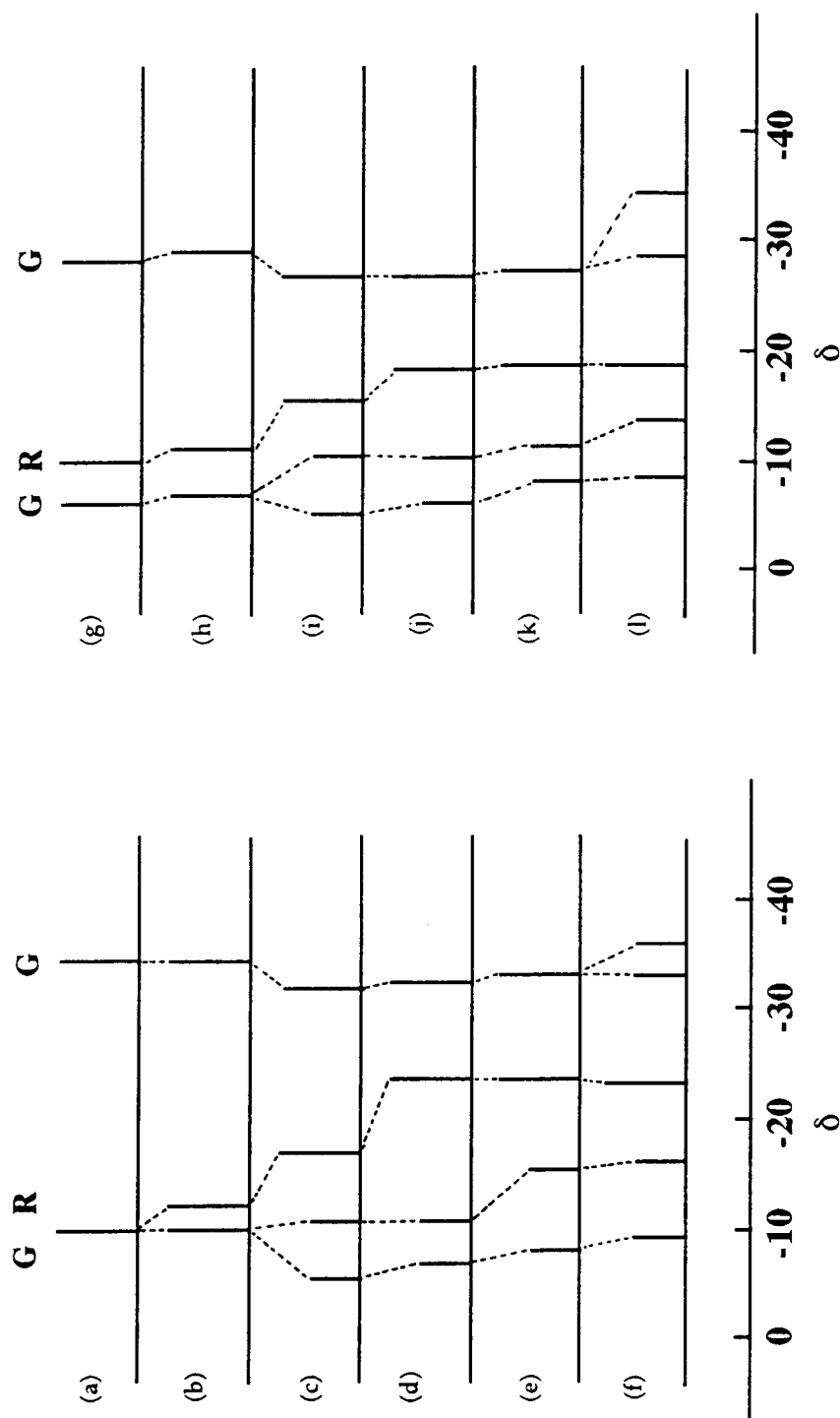


Figure 4-7. A schematic representation of the ^2H NMR chemical shift of

$[(\text{nta-d}_6)\text{Cr}(\text{OH})_2\text{M}(\text{N})_4]^{+}$; $M = \text{Co}^{3+}$ and $(N)_4 = (\text{en})_2$ (a) **A-2**, (tn) $_2$ (b) **A-3**, (picam) $_2$ (c) **A-6**, (bpy) $_2$ (d) **A-7**, (phen) $_2$ (e) **A-8** and $[(\text{nta-d}_6)\text{Cr}(\text{O})(\text{OH})\text{Cr}(\text{phen})_2]$ (f); $M = \text{Cr}^{3+}$ and $(N)_4 = (\text{en})_2$ (g) **B-2**, (tn) $_2$ (h) **B-3**, (picam) $_2$ (i) **B-6**, (bpy) $_2$ (j) **B-7**, (phen) $_2$ (k) **B-8** and $[(\text{nta-d}_6)\text{Cr}(\text{O})(\text{OH})\text{Co}(\text{phen})_2]$ (l). The dotted lines correlate inequivalent deuterons for the glycinato methylenes in the complexes.

Table 4-2. Tortion angles α (deg) (Cr-N-C-C(O)) and sum of angles(deg) of nta chelate rings^a for the dinuclear complexes **A-3**, **B-3** and **B-8**.

	Chelate rings	Tortion angles(α)	Sum of angles
[(nta)Cr(OH) ₂ Co(tn) ₂] ⁺ (A-3)			
R	Cr(1)N(1)C(1)C(2)	-14.1(3)	537.2
G ₁	Cr(1)N(1)C(3)C(4)	-37.6(3)	525.6
G ₂	Cr(1)N(1)C(5)C(6)	30.7(3)	531.5
[(nta)Cr(OH) ₂ Cr(tn) ₂] ⁺ (B-3)			
R	Cr(2)N(1)C(1)C(2)	-13.9(4)	537.5
G ₁	Cr(2)N(1)C(3)C(4)	-36.8(4)	526.0
G ₂	Cr(2)N(1)C(5)C(6)	30.4(3)	531.7
[(nta)Cr(OH) ₂ Cr(phen) ₂] ⁺ (B-8)			
molecule 1			
R	Cr(1)N(1)C(1)C(2)	-17(1)	540.3
G ₁	Cr(1)N(1)C(3)C(4)	-37(1)	523.0
G ₂	Cr(1)N(1)C(5)C(6)	27(1)	533.2
molecule 2			
R	Cr(4)N(11)C(11)C(11)	11(1)	536.6
G ₁	Cr(4)N(11)C(13)C(14)	-35(2)	527.0
G ₂	Cr(4)N(11)C(15)C(16)	31(2)	531.1

^a R- and G-rings are defined in the text.

different C values. Since the parameter C is a constant including the spin density, these difference are caused by the decrease in the effect by the paramagnetic unpaired electrons owing to the antiferromagnetic interaction in the [Cr(III)-Cr(III)] complexes.

4.3.3 ^2H NMR spectra and the influence of the ligands

i) The π -bond interaction of $\text{M}(\text{N})_4$ bond in $[(\text{nta})\text{Cr}(\text{OH})_2\text{M}(\text{N})_4]^+$. It is noted that not only the chemical shifts of the G-ring, but also those of the R-ring varied from δ -9.1 to -23.6. The variation of the ligands in the $\text{M}(\text{N})_4$ moieties is in accord with the changes in the chemical shifts of the R-ring as shown in Table 4-1 and Figure 4-7. The ^2H NMR chemical shifts of the R-ring methylene deuterons in the aliphatic amine complexes are located from δ -9.1 to -12.7 (**A-1 - 5** and **B-1 - 5**). The chemical shifts of the picam complexes are located at δ -14.0 and -15.6 (**A-6** and **B-6**). Those of the bpy and phen complexes with all aromatic nitrogen ligators are located from δ -17.9 to -23.6 (**A-7, 8, B-7** and **8**).

From the X-ray structure analysis in Chapter 3, it is expected that the signals of the R-rings also separate for complexes **A-3**, **B-3** and **8**, according to the reported result about the torsion angle α ,^{74b} but only one signal was obtained for all the complexes in this study. This result suggests that the R-ring becomes planar in the solution and the α values are equal to zero. From equation (3), thus, the shift differences between each complex are caused by the magnitude of the constant C . The constant C is affected by the spin density of the deuteron atom. As described in the crystal structures of the dinuclear complexes in Chapter 3, the $\text{Cr}(\text{nta})\text{-OH}$ bond lengths *trans* to the nta nitrogen atom vary with the kinds of the $(\text{N})_4$ ligand. Those of the aliphatic diamine complexes **A-3** and **B-3** are significantly shorter by about 0.03 Å than those of the aromatic diimine complex **B-8**. Though the obvious change in the $\text{Cr-N}(\text{nta})$ bond lengths is not detected from the structural analysis, the difference in the $\text{Cr}(\text{nta})\text{-OH}$ bond would affect the $\text{Cr-N}(\text{nta})$ bond owing to the *trans* influence. Therefore, it is considered that the unpaired electron density of the deuteron nuclei in the R-ring on the Cr_2O_2 plane or its isotropic contact shift increases with lengthening the $\text{M}(\text{N})_4\text{-OH}$ bond *trans* to the nta nitrogen atom. In other words, the ^2H NMR chemical shifts of the R-ring in the nta-d_6^{3-} ligand are sensitive to the π -bond

Table 4-4. ^2H NMR data for $[(\text{nta-d}_6)\text{Cr}(\text{OH})(\text{RCOO})\text{Cr}(\text{en})_2]^{+}$ in H_2O .

Complex	$\delta(\text{intensity})$	
	G-ring	R-ring
$[(\text{nta-d}_6)\text{Cr}(\text{OH})(\text{HCOO})\text{Cr}(\text{en})_2]^{+}$	-8.0(2)	-28.9(2)
$[(\text{nta-d}_6)\text{Cr}(\text{OH})(\text{CH}_3\text{COO})\text{Cr}(\text{en})_2]^{+}$	-11.0(2)	-31.5(2)
$[(\text{nta-d}_6)\text{Cr}(\text{OH})(\text{CH}_3\text{CH}_2\text{COO})\text{Cr}(\text{en})_2]^{+}$	-10.2(2)	-30.8(2)
$[(\text{nta-d}_6)\text{Cr}(\text{OH})(\text{CH}_3\text{CH}_2\text{CH}_2\text{COO})\text{Cr}(\text{en})_2]^{+}$	-10.8(2)	-31.5(2)
$[(\text{nta-d}_6)\text{Cr}(\text{OH})(\text{CH}_2\text{ClCOO})\text{Cr}(\text{en})_2]^{+}$	-10.1(2)	-27.6(2)
$[(\text{nta-d}_6)\text{Cr}(\text{OH})(\text{CH}_2\text{ClCH}_2\text{COO})\text{Cr}(\text{en})_2]^{+}$	-11.2(2)	-29.5(2)
$[(\text{nta-d}_6)\text{Cr}(\text{OH})(\text{CH}_3\text{OCH}_2\text{COO})\text{Cr}(\text{en})_2]^{+}$	-11.1(2)	-30.0(2)
$[(\text{nta-d}_6)\text{Cr}(\text{OH})(\text{C}_6\text{H}_5\text{COO})\text{Cr}(\text{en})_2]^{+}$	-11.2(2)	-31.7(2)

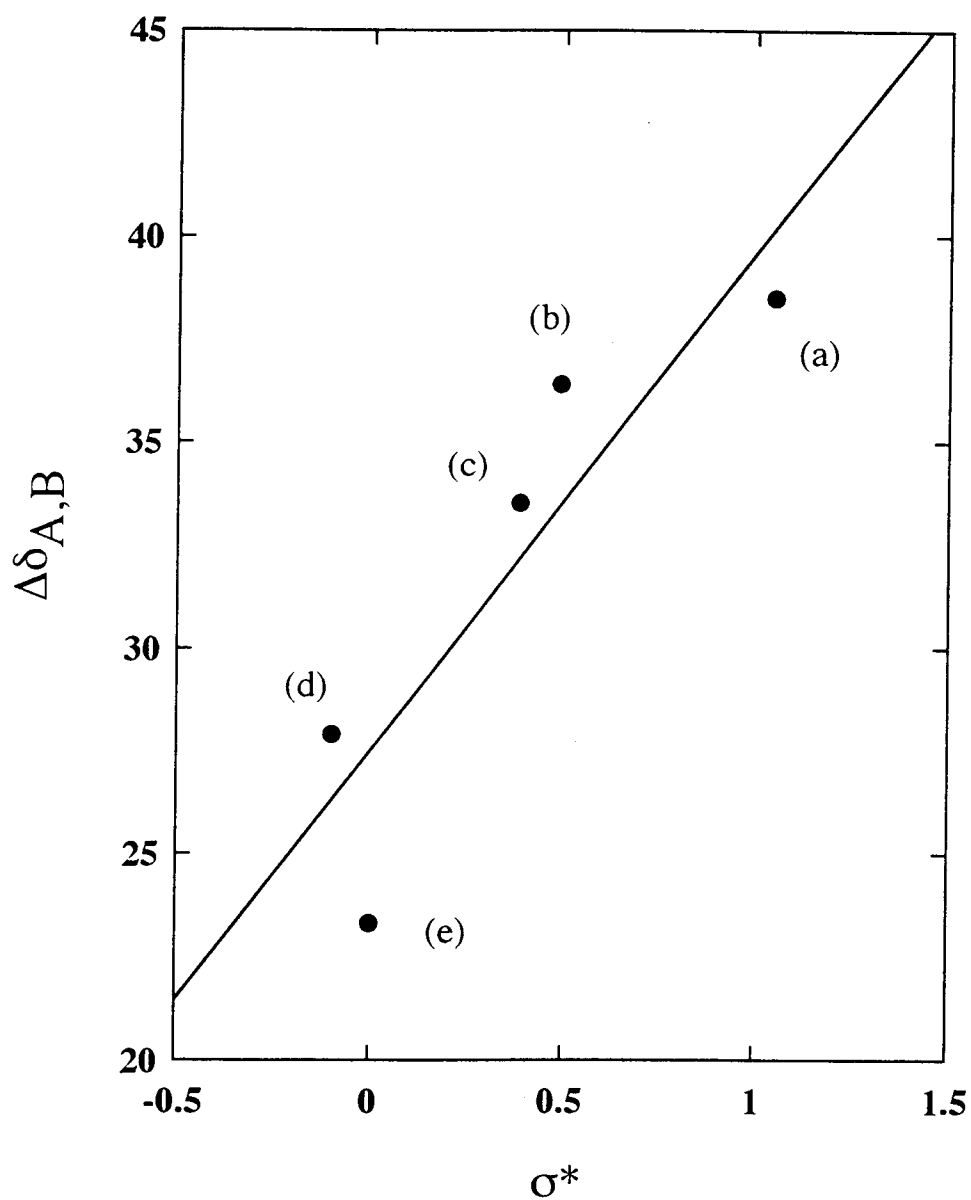


Figure 4-8. Relation between ^2H NMR shift differences and the inductive substituent constants for $[\text{Cr}_2(\text{OH})_2(\text{RCOO})(\text{bispicam-d}_1)_2]^{3+}$: $\text{R} = \text{CH}_2\text{Cl}$ (a), H (b), CH_2ClCH_2 (c), C_2H_5 (d) and CH_3 (e). The shift differences are adopted from Table 3-12. The inductive substituent constants are adopted from Table 6-5.

interaction of M-(N)₄ bond *via* the M(N)₄-OH bond in these dinuclear complexes through six bonds.

ii) Influence of the substituent R in [(nta-d₆)Cr(OH)(RCOO)Cr(en)₂]⁺. The ²H NMR data of [(nta-d₆)Cr(OH)(RCOO)Cr(en)₂]⁺ are summarized in Table 4-4. As described in above section, it is expected that the Cr-O(OOCR) bond which is governed by the substituent effect of RCOOH affects the ²H NMR signals. There is no significant relation between ²H NMR chemical shifts and RCOOH. This poor relation supports the expected structure of [(nta-d₆)Cr(OH)(RCOO)Cr(en)₂]⁺ as shown in Figure 3-7(a). The Cr-N(nta) bond is hardly affected by the Cr-O one *cis* to the nta nitrogen atom, no matter how the Cr-O(OOCR) bond changes significantly with the substituent R.

iii) Influence of the substituent R in [Cr₂(OH)₂(RCOO)(bispicam-d₁)₂]^{3+ or 4+} complexes. The ²H NMR of [Cr₂(OH)₂(RCOO)(bispicam-d₁)₂]^{3+ or 4+} were applied to determine the structure of the complexes in Chapter 3. Since all the complexes gave two ²H NMR signals, the Cr-N-C-C torsion angles α in the methylene ring of the bispicam ligand are averaged and constant in the solution. Therefore, the different C values are responsible for the shift differences Δδ between two signals in the equation $\Delta\delta_{A,B} = \delta_A - \delta_B = (-\sqrt{3}/2)C \sin(2\alpha)$ as described in above Section. There is a correlation between the shift differences Δδ and the inductive substituent constants of the R which will be explained detail in Chapter 6 as shown in Figure 4-8. This correlation means that the unpaired electron density in the deuterons in the methylene ring becomes larger with increasing inductive effect of the substituents. The increasing unpaired electron density is due to the shortened Cr-N(H) bond. Therefore, it was found that the Cr-O(OOCR) bond affected to the Cr-N(NH) one as a *trans* influences. The inductive effects as the properties of the substituent R were related to the ²H NMR chemical shift differences in the methylene deuterons in the bispicam ligand.

4.3.4 ¹⁴N NMR Spectra

The signal for the en ligands in [(nta)Cr(OH)₂Cr(en)₂]⁺ was observed at almost the

Table 4-5. Nitrogen-14 NMR spectral data for chromium(III) and cobalt(III) complexes.

Complex	δ ($\nu_{1/2}$ / Hz)
$[(\text{nta})\text{Cr}(\text{OH})_2\text{Cr}(\text{en})_2]^+$ (B-2)	-329.8 (81.0)
<i>cis</i> - $[\text{CrCl}_2(\text{en})_2]^+$	-338.8 (140.2)
<i>cis</i> - $[\text{CrF}_2(\text{en})_2]^+$	-338.8 (92.1)
<i>trans</i> - $[\text{CrF}_2(\text{en})_2]^+$	-346.8 (119.7)
$[\text{Cr}(\text{en})_3]^{3+}$	-322.7 (292.1)
$[(\text{nta})\text{Cr}(\text{OH})_2\text{Co}(\text{en})_2]^+$ (A-2)	-436 (1560), -481 (1870)
$[\text{Co}_2(\text{OH})_2(\text{en})_4]^{4+}$	-387, -408 (1800 ^a)
$[\text{Co}(\text{en})_2(\text{H}_2\text{O})_2]^{3+}$	-386, -403 (1260 ^a)
$[\text{Co}(\text{en})_2(\text{H}_2\text{O})_2]^{3+}$ ^b	-380, -396 (1880 ^a)

^a Linewidth for unresolved signals. ^b With addition of an equimolar amount of paramagnetic $[\text{Cr}(\text{nta})(\text{H}_2\text{O})_2]$ (see text).

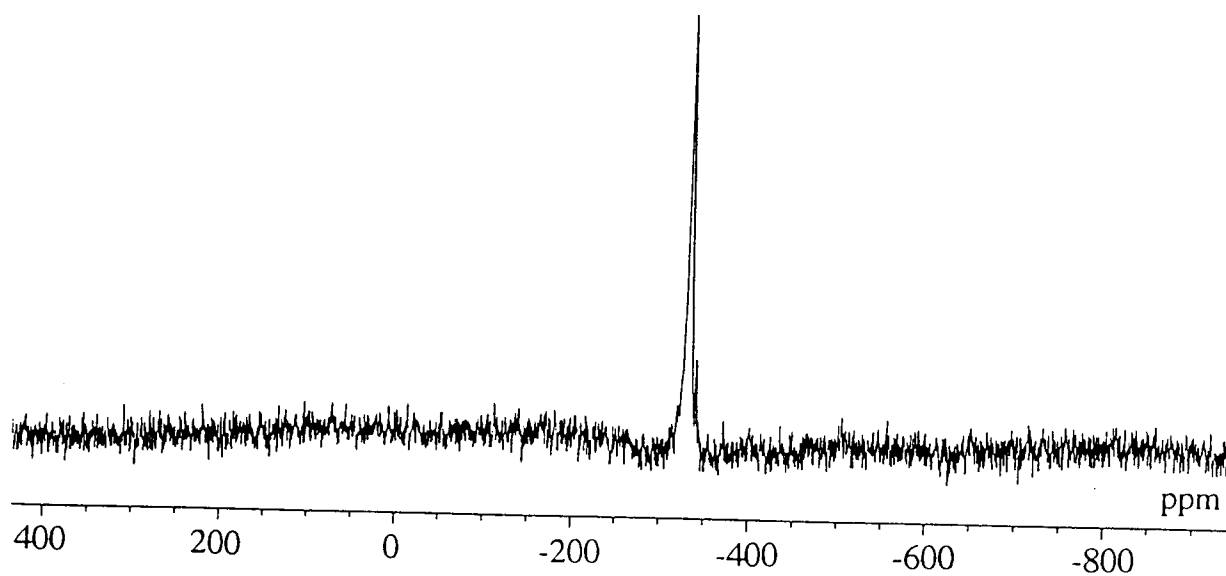


Figure 4-9. ^{14}N NMR spectrum of $[(\text{nta})\text{Cr}(\text{OH})_2\text{Cr}(\text{en})_2]^+$ at 25 °C.

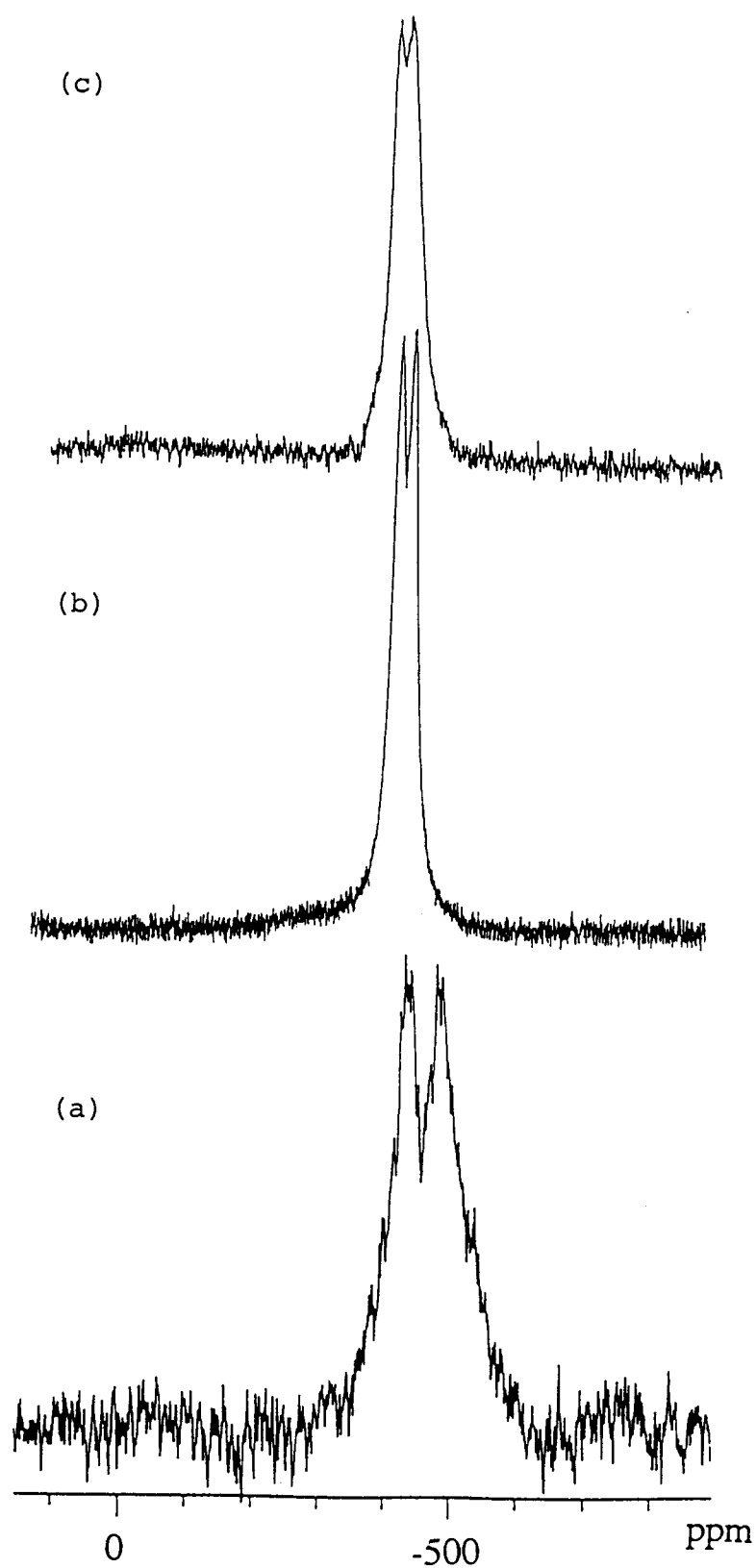


Figure 4-10. ^{14}N NMR spectra of $[(\text{nta})\text{Cr}(\text{OH})_2\text{Co}(\text{en})_2]^+$ (a), $\text{cis-}[\text{Co}(\text{en})_2(\text{H}_2\text{O})_2]^{3+}$ (b) and $\text{cis-}[\text{Co}(\text{en})_2(\text{H}_2\text{O})_2]^{3+}$ with equimolar amount of $[\text{Cr}(\text{nta})(\text{H}_2\text{O})_2]$ (c) at 25°C .

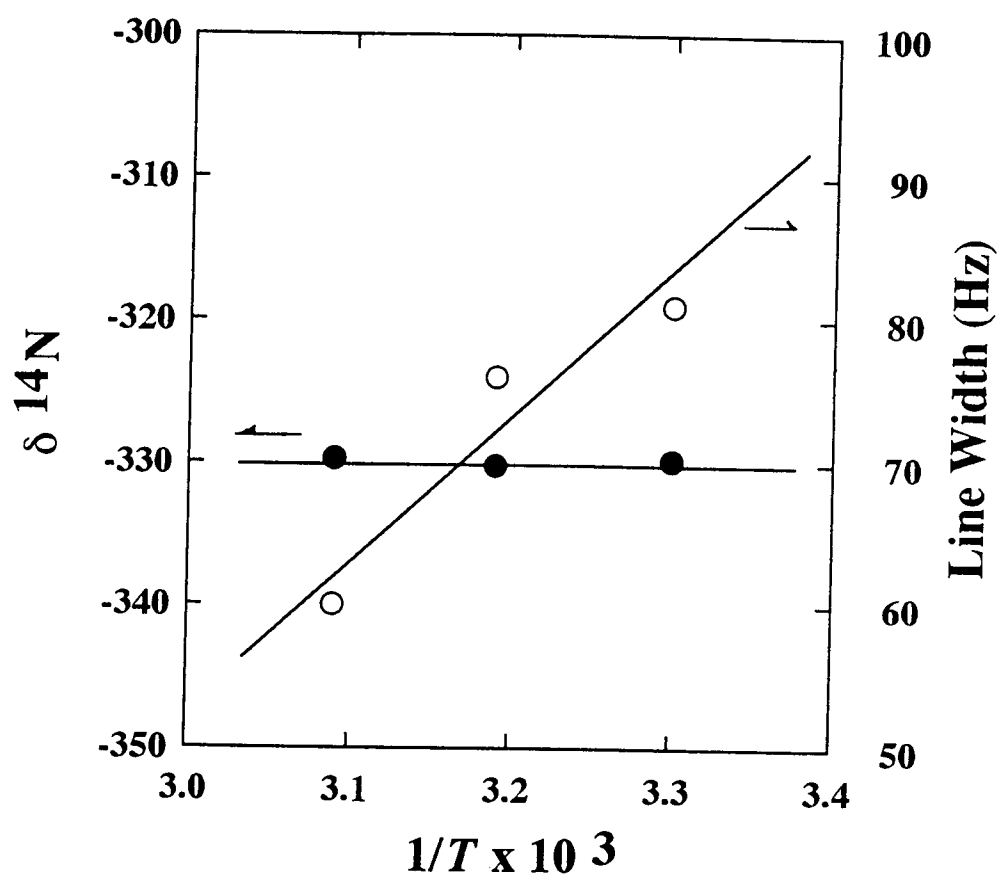


Figure 4-11. The relation among the ^{14}N NMR chemical shifts(●), linewidths (○) and temperature in $[(\text{nta})\text{Cr}(\text{OH})_2\text{Cr}(\text{en})_2]^+$ at 25 °C.

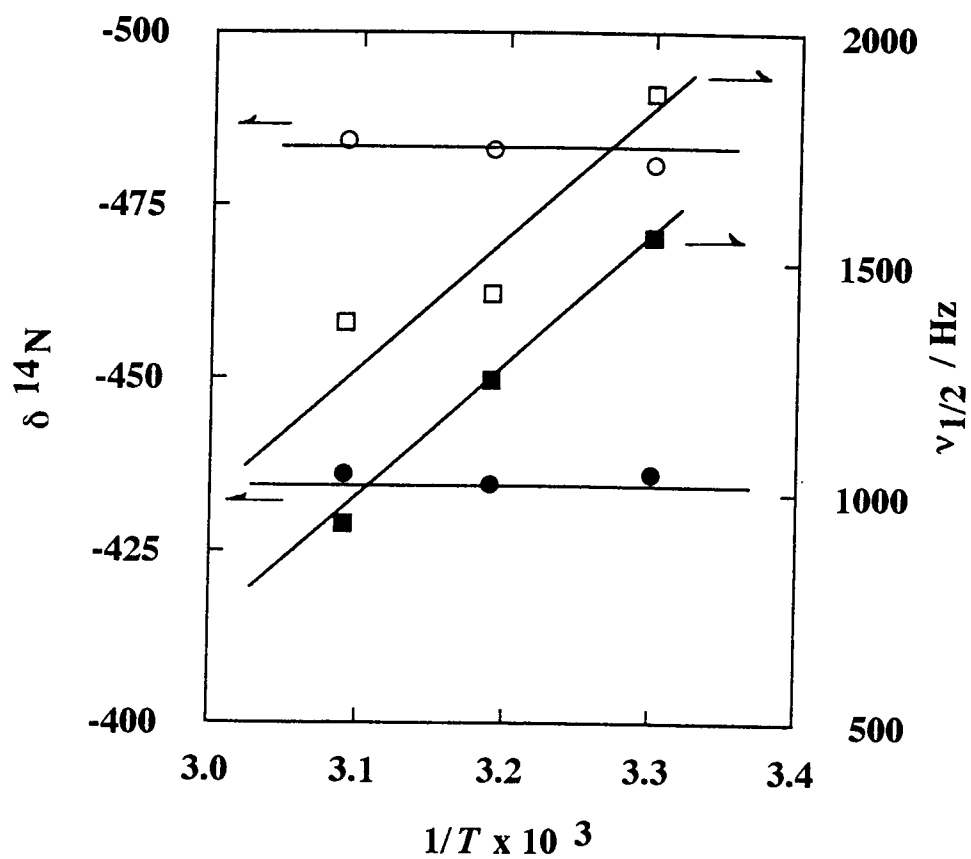


Figure 4-12. The relation among the ^{14}N NMR chemical shifts (● and ○), linewidths (■ and □) and temperature in $[(\text{nta})\text{Cr}(\text{OH})_2\text{Co}(\text{en})_2]^+$ at 25 °C.

same position as those of the mononuclear chromium(III) complexes (Table 4-5 and Figure 4-9). In addition, the linewidth is narrower than those of them. The ^{14}N signal of this dinuclear complex does not seem to be affected by the paramagnetic unpaired electrons in the $\text{Cr}(\text{nta})$ moiety. The only one resonance was observed, though there are two inequivalent nitrogen atoms *cis* and *trans* to the OH ligands. This is the same behavior to the mononuclear chromium(III) complexes.

In the ^{14}N NMR spectrum for the en ligands of $[(\text{nta})\text{Cr}(\text{OH})_2\text{Co}(\text{en})_2]^+$, two resolved signals owing to the inequivalent nitrogen atoms are obtained as shown in Figure 4-10a. These signals are shifted to higher field and broader than for the *cis*- $[\text{Co}(\text{en})_2(\text{H}_2\text{O})_2]^{3+}$ (Figure 4-10b) and $[\text{Co}_2(\text{OH})_2(\text{en})_4]^{4+}$ (Table 4-10). Therefore, the chemical shifts and linewidths of this complex do not result, respectively, from the coordination shift and the line broadening due to the enhanced rotation-correlation time. Moreover, the coexistence of *cis*- $[\text{Co}(\text{en})_2(\text{H}_2\text{O})_2]^{3+}$ in an equimolar amount (0.5 M) with the paramagnetic complex $[\text{Cr}(\text{nta})(\text{H}_2\text{O})_2]$ result in a small lower-field shift together with the line broadening (Table 4-5 and Figure 4-10c) for the ^{14}N NMR signals as observed for $[\text{NBu}_4]_2[\text{CoX}_4]$.⁷⁹ This small lower-field shift caused by adding the chromium(III) complex is in contrast to the large higher-field one for the $[\text{Cr}(\text{III})\text{-Co}(\text{III})]$ which exhibits the expected isotropic shift with paramagnetic relaxation line broadening. Their behavior is due to the effect of the paramagnetic unpaired electrons by the $(\text{nta})\text{Cr}^{\text{III}}$ moiety as observed in the ^1H NMR spectra for $[(\text{nta})\text{Cr}(\text{OH})_2\text{Co}(\text{bpy})_2]^+$.

However, no temperature dependence of the ^{14}N NMR chemical shifts was observed for each complexes as shown in Figure 4-11. The influences of paramagnetic unpaired electrons on the ^{14}N nuclei is not clear yet inspite of the large contact shifts of $[(\text{nta})\text{Cr}(\text{OH})_2\text{Co}(\text{en})_2]^+$. The temperature dependent linewidths are due to the increasing rotation-correlation time as shown in Figure 4-12.

4.3.5 ^{59}Co NMR Spectra

Cobalt-59 NMR chemical shifts and line widths for $[(\text{nta})\text{Cr}(\text{OH})_2\text{Co}(\text{N})_4]^+$ are shown in Table 4-6 together with the corresponding complexes. The spectra of

Table 4-6. Cobalt-59 NMR data and the positions of the first absorption maxima for cobalt(III) dinuclear and related mononuclear complexes.

Complex	$\delta(\nu_{1/2} / \text{Hz})$	$\lambda_{\text{obsd}}^a / \text{nm}$
$[(\text{nta})\text{Cr}(\text{OH})_2\text{Co}(\text{NH}_3)_4]^+$	8600 (10050)	545
$[(\text{nta})\text{Cr}(\text{OH})_2\text{Co}(\text{en})_2]^+$	8780 (3300)	510
$[(\text{nta})\text{Cr}(\text{OH})_2\text{Co}(\text{tn})_2]^+$	9250 (3230)	531
$[(\text{nta})\text{Cr}(\text{OH})_2\text{Co}\{(R,R)\text{chxn}\}_2]^+$	8490 (9800)	516
$[(\text{nta})\text{Cr}(\text{OH})_2\text{Co}(\text{trien})_2]^+$	8380 (2360)	508
$[(\text{nta})\text{Cr}(\text{OH})_2\text{Co}(\text{picam})_2]^+$	9250 (3230)	540
$[(\text{nta})\text{Cr}(\text{OH})_2\text{Co}(\text{bpy})_2]^+$	8210 (3290)	504
$[(\text{nta})\text{Cr}(\text{OH})_2\text{Co}(\text{phen})_2]^+$	8500 (3050)	512
$[(\text{H}_2\text{O})_2\text{Co}^{\text{II}}\{(\text{OH})_2\text{Co}(\text{en})_2\}_2]^{4+}$	9220 (6690)	— ^b
$[(\text{H}_2\text{O})_2\text{Zn}^{\text{II}}\{(\text{OH})_2\text{Co}(\text{en})_2\}_2]^{4+}$	8820 (4780)	— ^b
$[(\text{H}_2\text{O})_2\text{Ni}^{\text{II}}\{(\text{OH})_2\text{Co}(\text{en})_2\}_2]^{4+}$	8430 (10980)	— ^b
$[(\text{nta})\text{Co}(\text{OH})_2\text{Co}(\text{en})_2]^+$	9100 (7610)	512
<i>cis</i> - $[\text{Co}(\text{en})_2(\text{OH})_2]^+$	9380 (330)	516
<i>cis</i> - $[\text{Co}(\text{tn})_2(\text{OH})_2]^+$	9850 (320)	523
<i>cis</i> - $[\text{Co}(\text{bpy})_2(\text{OH})_2]^+$	8720 (2210)	516
<i>cis</i> - $[\text{Co}(\text{phen})_2(\text{OH})_2]^+$	9050 (1950)	508

^a Absorption maxima for $[\text{Co}(\text{N})_4(\text{O})_2]$ moiety. ^b This absorption maxima was not be estimated.

$[(nta)Cr(OH)_2Co(en)_2]^+$ is shown in Figure 4-13. There is a linear relationship between the chemical shifts of $[Cr(III)-Co(III)]$ ones and the corresponding mononuclear *cis*- $[Co(OH)_2(N)_4]^+$ ones (Figure 4-14). In the mononuclear cobalt(III) complexes, there is a linear relationship between chemical shifts δ and the first absorption band maxima $1/\Delta E$.⁸⁰ There is also the linear relationship between the chemical shifts and absorption band maxima in the first absorption band of $[Cr(III)-Co(III)]$ complexes (Figure 4-15).

In the paramagnetic compounds, the ^{59}Co NMR chemical shift δ is written as $\delta = \delta^{dia} + \delta^{con} + \delta^{dip}$, where δ^{dia} , δ^{con} and δ^{dip} are diamagnetic (temperature independent paramagnetic (TIP)), Fermi contact and dipolar term, respectively as described in the 1H NMR. In this case, the δ^{dia} term is proportional to the strength of the ligand field around the Co^{3+} ion. The δ^{con} and δ^{dip} are the influences of the paramagnetic unpaired electrons in the Cr^{3+} ion. The δ^{dip} term is proportional to the $1/R^3$ where R is the distance between the observed nuclei and paramagnetic center, but the δ^{con} one is not directly proportional to that. Since these dinuclear complexes are rigid bridging structures ($[Cr(\mu-OH)_2Co]$), the δ^{dip} terms which depends upon the distance from the paramagnetic center would be almost unchanged for all the dinuclear complexes. The remaining δ^{con} term would not be changed for each complex because of the above linear correlation.

To clarify the influences of the paramagnetic unpaired electrons, the temperature dependence chemical shifts were examined. The δ^{con} and δ^{dip} terms are closely related to the temperature (Curie law). Figures 4-16 and 4-17 show the relationships among chemical shifts, linewidths and temperature. In the chemical shift change, the slope for $[(nta)Cr(OH)_2Co(en)_2]^+$ was almost the same as those for *cis*- $[Co(en)_2(OH)_2]^+$. The behavior of the linewidths of $[(nta)Cr(OH)_2Co(en)_2]^+$ were also the same as those for the mononuclear one. In contrast to the fact that the ^{59}Co NMR for the Co_3O_4 polycrystalline which contains diamagnetic octahedral Co^{3+} and the paramagnetic tetrahedral Co^{2+} ions⁸¹ and ^{183}W NMR for the wolfram heteropoly complexes which contains paramagnetic tetrahedral Co^{2+} ion⁸² give large temperature dependent shifts in comparison with the corresponding diamagnetic species, there would be little influence by the paramagnetic electrons from $[(nta)Cr(\mu-OH)_2]$ moiety in the $[Cr(III)-Co(III)]$ complexes. In addition, the temperature

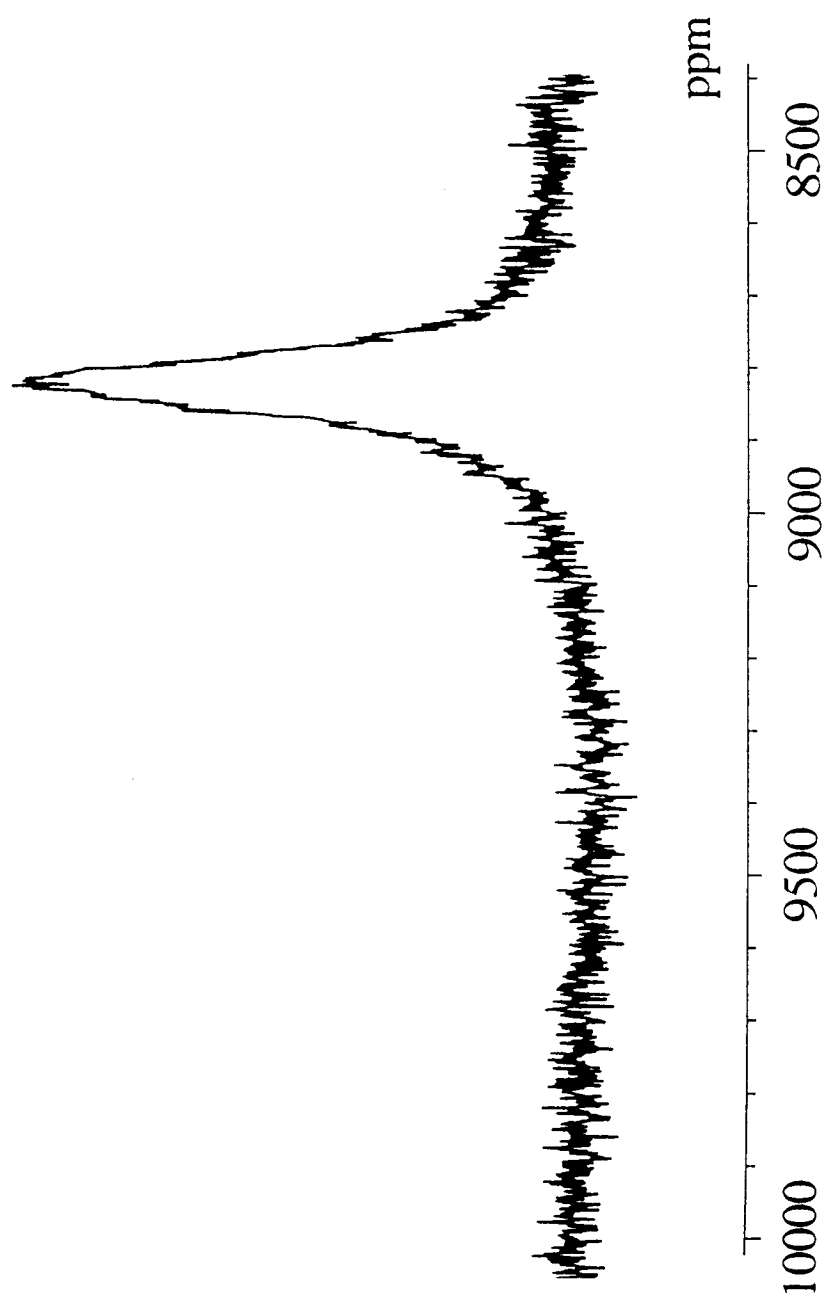


Figure 4-13. ^{59}Co NMR spectrum of $[(\text{nta})\text{Cr}(\text{OH})_2\text{Co}(\text{en})_2]^+$.

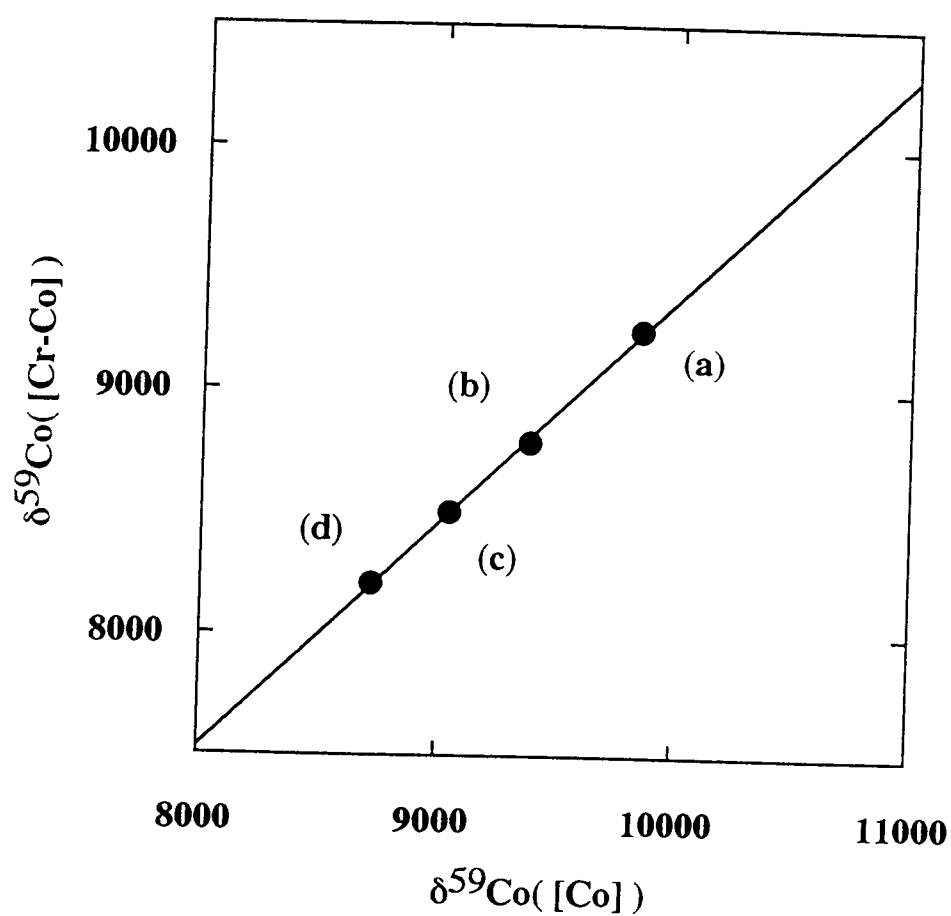


Figure 4-14. Correlation between ^{59}Co NMR chemical shifts of $[(nta)Cr-(OH)_2Co(N)_4]^+$ and $cis-[Co(OH)_2(N)_4]^+$: $(N)_4 = (tn)_2$ (a), $(en)_2$ (b), $(bpy)_2$ (c) and $(phen)_2$ (d).

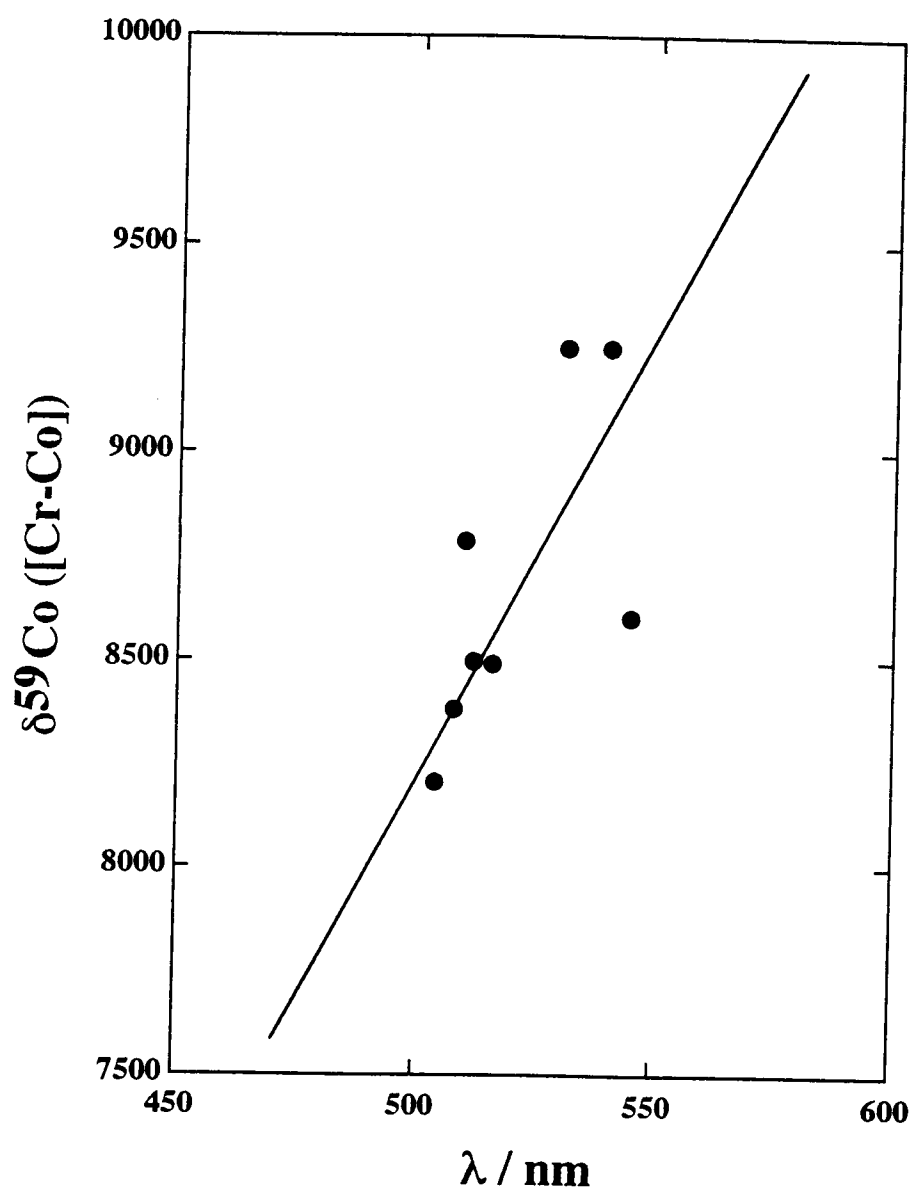


Figure 4-15. Correlation between ^{59}Co NMR chemical shifts of $[(\text{nta})\text{Cr}(\text{OH})_2\text{Co}(\text{N})_4]^+$ and their first absorption maxima. The data are obtained from Table 4-6. Line shown is least-squares fit.

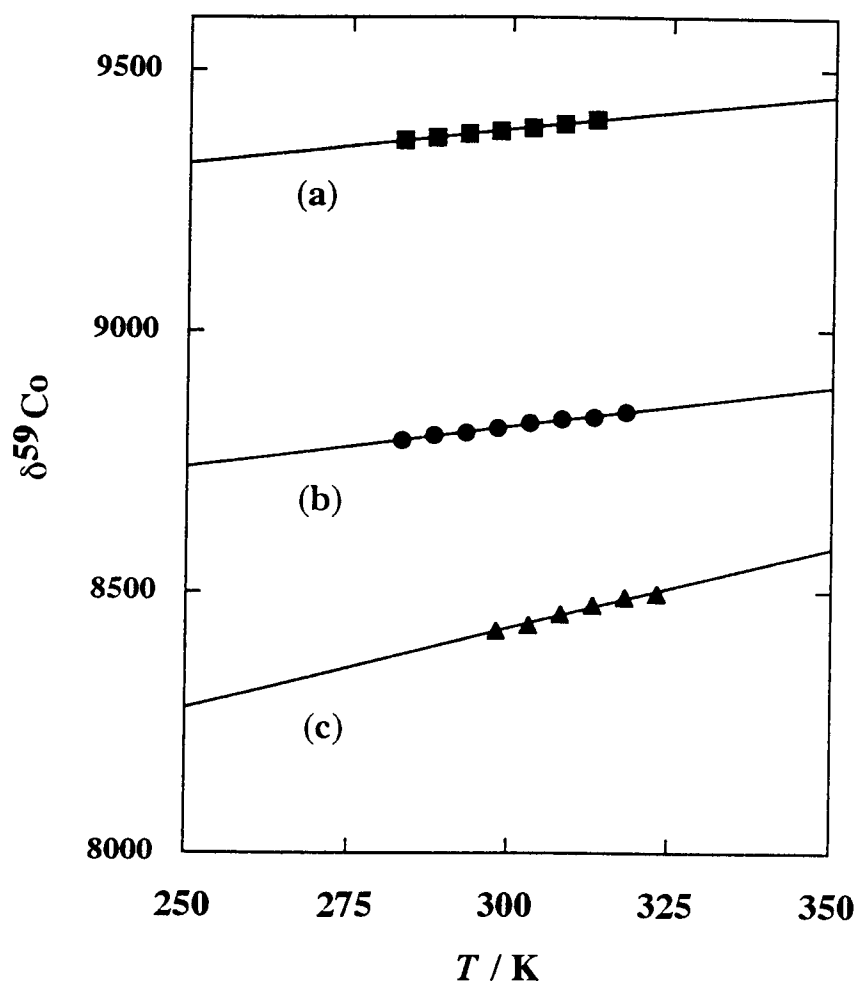


Figure 4-16. Relation between ^{59}Co NMR chemical shifts and temperature: *cis*- $[\text{Co}(\text{en})_2(\text{OH})_2]^+$ (a), $[(\text{nta})\text{Cr}(\text{OH})_2\text{Co}(\text{en})_2]^+$ (b) and $[(\text{H}_2\text{O})_2\text{Ni}\{(\mu\text{-OH})_2\text{-Co}(\text{en})_2\}_2]^{4+}$ (c).

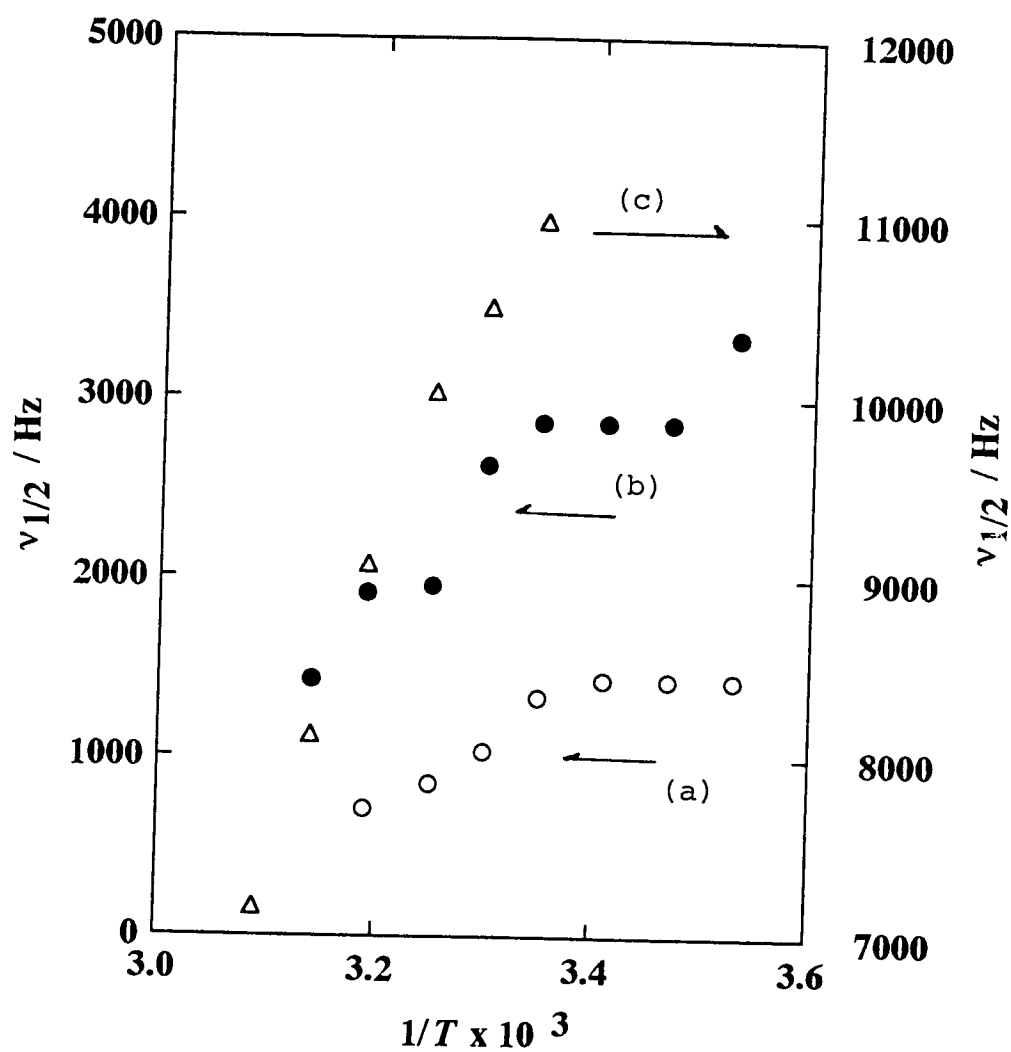


Figure 4-17. Relation between ^{59}Co NMR line widths and temperature:
 (a) $\text{cis-}[\text{Co}(\text{en})_2(\text{OH})_2]^+$ (○), (b) $[(\text{nta})\text{Cr}(\text{OH})_2\text{Co}(\text{en})_2]^+$ (●) and
 (c) $[(\text{H}_2\text{O})_2\text{Ni}\{(\mu\text{-OH})_2\text{Co}(\text{en})_2\}_2]^{4+}$ (△).

dependent chemical shifts of the cobalt(III) trinuclear $[(\text{H}_2\text{O})_2\text{Ni}^{\text{II}}\{(\text{OH})_2\text{Co}^{\text{III}}(\text{en})_2\}_2]^{4+}$ complex which contains octahedral (high spin d^8) Ni^{2+} ion, exhibited slightly larger slope $(\delta-1/T)$ than those of the *cis*- $[\text{Co}(\text{en})_2(\text{OH})_2]^+$ and $[(\text{nta})\text{Cr}(\text{OH})_2\text{Co}(\text{en})_2]^+$ as shown in Figure 4-16. The same structural $[(\text{H}_2\text{O})_2\text{Co}^{\text{II}}\{(\text{OH})_2\text{Co}^{\text{III}}(\text{en})_2\}_2]^{4+}$ complex also exhibited small influence of the paramagnetic unpaired electrons according to the ^{59}Co chemical shift and halfwidth. The effect of the paramagnetic unpaired electrons even in the e_g orbitals which form a σ -bond of Ni^{II} or Co^{II} ions is not so large to affect the ^{59}Co NMR shift apparently. As will be described in the Chapter 5, since the antiferromagnetic interaction is mainly *via* the π -overlap with magnetic t_{2g} orbital, the influence of the paramagnetic unpaired electrons in the σ -bond would not be so effective as expected.

Accordingly, the change in the higher field shifts in these complexes from the dihydroxo mononuclear complexes would result from the ligand field strengths of OH^- of $[\text{Co}(\text{N})_4(\text{O})_2]$ moiety. The order of the ligand field strengths of the OH^- ion is then as follows:

$$\begin{aligned} \Delta E([(\text{H}_2\text{O})_2\text{Ni}^{\text{II}}\{(\underline{\mu\text{-OH}})_2\text{Co}(\text{en})_2\}_2]^{4+}) &> \Delta E([(nta)\text{Cr}^{\text{III}}(\underline{\mu\text{-OH}})_2\text{Co}(\text{en})_2]^+) > \\ \Delta E([(\text{H}_2\text{O})_2\text{Zn}^{\text{II}}\{(\underline{\mu\text{-OH}})_2\text{Co}(\text{en})_2\}_2]^{4+}) &> \Delta E([(nta)\text{Co}^{\text{III}}(\underline{\mu\text{-OH}})_2\text{Co}(\text{en})_2]^+) > \\ \Delta E([(\text{H}_2\text{O})_2\text{Co}^{\text{II}}\{(\underline{\mu\text{-OH}})_2\text{Co}(\text{en})_2\}_2]^{4+}) &> \Delta E([\text{Co}(\underline{\text{OH}})_2(\text{en})_2]^+). \end{aligned}$$

The difference in the ^{59}Co NMR chemical shift among these complexes is mainly due to the difference of the ligand field strengths of the coordinating OH ligand to different metal ions. The bridging OH^- ion lies in the higher position of the spectrochemical series than the monodentate OH^- one.

5. Magnetic Exchange Interaction in Chromium(III)-Chromium(III) Dinuclear Complexes

5.1 Introduction

Since the octahedral chromium(III) ion has spin $S = 3/2$, the magnetic exchange interaction is one of the most interesting aspects in the dinuclear complexes as described in General Introduction. The extent of magnetic exchange interaction is usually obtained from the temperature dependent magnetic susceptibility data. The temperature dependent magnetic susceptibility data for chromium(III) dinuclear complexes were fitted by the Van Vleck equation,

$$\chi = \frac{Ng^2\beta^2}{kT} \cdot \frac{2\exp(2J/kT) + 10\exp(6J/kT) + 8\exp(12J/kT)}{1 + 3\exp(2J/kT) + 5\exp(6J/kT) + 7\exp(12J/kT)}$$

where J is the spin-exchange coupling constant in cm^{-1} by the exchange Hamiltonian expressed as $H = -2J (S_1 \cdot S_2)$.

There are several magneto-structural correlation about the exchange interaction in chromium(III) dinuclear complexes. For the chromium(III) dinuclear complexes with $[\text{Cr}(\mu\text{-OH})_2\text{Cr}]$ bridging unit, Glerup, Hodgson and Pedersen purposed a model (GHP model) which correlates the magnitude of the magnetic exchange interaction with structural parameters of Cr-O bond length r , Cr-O-Cr bridging angle ϕ and dihedral angle θ between the bridging plane and the OH vector of the bridging group (Figure 5-1).⁷² The observed exchange coupling constant J is the sum of the antiferro- (J_{af}) and ferromagnetic (J_{f}) contribution. They estimated each contributions to the above structural parameters on the basis of the angular overlap model (AOM) consideration. The overlap of the d_{zx} orbital in one chromium(III) ion and the d_{yz} orbital in another one *via* the p_z orbital on the bridging oxygen atom is mainly contributed to the antiferromagnetic interaction. The J_{af} term is proportional to $|\langle d_{zx}(a) | V_L | d_{yz}(b) \rangle|^2 / E_{\text{C.T.}}$ where $E_{\text{C.T.}}$ is the energy of the charge transfer configuration. On the other hand, the overlap of the d_{z^2} orbital in one chromium(III) ion and the d_{xy} orbital in another one is contributed to the ferromagnetic interaction. The J_{f} term is

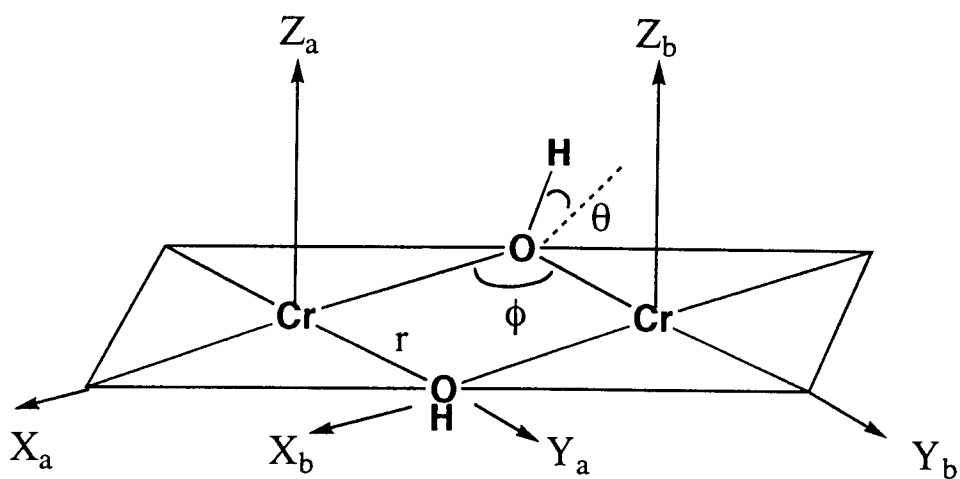


Figure 5-1. The coordination system for $[\text{Cr}(\mu\text{-OH})_2\text{Cr}]$ bridging unit in the GHP model.

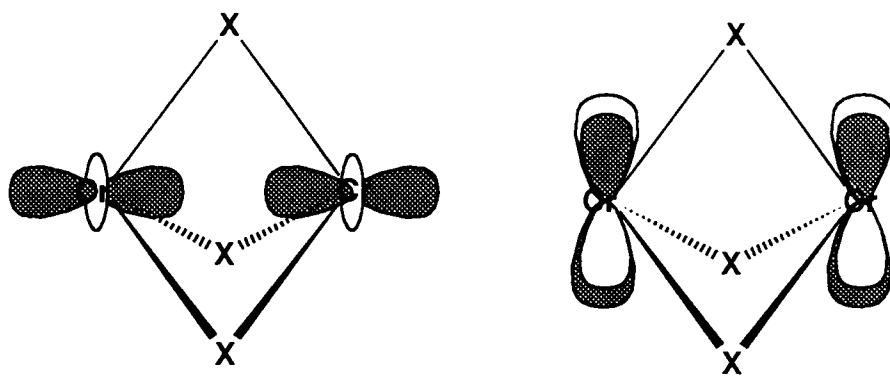


Figure 5-2. The magnetic exchange paths in face-sharing dinuclear complexes with d^3 - d^3 electronic configuration.

proportional to $|\langle d_{z^2}(a) | V_L | d_{xy}(b) \rangle|^2$. The total expression for $2J$ is the sum of J_a and J_f . Using these three structural parameters from X-ray structure, we can calculate the $2J$ value. According to the GHP's explanation, the $-2J$ value is obtained following equation:

$$-2J = e^{-a(r-1.8)} [b \cos^4 \theta / \{1 - \sin^2 \theta / \tan^2(\phi/2)\}^2 - c \sin^2 \phi / \{1 - \cos \phi\}^2]$$

where a , b and c are the parameters which were determined by the least-squares technique ($a = 19$, $b = 611$ and $c = 172$).⁷²

On the other hand, Wieghardt and co-workers reported that the direct metal-metal exchange interaction in the face-sharing transition metal dinuclear complexes with the d^3 - d^3 electronic configuration.⁸³ They demonstrated the only relevant structural parameter that correlates with the value of J is the distance between the two metal ions. Unlike the $\text{di}(\mu\text{-OH})$ chromium(III) dinuclear complexes, not the superexchange interaction, but the direct metal-metal interaction take place (Figure 5-2).

Although there are several magneto-structural correlations in the chromium(III) dinuclear complexes, a few studies on relation between magnetic exchange interaction and the coordinate bond characters of the ligands are reported. Nakahanada *et al.* reported that the one of the most appropriate series which make possible to relate the magnetic exchange interactions to the structural and the electronic properties of bridging moieties.⁸⁴ The magnetic exchange interactions in five $[\text{Cr}_2(\text{acac})_4(\text{X-PhO})_2]$ type $\text{bis}(\mu\text{-4-substituted-phenoxo})$ complexes tend to increase with increasing $\text{p}K_a$ values of 4-X-phenols or electron density at the bridging oxygen ligators. Gafford *et al.* found the relation of the $\text{p}K_a$ values of the carboxylic acids with the magnetic interactions in $[(\text{tmpa})\text{Cr}(\mu\text{-O})(\mu\text{-RCOO})\text{Cr}(\text{tmpa})]^{5+}$ type complexes.^{27,13}

In this chapter, the magnetic exchange interactions in the chromium(III)-chromium(III) dinuclear complexes are described. In $[(\text{nta})\text{Cr}(\text{OH})_2\text{Cr}(\text{N})_4]^+$ complexes, the correlation between structures and magnetic exchange coupling are investigated. In $[(\text{nta})\text{Cr}(\text{OH})(\text{RCOO})\text{Cr}(\text{en})_2]^+$ complexes, the contribution in the magnetic exchange interactions of the bridging carboxylates is examined. Since $[\text{Cr}_2(\text{OH})_2(\text{RCOO})(\text{bispicam})_2]^{3+ \text{ or } 4+}$ complexes have both face-sharing bridging unit and $\text{di}(\mu\text{-OH})$ one, it is interest of the correlation between structures and magnetic exchange

coupling. In addition, the contribution in the magnetic exchange interactions of the bridging carboxylates is also interest.

5.2 Experimental

5.2.1 Measurements

Magnetic susceptibilities were measured on powdered samples of chromium(III) dinuclear complexes by using a Faraday method. Corrections for diamagnetism were applied with use of Pascal's constants. The observed susceptibilities were fitted by a theoretical equation using a non-linear least-squares SIMPLEX parameter optimization routine, minimizing the residual function $R = [\sum(\chi_{\text{obs}} - \chi_{\text{calc}})^2 / \sum(\chi_{\text{obs}})^2]^{1/2}$. Magnetic moment in aqueous solution is measured using a Gouy method at room temperature.

5.3 Results and Discussion

5.3.1 [(nta)Cr(OH)₂Cr(N)₄]⁺ complexes

The best fit of the susceptibility data reveals that the [Cr(III)-Cr(III)] complexes give antiferromagnetic coupling and that their $2J$ values are -17.2 to -31.4 cm⁻¹ as summarized in Table 5-1. These $2J$ values are in the range of the dinuclear di(μ -OH) chromium(III) complexes.⁷² The experimental data for the temperature dependence of the magnetic susceptibility and magnetic moment of [(nta)Cr(OH)₂Cr(tn)₂]Cl·1.5H₂O is shown in Figure 5-3.

The X-ray structure analysis for [(nta)Cr(OH)₂Cr(tn)₂]Cl·1.5H₂O as described in Chapter 3 reveals that the angle θ , which consists of the Cr₂O₂ plane and the hydrogen atom of bridging hydroxo ligand is 22.7°(average). From the GHP model, the coupling constants ($2J$) for [(nta)Cr(OH)₂Cr(tn)₂]Cl·1.5H₂O is expected to be -23.1 cm⁻¹, compared with the observed value -17.2 cm⁻¹. The calculated value in this study is fairly in agreement with the observed one.

The $2J$ value of [Cr₂(OH)₂(phen)₄]Cl₄·6H₂O (-43.0 cm⁻¹)⁷² is larger than that of [Cr₂(OH)₂(en)₄]Cl₄·H₂O (-29.4 cm⁻¹).⁷² Since the magnetic exchange interaction in di(μ -OH) chromium(III) dinuclear complexes is largely dependent on Cr-OH bond length as

Table 5-1. Magnetic parameters for $[(\text{nta})\text{Cr}(\text{OH})_2\text{Cr}(\text{N})_4]^+{}^{\text{a}}$.

Complex	g	$2J / \text{cm}^{-1}{}^{\text{b}}$
$[(\text{nta})\text{Cr}(\text{OH})_2\text{Cr}(\text{NH}_3)_4]^+$	2.01	-19.5
$[(\text{nta})\text{Cr}(\text{OH})_2\text{Cr}(\text{en})_2]^+$	2.01	-19.8
$[(\text{nta})\text{Cr}(\text{OH})_2\text{Cr}(\text{tn})_2]^+$	2.01	-17.2
$[(\text{nta})\text{Cr}(\text{OH})_2\text{Cr}\{R,R(\text{chxn})\}_2]^+$	1.98	-25.5
$[(\text{nta})\text{Cr}(\text{OH})_2\text{Cr}(\text{trien})_2]^+$	1.96	-21.5
$[(\text{nta})\text{Cr}(\text{OH})_2\text{Cr}(\text{picam})_2]^+$	1.99	-20.5
$[(\text{nta})\text{Cr}(\text{OH})_2\text{Cr}(\text{bpy})_2]^+$	2.02	-31.4
$[(\text{nta})\text{Cr}(\text{OH})_2\text{Cr}(\text{phen})_2]^+$	1.98	-22.6

^aChloride salts. ^b $2J$ refers to the coupling constant determined from the observed susceptibility data.

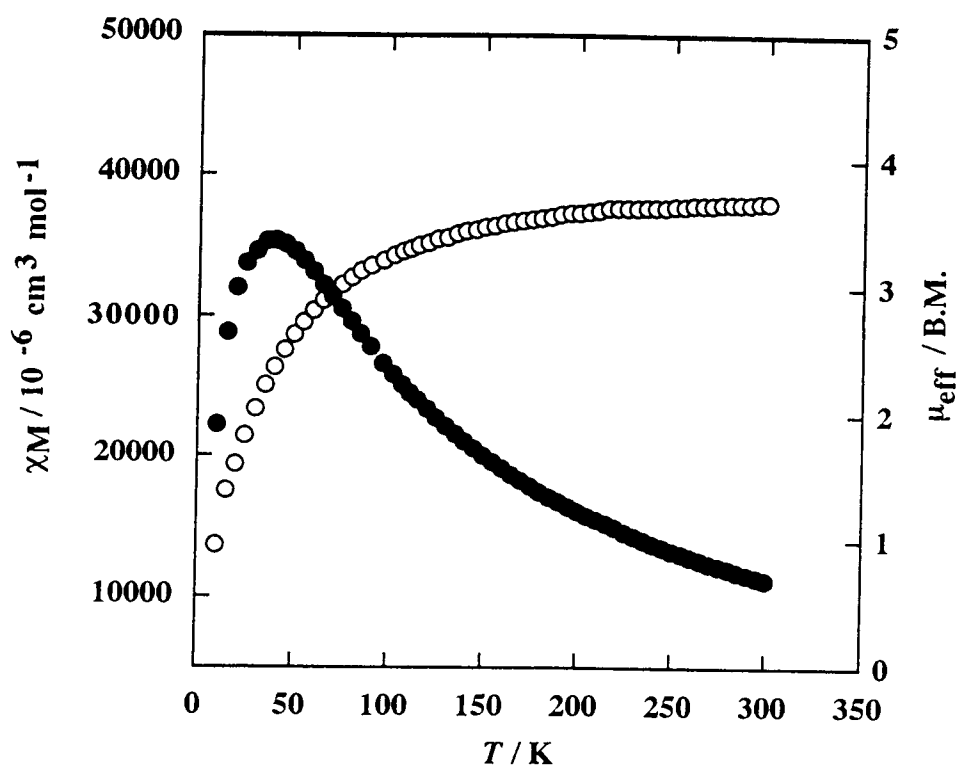


Figure 5-3. Temperature dependent magnetic susceptibility (χ_M , left scale, ●) and effective magnetic moment (μ_{eff} , right scale, ○) for $[(nta)Cr(OH)_2Cr(tn)_2]Cl \cdot 1.5H_2O$ (B-3).

Table 5-2. Magnetic parameters for $[(\text{nta})\text{Cr}(\text{OH})(\text{RCOO})\text{Cr}(\text{en})_2]^+$

R	g	$2J / \text{cm}^{-1\text{a}}$
H	2.01	-22.6
CH ₃	1.99	-20.0
CH ₃ CH ₂ CH ₂	1.98	-20.8
C ₆ H ₅	2.00	-21.1
CH ₃ CH ₂	1.97	-20.2
CH ₂ Cl	2.00	-22.5
CH ₂ ClCH ₂	2.01	-21.6
CH ₃ OCH ₂	1.99	-22.0

^a $2J$ refers to the coupling constant determined from the observed susceptibility data.

GHP model described, this difference in magnetic exchange interaction would be mainly due to the Cr-O bond difference between two complexes (see Table 3-6). Since the Cr-O bond lengths of the $[(\text{nta})\text{Cr}(\text{OH})_2\text{Cr}(\text{N})_4]^+$ complexes are also varied with $(\text{N})_4$ ligands described in Chapter 3, it is of interest in variation of their magnetic exchange coupling. As shown in Table 5-1, the $2J$ values are not so varied in wide range. From the X-ray structures, the $(\text{N})_4\text{Cr-OH}$ bond of $[(\text{nta})\text{Cr}(\text{OH})_2\text{Cr}(\text{tn})_2]\text{Cl}\cdot 1.5\text{H}_2\text{O}$ (**B-3**) is longer by 0.04\AA than that of $[(\text{nta})\text{Cr}(\text{OH})_2\text{Cr}(\text{phen})_2]\text{Cl}\cdot 7\text{H}_2\text{O}$ (**B-8**). On the other hand, the $(\text{nta})\text{Cr-OH}$ bond *trans* to the nitrogen atom of nta in $[(\text{nta})\text{Cr}(\text{OH})_2\text{Cr}(\text{tn})_2]\text{Cl}\cdot 1.5\text{H}_2\text{O}$ (**B-3**) is shorter by 0.03\AA than that in $[(\text{nta})\text{Cr}(\text{OH})_2\text{Cr}(\text{phen})_2]\text{Cl}\cdot 7\text{H}_2\text{O}$ (**B-8**). Since the magnetic exchange interaction mainly depends on the overlap between $d_{xz}(\text{a})$ and $d_{yz}(\text{b})$ orbitals *via* the p_z one on the bridging oxygen atom in $\text{di}(\mu\text{-OH})$ chromium(III) dinuclear complexes according to the GHP model, the averaged Cr-O bond length should be rather considered in this unsymmetrical dinuclear complexes. The average Cr-OH bond lengths are 1.954\AA and 1.94\AA for complex **B-3** and **B-8**, respectively. These average Cr-O bond lengths are not so changed to reveal the difference in the exchange coupling constant. Therefore the $2J$ values are not so different from each other in the $[(\text{nta})\text{Cr}(\text{OH})_2\text{Cr}(\text{N})_4]^+$ complexes, though $(\text{N})_4\text{Cr-OH}$ bonds are affected by the coordination bond character of $(\text{N})_4$ ligand as seen in X-ray structures.

5.3.2 $[(\text{nta})\text{Cr}(\text{OH})(\text{RCOO})\text{Cr}(\text{en})_2]^+$ complexes

The magnetic exchange interaction of $2J$ values varied from -20.0 to -22.6 cm^{-1} for $[(\text{nta})\text{Cr}(\text{OH})(\text{RCOO})\text{Cr}(\text{en})_2]^+$ complexes as shown in Table 5-2. Small change of $2J$ values are obtained in spite of the variation of bridging ligands. The bridging carboxylates are not affected in the magnetic exchange interaction. The Cr-O(H)-Cr exchange path would contribute mainly to the magnetic exchange interaction in these complexes. The structural parameters mainly Cr-O(H) bond would not be changed in each complexes, since the first absorption band maxima which is affected by the ligand field strength. Therefore the magnetic exchange interaction are not varied with complexes. This result indicates the direct contribution to the magnetic exchange interaction as an exchange path of the bridging

carboxylato ligand is not effective in these complexes.

5.3.3 $[\text{Cr}_2(\text{OH})_2(\text{RCOO})(\text{bispicam})_2]^{3+ \text{ or } 4+}$ complexes

Table 5-3 shows the summarized magnetic properties of μ -carboxylato chromium(III) dinuclear complexes. In Figure 5-4, plots of χ vs. T are shown for $[\text{Cr}_2(\text{OH})_2(\text{HCOO})(\text{bispicam})_2](\text{ClO}_4)_3 \cdot 0.5\text{H}_2\text{O}$ (**D-1**) and $[\text{Cr}_2(\text{OH})_2(\text{HCOO})(\text{bispicam})_2](\text{PF}_6)_3 \cdot 0.5\text{H}_2\text{O}$ (**D-5**). The results of the data fitting showed ferromagnetic exchange interactions between two chromium(III) ions in complexes **D-1**, **D-4** and **D-11** as shown in Table 5-3. The magnetic exchange interactions were changed from antiferromagnetic to ferromagnetic one depending upon the changes of the anion in the μ -HCOO and μ -CH₂ClCOO complexes. This remarkable change in magnetic exchange interactions for chromium(III) dinuclear complexes is firstly observed in this study. The bridging structure of these dinuclear complexes is intermediate between the edge-sharing and the face-sharing form as shown in Figure 5-5. The ferromagnetic exchange coupling in the μ -hydroxo bridged chromium(III) dinuclear complexes has been reported as $\text{Na}_4[\text{Cr}_2(\text{mal})_4(\text{OH})_2] \cdot \text{H}_2\text{O}$ ($2J = +2.16 \text{ cm}^{-1}$)⁸⁵ and $[\text{Cr}_2(\text{OH})_2(\text{histidine})_4]$ ($2J = +0.15 \text{ cm}^{-1}$).⁸⁶ The reason of this ferromagnetic exchange coupling was not explained in the literatures.^{85,86} Though the complexes in this study have the di(μ -hydroxo) structure, the $2J$ value of $[\text{Cr}_2(\text{OH})_2(\text{HCOO})(\text{bispicam})_2](\text{ClO}_4)_3 \cdot 0.5\text{H}_2\text{O}$ (**D-1**) ($2J = +28.0 \text{ cm}^{-1}$) is larger than those of $\text{Na}_4[\text{Cr}_2(\text{mal})_4(\text{OH})_2] \cdot \text{H}_2\text{O}$ and $[\text{Cr}_2(\text{OH})_2(\text{histidine})_4]$. This large ferromagnetic exchange interaction is also remarkable. On the other hand, the strong antiferromagnetic coupling ($2J = -67 \text{ cm}^{-1}$) was observed in the $[\text{Cr}_2(\text{OH})_2(\text{CH}_3\text{COO})(\text{tpen})](\text{ClO}_4)_3$ ¹⁸ which has the similar structures to the present dinuclear complexes. Moreover, it is noted that the $[\text{Cr}_2(\text{OH})_2(\text{SO}_4)(\text{bispicam})_2](\text{S}_2\text{O}_6) \cdot 3\text{H}_2\text{O}$ which has almost the same structure revealed antiferromagnetic coupling ($2J = -14.4 \text{ cm}^{-1}$).²⁸

Toftlund, Simonsen and Pedersen suggested that the strong antiferromagnetic exchange coupling in $[\text{Cr}_2(\text{OH})_2(\text{CH}_3\text{COO})(\text{tpen})](\text{ClO}_4)_3$ would be due to the existence of the exchange paths through the hydroxo ligands and the acetato one.¹⁸ However, another

Table 5-3. Magnetic parameters of $[\text{Cr}(\text{OH})_2(\text{HCOO})(\text{bispicam})_2]^{3+ \text{ or } 4+}$ complexes.

Complex	No.	$2J / \text{cm}^{-1}$	g value
$[\text{Cr}(\text{OH})_2(\text{HCOO})(\text{bispicam})_2](\text{ClO}_4)_3 \cdot 0.5\text{H}_2\text{O}$	C-1	28.0	1.96
$[\text{Cr}(\text{OH})_2(\text{HCOO})(\text{bispicam})_2]\text{I}_3 \cdot 5\text{H}_2\text{O}$	C-2	-2.04	2.02
$[\text{Cr}(\text{OH})_2(\text{HCOO})(\text{bispicam})_2]\text{Br}_3 \cdot 5\text{H}_2\text{O}$	C-3	-8.00	2.04
$[\text{Cr}(\text{OH})_2(\text{HCOO})(\text{bispicam})_2](\text{BF}_4)_3 \cdot 0.5\text{H}_2\text{O}$	C-4	1.32	1.96
$[\text{Cr}(\text{OH})_2(\text{HCOO})(\text{bispicam})_2](\text{PF}_6)_3 \cdot 1.5\text{H}_2\text{O}$	C-5	-9.01	2.02
$[\text{Cr}(\text{OH})_2(\text{CH}_3\text{COO})(\text{bispicam})_2](\text{ClO}_4)_3 \cdot 2.5\text{H}_2\text{O}$	C-6	-3.95	1.98
$[\text{Cr}(\text{OH})_2(\text{CH}_3\text{COO})(\text{bispicam})_2]\text{I}_3 \cdot 3\text{H}_2\text{O}$	C-7	-9.86	2.04
$[\text{Cr}(\text{OH})_2(\text{CH}_3\text{COO})(\text{bispicam})_2](\text{BF}_4)_3 \cdot \text{H}_2\text{O}$	C-8	-5.38	2.03
$[\text{Cr}(\text{OH})_2(\text{CH}_3\text{CH}_2\text{COO})(\text{bispicam})_2](\text{ClO}_4)_3 \cdot 0.5\text{H}_2\text{O}$	C-9	-2.17	2.00
$[\text{Cr}(\text{OH})_2(\text{CH}_2\text{ClCOO})(\text{bispicam})_2](\text{ClO}_4)_3 \cdot \text{H}_2\text{O}$	C-10	-3.11	2.02
$[\text{Cr}(\text{OH})_2(\text{CH}_2\text{ClCOO})(\text{bispicam})_2]\text{I}_3 \cdot 3\text{H}_2\text{O}$	C-11	11.9	1.94
$[\text{Cr}(\text{OH})_2(\text{CH}_2\text{ClCH}_2\text{COO})(\text{bispicam})_2](\text{ClO}_4)_3 \cdot 0.5\text{H}_2\text{O}$	C-12	-1.80	2.03
$[\text{Cr}(\text{OH})_2(\text{CH}_2\text{ClCH}_2\text{COO})(\text{bispicam})_2]\text{I}_3 \cdot 0.5\text{H}_2\text{O}$	C-13	-14.6	2.00
$[\text{Cr}_2(\text{OH})_2(\text{H}_3\text{NCH}_2\text{COO})(\text{bispicam})_2](\text{ClO}_4)_3 \cdot 3\text{H}_2\text{O}$	C-14	-2.01	1.99
$[\text{Cr}_2(\text{OH})_2(\text{H}_3\text{NCH}_2\text{CH}_2\text{COO})(\text{bispicam})_2](\text{ClO}_4)_3 \cdot 3\text{H}_2\text{O}$	C-15	-3.05	1.98
$[\text{Cr}_2(\text{OH})_2(\text{H}_3\text{NCH}_2\text{CH}_2\text{CH}_2\text{COO})(\text{bispicam})_2](\text{ClO}_4)_3$	C-16	-2.12	2.02
$[\text{Cr}_2(\text{OH})_2(\text{H}_3\text{NCH}(\text{CH}_3)\text{COO})(\text{bispicam})_2](\text{ClO}_4)_3 \cdot 3\text{H}_2\text{O}$	C-17	-3.41	2.01
$[\text{Cr}_2(\text{OH})_2(\text{H}_3\text{NCH}(\text{OH})\text{COO})(\text{bispicam})_2](\text{ClO}_4)_3 \cdot 3\text{H}_2\text{O}$	C-18	-4.03	2.02

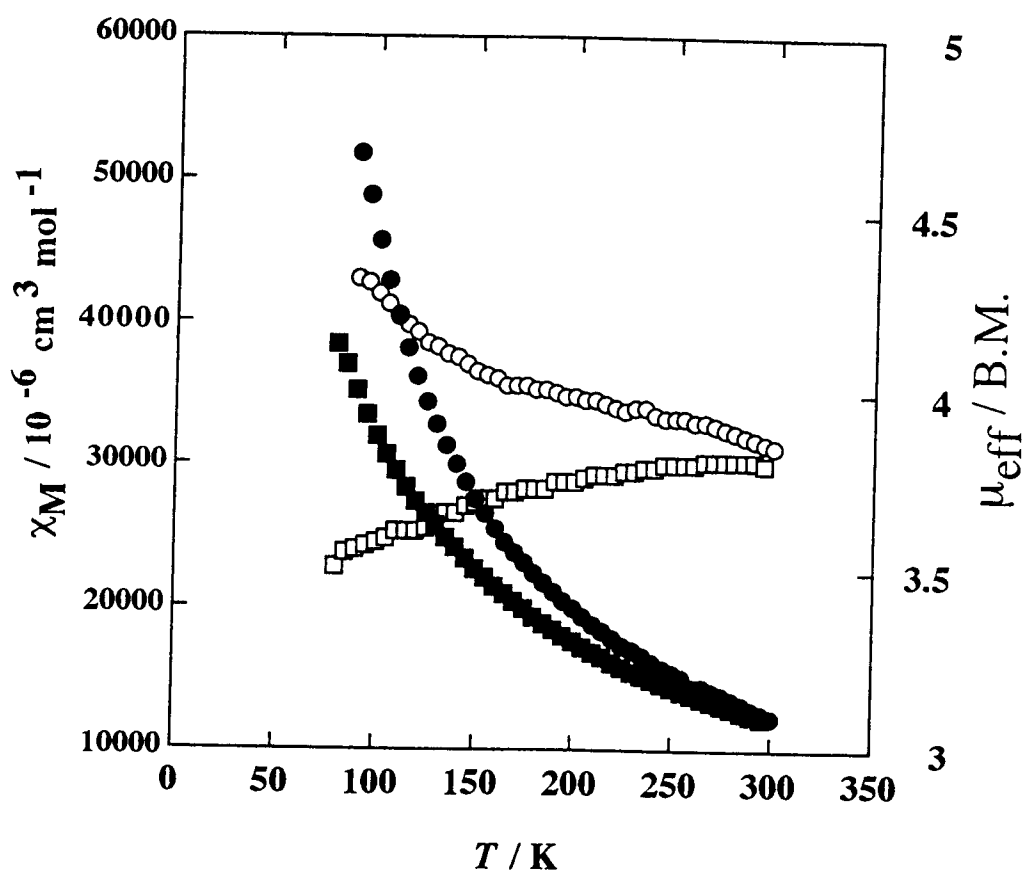


Figure 5-4. Temperature dependent magnetic susceptibility (χ_M , left scale) and effective magnetic moment (μ_{eff} , right scale) of $[\text{Cr}_2(\text{OH})_2(\text{HCOO})(\text{bispicam})_2](\text{ClO}_4)_3 \cdot 0.5\text{H}_2\text{O}$ (D-1) (\bullet , \circ) and $[\text{Cr}_2(\text{OH})_2(\text{HCOO})(\text{bispicam})_2](\text{PF}_6)_3 \cdot 1.5\text{H}_2\text{O}$ (D-5) (\blacksquare , \square).

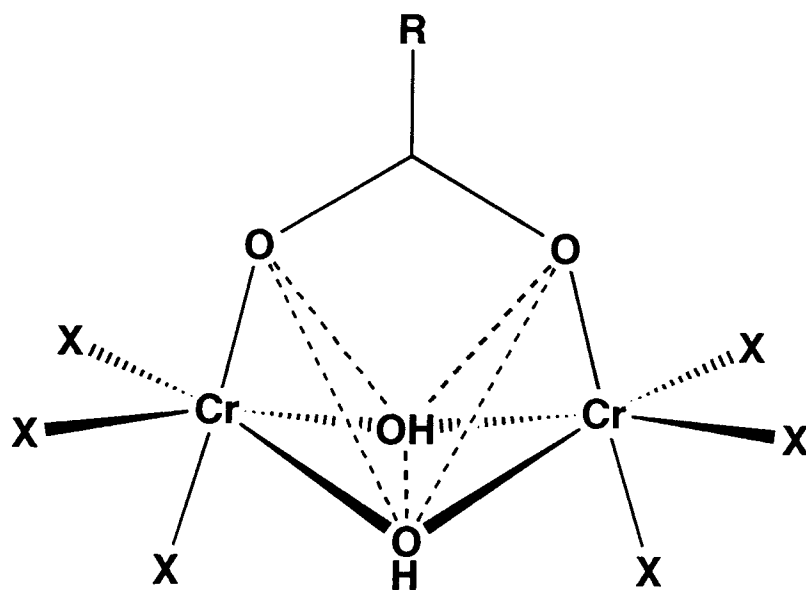


Figure 5-5. The bridging structure of $[\text{Cr}_2(\text{OH})_2(\text{RCOO})(\text{bispicam})_2]^{3+ \text{ or } 4+}$ type complexes.

exchange path which can perform antiferromagnetic exchange exists in the chromium(III) dinuclear complexes. Since this complex has a relatively short metal-metal distance, the strong antiferromagnetic coupling is anticipated to be due to a direct metal-metal interaction as described in the introduction. The coupling constant for $[\text{Cr}_2(\text{OH})_2(\text{CH}_3\text{COO})(\text{tpen})](\text{ClO}_4)_3$ is very applicable for their relationship between the metal-metal distances and $\ln|-2J|$ (the result is shown in Figure 5-6). From this result, in the magnetic exchange coupling of $[\text{Cr}_2(\text{OH})_2(\text{CH}_3\text{COO})(\text{tpen})](\text{ClO}_4)_3$, the direct metal-metal interaction is a predominant exchange path. Therefore, the existence of the exchange path through the carboxylate in $[\text{Cr}_2(\text{OH})_2(\text{CH}_3\text{COO})(\text{tpen})](\text{ClO}_4)_3$ is not clear. On the other hand, the possibility of the contribution of the direct metal-metal interaction in the face-sharing type dinuclear complexes is not favorable for the present ferromagnetic $[\text{Cr}_2(\text{OH})_2(\text{HCOO})(\text{bispicam})_2]^{3+ \text{ or } 4+}$ complexes, since that interaction reveals antiferromagnetic coupling in d^3 - d^3 electronic configuration as Wiegardt explained.^{83a} In addition, the antiferromagnetic exchange interactions of $[\text{Cr}_2(\text{OH})_2(\text{HCOO})(\text{bispicam})_2]^{3+ \text{ or } 4+}$ can not be explained by the metal-metal direct interaction. The $\ln|-2J|$ values of $[\text{Cr}_2(\text{OH})_2(\text{HCOO})(\text{bispicam})_2]^{3+ \text{ or } 4+}$ are plotted using the metal-metal distance of $[\text{Cr}_2(\text{OH})_2(\text{HCOO})(\text{bispicam})_2](\text{ClO}_4)_3 \cdot 0.5\text{H}_2\text{O}$ (**D-1**) in Figure 5-6. The $\ln|-2J|$ values of $[\text{Cr}_2(\text{OH})_2(\text{HCOO})(\text{bispicam})_2]^{3+ \text{ or } 4+}$ are widely distributed as surrounded by the dotted ellipsoids. The magnetic exchange interactions of these complexes cannot be explained by the face-sharing model.

Larsen, Michelsen and Pedersen reported that the calculated $2J$ value of $[\text{Cr}_2(\text{OH})_2(\text{SO}_4)(\text{bispicam})_2](\text{S}_2\text{O}_6) \cdot 3\text{H}_2\text{O}$ ($2J_{\text{calcd}} = -15 \text{ cm}^{-1}$) using GHP model was in agreement with the fitting data and the bridging sulfate ion was not an effective exchange path. Using the structural parameters of $r = 1.977 \text{ \AA}$, $\phi = 96.97^\circ$ and $\theta = 25.75^\circ$ in the $[\text{Cr}_2(\text{OH})_2(\text{HCOO})(\text{bispicam})_2](\text{ClO}_4)_3 \cdot 0.5\text{H}_2\text{O}$, the $2J$ value is calculated according to the GHP model. The calculated $2J$ values is -22.8 cm^{-1} (antiferromagnetic coupling) and different from the observed value. In addition, it assumes that the structural parameters of the other $[\text{Cr}_2(\text{OH})_2(\text{HCOO})(\text{bispicam})_2]^{3+ \text{ or } 4+}$ complexes are not so different from those of complex **D-1**, the observed $2J$ values of them are also smaller than this calculated one. The

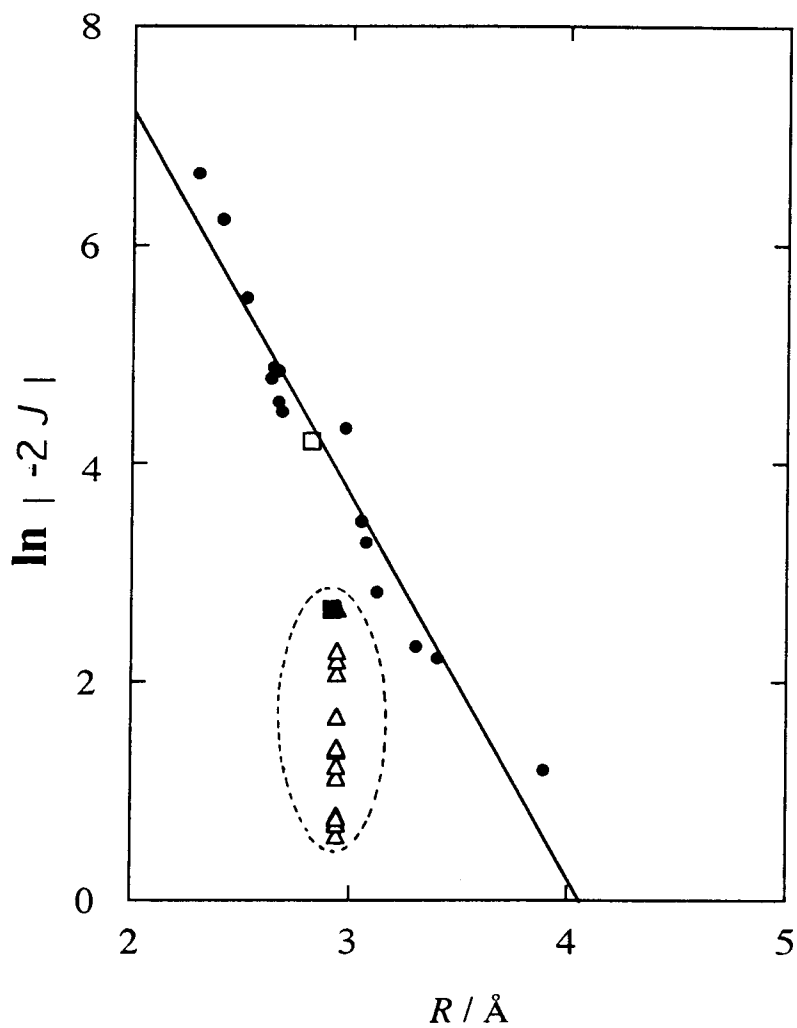


Figure 5-6. A plot of $\ln |-2J|$ vs. metal-metal distance R for face-sharing dinuclear complexes. The symbols \square and \blacksquare denote $[\text{Cr}_2(\text{OH})_2(\text{CH}_3\text{COO})(\text{tpen})](\text{ClO}_4)_3$ and $[\text{Cr}_2(\text{OH})_2(\text{SO}_4)(\text{bispicam})_2](\text{S}_2\text{O}_6) \cdot 3\text{H}_2\text{O}$, respectively. The $2J$ values for $[\text{Cr}_2(\text{OH})_2(\text{RCOO})(\text{bispicam})_2]^{3+ \text{ or } 4+}$ are indicated as symbol \triangle . The data (●) for $[\text{M}(\mu\text{-X})_3\text{M}]$ type are from reference 83.

GHP model also cannot elucidate observed magnetic exchange coupling in $[\text{Cr}_2(\mu\text{-OH})_2(\mu\text{-RCOO})(\text{bispicam})_2]^{3+ \text{ or } 4+}$.

The carboxylato bridging ligand must be taken into account as an additional effective exchange path in $[\text{Cr}_2(\text{OH})_2(\text{RCOO})(\text{bispicam})_2]^{3+ \text{ or } 4+}$. The apparent magnetic interaction would be a sum of the two hydroxo bridged path and carboxylato bridged one as following equation:

$$J_{\text{obsd}} = J_{\text{OH}} + J_{\text{RCOO}}$$

where J_{obsd} , J_{OH} and J_{RCOO} are the observed coupling constant, the contribution of the OH path and that of the RCOO one, respectively. Since the ferromagnetic term in OH path is small according to the GHP model, the ferromagnetic contribution in apparent magnetic coupling constant would be due to the RCOO path. Assuming almost the constant of ferromagnetic contribution in RCOO path in the J_{RCOO} value in each complexes, the remarkable change in magnetic exchange interaction from antiferromagnetic to ferromagnetic is due to the change of the J_{OH} one which is influenced by the structural parameters of bridging unit. While the crystal structures which exhibit antiferromagnetic coupling are not obtained, the small antiferromagnetic contribution of OH path arise from the decrease of the overlap between p_z and d_{yz} or d_{xz} because of the large θ values in the crystals. The large θ value brings to the change the hybridized orbital from sp^2 to sp^3 in the bridging OH, and then the Cr-O bond becomes longer.⁷²

The carboxylato bridging ligand as an exchange path was reported by Inoue and Kubo in the formate-copper(II) complexes.⁸⁷ They claimed that there are ferromagnetic σ -exchange path and antiferromagnetic π -exchange path in the formate bridging ligand. The contribution of the substituent R in the carboxylato ligand is not clear in $[\text{Cr}_2(\text{OH})_2(\text{RCOO})(\text{bispicam})_2]^{3+ \text{ or } 4+}$.

It is concluded that this is a certain first example to suggest that the carboxylato bridging ligands are the obvious important magnetic exchange path in the chromium(III) dinuclear complexes.

6. Base Hydrolysis Reaction in Chromium(III)-Chromium(III) Dinuclear Complexes

6.1 Introduction

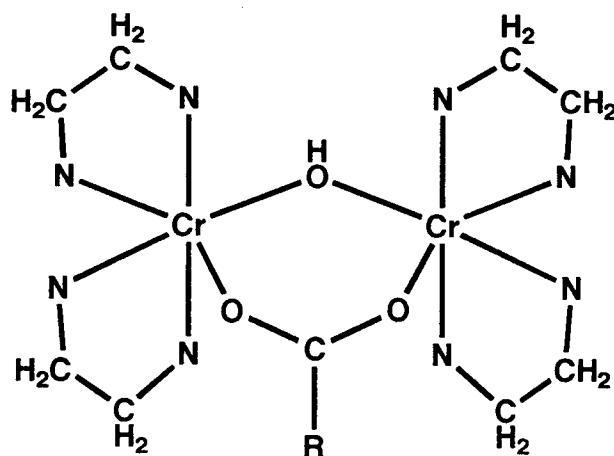
Though a number of chromium(III) dinuclear complexes have been also investigated from the kinetic view points,^{11,12,13,15,45,88} there has been few studies on the correlation between properties of the ligands and the reactivities in the bridging units. Springborg and Toftlund reported that the base hydrolysis of $[\text{Cr}_2(\text{OH})(\text{RCOO})(\text{en})_4]^{4+}$ with $\text{R} = \text{H}, \text{CH}_3$, and NH_3CH_2 were presumed to be affected by acid strengths of free carboxylic acids from the semiquantitative comparison of the half-life times.⁴⁵ The recent kinetic study on the $\mu\text{-CF}_3\text{COO}$ bridging complex $[\text{Cr}_2(\text{OH})(\text{CF}_3\text{COO})(\text{en})_4]^{4+}$ revealed that the hydrolysis reaction undertakes through two stages with easy loss of the bridging carboxylate ligand.¹⁵

As described in Chapters 2, it was found that $[(\text{nta})\text{Cr}(\text{OH})_2\text{Cr}(\text{en})_2]^+$ reacts with many carboxylic acids (RCOOH) to form $[(\text{nta})\text{Cr}(\text{OH})(\text{RCOO})\text{Cr}(\text{en})_2]^+$ in aqueous solution. These dinuclear complexes are expected to a suitable candidate to clarify the reaction mechanism related to the on substituent effects of the bridging carboxylates and the effect of the ligands in comparison with those for $[\text{Cr}_2(\text{OH})(\text{RCOO})(\text{en})_4]^{4+}$. Their structures which confirmed in Chapter 3, are shown in Figure 6-1.

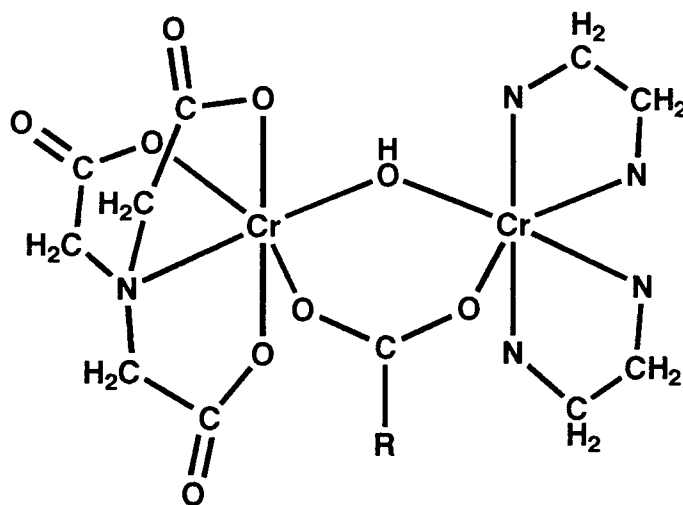
In this chapter, the kinetics of base hydrolysis of $[\text{Cr}_2(\text{OH})(\text{RCOO})(\text{en})_4]^{4+}$ and $[(\text{nta})\text{Cr}(\text{OH})(\text{RCOO})\text{Cr}(\text{en})_2]^+$ at 25 °C were described. The effects of substituent groups of carboxylates and of non-bridging ligand on the base hydrolysis reaction rates and the reaction mechanisms will be discussed.

6.2 Experimental

6.2.1 Instruments. UV/VIS spectra were recorded on a HITACHI 330 and a Shimadzu UV-2100 spectrophotometers at room temperature. Stopped flow measurements were carried out by an Union Giken Stopped-flow RA-401 spectrophotometer. Deuteron-2 NMR spectra were measured using a JEOL JNM-GSX-270 FT NMR spectrometer at 25 °C. The data were collected on mixing solutions initially containing equivalent volume of 0.01



(a)



(b)

Figure 6-1. Molecular structures of $[\text{Cr}_2(\mu\text{-OH})(\mu\text{-RCOO})(\text{en})_4]^{4+}$ (a) and $[(\text{nta})\text{Cr}(\mu\text{-OH})(\mu\text{-RCOO})\text{Cr}(\text{en})_2]^+$ (b).

M solution of the complexes and 1 M NaOH solution in 10 mm tubes. The external standard was C^2HCl_3 7.24 ppm with the downfield shift defined as positive.

The column chromatography to separate the reaction intermediates from the reaction solution was carried out in the following conditions with SP-Sephadex (C-25 Na^+ form and 1.5 x 20 cm) and/or QAE-Sephadex (A-25 Cl^- form and 1.5 x 20 cm) ion exchanger. The eluting solution was 0.1 M $\text{NH}_3/\text{NH}_4\text{Cl}$ aqueous buffered solution at pH 9.5.

6.2.2 Kinetic measurements. The kinetics of base hydrolysis for $[\text{Cr}_2(\text{OH})(\text{RCOO})(\text{en})_4]^{4+}$ (**C-1a - 7a**) were monitored at 363 and 527 nm in 10 mm quartz cells thermostated at 25 ± 0.1 °C using a Shimadzu UV-2100 spectrophotometer. Since the reactions of the μ -formato and μ -monochloroacetato complexes were very fast, they were followed at 363 nm by employing the stopped flow method. The hydroxide ion concentration dependence of the rates were investigated for the reactions with NaOH solution ranging in concentration from 0.1 to 0.5 M. The initial concentrations of the complexes were 3×10^{-3} M. All spectrophotometric measurements were made by mixing equivalent volume of each solution in a cell at constant ionic strengths of 0.5 M adjusted with NaClO_4 .

The base hydrolysis of $[(\text{nta})\text{Cr}(\text{OH})(\text{RCOO})\text{Cr}(\text{en})_2]^+$ (**C-1b - 8b**) were followed spectrometrically by using a Shimadzu UV-160 or UV-2100 spectrophotometer at 700 nm in 10 mm cells thermostated at 25 ± 0.1 °C. The hydroxide ion concentration dependence of the rates were investigated for the reactions with NaOH solution ranging in concentration from 0.05 to 2 M at constant ionic strengths of 2 M adjusted with NaClO_4 . The initial concentrations of the complexes are 5×10^{-3} M.

Pseudo-first-order rate constants (k_{obsd}) were determined by plotting $\ln(A_t - A_{\text{inf}})$ vs. time. Reactions were followed for at least 4 half-lives. Rate constants were calculated from the slope of the plots using the following relationship

$$\ln(A_t - A_{\text{inf}}) = -k_{\text{obsd}}t + \ln(A_0 - A_{\text{inf}}) \quad (1),$$

where A_0 , A_{inf} , and A_t refer to the absorbances at the initial, infinite, and t time, respectively. Kinetic runs are carried out at least three times. The reproducibility of rate constants for the repeated experiments was found to be within 9%.

6.3 Results and Discussion

6.3.1 Kinetics of base hydrolysis for $[\text{Cr}_2(\text{OH})(\text{RCOO})(\text{en})_4]^{4+}$ (en complexes, **C-1a - 7a**). The color of the aqueous solution of $[\text{Cr}_2(\text{OH})(\text{RCOO})(\text{en})_4]^{4+}$ changed rapidly from red to blue by addition of hydroxide ion. This color change is due to the deprotonation of the hydroxo bridge as reported by Springborg and Toftlund.⁴⁵ The deprotonation reaction rate is too fast to follow it even with a stopped-flow method. After deprotonation, the UV/VIS spectra of the blue complex giving absorption maxima at 580, 450 and 363 nm changed with time. The isosbestic points are observed at 385, 430 and 558 nm in the early phase of the reaction as shown in Figure 6-2. At 363 nm, the absorbance was simply decreased and converged to A_{inf} whereas at 527 nm it was initially increased and then decreased. The isosbestic points vanished as the reaction proceeded. These spectral changes are ascribed to the first and second stages in the whole reaction.

The SP-Sephadex column chromatography at 5 min and 60 min during the base hydrolysis gave two bands, showing a tripositive and an unipositive complex ion in view of the concentrations of the eluting solutions. The amount of the former and the latter bands decreased and increased, respectively, at 60 min as compared with those at 5 min. They are identified as mono- μ -OH dinuclear $[(\text{OH})(\text{en})_2\text{Cr}(\mu\text{-OH})\text{Cr}(\text{OH})(\text{en})_2]^{3+}$ and mononuclear *cis*- $[\text{Cr}(\text{OH})_2(\text{en})_2]^+$ not only by the UV/VIS spectra,⁶⁸ but also by the ^2H NMR spectra of the $\mu\text{-CD}_3\text{COO}^-$ complex as follows.

The ^2H NMR chemical shift behavior of CD_3COO^- makes possible to distinguish among an uncoordinated form, monodentate one and a bridged ligand coordinated to chromium(III) ions. The NMR signals for the monodentate acetato ligand appear at about 20 ppm.^{55,89} On the other hand, the bridging acetato ligands exhibit a signal ranging in chemical shifts from about 60 to 40 ppm.^{55,89} Before addition of hydroxide ion, only one ^2H NMR signal was observed at 56 ppm as in Figure 6-3a. This is assignable to the bridging deuteriated acetato ligand in $[\text{Cr}_2(\text{OH})(\text{CD}_3\text{COO})(\text{en})_4]^{4+}$. When hydroxide ion was added, three signals at 39.0, 17.8 and 3.0 ppm appeared (Figure 6-3b). Among them, the signal intensity at 3.0 ppm increased with time and kept almost unchanged after

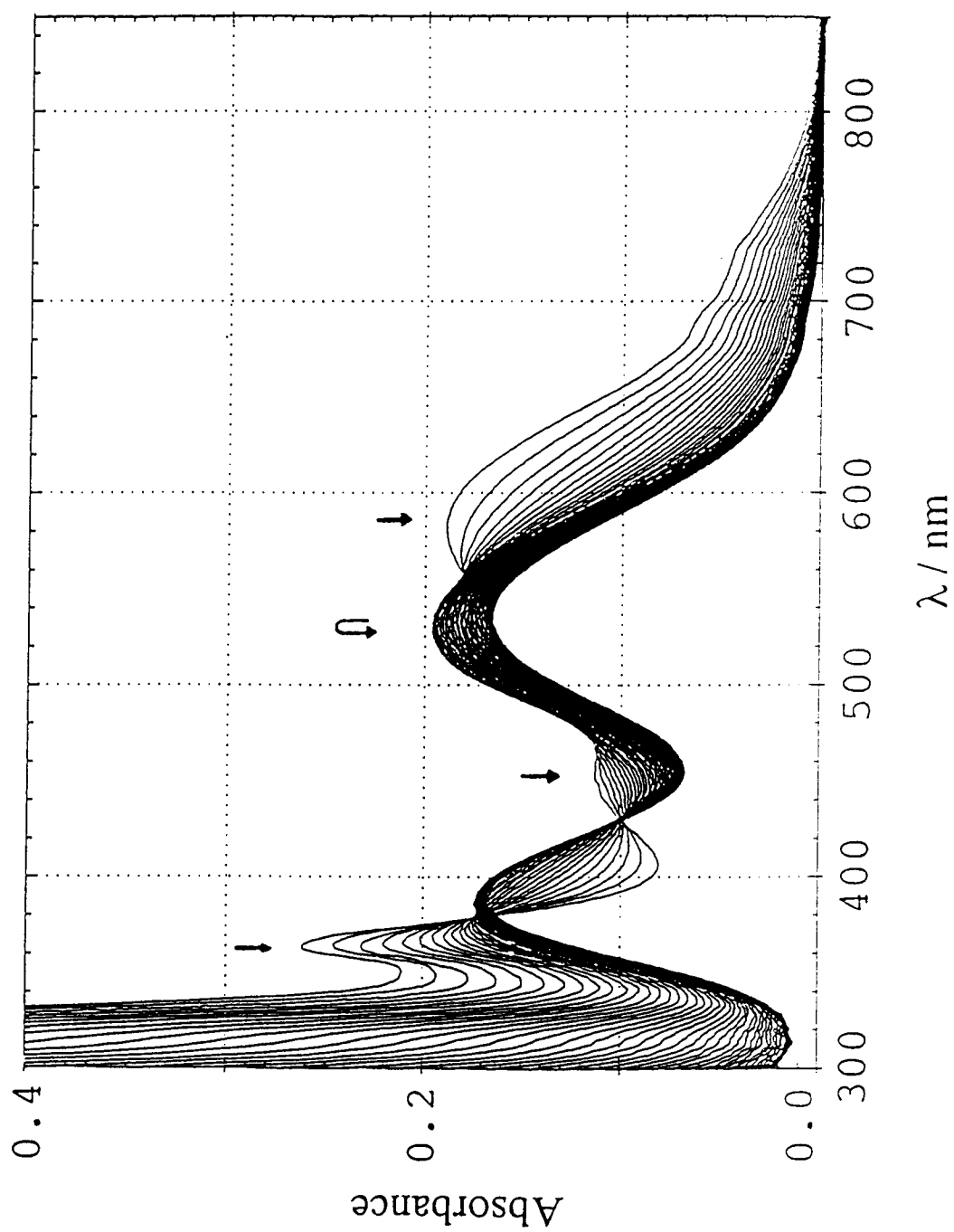


Figure 6-2. Absorption spectral change of $[\text{Cr}_2(\mu\text{-OH})(\mu\text{-CH}_3\text{COO})(\text{en})_4]^{++}$ solution (**C-2a**) (initial 5 mM) over two hours after adding NaOH aqueous solution ($[\text{OH}] = 0.5 \text{ M}$) at 25°C . Total scanning time is 90 min. Time interval between scans was 90 sec.

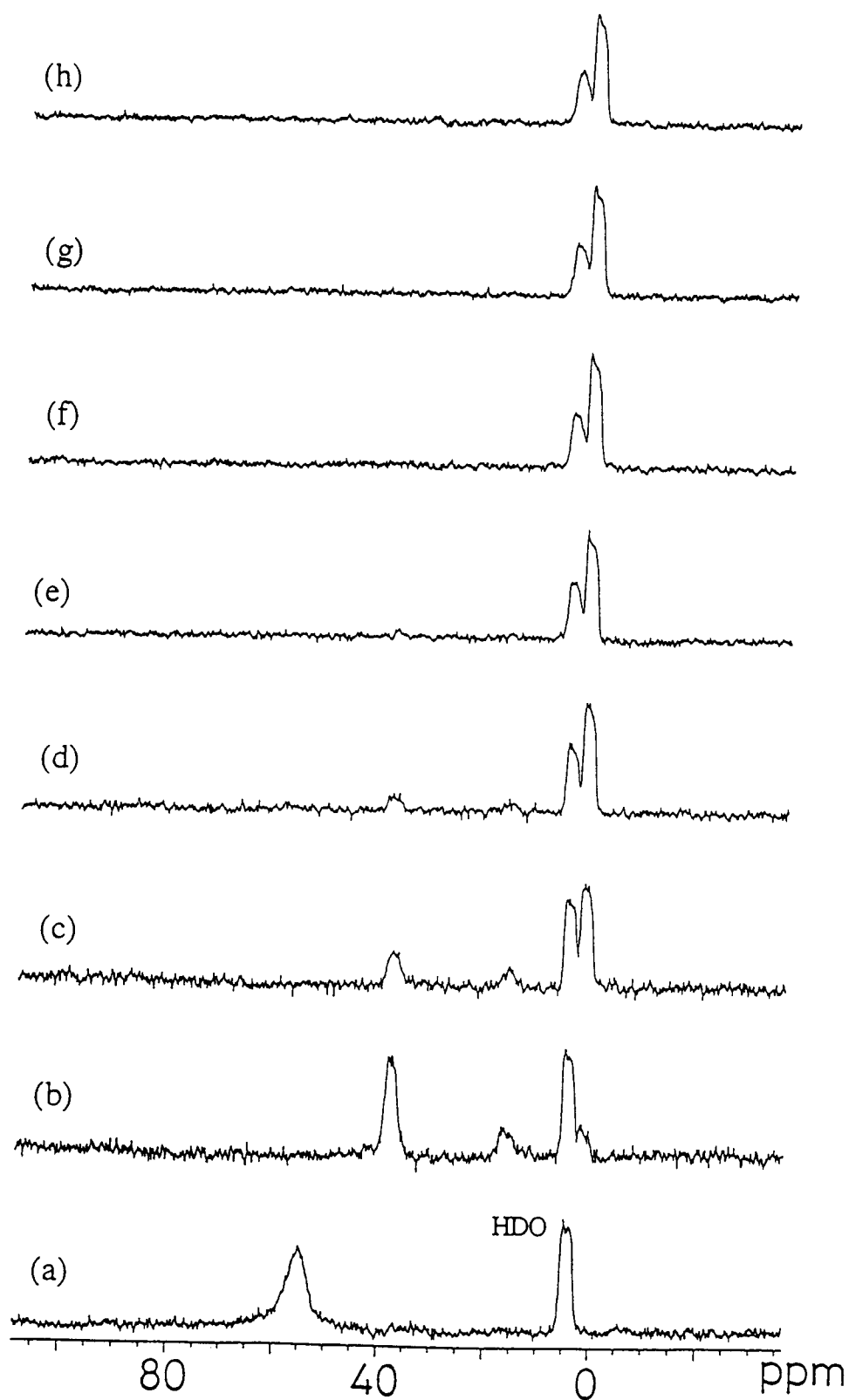
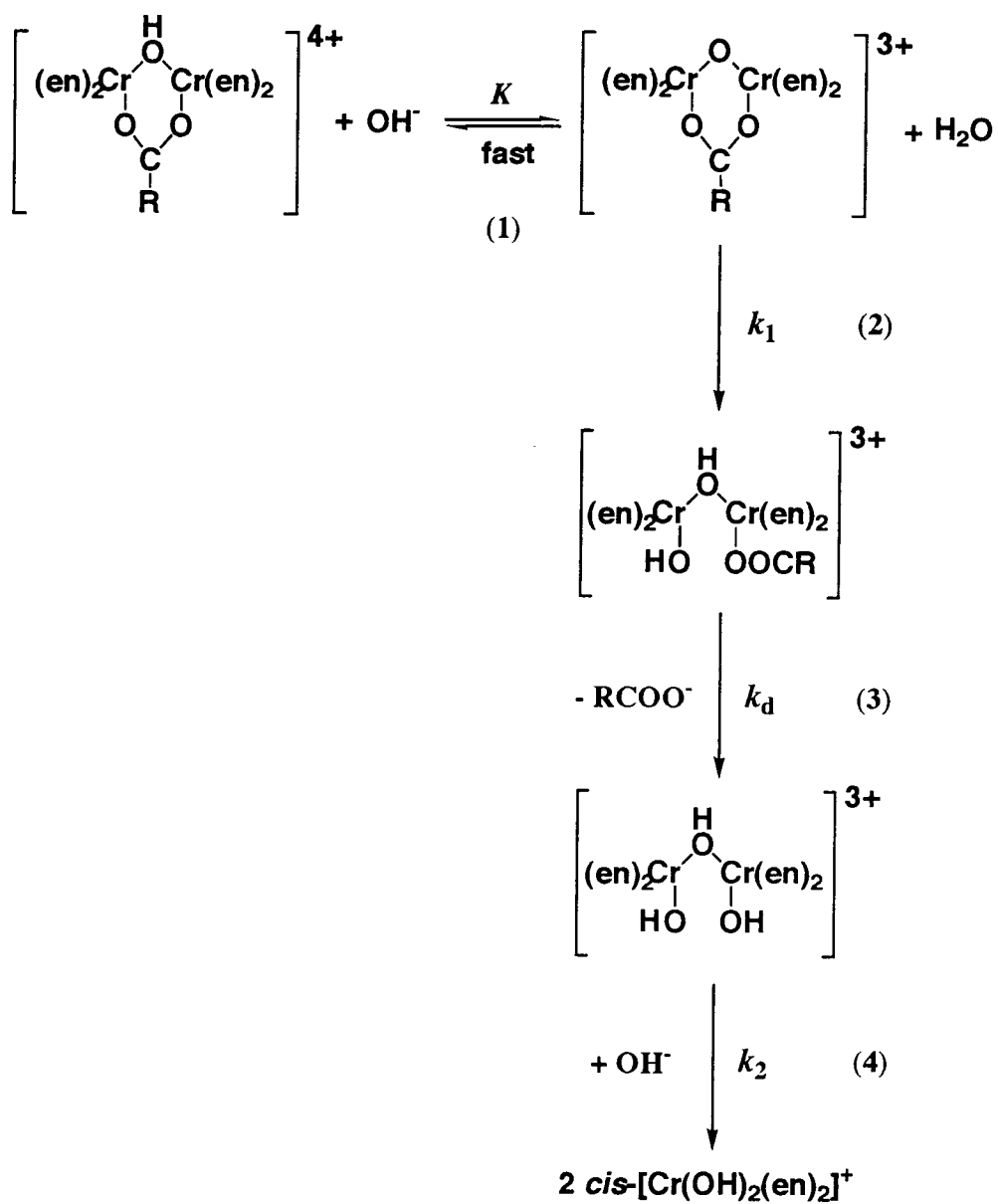


Figure 6-3. ^2H NMR spectral change of $[\text{Cr}_2(\mu\text{-OH})(\mu\text{-CD}_3\text{COO})(\text{en})_4]^{4+}$ solution (a), before adding NaOH solution; after adding NaOH aqueous solution (b) 5 min, (c) 10 min, (d) 15 min, (e) 20 min, (f) 30 min, (g) 40 min and (h) 50 min.



Scheme 6-1. Base hydrolysis reaction mechanism of $[\text{Cr}_2(\mu\text{-OH})(\mu\text{-RCOO})(\text{en})_4]^{4+}$.

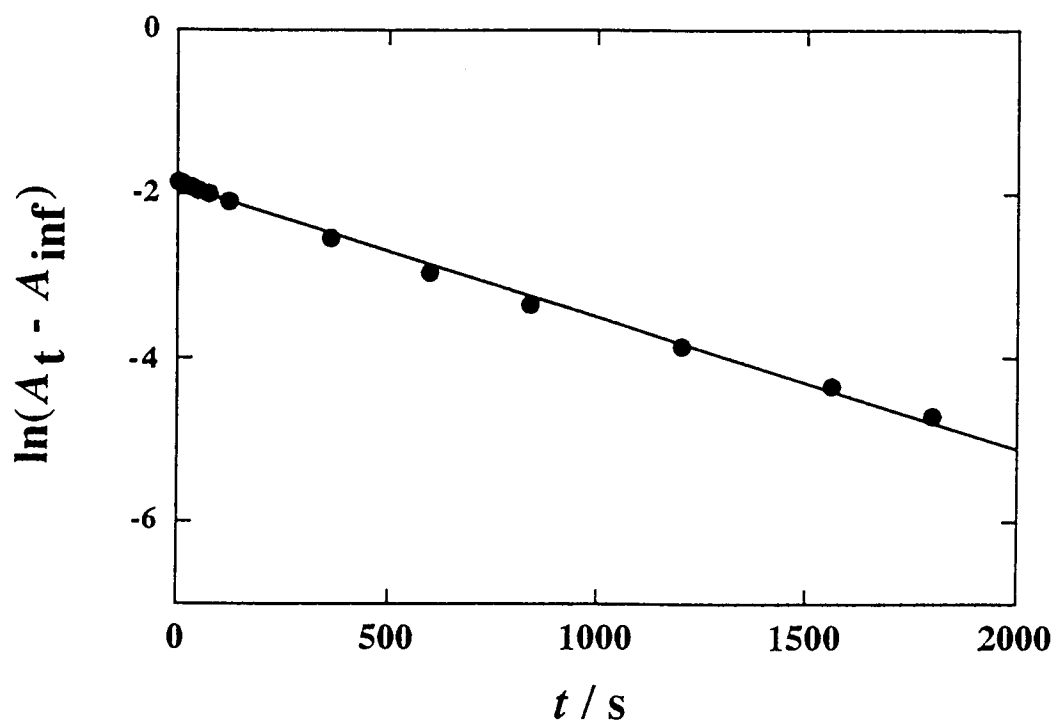


Figure 6-4. Plot of $\ln(A_t - A_{\text{inf}})$ at 363 nm vs. time for the reaction of $[\text{Cr}_2(\mu\text{-OH})(\mu\text{-CH}_3\text{COO})(\text{en})_4]^{4+}$ (**C-2a**) with NaOH aqueous solution ($[\text{OH}] = 0.5 \text{ M}$) at 25°C and $I = 0.5 \text{ M}$ (NaClO_4).

about 40 min. This signal is due to free uncoordinated CD_3COO^- ion in view of the chemical shift. The remaining two signals at 39.0 and 17.8 ppm decreased with time and finally disappeared. The signal at 39.0 ppm is assigned to the bridging acetato in the deprotonated $[\text{Cr}_2(\mu\text{-O})(\mu\text{-CD}_3\text{COO})(\text{en})_4]^{3+}$. Since this deprotonated complex changed to $[(\text{OH})(\text{en})_2\text{Cr}(\text{OH})\text{Cr}(\text{OH})(\text{en})_2]^{3+}$ complex in the early phase of the reaction, there can be no formation of a mononuclear complex containing monodentate CD_3COO^- like $[\text{Cr}(\text{OH})(\text{CD}_3\text{COO})(\text{en})_2]^+$. Thus, the other signal at 17.8 ppm is due to monodentate CD_3COO^- ligand in $[(\text{OH})(\text{en})_2\text{Cr}(\mu\text{-OH})\text{Cr}(\text{CD}_3\text{COO})(\text{en})_2]^{3+}$, of which the amount is small in view of the intensity. This is supported by ^2H NMR spectral change exhibiting a complete disappearance of the coordinated CD_3COO^- signal and an appearance of free CD_3COO^- signal in the acetato bridge cleavage reaction.

From these experimental results, the first stage reaction involves an acetato bridge cleavage giving mono- $\mu\text{-OH}$ complex as Springborg and Toftlund claimed.⁴⁵ The second stage reaction is a decomposition of the dinuclear complex. The rate-determining steps exist in the first and second stage reactions. Almost the same absorption spectral changes were observed for all the $\mu\text{-carboxylato}$ complexes as well as the $\mu\text{-acetato}$ complex. In addition, the column chromatography for all the $\mu\text{-carboxylato}$ complexes gave two eluates corresponding to $[(\text{OH})(\text{en})_2\text{Cr}(\text{OH})\text{Cr}(\text{OH})(\text{en})_2]^{3+}$ and *cis*- $[\text{Cr}(\text{OH})_2(\text{en})_2]^+$. Accordingly, the reaction mechanism for the $\mu\text{-carboxylato}$ complexes is the same as that for the $\mu\text{-acetato}$ complex. Therefore, the reaction mechanism for the $\mu\text{-carboxylato}$ en complexes is depicted as in Scheme 6-1.

The apparent rate constant ($k_1(\text{obsd})$) for the first stage reaction (carboxylato bridge cleavage) and the second stage (k_2) reaction (decomposition to the mononuclear complex) rates in Scheme 6-1(2) and (4) were obtained by monitoring the absorbances at 363 nm (Figure 6-4) and 527 nm (arrows in Figure 6-2), respectively. The obtained kinetic data were summarized in Table 6-1. The influence from the second stage reaction rate is removed by the monitor at 363 nm, where only the first one is observed, and vice versa at 527 nm. For the monodentate carboxylato ligand dissociation reaction in Scheme 6-1(3), the rate constant (k_d) can not be estimated in this experiment, in view of a small amount of

Table 6-1. Rate constants for $[\text{Cr}_2(\text{OH})(\text{RCOO})(\text{en})_4]^{4+}$ complexes^a

R	$[\text{OH}^-] / \text{mol dm}^{-3}$	$k_1(\text{obsd}) / \text{s}^{-1}$	$k_2 / 10^{-4} \text{ s}^{-1}$
H	0.1	0.299 ± 0.016	3.14 ± 0.04^b
	0.2	0.543 ± 0.011	3.13 ± 0.04^c
	0.25	0.649 ± 0.004	3.16 ± 0.04^d
	0.4	0.909 ± 0.022	3.15 ± 0.04^e
CH_2Cl	0.1	0.070 ± 0.001	3.14 ± 0.06^b
	0.2	0.108 ± 0.003	3.18 ± 0.08^c
	0.25	0.121 ± 0.001	3.26 ± 0.08^d
	0.4	0.159 ± 0.006	3.12 ± 0.02^e
CH_3OCH_2	0.1	$(0.660 \pm 0.008) \times 10^{-2}$	3.15 ± 0.04
	0.25	$(1.04 \pm 0.02) \times 10^{-2}$	3.16 ± 0.07
	0.4	$(1.24 \pm 0.01) \times 10^{-2}$	3.18 ± 0.03
	0.5	$(1.40 \pm 0.02) \times 10^{-2}$	3.19 ± 0.02
CH_2ClCH_2	0.1	$(1.46 \pm 0.02) \times 10^{-3}$	3.13 ± 0.07
	0.25	$(1.51 \pm 0.01) \times 10^{-3}$	3.17 ± 0.06
	0.4	$(1.51 \pm 0.02) \times 10^{-3}$	3.18 ± 0.05
	0.5	$(1.52 \pm 0.02) \times 10^{-3}$	3.28 ± 0.02
CH_3	0.1	$(1.47 \pm 0.02) \times 10^{-3}$	3.21 ± 0.05
	0.25	$(1.50 \pm 0.01) \times 10^{-3}$	3.24 ± 0.03
	0.4	$(1.57 \pm 0.02) \times 10^{-3}$	3.24 ± 0.06
	0.5	$(1.59 \pm 0.01) \times 10^{-3}$	3.35 ± 0.05
C_2H_5	0.1	$(7.35 \pm 0.03) \times 10^{-4}$	3.21 ± 0.02
	0.25	$(8.64 \pm 0.03) \times 10^{-4}$	3.14 ± 0.04
	0.4	$(8.80 \pm 0.02) \times 10^{-4}$	3.15 ± 0.04
	0.5	$(9.24 \pm 0.02) \times 10^{-4}$	3.20 ± 0.03
$\text{n-C}_3\text{H}_7$	0.1	$(6.78 \pm 0.03) \times 10^{-4}$	3.07 ± 0.04
	0.25	$(7.37 \pm 0.04) \times 10^{-4}$	3.11 ± 0.01
	0.4	$(7.57 \pm 0.03) \times 10^{-4}$	3.11 ± 0.04
	0.5	$(7.60 \pm 0.01) \times 10^{-4}$	3.08 ± 0.04
$\{[\text{Cr}(\text{OH})(\text{en})_2]_2(\mu\text{-OH})\}^{3+}$ ^f	0.1		3.07 ± 0.02
	0.25		3.08 ± 0.01
	0.4		3.09 ± 0.01
	0.5		3.14 ± 0.03

^a $I = 0.5 \text{ mol dm}^{-3} \text{ NaClO}_4$ at 25°C . ^b 0.1 mol dm^{-3} of $[\text{OH}^-]$. ^c 0.25 mol dm^{-3} of $[\text{OH}^-]$. ^d 0.4 mol dm^{-3} of $[\text{OH}^-]$. ^e 0.5 mol dm^{-3} of $[\text{OH}^-]$. ^f Rate constants of the decomposition reaction of the dinuclear complex to the mononuclear one.

$[(\text{OH})(\text{en})_2\text{Cr}(\text{OH})\text{Cr}(\text{CD}_3\text{COO})(\text{en})_2]^{3+}$ as observed for the NMR spectra and of only the early phase detection of the kinetic measurements in the decarboxylation of the μ -oxo- μ -carboxylato complexes (Scheme 6-1(2) and (3)).

The half-lives estimated from the $k_1(\text{obsd})$ values for the μ -acetato (**C-2a**) and μ -formato (**C-1a**) complexes are in the similar order of magnitude ($t_{1/2} \sim 6$ min and 1 sec, respectively) to those for the these complexes reported by Springborg and Toftlund.⁴⁵ The hydroxide ion concentration dependence was observed for the apparent rate constant ($k_1(\text{obsd})$) of the first stage reaction, but not for the second stage (k_2) ones.

Taking into account the acid-base equilibrium of $[\text{Cr}_2(\text{OH})(\text{RCOO})(\text{en})_4]^{4+}$ as shown in Scheme 6-1(1), these reactions lead to the rate laws about the pseudo-first-order constant $k_1(\text{obsd})$:

$$-\frac{d[\text{Cr}_2(\mu\text{-O})(\mu\text{-RCOO})(\text{en})_4]^{3+}}{dt} = k_1([\text{Cr}_2(\mu\text{-O})(\mu\text{-RCOO})(\text{en})_4]^{3+})$$

let

a = initial concentration of $[\text{Cr}_2(\text{OH})(\text{RCOO})(\text{en})_4]^{4+}$ complexes,

x = fraction of carboxylato bridge cleavaged complex at time t ,

$[A]$ = concentration of species of $[\text{Cr}_2(\text{OH})(\text{RCOO})(\text{en})_4]^{4+}$ complex at time t ,

$[B]$ = concentration of species of deprotonated $[\text{Cr}_2(\mu\text{-O})(\mu\text{-RCOO})(\text{en})_4]^{3+}$ complex at time t ,

$[\text{OH}^-]$ = hydroxide ion concentration ($[\text{OH}^-] \gg a$).

Then

$$K = \frac{[B][\text{H}_2\text{O}]}{[A][\text{OH}^-]}$$

and $a - x = [A] + [B]$.

$$\text{So that } [B] = \frac{K[\text{OH}^-]}{1+K[\text{OH}^-]} (a - x)$$

$$\text{Then } \frac{d[\text{carboxylato bridge cleavaged complex}]}{dt} = k_1[B] = \frac{k_1 \cdot K[\text{OH}]}{1+K[\text{OH}]} (a - x)$$

Integrating this equation, we can obtain

$$\ln \frac{a}{a-x} = \frac{k_1 \cdot K[\text{OH}]}{1+K[\text{OH}]} t = k_1(\text{obsd})t$$

Hence the obtained pseudo-first-order constant $k_1(\text{obsd})$ is given by

$$k_1(\text{obsd}) = \frac{K[\text{OH}]}{1+K[\text{OH}]} k_1$$

This equation can be rearranged to following form

$$\frac{1}{k_1(\text{obsd})} = \frac{1}{k_1} + \frac{1}{k_1 \cdot K} \cdot \frac{1}{[\text{OH}]} \quad (2)$$

As seen in Figure 6-5, plots of $1/k_1(\text{obsd})$ vs. $1/[\text{OH}]$ give straight lines. Thus, we can obtain the reaction rate constant k_1 and the equilibrium constant K from the slope and intercept of the $1/k_1(\text{obsd})$ vs. $1/[\text{OH}]$ plot, respectively.

Using the equilibrium constant K , the acid strengths of the bridging hydroxo ligand ($\text{p}K_a = -\log(K \cdot K_w)$) can be calculated. The k_1 , k_2 , K and $\text{p}K_a$ values are summarized in Table 6-2. For the $\mu\text{-CH}_3\text{COO}^-$ complex, the $\text{p}K_a$ value (12.0) agrees with the estimated value of Springborg and Toftlund.³ The first stage reaction rate constants k_1 varied largely from 2.88 s^{-1} to $7.88 \times 10^{-4} \text{ s}^{-1}$ with variation of carboxylates in $[\text{Cr}_2(\mu\text{-OH})(\mu\text{-RCOO})(\text{en})_4]^{4+}$. Springborg and Toftlund concluded that the carboxylato bridge cleavage reaction becomes plausibly slower as acid strengths ($\text{p}K_a'$) of the corresponding carboxylic acids decrease.⁴⁵ On this basis, the reaction rate (k_1) of the μ -monochloroacetato (**C-5a**, $\text{p}K_a' = 2.68$) and μ -methoxyacetato (**C-7a**, $\text{p}K_a' = 3.31$) complex is supposed to be faster than that of the μ -formato (**C-1a**, $\text{p}K_a' = 3.55$) one. However, the k_1 values for the former two complexes are found to be smaller by one or two order of magnitude than the latter one. These data cannot be accounted for only by the

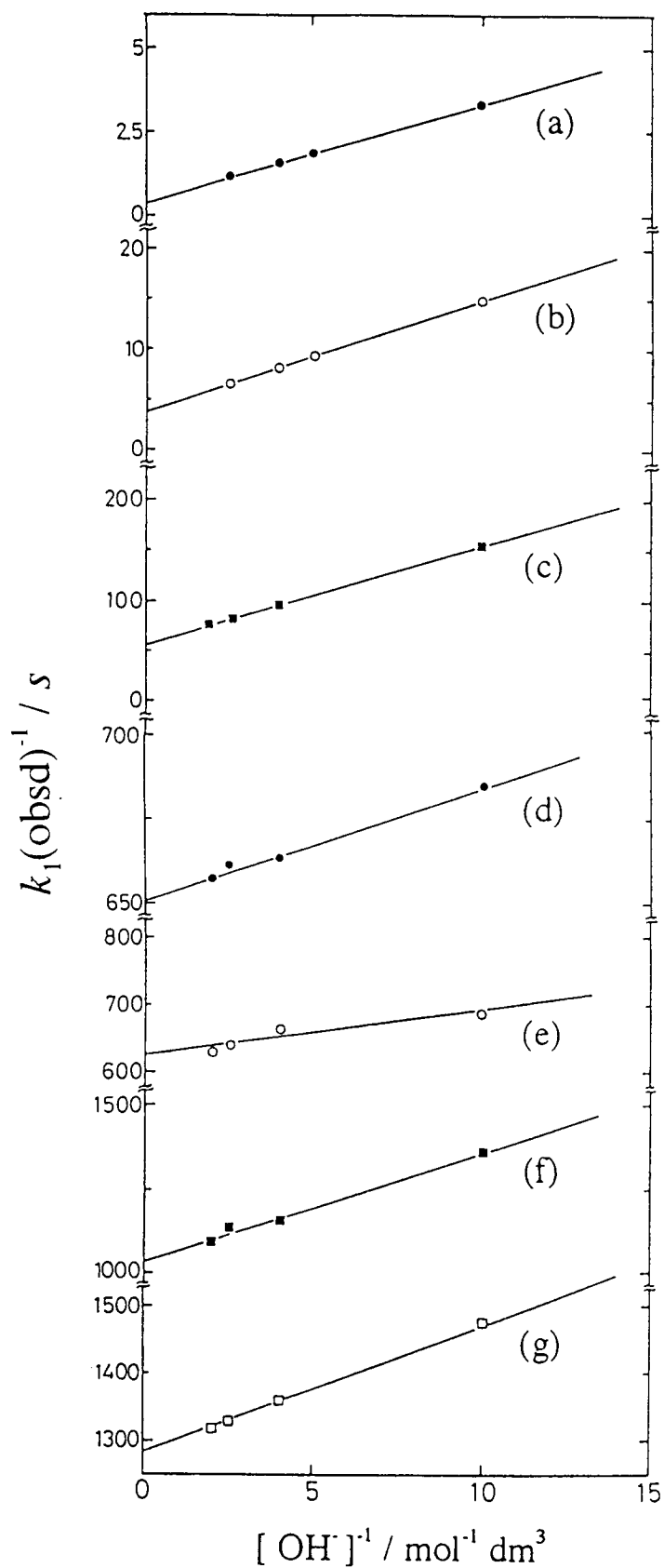


Figure 6-5. Plots of $k_1(\text{obsd})^{-1}$ vs. $[\text{OH}^-]^{-1}$ of $[\text{Cr}_2(\mu\text{-OH})(\mu\text{-RCOO})(\text{en})_4]^{4+}$; (a), R = H; (b), CH_2Cl ; (c), CH_3OCH_2 ; (d), CH_2ClCH_2 ; (e), CH_3 ; (f), CH_3CH_2 ; (g), $\text{CH}_3\text{CH}_2\text{CH}_2$.

Table 6-2. Kinetic data for $[\text{Cr}_2(\text{OH})(\text{RCOO})(\text{en})_4]^{4+}$ complexes^a

R	k_1 / s^{-1b}	$k_2 / 10^{-4} \text{s}^{-1bc}$	K^{bd}	$\text{p}K_a^{ef}$	$\text{p}K_a^{fg}$
H	2.88(4)	3.15(1)	1.16(2)	13.9	3.75
CH_2Cl	$2.57(16) \times 10^{-1}$	3.18(6)	3.71(27)	13.4	2.87
CH_3OCH_2	$1.83(9) \times 10^{-2}$	3.17(7)	5.58(39)	13.3	3.57
CH_2ClCH_2	$1.54(1) \times 10^{-3}$	3.19(10)	193(24)	11.7	4.11
CH_3	$1.60(3) \times 10^{-3}$	3.26(9)	109(42)	12.0	4.76
CH_3CH_2	$9.70(2) \times 10^{-4}$	3.18(5)	31.4(30)	12.5	4.87
$\text{CH}_3\text{CH}_2\text{CH}_2$	$7.88(2) \times 10^{-4}$	3.09(6)	63.1(21)	12.2	4.82

^a $I = 0.5 \text{ mol dm}^{-3}$ with NaClO_4 at 25°C . ^b Standard deviations are given in parentheses in units of the last decimal. ^c Average value. ^d Equilibrium constant for the Scheme 6-1 (1). ^e $\text{p}K_a = -\log(K \cdot K_w)$ for $\mu\text{-OH}$ moiety. ^f The uncertainty estimated at $\pm 0.2 \text{ p}K_a$ unit. ^g Acid dissociation constants for RCOOH from *Critical Stability Constants*; Smith, R. M., Martell, A. E. Eds.; Plenum Press: New York, 1989; Vol 6.

acidity of the carboxylates in the bridging unit. This subject will be discussed later in detail on the basis of the substituent effect other than the acidity of the carboxylic acid.

The k_2 values are almost the same for all the complexes. Since the rate-determining step reaction in the second stage one is a decomposition of the mono- μ -OH complex $[(\text{OH})(\text{en})_2\text{Cr}(\mu\text{-OH})\text{Cr}(\text{OH})(\text{en})_2]^{3+}$ to the mononuclear complexes, it is reasonable that the k_2 values of each complex are independent of the substituent group R of the μ -RCOO complexes.

6.3.2 Kinetics of base hydrolysis of $[(\text{nta})\text{Cr}(\text{OH})(\text{RCOO})\text{Cr}(\text{en})_2]^+$ (nta complex, **C-1b - 8b**). As in the case of the en complexes, by addition of NaOH solution to aqueous solution of the nta complexes, the rapid color change occurred from reddish violet to blue. This observation suggests the deprotonation of the hydroxo bridge in $[(\text{nta})\text{Cr}(\text{OH})(\text{RCOO})\text{Cr}(\text{en})_2]^+$. The absorption spectra of the blue solution showed maxima at 510 and 372 nm and an inflection at 700 nm. After deprotonation, the UV-vis spectra changed with time as in Figure 6-6.

Successive column chromatography with SP-Sephadex cation and QAE-Sephadex anion ion-exchangers at 2 and 40 min after addition of hydroxide ion gave one and two bands for an uncharged red band and a unipositive and a dinegative ones, respectively in view of the elution behavior. The amounts of the latter two complexes increased with time.

These species were characterized by the ^2H NMR spectral change of the reaction solution for the μ - CD_3COO^- complex. A signal at 47.4 ppm observed before addition of OH^- ion is assigned to $[(\text{nta})\text{Cr}(\mu\text{-OH})(\mu\text{-CD}_3\text{COO})\text{Cr}(\text{en})_2]^+$ (Figure 6-7a). When OH^- ion was added, two signals appeared at 40.0 and 18.0 ppm (Figure 6-7b). The 40.0 ppm signal completely disappeared after 10 min (Figure 6-7c). The 18.0 ppm signal decreased with time, and a new 20.0 ppm one appeared. After then the signal intensity remained unchanged. The signals at 18.0 and 20.0 ppm are assigned to the monodentate CD_3COO^- ligand coordinated to the μ -OH dinuclear and mononuclear complexes, respectively, according to the column chromatographic behavior and the reported data.^{55,89} Unlike $[\text{Cr}_2(\text{OH})(\text{CD}_3\text{COO})(\text{en})_4]^{4+}$, the half-life of a signal attributable to the coordinated

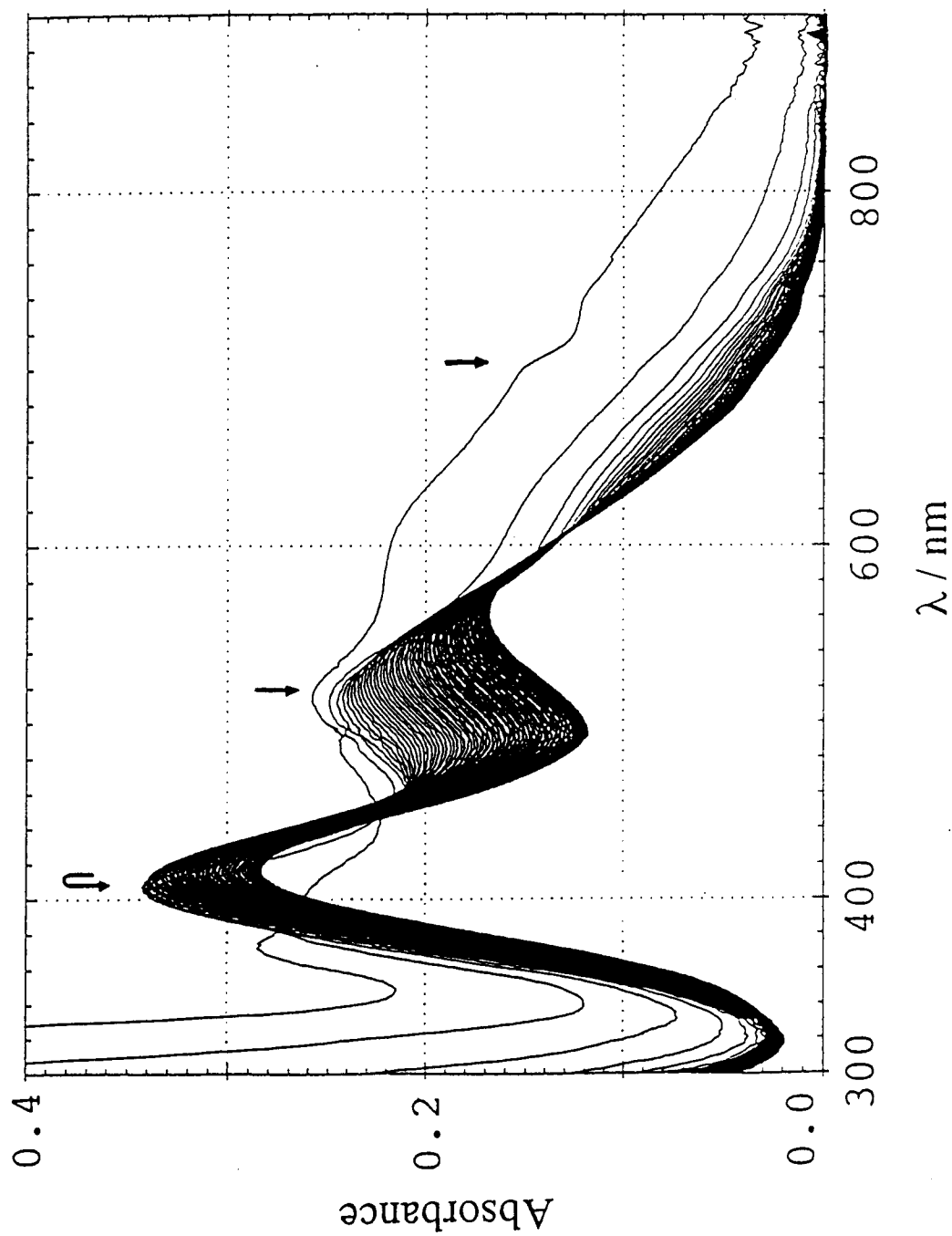


Figure 6-6. Absorption spectral change of $[(\text{nia})\text{Cr}(\mu\text{-OH})(\mu\text{-CH}_3\text{COO})\text{Cr}(\text{en})_2]^+$ solution (C-2b) (initial 3 mM) over one hour after adding aqueous NaOH solution ($[\text{OH}^-] = 0.5 \text{ M}$) at 25°C . Total scanning time is 60 min. Time interval between scans was 90 sec.

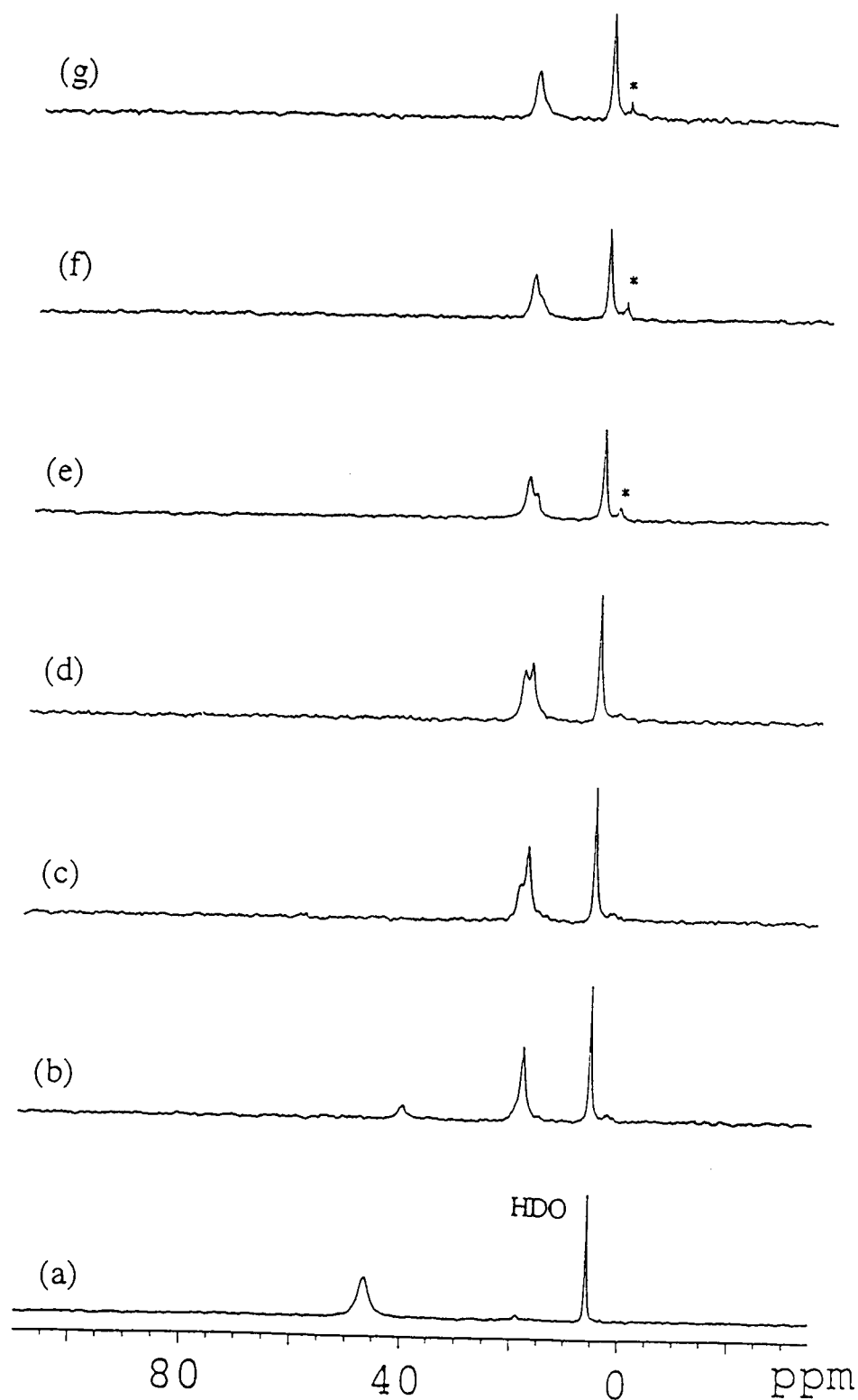
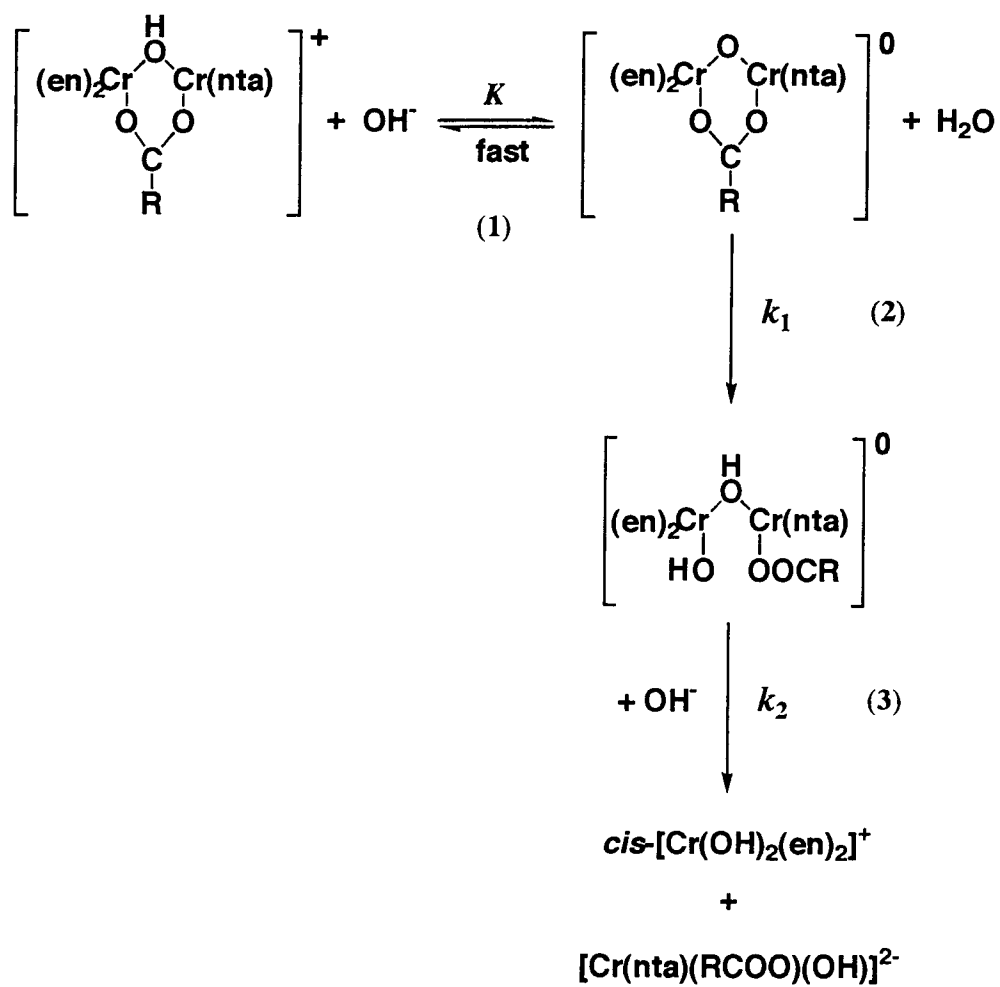


Figure 6-7. ^2H NMR spectral change of $[(\text{nta})\text{Cr}(\mu\text{-OH})(\mu\text{-CD}_3\text{COO})\text{Cr}(\text{en})_2]^+$ solution after adding NaOH aqueous solution; (a) before adding NaOH solution, (b) 5 min after, (c) 10 min, (d) 15 min, (e) 20 min, (f) 30 min and (g) 40 min. Asterisks exhibit free CD_3COO^- anion due to the decomposition of the reaction product.



Scheme 6-2. Base hydrolysis reaction mechanism of $[(\text{nta})\text{Cr}(\mu\text{-OH})(\mu\text{-RCOO})\text{Cr}(\text{en})_2]^+$.

CD₃COO⁻ ligand is longer in this reaction; showing the formation of the monodentate acetato complex. This fact gives a clue to determine a cleavage reaction site of the carboxylato bridges (Cr(en)₂ or Cr(nta) site). If the cleavage occurs at the Cr(nta) site, the CD₃COO⁻ ligand could remain at the Cr(en)₂ one. In this case, the ²H NMR signal of the monodentate acetate must appear but disappear within a few minutes similarly as for [Cr₂(OH)(CD₃COO)(en)₄]⁴⁺. This is contrary to the observation for the nta complex.

The Cr-O bond of the μ-RCOO⁻ *cis* to the tertiary amine of the nta in the structure of [(nta)Cr(OH)(RCOO)Cr(en)₂]⁺ (Figure 6-1(b)) is assumed to be relatively inert as claimed for the aquation of [Cr(nta)(im)₂].⁵⁷ Therefore, the first stage reaction of the carboxylato bridge cleavage occurs at the Cr(en)₂ site to give the mono-μ-OH complex [(CD₃COO)(nta)Cr(μ-OH)Cr(OH)(en)₂].

Furthermore, a ln(A_t - A_{inf}) vs. time plot of the absorbance at 700 nm reveals two stage reactions as shown in Figure 6-8. The apparent rate constants (k₁(obsd)) for the first stage reaction were obtained from the early steep line (insert in Figure 6-8) and the second ones (k₂) from the late less steep line. The obtained kinetic data were summarized in Table 6-3. All the carboxylato bridging complexes as well as the μ-acetato complex showed almost the same absorption spectral changes. The similar column chromatographic behavior were observed for all the μ-carboxylato complexes. Accordingly, the reaction mechanism for the μ-carboxylato complexes appears to be the same as that for the μ-acetato complex.

From the above results, the reaction mechanism is proposed as the following Scheme 6-2. Scheme 6-2 is analogous to Scheme 6-1 except that one of the final products contain the monodentate carboxylato ligand. For these complexes, both the k₁(obsd) and k₂ rate constants exhibit no hydroxide ion concentration dependence. According to the equation (2), therefore, the observed k₁(obsd) values equal the first stage reaction rate constant k₁. In this condition, K[OH⁻] >> 1 holds, resulting in much larger values for K than those of the en complexes. It is noted that the acid strengths for the unipositive nta complexes are unexpectedly much stronger than those for the tetrapositive en complexes. The k₁ (= k₁(obsd)) and k₂ values are summarized in Table 6-4.

As compared with the k₁ values for [Cr₂(OH)(RCOO)(en)₄]⁴⁺,

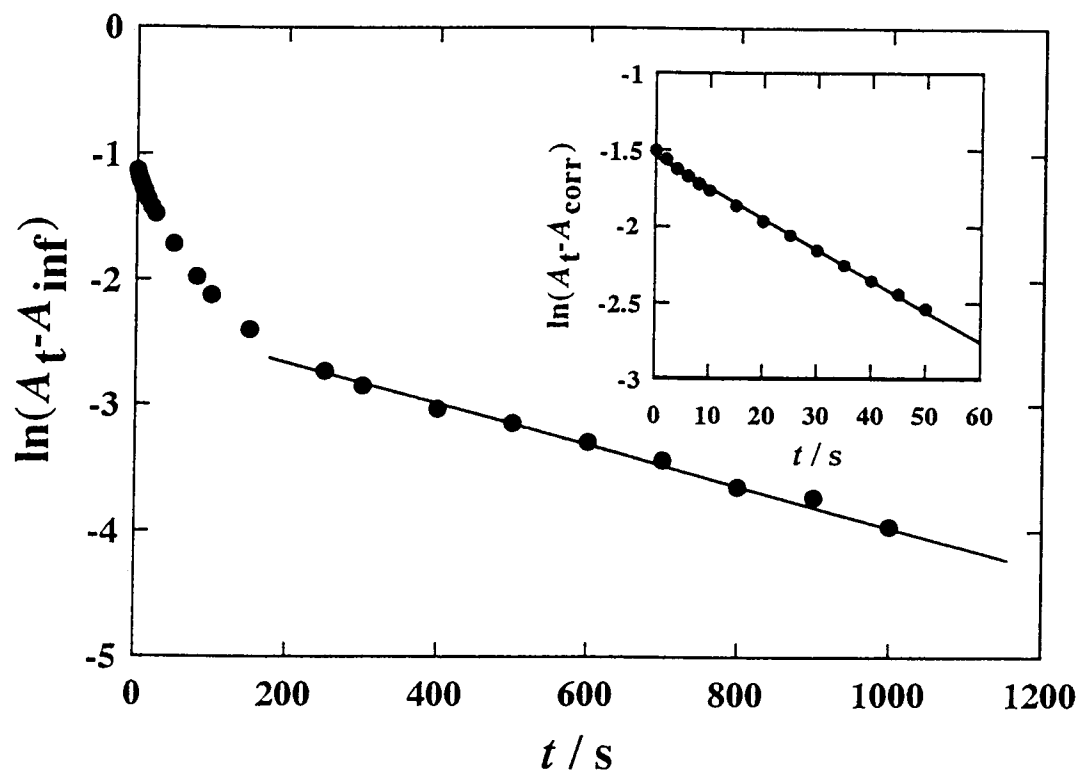


Figure 6-8. Plot of $\ln(A_t - A_{\text{inf}})$ vs. time at 700 nm for the reaction of $[(\text{nta})\text{Cr}(\mu\text{-OH})(\mu\text{-CH}_3\text{COO})\text{Cr}(\text{en})_2]^+$ (**C-2b**) with NaOH aqueous solution ($[\text{OH}] = 0.5 \text{ M}$) at 25°C and $I = 2 \text{ M}$ (NaClO_4). The insert shows plot of $\ln(A_t - A_{\text{corr}})$ vs. time.

Table 6-3. Rate constants for [(nta)Cr(OH)(RCOO)Cr(en)₂]⁺ complexes^a

R	[OH ⁻] / mol dm ⁻³	<i>k</i> ₁ (obsd) / 10 ⁻² s ⁻¹	<i>k</i> ₂ / 10 ⁻³ s ⁻¹
H	0.05	6.77 ± 0.03	1.98 ± 0.08
	0.5	6.78 ± 0.04	1.90 ± 0.05
	1.0	6.90 ± 0.05	1.95 ± 0.06
	2.0	6.92 ± 0.06	1.99 ± 0.04
CH ₃	0.05	2.10 ± 0.04	1.96 ± 0.04
	0.5	2.01 ± 0.06	1.85 ± 0.03
	1.0	1.88 ± 0.01	1.76 ± 0.04
	2.0	1.95 ± 0.01	1.71 ± 0.02
n-C ₃ H ₇	0.05	1.77 ± 0.02	1.93 ± 0.02
	0.5	1.68 ± 0.02	1.93 ± 0.03
	1.0	1.76 ± 0.02	2.00 ± 0.02
	2.0	1.73 ± 0.02	2.04 ± 0.04
C ₆ H ₅	0.05	1.68 ± 0.02	1.76 ± 0.02
	0.5	1.74 ± 0.02	1.81 ± 0.04
	1.0	1.72 ± 0.03	1.79 ± 0.04
	2.0	1.73 ± 0.04	1.90 ± 0.03
C ₂ H ₅	0.05	1.65 ± 0.01	1.76 ± 0.01
	0.5	1.62 ± 0.01	1.78 ± 0.01
	1.0	1.64 ± 0.02	1.77 ± 0.02
	2.0	1.65 ± 0.03	1.76 ± 0.03
CH ₂ Cl	0.05	1.56 ± 0.03	1.61 ± 0.03
	0.5	1.57 ± 0.03	1.74 ± 0.02
	1.0	1.58 ± 0.02	1.68 ± 0.01
	2.0	1.60 ± 0.02	1.90 ± 0.04
CH ₃ OH ₂	0.05	1.55 ± 0.02	1.94 ± 0.02
	0.5	1.52 ± 0.01	1.99 ± 0.01
	1.0	1.56 ± 0.02	2.03 ± 0.02
	2.0	1.56 ± 0.02	1.97 ± 0.02
CH ₂ ClCH ₂	0.05	1.64 ± 0.03	1.91 ± 0.04
	0.5	1.63 ± 0.02	1.98 ± 0.04
	1.0	1.61 ± 0.03	1.95 ± 0.05
	2.0	1.61 ± 0.01	1.84 ± 0.07

^a *I* = 2 mol dm⁻³ NaClO₄ at 25 °C.

Table 6-4. Kinetic data for $[(\text{nta})\text{Cr}(\text{OH})(\text{RCOO})\text{Cr}(\text{en})_2]^+$ complexes^a

R	$k_1/10^{-2} \text{ s}^{-1\text{b,c}}$	$k_2/10^{-3} \text{ s}^{-1\text{b,c}}$
H	6.87(8)	1.96(4)
CH ₃	1.99(9)	1.82(11)
CH ₃ CH ₂ CH ₂	1.74(4)	1.98(5)
C ₆ H ₅	1.72(3)	1.82(6)
CH ₃ CH ₂	1.64(1)	1.77(1)
CH ₂ Cl	1.58(2)	1.73(12)
CH ₂ ClCH ₂	1.62(2)	1.92(6)
CH ₃ OCH ₂	1.55(2)	1.98(4)

^a $I = 2 \text{ mol dm}^{-3}$ at 25 °C. ^b Average value. ^c Standard deviations are given in parentheses in units of the last decimal.

$[(\text{nta})\text{Cr}(\text{OH})(\text{RCOO})\text{Cr}(\text{en})_2]^+$ give little variation of the k_1 ones with the same order of magnitude. On the other hand, the k_2 values of $[(\text{nta})\text{Cr}(\text{OH})(\text{RCOO})\text{Cr}(\text{en})_2]^+$ are almost the same for all the complexes. The k_2 values correspond to the rates of the hydroxo bridge cleavage reaction of mono- μ -OH complexes to the mononuclear ones. In the mono- μ -OH complex $[(\text{RCOO})(\text{nta})\text{Cr}(\mu\text{-OH})\text{Cr}(\text{OH})(\text{en})_2]$, there are two reaction sites of the hydroxo bridges ($\text{Cr}(\text{en})_2$ or $\text{Cr}(\text{nta})$ site). If the cleavage occurs at the $\text{Cr}(\text{en})_2$ -OH site, the k_2 values should be close to those for the $[\text{Cr}_2(\text{OH})(\text{RCOO})(\text{en})_4]^{4+}$. However, the present reactions for the nta complexes are about six times faster than those of the corresponding $[\text{Cr}_2(\text{OH})(\text{RCOO})(\text{en})_4]^{4+}$. In this reaction stage, therefore, the hydroxo bridge cleavage in the nta complexes would occur at the $\text{Cr}(\text{nta})$ site in accordance with the carboxylate *cis* labilization effect.⁵⁷

In order to reveal the fundamental difference in the substituent effect or the effect of the nonbridging ligand together with the reaction mechanism, The kinetic data in terms of the substitutional parameters will be examined in the next section.

6.3.3 Substituent effects of carboxylato bridged ligands. In the reaction series of the *m*- and *p*-substituted derivatives of benzene, the substituent effects on the reaction are simply correlated to the polar effect of the substituent as the Hammet equation⁹⁰

$$\log(k / k_0) = \rho \sigma \quad (3),$$

where σ and ρ are substituent constant and adjustable parameter, respectively. In this case, the substituents must be held rigidly and the steric interactions must not be changed about the reaction center.

On the other hand, since the aliphatic compounds have many conformations, the steric effects must be considered in the substituent effects. Taft separated the substituent effects to the inductive and the steric ones and estimated their parameters. He expressed the relationship between the reaction rate constants and the substituent effects as Taft's equation⁹¹

$$\log(k / k_0) = \rho^* \sigma^* + \delta E_s \quad (4),$$

where σ^* and E_s are the inductive and the steric aliphatic substituent constants, respectively

Table 6-5. The inductive and steric substituent constants for aliphatic series.^a

Substituent R	σ^*	E_s
CCl ₃	2.65	-2.06
CHF ₂	2.05	-0.67
CHCl ₂	1.940	-1.54
CH ₂ F	1.10	-0.24
CH ₂ Cl	1.050	-0.24
CH ₂ Br	1.000	-0.27
CH ₂ I	0.85	-0.37
C ₆ H ₅	0.600	—
CH ₃ OCH ₂	0.520	-0.19
H	0.490	+1.24
(C ₆ H ₅) ₂ CH	0.405	-1.76
CH ₂ ClCH ₂	0.385	-0.90
C ₆ H ₅ CH ₂	0.215	-0.38
C ₆ H ₅ CH ₂ CH ₂	0.080	-0.38
C ₆ H ₅ (C ₂ H ₅)CH	0.04	-1.50
C ₆ H ₅ CH ₂ CH ₂ CH ₂	0.02	-0.45
CH ₃	0.000	0.00
cyclo-C ₆ H ₁₁ CH ₂	-0.06	-0.98
C ₂ H ₅	-0.100	-0.07
n-C ₃ H ₇	-0.115	-0.36
i-C ₄ H ₉	-0.125	-0.93
n-C ₄ H ₉	-0.130	-0.39
cyclo-C ₆ H ₁₁	-0.15	-0.79
t-C ₄ H ₉ CH ₂	-0.165	-1.74
i-C ₃ H ₇	-0.190	-0.47
cyclo-C ₅ H ₉	-0.20	-0.51
(C ₂ H ₅) ₂ CH	-0.225	-1.98
(t-C ₄ H ₉)(CH ₃)CH	-0.28	-3.33
t-C ₄ H ₉	-0.300	-1.54

^a Data from reference 91.

as shown in Table 6-5. The σ^* depends only on polar effects and is analogous to the Hammett substituent constant σ . The E_s represents the degree of the steric effect of a substituent. The adjustable parameters ρ^* and δ are the constant values through a reaction series and independent of the nature of the substituent groups. They give a measure of the relative susceptibility to the inductive and steric requirements of the aliphatic substituents in the reaction series. The k / k_0 is the relative rate of the reaction series for any substituent. The k_0 is the rate constant for the standard reactant. In this study, the μ -acetato complexes are used as the standard reactant.

This Taft's equation was applied to the base hydrolysis reaction rate constant k_1 values for a series of $[\text{Cr}_2(\text{OH})(\text{RCOO})(\text{en})_4]^{4+}$ which vary largely with kinds of the carboxylato bridges. Using a regression analysis for the least squared fitting, it is found that $\log(k / k_0)$ for the rates of the base hydrolysis for all the seven μ -RCOO⁻ complexes are satisfactorily fitted with the correlation coefficient 0.992 to give the parameter values $\rho^* = 2.28 \pm 0.21$ and $\delta = 1.43 \pm 0.13$ in the equation (3) (Figure 6-9).

This result means that the carboxylato bridge cleavage base hydrolysis reaction for $[\text{Cr}_2(\text{OH})(\text{RCOO})(\text{en})_4]^{4+}$ is influenced by both the inductive and the steric effects in similar extents. The reaction coefficients (ρ^* and δ) in $[\text{Cr}_2(\text{OH})(\text{RCOO})(\text{en})_4]^{4+}$ are relatively large and similar to those in the methanolysis reaction of *l*-menthylester ($\rho^* = 2.70$ and $\delta = 1.30$)⁹²

The reaction mechanism of the methanolysis reaction of *l*-menthylester is shown in Scheme 6-3. In accordance with the mechanism in the methanolysis of *l*-menthylester, therefore, the carboxylic acyl carbon atom is attacked nucleophilically by OH⁻ followed by the C-O bond cleavage as shown in Scheme 6-4a.

As Basolo *et al.* reported, the Co-O(carboxylato) bond cleavage occurred in the base hydrolysis reactions of the $[\text{Co}(\text{NH}_3)_5(\text{OOCR})]^{2+}$,⁹³ while the C-O bond cleavage reaction occurred only for $[\text{Co}(\text{NH}_3)_5(\text{OOC}\text{CF}_3)]^{2+}$ ⁹⁴ and $[\text{Cr}(\text{NH}_3)_5(\text{OOC}\text{CF}_3)]^{2+}$.⁹⁵ This is because the acyl carbon is significantly activated by the strong inductive CF_3 substituent. In our experimental results for the base hydrolysis reaction of $[\text{Cr}_2(\text{OH})(\mu\text{-RCOO})(\text{en})_4]^{4+}$, it is to be noted that the C-O bond cleavage occurs in all the complexes without the strong inductive

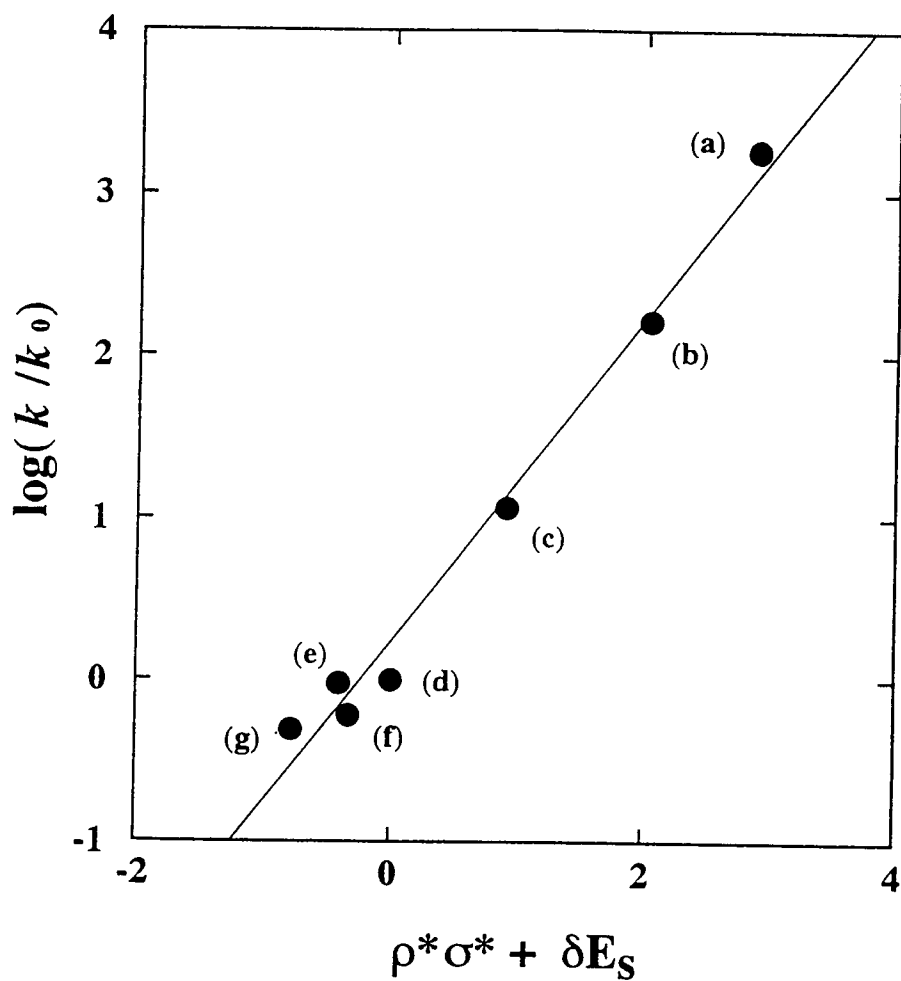
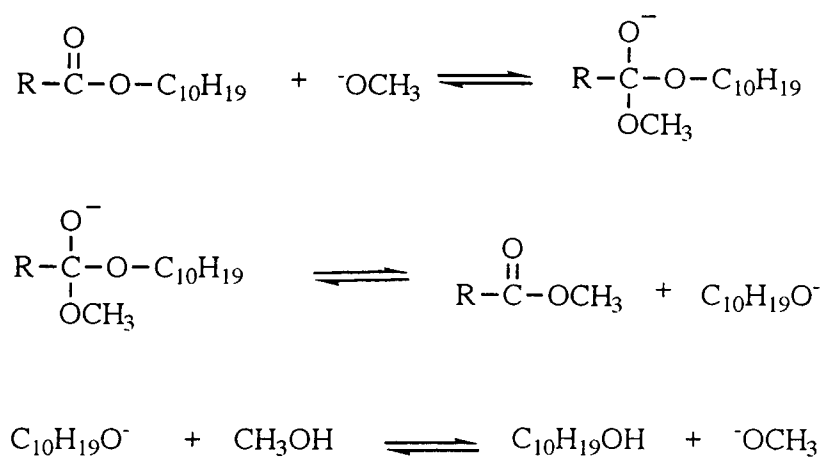
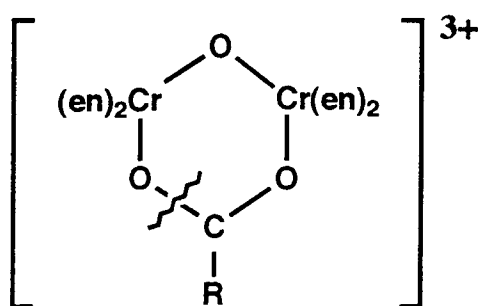


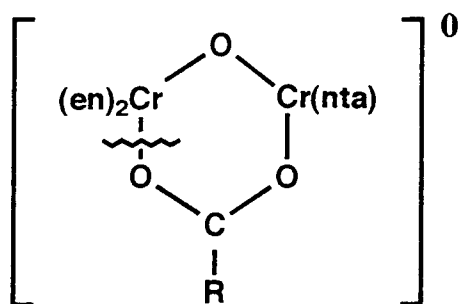
Figure 6-9. Relationship between $\log(k/k_0)$ vs. the inductive and steric substituent constants for carboxylato bridge cleavage reaction constants (k_1) of $[\text{Cr}_2(\mu\text{-OH})(\mu\text{-RCOO})(\text{en})_4]^{4+}$: (a) H, (b) CH_2Cl , (c) CH_3OCH_2 , (d) CH_3 , (e) CH_2ClCH_2 , (f) CH_3CH_2 and (g) $\text{CH}_3\text{CH}_2\text{CH}_2$.



Scheme 6-3. Reaction mechanism of the sodium methoxide-catalyzed methanolysis of *l*-menthylester.



(a)



(b)

Scheme 6-4. Proposed reaction sites of carboxylato bridge cleavage reaction.

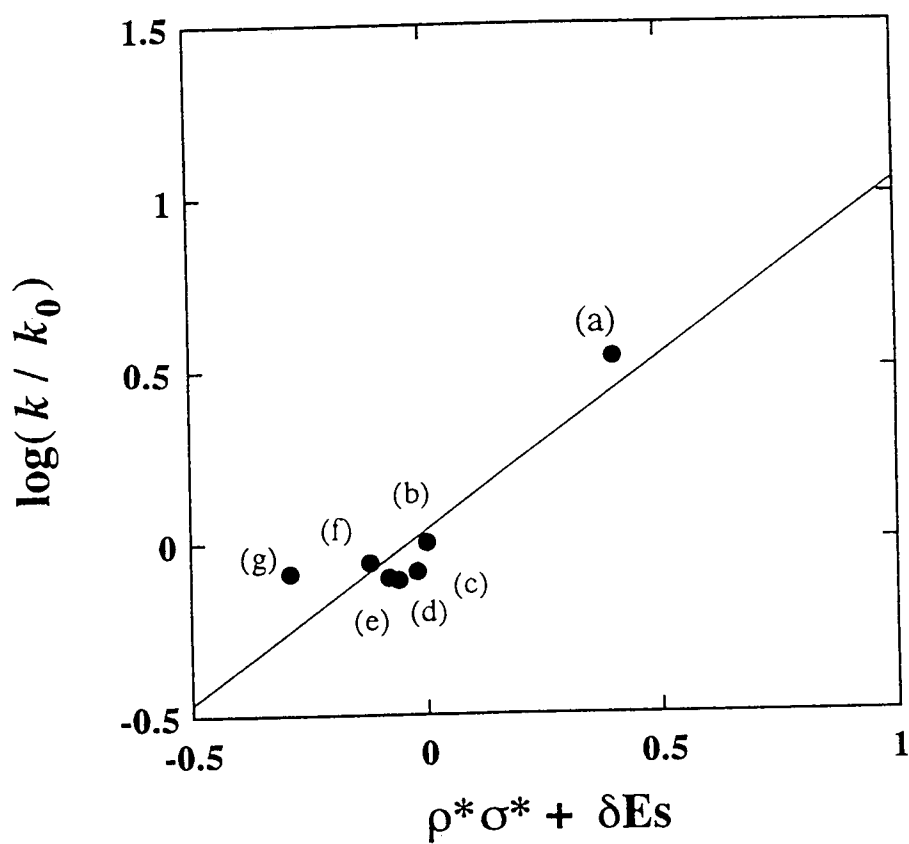


Figure 6-10. Relationship between $\log(k/k_0)$ vs. the inductive and steric substituent constants for carboxylato bridge cleavage reaction constants (k_1) of $[(\text{nta})\text{Cr}(\mu\text{-OH})(\mu\text{-RCOO})\text{Cr}(\text{en})_2]^+$: (a) H, (b) CH_3 , (c) CH_3CH_2 , (d) CH_3OCH_2 , (e) CH_2Cl , (f) $\text{CH}_3\text{CH}_2\text{CH}_2$ and (g) CH_2ClCH_2 .

substituents like CF_3 group. Though the base hydrolysis for the μ -trifluoroacetato complex $[\text{Cr}_2(\text{OH})(\text{CF}_3\text{COO})(\text{en})_4]^{4+}$ is assumed to be the C-O bond cleavage mechanism from a comparison with the reaction for $[\text{Cr}(\text{NH}_3)_5(\text{OOC}\text{CF}_3)]^{2+}$,¹⁵ it is reasonable that the C-O bond rupture in the $(\mu\text{-OH})(\mu\text{-RCOO})$ dinuclear complexes is ascribed to the acyl carbon activation due to the bidentate bridging ligation rather than due to only the strong inductive effect of CF_3 group.

For $[(\text{nta})\text{Cr}(\text{OH})(\text{RCOO})\text{Cr}(\text{en})_2]^+$, the k_1 values also varied with kinds of the carboxylato bridges (6.87×10^{-2} to $1.55 \times 10^{-2} \text{ s}^{-1}$). The range in the rate constants is smaller than that of $[\text{Cr}_2(\text{OH})(\text{RCOO})(\text{en})_4]^{4+}$. In the same manner as the above mentioned procedure for the en complexes, the least squared fitting for the relationship between the reaction rate constants and the substituent effect in the equation (3) gives the parameter values $\rho^* = 0.01 \pm 0.12$ and $\delta = 0.32 \pm 0.08$ with the correlation coefficient 0.904 as shown in Figure 6-10.

For the nta complexes, the carboxylato bridge cleavage base hydrolysis reaction is entirely different from that for the en complex and influenced mainly by the steric effect but only little by the inductive one, though the estimated uncertainty for the ρ^* is rather larger than the parameter value itself. The susceptibility to the steric effect is smaller by about one fourth than that of the en complexes. Thus, the cleavage reaction occurs in the Cr-O(carboxylato oxygen) bond at the $\text{Cr}(\text{en})_2$ site remote from the substituent group R as Scheme 6-4b.

In view of the above examinations of the kinetics for the μ -carboxylato complexes, the difference in reaction mechanisms between the en and the nta complexes may be ascribed to the kinetic lability resulting from the relative charge imbalance among the acyl carbon, $\text{Cr}(\text{en})_2$, and $\text{Cr}(\text{nta})$ sites. The intrinsic difference in the thermodynamic instability or the coordination bond (ligand field) properties between the $(\text{en})_2\text{Cr-O}$ and $(\text{nta})\text{Cr-O}$ bonds would not be responsible for the difference in the reaction mechanisms, in agreement with the similarity in the ligand field absorption maxima as well as the magnetic interaction (2J) for these complexes as described above. This is the first example for differentiating the base-hydrolysis reaction mechanisms by non-bridging ligands in dinuclear complexes.

7. Concluding Remarks

As described in Chapter 1 (General Introduction), this work directs toward the elucidation of the influences of the coordination bond characters of the ligands on the physical and chemical properties of the chromium(III)-cobalt(III) and chromium(III)-chromium(III) dinuclear complexes.

1) About 40 new chromium(III)-cobalt(III) and chromium(III)-chromium(III) dinuclear complexes with various ligands have been prepared. The $[(nta)Cr(OH)_2M(N)_4]^+$ ($M = Cr(III)$ and $Co(III)$) type complexes have been synthesized by the aqueous hydrolysis reaction. The resulted heterometal $[(nta)Cr(OH)_2Co(N)_4]^+$ complexes are very stable in aqueous solution. The systematic synthesis of the stable $di(\mu-OH)$ $[Cr(III)-Co(III)]$ dinuclear complexes is firstly confirmed. The $[(nta)Cr(OH)(RCOO)Cr(en)_2]^+$ and $[Cr_2(OH)(RCOO)(en)_4]^{4+}$ type ones have been prepared by the reaction of $di(\mu-OH)$ complexes with $RCOOH$ in aqueous solution. $[Cr_2(OH)(RCOO)(bispicam)_2]^{3+}$ or $4+$ type ones have been obtained by oxidation reactions of air sensitive $[Cr^{II}(RCOO)_4X_2]$ type ones with the amine ligand. They have been characterized by the UV/VIS, infra-red, CD spectra, acid dissociation constants, magnetic properties, NMR spectra and single crystal X-ray structure analysis and those result helped to examine the various properties of the dinuclear complexes.

2) The structures of the unsymmetrical $[(nta)Cr(OH)_2M(N)_4]^+$ complexes have been confirmed by the X-ray crystal structure analysis. The bond lengths and angles in the bridging units were found to correspond to those of the symmetrical $[L_nM(OH)_2ML_n]$ type dinuclear complexes. The $(nta)Cr-OH$ bond *trans* to the *nta* amine nitrogen atom is changed accompanying with the changes of the $(N)_4Cr-OH$ bond. The acid strengths of the bridging hydroxide ligands are influenced by the π -bond characters of the $M-(N)_4$ bond.

3) The 2H NMR spectra of the $[(nta-d_6)Cr(OH)_2M(N)_4]^+$ complexes have been influenced by the interaction between non-bridging ligands and the long-range influences by the coordinate bond characters of the $(N)_4$ ligands. The 1H , ^{14}N and ^{59}Co NMR spectra of the $[(nta)Cr(OH)_2M(N)_4]^+$ complexes have been examined the paramagnetic influences.

4) The ^2H NMR spectra of the $[\text{Cr}_2(\text{OH})(\text{RCOO})(\text{bispicam-d}_1)_2]^{3+}$ complexes have been influenced by the inductive substituent effect of the carboxylic acid.

5) The magnetic exchange interaction in $[(\text{nta})\text{Cr}(\text{OH})_2\text{Cr}(\text{N})_4]^+$ and $[(\text{nta})\text{Cr}(\text{OH})(\text{RCOO})\text{Cr}(\text{en})_2]^+$ complexes were not appreciably changed by the $(\text{N})_4$ and RCOO ligands, since the average Cr-OH bond distance which governs the magnetic exchange interaction are not changed within these complexes according to the X-ray structures and the UV/VIS absorption spectra. In contrast to the above complexes, the magnetic exchange interaction in $[\text{Cr}_2(\text{OH})(\text{RCOO})(\text{bispicam})_2]^{3+ \text{ or } 4+}$ ones widely changed from antiferromagnetic to ferromagnetic exchange coupling with the variation of the counter anions. This remarkable change in the magnetic exchange interaction is due to the competition between the ferromagnetic contribution of the carboxylato bridging ligands and the antiferromagnetic one of the OH bridging ligands.

6) The base hydrolysis reaction of the chromium(III)-chromium(III) complexes were examined. The carboxylato bridge cleavage reaction is influenced by both the inductive and the steric effects of the substituents in $[\text{Cr}_2(\text{OH})(\text{RCOO})(\text{en})_4]^{4+}$ complexes, but is mainly influenced by the steric effect in $[(\text{nta})\text{Cr}(\text{OH})(\text{RCOO})\text{Cr}(\text{en})_2]^+$ ones. The former complexes cleavage at carboxylic acyl carbon-oxygen bond (C-O) and the latter ones cleavage at chromium-oxygen bond (Cr-O) in the $\text{Cr}(\text{en})_2$ site. These different cleavage sites come from the relative charge imbalance among the acyl carbon, $\text{Cr}(\text{en})_2$ and $\text{Cr}(\text{nta})$ sites.

References

- (1) S. M. Jørgensen, *J. Prakt. Chem.*, 1882, **25**, 321.
- (2) S. M. Jørgensen, *J. Prakt. Chem.*, 1892, **45**, 260.
- (3) S. M. Jørgensen, *Z. Anorg. Allg. Chem.*, 1898, **16**, 184.
- (4) A. Werner and A. Mylius, *Z. Anorg. Allg. Chem.*, 1898, **16**, 245.
- (5) A. Werner, *Liebigs Ann. Chem.*, 1910, **375**, 1.
- (6) A. Werner, *Liebigs Ann. Chem.*, 1910, **375**, 72.
- (7) A. Werner, *Liebigs Ann. Chem.*, 1910, **375**, 84.
- (8) A. Werner, *Liebigs Ann. Chem.*, 1914, **375**, 286.
- (9) A. Werner, *Ber.*, 1914, **47**, 3087.
- (10) A. Werner, *Ber.*, 1907, **40**, 2119.
- (11) J. Springborg, *Adv. in Inorg. Chem.* 1988, **32**, 55.
- (12) P. Andersen, *Coord. Chem. Rev.*, 1989, **94**, 47.
- (13) T. F. Tekut, C. J. O'Connor and R. Holwerda, *Inorg. Chim. Acta*, 1993, **214**, 145.
- (14) J. Grelup, S. Larsen and H. Weihe, *Acta Chem. Scand.*, 1993, **47**, 1154.
- (15) J. Springborg, *Acta Chem. Scand.*, 1992, **46**, 1047.
- (16) R. Hotzelmann, K. Wieghardt, U. Flörke, H-J. Haupt, D. C. Weatherburn, J. Bovinson, G. Blondin and J-J. Girerd, *J. Am. Chem. Soc.*, 1992, **114**, 1681.
- (17) P. N. Turowski, A. Bino and S. J. Lippard, *Angew. Chem. Int. Ed. Engl.*, 1990, **29**, 811.
- (18) H. Toftlund, O. Simonsen and E. Pedersen, *Acta Chem. Scand.*, 1990, **44**, 676.
- (19) L. L. Martin, K. Wieghardt, G. Blondin, J. J. Girerd, B. Nuber and J. Weiss, *J. Chem. Soc. Chem. Commun.*, **1990**, 1767.
- (20) P. Andersen, A. Dossing and S. Larsen, *Acta Chem. Scand.*, 1990, **44**, 455.
- (21) U. Bossek, T. Weyhermüller, K. Wieghardt, J. Bonvoisin and J. J. Girerd, *J. Chem. Soc. Chem. Commun.*, **1989**, 633.
- (22) K. Wieghardt, U. Bossek, D. Ventur and J. Weiss, *J. Chem. Soc. Chem. Commun.*, **1985**, 347.
- (23) P. Chaudhuri, K. Wieghardt, B. Nuber and J. Weiss, *Angew. Chem. Int. Ed. Engl.*, 1985, **24**, 727.
- (24) W. H. Armstrong and S. J. Lippard, *J. Am. Chem. Soc.*, 1983, **105**, 4837.
- (25) K. Wieghardt, K. Pohl and W. Gebert, *Angew. Chem. Int. Ed. Engl.*, 1983, **22**, 727.
- (26) T. F. Tekut and R. Holwerda, *Inorg. Chem.*, 1993, **32**, 3196.

- (27) B. G. Gafford, R. E. Marsh, W. P. Schaefer, J. H. Zhang, C. J. O'Connor and R. A. Holwerda, *Inorg. Chem.*, 1990, **29**, 4652.
- (28) S. Larsen, K. Michelsen and E. Pedersen, *Acta Chem. Scand.*, 1986, **A40**, 63.
- (29) E. bang, K. Michelsen, K. M. Nielsen and E. Pedersen, *Acta Chem. Scand.*, 1989, **43**, 748.
- (30) P. Chaudhuri, M. Winter, H.-J. Küppers, K. Wieghardt, B. Nuber and J. Weiss, *Inorg. Chem.*, 1987, **26**, 3302.
- (31) N. Koine, R. Bianchini and J. I. Legg, *Inorg. Chem.*, 1988, **25**, 2835.
- (32) S. M. Jørgensen, *Z. Anorg. Chem.*, 1892, **2**, 297.
- (33) P. Pfeiffer and O. Angern, *Chem. Ber.*, 1927, **60**, 308.
- (34) Y. Kojima, *Bull. Chem. Soc. Jpn.*, 1975, **48**, 2033.
- (35) R. S. Treptow, *Inorg. Chem.*, 1966, **5**, 1593.
- (36) A. M. Sargeson and G. H. Searle, *Inorg. Chem.*, 1967, **6**, 787.
- (37) K. Michelsen, *Acta Chem. Scand.*, 1972, **26**, 769.
- (38) K. Kashiwabara, K. Igi and B. E. Douglas, *Bull. Chem. Soc. Jpn.*, 1976, **49**, 1573.
- (39) M. Mori, *Nippon Kagaku Zashhi*, 1953, **74**, 253.
- (40) E. Pedersen, *Acta Chem. Scand.*, 1970, **24**, 3362.
- (41) M. Nakano and S. Kawaguchi, *Bull. Chem. Soc. Jpn.*, 1979, **52**, 3563.
- (42) D. A. House and C. S. Garner, *J. Am. Chem. Soc.*, 1968, **88**, 2156.
- (43) K. Michelsen, *Acta Chem. Scand.*, 1972, **26**, 1517.
- (44) M. P. Hancock, J. Josephsen and C. E. Schäffer, *Acta Chem. Scand.*, 1976, **A30**, 79.
- (45) J. Springborg and H. Toftlund, *Acta Chem. Scand.*, 1979, **A33**, 31.
- (46) L. C. Craig and R. M. Hixon, *J. Am. Chem. Soc.*, 1931, **53**, 4367.
- (47) a) S. Herzog and W. Kalies, *Z. Anorg. allg. Chem.*, 1964, **329**, 83.
b) S. Herzog and W. Kalies, *Z. Anorg. allg. Chem.*, 1967, **351**, 237.
- (48) L. Mønsted and O. Mønsted, *Acta Chem. Scand.*, 1976, **A30**, 203.
- (49) TEXSAN-TEXRAY Structure Analysis Package, Molecular Structure Corporation, 1985.
- (50) M. Ardon and A. Bino, *Inorg. Chem.*, 1985, **24**, 1343; *Struct. Bond.*, 1987, **65**, 1:
S. Larsen, K. B. Nielsen and I. Trabjerg, *Acta Chem. Scand.*, 1983, **A37**, 833.
- (51) J. Springborg and C. E. Schäffer, *Acta Chem. Scand.*, 1976, **A30**, 787:
J. Springborg and C. E. Schäffer, *Inorg. Chem.*, 1976, **15**, 1744.
- (52) a) T. Ama, H. Kawaguchi and T. Yasui, *Bull. Chem. Soc. Jpn.*, 1987,

- 60**, 1183; 1988 , **61**, 1141.
- b) K. Okamoto, J. Hidaka, T. Ama and T. Yasui, *Acta Cryst.*, **1991**, C47, 2099.
- (53) T. Ama, T. Yonemura, H. Kawaguchi and T. Yasui, *Bull. Chem. Soc. Jpn.*, 1994, **67**, 410.
- (54) R. G. Geue and M. R. Snow, *J. Chem. Soc., (A)* **1971**, 1981;
T. Nomura, F. Marumo and Y. Saito, *Bull. Chem. Soc. Jpn.*, 1969, **42**, 1016;
H. V. F. Schousboe-Jensen, *Acta Chem. Scand.*, 1972, **26**, 3143;
R. Nagao, F. Marumo and Y. Saito, *Acta Cryst.*, 1973, **B29**, 2438;
K. Matsumoto, H. Kawaguchi, H. Kuroya and S. Kawaguchi, *Bull. Chem. Soc. Jpn.*, 1973, **46**, 2424;
G. Srdanov, R. Herak and B. Prelesnik, *Inorg. Chim. Acta*, 1979, **33**, 23.
- (55) C. A. Green, N. Koine, J. I. Legg and R. D. Willett, *Inorg. Chim. Acta*, 1990, **176**, 87.
- (56) N. Koine, *personal communication*.
- (57) J. R. Bocarsly, M. Y. Chiang, L. Bryant and J. K. Barton, *Inorg. Chem.*, 1990 , **29**, 4898.
- (58) U. Thewalt and M. Zehnder, *Helv. Chim. Acta*, 1970, **60**, 2000.
- (59) F. A. Journak and K. N. Raymond, *Inorg. Chem.*, 1972, **11**, 3149.
- (60) P. Andersen, A. Døssing and K. M. Nielsen, *Acta Chem. Scand.*, 1986, **A40**, 142.
- (61) G. H. Stout and L. H. Jensen, *X-ray Structure Determination*, Macmillan, New York, **1968**.
- (62) F. A. Journak and K. N. Raymond, *Inorg. Chem.*, 1974, **13**, 2387;
E. N. Dueslen and K. N. Raymond, *Inorg. Chim. Acta*, 1978, **30**, 87;
X. Solans, M. Font-Altaba, M. Montfort and J. Ribas, *Acta Cryst.*, 1982, **B38**, 2899;
X. Solans, M. Font-Altaba, J. L. Brianso, A. Solans, J. Casabo and J. Ribas, *Cryst. Struct. Commun.*, 1982, **11**, 1199.
- (63) J. T. Veal, W. E. Hatfield and D. J. Hodgson, *Acta Cryst.*, 1973, **B29**, 12.
- (64) R. P. Scaringe, P. Singh, R. P. Eckberg, Hatfield and D. J. Hodgson, *Inorg. Chem.*, 1975, **14**, 1127.
- (65) K. Kaas, *Acta Cryst.*, 1976, **B32**, 2021.
- (66) J. Josephsen and C. E. Schäffer, *Acta Chem. Scand.*, 1970, **24**, 2929.
- (67) J. Springborg and C. E. Schäffer, *Inorg. Synth.*, 1978, **18**, 75.
- (68) J. Springborg and H. Toftlund, *Acta Chem. Scand.*, 1976, **A30**, 171;
J. Chem. Soc. Dalton Trans., **1976**, 1017.

- (69) J. Springborg, *Acta Chem. Scand.*, 1978, **A32**, 231.
- (70) Y. Inamura and Y. Kondo, *Nippon Kagaku Zasshi*, 1953, **74**, 627.
- (71) L. Spiccia, G. D. Fallon, A. Markiewicz, K. S. Murray and H. Riesen, *Inorg. Chem.*, 1992, **31**, 1066.
- (72) J. Glerup, D. J. Hodgson and E. Pedersen, *Acta Chem. Scand.*, 1983, **A37**, 161.
- (73) P. N. Turowski, A. Bino and S. J. Lippard, *Angew. Chem. Int. Ed. Engl.*, 1990, **29**, 811.
- (74) a) W. D. Wheeler, S. Kaizaki and J. I. Legg, *Inorg. Chem.*, 1982, **21**, 3248; F. H. Kohler, Ren de Cao, K. Ackermann and J. Sedlmair, *Z. Naturforsch, Teil B*, 1983, **38**, 1406;
W. D. Wheeler and J. I. Legg, *Inorg. Chem.*, 1984, **23**, 3798; C. A. Green, R. J. Bianchini and J. I. Legg, *Inorg. Chem.*, 1984, **23**, 2713;
W. D. Wheeler and J. I. Legg, *Inorg. Chem.*, 1985, **24**, 1292;
R. J. Bianchini, U. Geiser, H. Place, S. Kaizaki, Y. Morita and J. I. Legg, *Inorg. Chem.*, 1986, **25**, 4672;
C. A. Green, H. Place, R. D. Willett and J. I. Legg, *Inorg. Chem.*, 1986, **25**, 4672;
R. J. Bianchini and J. I. Legg, *Inorg. Chem.*, 1986, **25**, 3263;
C. Cornioley-Deuschel and A. von Zelewsky, *Inorg. Chem.*, 1987, **26**, 2835;
S. Kaizaki, M. Byakuno, M. Hayashi, J. I. Legg, K. Umakoshi and S. Ooi, *Inorg. Chem.*, 1987, **26**, 2395;
S. Kaizaki and H. Takemoto, *Inorg. Chem.*, 1990, **29**, 4960.
b) S. Kaizaki and M. Hayashi, *J. Chem. Soc. Dalton Trans.*, **1989**, 1947.
- (75) G. Fisher, *Synthesis*, **1973**, 218.
- (76) M. Mori, *Shin Jikken Kagaku Kōza*, Maruzen, Tokyo, 1977, vol 8, p. 1402.
- (77) *NMR of Paramagnetic Molecules*, eds. G. N. La Mar, W. D. Horrocks, Jr. and R. H. Holm, Academic Press, 1973.
- (78) J. Josephsen and C. E. Schäffer, *Acta Chem. Scand.*, 1970, **24**, 2929.
- (79) D. G. Brown and R. S. Drago, *J. Am. Chem. Soc.*, 1970, **92**, 1871.
- (80) R. G. Kidd and R. J. Goodfellow, *NMR and the Periodic Table*, eds. R. K. Harris and B. E. Mann, Academic Press, New York 1978, ch. 8, pp. 225-244.
- (81) K. Miyatani, K. Kohn, H. Kamimura and S. Iida, *J. Phys. Soc. Jpn.*, 1966, **21**, 464;
H. Kamimura, *J. Phys. Soc. Jpn.*, 1966, **21**, 484.
- (82) R. Acerete, N. Casan-Pastor, J. Bas-Serra and L. C. W. Baker, *J. Am.*

- Chem. Soc.*, 1989, **111**, 6049.
- (83) a) A. Niemann, U. Bossek, K. Wieghardt, C. Butzlaff, A. X. Trautwein and B. Nuber, *Angew. Chem. Int. Ed. Engl.*, 1992, **31**, 311;
 b) G. Frei, M. G. Colombo and H.-O. Güdel, *Perspectives in Coordination Chemistry*, Verlag Helvetic Chimica Acta, Basel, 1992; p183.
- (84) M. Nakahanada, T. Fujihara, A. Fuyuhiko and S. Kaizaki, *Inorg. Chem.*, 1992, **31**, 1315.
- (85) R. P. Scaringe, W. E. Hatfield and D. J. Hodgson, *Inorg. Chem.*, 1977, **16**, 1600.
- (86) E. E. Eduok, J. W. Owens and C. J. O'Connor, *Polyhedron*, 1984, **3**, 17.
- (87) M. Inoue and M. Kubo, *Inorg. Chem.*, 1970, **9**, 2310.
- (88) K. Kaas and J. Springborg, *Acta Chem. Scand.*, 1986, **A40**, 515.
- (89) J. E. Tackett, *Applied Spectrosc.*, 1989, **43**, 490.
- (90) L. P. Hammett, *Chem. Revs.*, 1935, **17**, 125; L. P. Hammett, *Physical Organic Chemistry*, Mc-GrowHill, New York, 1940;
 H. H. Jaffe, *Chem. Revs.*, 1953, **53**, 191.
- (91) R. W. Taft, Jr., *Steric Effects in Organic Chemistry*, M. S. Newman, Ed.; John Wiley & Sons: New York, 1956; ch. 13.
- (92) W. A. Pavelich and R. W. Taft, Jr., *J. Am. Chem. Soc.*, 1957, **79**, 4935.
- (93) F. Basolo and J. G. Bergmann and R. G. Pearson, *J. Phys. Chem.*, 1952, **56**, 22.
- (94) R. B. Jordan and H. Taube, *J. Am. Chem. Soc.*, 1964, **86**, 3890.
- (95) R. Davies, G. B. Evans and R. B. Jordan, *Inorg. Chem.*, 1969, **8**, 2025.

Appendixes

Table AI-1. Positional parameters and equivalent isotropic thermal parameters (\AA^2) for $[(\text{nta})\text{Cr}(\text{OH})_2\text{Co}(\text{tn})_2]\text{Cl} \cdot 1.5\text{H}_2\text{O}$ (**A-3**).

Atom	x / a	y / b	z / c	$B(\text{eq})$
Co	0.29853(2)	0.66786(3)	0.36213(2)	1.47(1)
Cr	0.25972(3)	0.54968(3)	0.47265(3)	1.59(2)
O(1)	0.3134(1)	0.5304(2)	0.5823(1)	2.51(8)
O(2)	0.3175(2)	0.4344(2)	0.6741(1)	3.6(1)
O(3)	0.1663(1)	0.6272(1)	0.4863(1)	2.13(8)
O(4)	0.0239(2)	0.6288(2)	0.4634(2)	4.0(1)
O(5)	0.3269(1)	0.4455(1)	0.4562(1)	2.28(1)
O(6)	0.3198(2)	0.2971(2)	0.4329(2)	4.0(1)
O(7)	0.2122(1)	0.5786(1)	0.3638(1)	1.81(7)
O(8)	0.3369(1)	0.6461(1)	0.4693(1)	1.93(7)
O(9)	-0.0038(2)	0.8174(2)	0.4386(2)	4.0(1)
O(10)	1.0000	0.4923(8)	0.7500	14.5(6)
N(1)	0.1742(2)	0.4487(2)	0.4772(1)	1.81(9)
N(2)	0.2226(2)	0.7625(2)	0.3793(1)	2.2(1)
N(3)	0.2488(2)	0.6928(2)	0.2533(1)	2.12(9)
N(4)	0.3893(2)	0.7607(2)	0.3775(2)	2.5(1)
N(5)	0.3689(2)	0.5641(2)	0.3463(2)	2.3(1)
C(1)	0.1954(2)	0.4267(2)	0.5595(2)	2.5(1)
C(2)	0.2827(2)	0.4652(2)	0.6102(2)	2.4(1)
C(3)	0.0868(2)	0.4899(2)	0.4427(2)	2.4(1)
C(4)	0.0909(2)	0.5900(2)	0.4661(2)	2.4(1)
C(5)	0.1913(2)	0.3702(2)	0.4351(2)	2.4(1)
C(6)	0.2861(2)	0.3684(2)	0.4419(2)	2.5(1)
C(7)	0.1292(2)	0.7684(2)	0.3318(2)	2.5(1)
C(8)	0.1162(2)	0.7752(3)	0.2490(2)	2.9(1)
C(9)	0.1528(2)	0.6969(2)	0.2178(2)	2.6(1)
C(10A) ^a	0.4764(4)	0.7486(5)	0.3763(4)	3.2(3)
C(10B) ^a	0.4605(5)	0.7340(6)	0.3404(5)	4.4(4)
C(11A) ^a	0.4860(6)	0.6659(7)	0.3362(6)	5.7(5)
C(11B) ^a	0.5107(4)	0.6485(5)	0.3791(4)	3.2(3)
C(12A) ^a	0.4672(5)	0.5739(6)	0.3749(6)	5.0(4)
C(12B) ^a	0.4567(5)	0.5716(5)	0.3381(5)	3.4(3)
Cl	0.81960(8)	0.57712(7)	0.75965(7)	4.75(5)

^a The population parameter is 0.5.

Table AI-2. Positional parameters and equivalent isotropic thermal parameters (\AA^2) for $[(\text{nta})\text{Cr}(\text{OH})_2\text{Co}(\text{tn})_2]\text{Cl} \cdot 1.5\text{H}_2\text{O}$ (**A-3**) (Hydrogen atoms).

Atom	x / a	y / b	z / c	$B(\text{eq})$
H(1)	0.203(2)	0.547(2)	0.340(2)	1.7(6)
H(2)	0.375(3)	0.643(2)	0.490(2)	2.8(8)
H(3)	0.154(2)	0.452(2)	0.577(2)	3.7(9)
H(4)	0.200(2)	0.361(2)	0.569(2)	2.6(7)
H(5)	0.071(2)	0.489(2)	0.386(2)	2.3(7)
H(6)	0.044(2)	0.460(2)	0.450(2)	2.2(7)
H(7)	0.180(2)	0.315(2)	0.454(2)	2.0(7)
H(8)	0.160(2)	0.375(2)	0.384(2)	2.3(7)
H(9)	0.238(2)	0.805(2)	0.381(2)	2.5(7)
H(10)	0.225(2)	0.756(3)	0.427(2)	3.9(9)
H(11)	0.103(2)	0.814(2)	0.350(2)	3.0(8)
H(13)	0.137(3)	0.825(3)	0.250(3)	6(1)
H(14)	0.060(2)	0.779(2)	0.223(2)	2.7(8)
H(15)	0.138(2)	0.703(2)	0.161(2)	2.3(7)
H(16)	0.129(2)	0.635(2)	0.225(2)	3.5(8)
H(17)	0.267(2)	0.736(2)	0.245(2)	2.8(8)
H(18)	0.267(2)	0.650(2)	0.222(2)	3.2(8)
H(51)	-0.053(3)	0.823(3)	0.433(2)	5(1)
H(52)	0.013(4)	0.739(5)	0.423(4)	14(2)

Table AI-3. Thermal parameters for [(nta)Cr(OH)₂Co(tn)₂]Cl·1.5H₂O (**A-3**).

Atom	U ₁₁	U ₂₂	U ₃₃	U ₁₂	U ₁₃	U ₂₃
Co	0.0203(2)	0.0176(2)	0.0171(2)	-0.0015(2)	0.0057(1)	0.0006(1)
Cr	0.0234(2)	0.0170(2)	0.0202(2)	-0.0030(2)	0.0081(2)	0.0013(2)
Cl	0.0714(7)	0.0444(6)	0.0598(7)	-0.0022(5)	0.0171(6)	-0.0256(5)
O(1)	0.039(1)	0.031(1)	0.023(1)	-0.009(1)	0.007(1)	0.006(1)
O(2)	0.054(2)	0.053(2)	0.029(1)	-0.003(1)	0.013(1)	0.017(1)
O(3)	0.032(1)	0.023(1)	0.028(1)	-0.0005(9)	0.014(1)	-0.0026(9)
O(4)	0.039(1)	0.038(1)	0.086(2)	0.008(1)	0.034(1)	0.004(1)
O(5)	0.027(1)	0.022(1)	0.040(1)	0.0029(9)	0.016(1)	0.005(1)
O(6)	0.057(2)	0.024(1)	0.085(2)	0.007(1)	0.043(2)	0.000(1)
O(7)	0.026(1)	0.021(1)	0.021(1)	-0.0049(8)	0.0072(8)	-0.0037(8)
O(8)	0.025(1)	0.027(1)	0.018(1)	-0.0064(8)	0.0025(8)	0.0038(8)
O(9)	0.028(1)	0.068(2)	0.049(2)	-0.006(1)	0.005(1)	-0.015(1)
O(10)	0.117(6)	0.29(1)	0.144(8)	0	0.042(6)	0
N(1)	0.026(1)	0.020(1)	0.025(1)	-0.001(1)	0.011(1)	0.001(1)
N(2)	0.031(1)	0.023(1)	0.026(1)	0.002(1)	0.004(1)	-0.004(1)
N(3)	0.030(1)	0.031(1)	0.020(1)	0.002(1)	0.010(1)	0.001(1)
N(4)	0.028(1)	0.031(1)	0.033(1)	-0.011(1)	0.008(1)	0.006(1)
N(5)	0.029(1)	0.026(1)	0.033(1)	0.005(1)	0.015(1)	0.000(1)
C(1)	0.040(2)	0.028(2)	0.033(2)	-0.04(1)	0.019(2)	0.006(1)
C(2)	0.039(2)	0.031(2)	0.027(2)	0.002(1)	0.018(1)	0.003(1)
C(3)	0.022(1)	0.028(2)	0.042(2)	-0.004(1)	0.013(1)	-0.002(1)
C(4)	0.037(2)	0.025(2)	0.033(2)	0.003(1)	0.019(1)	0.002(1)
C(5)	0.038(2)	0.018(1)	0.042(2)	-0.006(1)	0.021(2)	-0.007(1)
C(6)	0.039(2)	0.022(1)	0.038(2)	0.002(1)	0.020(2)	0.003(1)
C(7)	0.027(2)	0.039(2)	0.028(2)	0.007(1)	0.009(1)	-0.001(1)
C(8)	0.029(2)	0.050(2)	0.028(2)	0.012(2)	0.007(1)	0.005(2)
C(9)	0.031(2)	0.047(2)	0.016(1)	0.002(1)	0.003(1)	-0.001(1)
C(10A)	0.024(3)	0.049(4)	0.053(4)	-0.002(3)	0.018(3)	-0.002(4)
C(10B)	0.047(5)	0.053(5)	0.082(6)	0.004(4)	0.038(5)	0.023(5)
C(11A)	0.069(6)	0.076(7)	0.099(8)	-0.025(5)	0.065(6)	-0.020(6)
C(11B)	0.026(3)	0.043(4)	0.049(4)	0.000(3)	0.011(3)	0.007(3)
C(12A)	0.035(4)	0.064(6)	0.086(7)	0.016(4)	0.017(5)	-0.006(5)
C(12B)	0.029(4)	0.054(5)	0.049(4)	0.002(3)	0.019(3)	0.004(4)

Table AI-4. Positional parameters and equivalent isotropic thermal parameters (\AA^2) for $[(\text{nta})\text{Cr}(\text{OH})_2\text{Cr}(\text{tn})_2]\text{Cl} \cdot 1.5\text{H}_2\text{O}$ (**B-3**).

Atom	x / a	y / b	z / c	$B(\text{eq})$
Cr(1)	0.29950(3)	0.66725(4)	0.36365(3)	1.36(2)
Cr(2)	0.26165(3)	0.54800(3)	0.47498(3)	1.47(2)
O(1)	0.3136(2)	0.5295(2)	0.5827(1)	2.4(1)
O(2)	0.3157(2)	0.4356(2)	0.6741(2)	3.7(1)
O(3)	0.1683(2)	0.6245(2)	0.4882(1)	2.03(9)
O(4)	0.0261(2)	0.6254(2)	0.4647(2)	3.7(1)
O(5)	0.3296(2)	0.4453(2)	0.4586(1)	2.2(1)
O(6)	0.3248(2)	0.2975(2)	0.4362(2)	3.7(1)
O(7)	0.2144(1)	0.5750(2)	0.3668(1)	1.66(8)
O(8)	0.3383(1)	0.6447(2)	0.4711(1)	1.91(8)
O(9)	-0.0013(2)	0.8128(2)	0.4390(2)	3.7(1)
O(10)	1.0000	0.4842(7)	0.7500	11.7(5)
N(1)	0.1775(2)	0.4473(2)	0.4795(2)	1.7(1)
N(2)	0.2180(2)	0.7664(2)	0.3795(2)	2.3(1)
N(3)	0.2472(2)	0.6956(2)	0.2500(2)	2.1(1)
N(4)	0.3956(2)	0.7640(2)	0.3778(2)	2.4(1)
N(5)	0.3753(2)	0.5616(2)	0.3448(2)	2.4(1)
C(1)	0.1968(2)	0.4259(2)	0.5604(2)	2.3(1)
C(2)	0.2824(2)	0.4655(2)	0.6106(2)	2.3(1)
C(3)	0.0902(2)	0.4869(2)	0.4456(2)	2.1(1)
C(4)	0.0935(2)	0.5867(2)	0.4678(2)	2.2(1)
C(5)	0.1956(2)	0.3687(2)	0.4383(2)	2.4(1)
C(6)	0.2905(2)	0.3681(2)	0.4451(2)	2.2(1)
C(7)	0.1256(2)	0.7679(2)	0.3302(2)	2.5(1)
C(8)	0.1164(2)	0.7787(2)	0.2491(2)	2.9(5)
C(9)	0.1511(2)	0.7002(3)	0.2173(2)	2.7(1)
C(10)	0.4770(4)	0.7449(4)	0.3639(5)	7.3(3)
C(11)	0.5030(5)	0.6577(5)	0.3598(6)	10.4(5)
C(12)	0.4670(3)	0.5728(4)	0.3513(5)	7.1(3)
Cl	0.82218(9)	0.57819(9)	0.75564(7)	4.79(5)

Table AI-5. Positional parameters and equivalent isotropic thermal parameters (\AA^2) for $[(\text{nta})\text{Cr}(\text{OH})_2\text{Cr}(\text{tn})_2]\text{Cl} \cdot 1.5\text{H}_2\text{O}$ (**B-3**) (Hydrogen atoms).

Atom	x / a	y / b	z / c	$B(\text{eq})$
H(1)	0.200(2)	0.536(2)	0.334(2)	2.8(9)
H(2)	0.373(2)	0.648(3)	0.492(2)	2.7(9)
H(3)	0.152(2)	0.456(2)	0.570(2)	2.6(9)
H(4)	0.194(2)	0.368(2)	0.564(2)	2.3(8)
H(5)	0.073(2)	0.485(2)	0.391(2)	1.3(7)
H(6)	0.048(3)	0.457(3)	0.456(2)	4(1)
H(7)	0.180(2)	0.316(2)	0.454(2)	3.0(9)
H(8)	0.157(3)	0.381(3)	0.382(2)	5(1)
H(9)	0.237(2)	0.811(2)	0.381(2)	2.7(9)
H(10)	0.223(3)	0.761(3)	0.425(2)	4(1)
H(11)	0.101(2)	0.816(2)	0.347(2)	1.8(7)
H(12)	0.102(2)	0.704(3)	0.340(2)	3(1)
H(13)	0.145(3)	0.826(3)	0.245(3)	4(1)
H(14)	0.057(3)	0.777(3)	0.227(3)	5(1)
H(15)	0.132(2)	0.706(2)	0.165(2)	2.7(8)
H(16)	0.128(3)	0.635(3)	0.231(2)	4(1)
H(17)	0.269(2)	0.749(3)	0.248(2)	2.6(8)
H(18)	0.261(3)	0.661(3)	0.226(2)	4(1)
H(19)	0.372(2)	0.808(3)	0.345(3)	5(1)
H(20)	0.401(3)	0.783(3)	0.420(2)	4(1)
H(27)	0.379(3)	0.526(3)	0.375(2)	4(1)
H(28)	0.342(3)	0.542(3)	0.306(2)	5(1)
H(51)	-0.050(3)	0.812(3)	0.438(2)	5(1)
H(52)	-0.003(4)	0.747(4)	0.433(3)	6(1)

Table AI-6. Thermal parameters for [(nta)Cr(OH)₂Cr(tn)₂]Cl · 1.5H₂O (**B-3**).

Atom	U ₁₁	U ₂₂	U ₃₃	U ₁₂	U ₁₃	U ₂₃
Cr(1)	0.0184(2)	0.0171(2)	0.0159(2)	-0.009(2)	0.0054(2)	0.0007(2)
Cr(2)	0.0216(3)	0.0160(2)	0.0186(2)	-0.0028(2)	0.0073(2)	0.0011(2)
Cl	0.0705(9)	0.0453(7)	0.0589(8)	0.0009(6)	0.0130(7)	-0.0285(6)
O(1)	0.037(1)	0.030(1)	0.021(1)	-0.008(1)	0.007(1)	0.005(1)
O(2)	0.056(2)	0.055(2)	0.027(1)	-0.006(2)	0.011(1)	0.016(1)
O(3)	0.030(1)	0.021(1)	0.028(1)	-0.001(1)	0.013(1)	-0.003(1)
O(4)	0.038(2)	0.037(2)	0.076(2)	0.010(1)	0.032(2)	0.005(2)
O(5)	0.027(1)	0.022(1)	0.038(1)	0.002(1)	0.016(1)	0.003(1)
O(6)	0.052(2)	0.022(1)	0.078(2)	0.004(1)	0.037(2)	-0.000(1)
O(7)	0.024(1)	0.020(1)	0.019(1)	-0.005(1)	0.006(1)	-0.003(1)
O(8)	0.024(1)	0.026(1)	0.018(1)	-0.008(1)	0.002(1)	0.002(1)
O(9)	0.028(1)	0.057(2)	0.048(2)	-0.007(1)	0.006(1)	-0.012(2)
O(10)	0.102(6)	0.20(1)	0.142(8)	0	0.040(5)	0
N(1)	0.024(1)	0.018(1)	0.026(1)	-0.001(1)	0.011(1)	0.001(1)
N(2)	0.030(2)	0.027(2)	0.023(2)	0.004(1)	0.001(1)	-0.005(1)
N(3)	0.030(2)	0.031(2)	0.021(1)	0.005(1)	0.010(1)	0.001(1)
N(4)	0.033(2)	0.031(2)	0.027(2)	-0.007(1)	0.009(1)	0.005(1)
N(5)	0.035(2)	0.028(2)	0.029(2)	0.007(1)	0.015(1)	0.002(1)
C(1)	0.036(2)	0.026(2)	0.028(2)	-0.006(2)	0.015(2)	0.005(1)
C(2)	0.038(2)	0.026(2)	0.025(2)	0.002(2)	0.016(2)	0.002(1)
C(3)	0.021(2)	0.025(2)	0.034(2)	-0.003(1)	0.010(1)	-0.001(1)
C(4)	0.035(2)	0.025(2)	0.029(2)	0.004(2)	0.017(2)	0.002(1)
C(5)	0.035(2)	0.017(2)	0.043(2)	-0.008(1)	0.020(2)	-0.007(2)
C(6)	0.034(2)	0.022(2)	0.034(2)	0.003(2)	0.018(2)	0.002(2)
C(7)	0.026(2)	0.039(2)	0.028(2)	0.006(2)	0.009(2)	-0.004(2)
C(8)	0.028(2)	0.048(3)	0.030(2)	0.011(2)	0.007(2)	0.007(2)
C(9)	0.027(2)	0.051(2)	0.017(2)	0.006(2)	0.000(1)	0.002(2)
C(10)	0.051(3)	0.061(4)	0.192(8)	0.009(3)	0.076(4)	0.038(4)
C(11)	0.077(5)	0.089(5)	0.28(1)	-0.041(4)	0.125(6)	-0.078(6)
C(12)	0.040(3)	0.062(4)	0.184(7)	0.010(3)	0.059(4)	0.013(4)

Table AI-7. Positional parameters and equivalent isotropic thermal parameters (\AA^2) for $[(\text{nta})\text{Cr}(\text{OH})_2\text{Cr}(\text{phen})_2]\text{Cl}\cdot 7\text{H}_2\text{O}$ (**B-8**).

Atom	x / a	y / b	z / c	$B(\text{eq})$
Cr(1)	0.6867(1)	0.1863(1)	0.7084(1)	2.60(8)
Cr(2)	0.7351(1)	0.0724(1)	0.8454(2)	2.53(8)
O(1)	0.7032(6)	0.2112(5)	0.5687(7)	3.8(4)
O(2)	0.6773(7)	0.2900(6)	0.4531(8)	5.2(5)
O(3)	0.5648(6)	0.1210(5)	0.6388(7)	3.2(3)
O(4)	0.4252(6)	0.1099(6)	0.6505(8)	4.7(4)
O(5)	0.7878(6)	0.2748(5)	0.7815(7)	3.4(4)
O(6)	0.8236(7)	0.3963(5)	0.8640(8)	4.7(4)
O(7)	0.6756(5)	0.1544(4)	0.8485(6)	2.3(3)
O(8)	0.7467(6)	0.1026(5)	0.7084(6)	2.8(3)
N(1)	0.6148(7)	0.2682(5)	0.7054(8)	2.7(4)
N(2)	0.6173(7)	-0.0093(6)	0.7777(8)	2.7(4)
N(3)	0.7051(7)	0.0385(6)	0.9859(8)	2.4(4)
N(4)	0.8062(7)	-0.0110(6)	0.8316(9)	3.3(4)
N(5)	0.8632(7)	0.1377(6)	0.9221(9)	3.0(4)
C(1)	0.602(1)	0.2890(8)	0.594(1)	3.5(5)
C(2)	0.667(1)	0.2640(8)	0.533(1)	3.7(5)
C(3)	0.5283(9)	0.2295(8)	0.724(1)	3.3(5)
C(4)	0.5018(8)	0.1469(8)	0.666(1)	3.1(5)
C(5)	0.667(1)	0.3325(8)	0.790(1)	3.7(6)
C(6)	0.768(1)	0.3371(7)	0.814(1)	3.5(5)
C(7)	0.575(1)	-0.0316(7)	0.673(1)	3.7(6)
C(8)	0.493(1)	-0.0865(8)	0.638(1)	4.1(6)
C(9)	0.453(1)	-0.1170(8)	0.714(1)	4.6(6)
C(10)	0.4968(9)	-0.0974(7)	0.828(1)	3.7(6)
C(11)	0.464(1)	-0.1278(8)	0.916(1)	4.4(6)
C(12)	0.509(1)	-0.1050(8)	1.019(1)	4.9(7)
C(13)	0.596(1)	-0.0476(7)	1.048(1)	3.4(5)
C(14)	0.645(1)	-0.020(1)	1.156(1)	5.0(7)
C(15)	0.721(1)	0.0367(9)	1.174(1)	4.3(6)
C(16)	0.7495(9)	0.0660(8)	1.089(1)	3.4(5)
C(17)	0.6269(8)	-0.0168(7)	0.965(1)	2.6(5)
C(18)	0.5794(8)	-0.0411(7)	0.853(1)	2.7(5)
C(19)	0.779(1)	-0.0844(7)	0.794(1)	4.4(6)
C(20)	0.836(1)	-0.1305(9)	0.780(1)	5.7(7)
C(21)	0.922(1)	-0.101(1)	0.805(1)	7.0(9)
C(22)	0.962(1)	-0.019(1)	0.843(1)	6.1(8)
C(23)	1.056(1)	0.023(1)	0.872(2)	8(1)
C(24)	1.084(1)	0.098(1)	0.919(1)	6.9(9)

Table AI-7. continued.

C(25)	1.021(1)	0.139(1)	0.938(1)	4.6(6)
C(26)	1.045(1)	0.2141(9)	0.989(1)	4.6(6)
C(27)	0.979(1)	0.2503(8)	1.009(1)	4.2(6)
C(28)	0.8897(9)	0.2114(7)	0.972(1)	3.4(5)
C(29)	0.9271(8)	0.1006(8)	0.907(1)	3.2(5)
C(30)	0.897(1)	0.0219(8)	0.860(1)	3.9(6)
Cr(3)	0.7253(1)	-0.4724(1)	0.2911(2)	2.21(7)
Cr(4)	0.7201(1)	-0.3151(1)	0.3892(2)	2.61(7)
O(11)	0.6371(6)	-0.2776(5)	0.4588(8)	4.1(4)
O(12)	0.6321(8)	-0.1834(7)	0.580(1)	7.1(6)
O(13)	0.7873(5)	-0.3189(5)	0.5388(7)	2.9(3)
O(14)	0.9163(6)	-0.2622(5)	0.6605(8)	3.4(4)
O(15)	0.6780(6)	-0.2812(5)	0.2551(7)	3.7(4)
O(16)	0.7142(8)	-0.1919(7)	0.150(1)	7.1(5)
O(17)	0.8005(5)	-0.3691(5)	0.3334(7)	2.8(3)
O(18)	0.6457(5)	-0.4202(5)	0.3434(7)	2.9(3)
N(11)	0.7973(7)	-0.2045(6)	0.429(1)	3.6(4)
N(12)	0.7661(6)	-0.5055(5)	0.4378(8)	2.1(4)
N(13)	0.8218(6)	-0.5261(5)	0.2591(8)	2.3(4)
N(14)	0.6263(7)	-0.5278(6)	0.2318(8)	2.6(4)
N(15)	0.6868(7)	-0.4599(6)	0.1304(8)	3.2(4)
C(51)	0.745(1)	-0.1603(8)	0.483(1)	4.5(6)
C(52)	0.666(1)	-0.2099(9)	0.511(1)	4.5(6)
C(53)	0.8806(8)	-0.2068(7)	0.503(1)	3.2(5)
C(54)	0.8606(8)	-0.2676(7)	0.574(1)	2.7(5)
C(55)	0.808(1)	-0.1794(8)	0.326(1)	4.5(6)
C(56)	0.726(1)	-0.218(1)	0.235(1)	4.7(6)
C(57)	0.7370(9)	-0.4938(8)	0.527(1)	3.2(5)
C(58)	0.775(1)	-0.5151(8)	0.623(1)	3.6(6)
C(59)	0.843(1)	-0.5494(8)	0.628(1)	3.8(6)
C(60)	0.8748(9)	-0.5647(8)	0.537(1)	3.4(5)
C(61)	0.947(1)	-0.6001(8)	0.533(1)	4.4(6)
C(62)	0.975(1)	-0.6109(9)	0.442(1)	4.9(7)
C(63)	0.9348(9)	-0.5874(7)	0.345(1)	3.3(5)
C(64)	0.960(1)	-0.5992(8)	0.247(1)	4.0(6)
C(65)	0.917(1)	-0.5279(9)	0.158(1)	4.1(6)
C(66)	0.8460(8)	-0.5381(8)	0.167(1)	3.1(5)
C(67)	0.8638(8)	-0.5518(7)	0.346(1)	2.8(5)
C(68)	0.8340(8)	-0.5400(7)	0.443(1)	2.5(5)
C(69)	0.5941(9)	-0.6255(8)	0.287(1)	4.0(6)

Table AI-7. continued.

C(70)	0.525(1)	-0.6907(9)	0.238(2)	5.6(7)
C(71)	0.490(1)	-0.6987(8)	0.126(2)	6.0(7)
C(72)	0.5186(9)	-0.6454(8)	0.068(1)	4.4(6)
C(73)	0.485(1)	-0.648(1)	-0.047(1)	5.3(6)
C(74)	0.517(1)	-0.591(1)	-0.100(1)	5.3(7)
C(75)	0.586(1)	-0.527(1)	-0.043(1)	4.2(6)
C(76)	0.623(1)	-0.465(1)	-0.090(1)	5.8(7)
C(77)	0.689(1)	-0.405(1)	-0.029(1)	5.0(7)
C(78)	0.721(1)	-0.402(1)	0.083(1)	4.1(6)
C(79)	0.6220(9)	-0.5213(8)	0.070(1)	3.1(5)
C(80)	0.5893(8)	-0.5812(8)	0.126(1)	3.2(5)
Cl(1)	0.7070(3)	0.2768(2)	0.0481(3)	4.4(2)
Cl(2)	0.4677(5)	0.5121(4)	0.3794(6)	12.0(2)
O(101)	0.0488(5)	0.2900(4)	0.7423(6)	2.4(2)
O(102)	0.1233(7)	0.4433(6)	0.0805(9)	5.6(3)
O(103)	0.1858(7)	0.3394(6)	0.2052(9)	5.8(3)
O(104)	1.0009(8)	0.4002(7)	0.882(1)	6.9(3)
O(105)	0.7647(8)	0.2459(7)	0.288(1)	6.7(3)
O(106)	0.9072(9)	0.1790(7)	0.293(1)	7.6(3)
O(107)	0.705(1)	0.023(1)	0.474(1)	11.9(5)

Table AI-8. Positional parameters and equivalent isotropic thermal parameters (\AA^2) for $[(\text{nta})\text{Cr}(\text{OH})_2\text{Cr}(\text{phen})_2]\text{Cl}\cdot 7\text{H}_2\text{O}(\text{B-8})(\text{Hydrogen atoms})$.

Atom	x / a	y / b	z / c	$B(\text{eq})$
H(1)	0.6487	0.1742	0.9027	2.8
H(2)	0.7747	0.0823	0.6552	3.5
H(3)	0.5408	0.2653	0.5542	4.3
H(4)	0.6092	0.3443	0.6005	4.3
H(5)	0.5324	0.2309	0.8014	4.4
H(6)	0.4828	0.2562	0.6984	4.4
H(7)	0.6562	0.3804	0.7693	4.5
H(8)	0.6462	0.3276	0.8562	4.5
H(9)	0.6052	-0.0096	0.6197	4.4
H(10)	0.4648	-0.1020	0.5611	5.1
H(11)	0.3940	-0.1532	0.6908	5.4
H(12)	0.4071	-0.1660	0.8997	5.5
H(13)	0.4854	-0.1269	1.0769	6.3
H(14)	0.6252	-0.0417	1.2167	6.3
H(15)	0.7547	0.0577	1.2488	5.2
H(16)	0.8041	0.1075	1.1044	4.3
H(17)	0.7141	-0.1082	0.7756	5.5
H(18)	0.8114	-0.1853	0.7517	6.6
H(19)	0.9617	-0.1350	0.7997	8.1
H(20)	1.1008	-0.0036	0.8567	9.2
H(21)	1.1473	0.1256	0.9359	7.9
H(22)	1.1076	0.2427	1.0123	5.5
H(23)	0.9959	0.3029	1.0480	5.0
H(24)	0.8447	0.2383	0.9837	4.2
H(25)	0.8610	-0.3494	0.3282	3.4
H(26)	0.5845	-0.4411	0.3459	3.6
H(27)	0.7851	-0.1279	0.5483	5.2
H(28)	0.7254	-0.1258	0.4358	5.2
H(29)	0.9226	-0.2188	0.4622	3.6
H(30)	0.9098	-0.1568	0.5478	3.6
H(31)	0.8193	-0.1238	0.3337	5.4
H(32)	0.8609	-0.1920	0.3090	5.4
H(33)	0.6867	-0.4699	0.5252	3.9
H(34)	0.7529	-0.5048	0.6885	4.3
H(35)	0.8701	-0.5633	0.6968	4.5
H(36)	0.9767	-0.6164	0.5976	5.1
H(37)	1.0243	-0.6359	0.4424	5.7
H(38)	1.0066	-0.6259	0.2410	4.7
H(39)	0.9362	-0.5765	0.0904	5.1

Table AI-8. continued.

H(40)	0.8135	-0.5226	0.1031	3.8
H(41)	0.6188	-0.6185	0.3657	4.7
H(42)	0.5032	-0.7298	0.2807	6.8
H(43)	0.4413	-0.7446	0.0916	6.8
H(44)	0.4375	-0.6925	-0.0880	5.8
H(45)	0.4931	-0.5950	-0.1781	6.0
H(46)	0.6034	-0.4636	-0.1664	7.1
H(47)	0.7144	-0.3616	-0.0622	6.3
H(48)	0.7683	-0.3580	-0.1268	5.4

Table AI-9. Thermal parameters for [(nta)Cr(OH)₂Cr(phen)₂]Cl·7H₂O (**B-8**).

Atom	U ₁₁	U ₂₂	U ₃₃	U ₁₂	U ₁₃	U ₂₃
Cr(1)	0.038(1)	0.031(1)	0.031(1)	0.008(1)	0.009(1)	0.006(1)
Cr(2)	0.037(1)	0.028(1)	0.032(1)	0.009(1)	0.009(1)	0.006(1)
O(1)	0.067(7)	0.055(6)	0.038(6)	0.028(6)	0.022(5)	0.020(5)
O(2)	0.099(9)	0.073(8)	0.036(6)	0.023(7)	0.028(6)	0.024(6)
O(3)	0.041(6)	0.039(6)	0.039(5)	0.007(5)	0.009(4)	0.005(4)
O(4)	0.039(6)	0.059(7)	0.075(8)	0.003(5)	0.011(5)	0.018(6)
O(5)	0.033(5)	0.040(6)	0.054(7)	0.003(4)	0.008(5)	0.014(5)
O(6)	0.070(7)	0.035(6)	0.059(7)	-0.001(5)	0.002(6)	0.005(5)
O(7)	0.033(5)	0.030(5)	0.028(5)	0.006(4)	0.013(4)	0.004(4)
O(8)	0.047(6)	0.037(5)	0.030(5)	0.015(4)	0.023(4)	0.008(4)
N(1)	0.044(7)	0.023(6)	0.032(6)	0.005(5)	0.006(5)	0.005(5)
N(2)	0.041(7)	0.031(6)	0.030(6)	0.005(5)	0.012(5)	0.004(5)
N(3)	0.030(6)	0.034(7)	0.032(7)	0.006(5)	0.015(5)	0.010(5)
N(4)	0.049(7)	0.043(7)	0.042(7)	0.022(6)	0.013(6)	0.014(6)
N(5)	0.039(7)	0.035(7)	0.041(7)	0.010(5)	0.007(5)	0.009(6)
C(1)	0.05(1)	0.039(9)	0.044(9)	0.018(7)	0.008(7)	0.015(7)
C(2)	0.05(1)	0.038(8)	0.034(8)	-0.004(7)	-0.002(7)	0.007(7)
C(3)	0.036(8)	0.042(9)	0.05(1)	0.006(7)	0.014(7)	0.016(7)
C(4)	0.035(8)	0.04(1)	0.040(9)	0.005(7)	0.004(7)	0.017(7)
C(5)	0.05(1)	0.43(9)	0.05(1)	0.015(7)	0.018(7)	0.013(7)
C(6)	0.05(1)	0.040(8)	0.042(9)	0.006(7)	0.010(7)	0.026(7)
C(7)	0.06(1)	0.029(8)	0.04(1)	0.006(7)	0.004(8)	0.006(7)
C(8)	0.07(1)	0.035(9)	0.05(1)	0.004(8)	0.016(8)	0.002(7)
C(9)	0.06(1)	0.036(9)	0.06(1)	0.006(8)	-0.007(8)	-0.012(8)
C(10)	0.043(9)	0.025(8)	0.07(1)	0.006(7)	0.021(8)	-0.002(7)
C(11)	0.05(1)	0.04(1)	0.08(1)	0.003(8)	0.029(9)	0.006(9)
C(12)	0.08(1)	0.04(1)	0.08(1)	0.012(9)	0.04(1)	0.017(9)
C(13)	0.05(1)	0.032(8)	0.049(9)	0.013(7)	0.020(7)	0.011(7)
C(14)	0.09(1)	0.06(1)	0.05(1)	0.02(1)	0.04(1)	0.029(9)
C(15)	0.06(1)	0.07(1)	0.037(9)	0.012(9)	0.004(8)	0.020(8)
C(16)	0.044(9)	0.046(9)	0.036(9)	0.007(7)	0.006(7)	0.009(7)
C(17)	0.040(8)	0.031(8)	0.035(8)	0.014(6)	0.016(6)	0.012(6)
C(18)	0.039(8)	0.024(7)	0.041(8)	0.010(6)	0.013(7)	-0.002(6)
C(19)	0.08(1)	0.025(8)	0.06(1)	0.020(8)	0.006(9)	-0.007(5)
C(20)	0.09(1)	0.05(1)	0.07(1)	0.04(1)	0.00(1)	-0.021(9)
C(21)	0.13(2)	0.08(1)	0.06(1)	0.08(1)	0.01(1)	-0.01(1)
C(22)	0.09(1)	0.109(1)	0.06(1)	0.07(1)	0.01(1)	0.01(1)
C(23)	0.06(1)	0.16(2)	0.10(2)	0.08(1)	0.01(1)	0.01(1)

Table AI-9. continued.

C(24)	0.05(1)	0.13(2)	0.08(1)	0.04(1)	-0.10(1)	-0.01(1)
C(25)	0.035(8)	0.07(1)	0.06(1)	0.08(8)	0.012(8)	0.00(1)
C(26)	0.05(1)	0.07(1)	0.05(1)	0.005(8)	-0.001(8)	0.006(8)
C(27)	0.04(1)	0.05(1)	0.05(1)	-0.002(8)	-0.001(8)	0.013(8)
C(28)	0.045(9)	0.032(8)	0.05(1)	0.004(7)	0.012(7)	0.008(7)
C(29)	0.033(8)	0.05(1)	0.036(8)	0.017(7)	0.007(6)	0.004(7)
C(30)	0.05(1)	0.06(1)	0.038(9)	0.03(8)	0.007(7)	-0.001(7)
Cr(3)	0.027(1)	0.033(1)	0.024(1)	0.009(1)	0.0056(9)	0.004(1)
Cr(4)	0.029(1)	0.030(1)	0.035(1)	0.008(1)	0.001(1)	-0.001(1)
O(11)	0.039(6)	0.046(6)	0.061(7)	0.015(5)	0.003(5)	-0.013(5)
O(12)	0.077(9)	0.08(1)	0.10(1)	0.022(7)	0.023(8)	-0.033(8)
O(13)	0.036(5)	0.036(6)	0.034(5)	0.003(4)	0.004(4)	0.003(4)
O(14)	0.043(6)	0.041(6)	0.040(6)	0.010(5)	0.005(5)	-0.000(5)
O(15)	0.052(6)	0.033(6)	0.043(6)	0.008(5)	-0.009(5)	0.003(5)
O(16)	0.10(1)	0.073(9)	0.067(8)	-0.002(7)	-0.023(7)	0.033(7)
O(17)	0.024(5)	0.032(5)	0.050(6)	0.004(4)	0.010(4)	0.000(4)
O(18)	0.029(5)	0.036(5)	0.044(6)	0.009(4)	0.011(4)	-0.002(4)
N(11)	0.048(7)	0.029(7)	0.051(8)	0.013(6)	-0.008(6)	0.006(6)
N(12)	0.025(5)	0.031(6)	0.023(6)	0.005(5)	0.008(5)	0.004(5)
N(13)	0.028(6)	0.028(6)	0.031(6)	0.008(5)	0.008(5)	0.003(5)
N(14)	0.037(6)	0.017(6)	0.040(7)	0.007(5)	-0.004(5)	0.004(5)
N(15)	0.043(7)	0.056(8)	0.024(6)	0.026(6)	0.005(5)	-0.002(6)
C(51)	0.05(1)	0.04(1)	0.07(1)	0.028(8)	0.000(8)	-0.004(8)
C(52)	0.04(1)	0.07(1)	0.06(1)	0.026(9)	0.001(8)	-0.007(8)
C(53)	0.034(8)	0.028(8)	0.050(9)	-0.000(6)	-0.002(7)	0.004(7)
C(54)	0.038(8)	0.033(8)	0.031(8)	0.018(6)	0.003(6)	-0.006(6)
C(55)	0.08(1)	0.04(1)	0.036(9)	0.000(9)	0.001(8)	0.010(7)
C(56)	0.06(1)	0.06(1)	0.05(1)	0.018(9)	-0.008(8)	0.008(8)
C(57)	0.044(9)	0.041(9)	0.035(8)	0.006(7)	0.009(7)	0.011(7)
C(58)	0.05(1)	0.05(1)	0.031(8)	0.005(8)	0.012(7)	0.003(7)
C(59)	0.05(1)	0.05(1)	0.032(8)	-0.004(8)	-0.002(7)	0.012(7)
C(60)	0.043(9)	0.040(9)	0.039(9)	0.003(7)	-0.001(7)	0.012(7)
C(61)	0.05(1)	0.05(1)	0.06(1)	0.021(8)	-0.010(8)	0.011(8)
C(62)	0.05(1)	0.05(1)	0.08(1)	0.033(9)	0.003(9)	0.005(9)
C(63)	0.038(8)	0.027(8)	0.05(1)	0.004(7)	0.002(7)	0.003(7)
C(64)	0.04(1)	0.05(1)	0.06(1)	0.018(8)	0.011(8)	-0.001(8)
C(65)	0.05(1)	0.07(1)	0.04(1)	0.020(9)	0.024(8)	0.002(8)
C(66)	0.031(8)	0.047(9)	0.041(9)	0.013(7)	0.008(7)	0.008(7)

Table AI-9. continued.

C(68)	0.034(7)	0.033(8)	0.023(7)	0.003(6)	0.005(6)	-0.001(6)
C(69)	0.041(9)	0.029(8)	0.07(1)	0.013(7)	-0.009(8)	0.005(8)
C(70)	0.06(1)	0.04(1)	0.11(2)	0.014(9)	0.01(1)	0.02(1)
C(71)	0.05(1)	0.030(9)	0.12(2)	0.012(8)	-0.01(1)	-0.02(1)
C(72)	0.037(8)	0.04(1)	0.08(1)	0.021(7)	-0.010(8)	-0.016(8)
C(73)	0.035(9)	0.09(1)	0.05(1)	0.03(1)	-0.018(7)	-0.05(1)
C(74)	0.06(1)	0.10(1)	0.03(1)	0.05(1)	-0.007(8)	-0.019(9)
C(75)	0.06(1)	0.09(1)	0.027(8)	0.04(1)	0.010(7)	0.003(8)
C(76)	0.08(1)	0.14(2)	0.03(1)	0.08(1)	0.016(9)	0.02(1)
C(77)	0.08(1)	0.09(1)	0.05(1)	0.05(1)	0.035(9)	0.03(1)
C(78)	0.06(1)	0.07(1)	0.04(1)	0.04(1)	0.029(8)	0.038(9)
C(79)	0.037(8)	0.05(1)	0.039(8)	0.033(8)	0.014(7)	0.009(7)
C(80)	0.035(8)	0.05(1)	0.037(8)	0.029(7)	-0.003(6)	-0.007(7)
Cl(1)	0.061(3)	0.055(3)	0.048(2)	0.006(2)	0.023(2)	-0.001(2)
Cl(2)	0.152(3)					
O(101)	0.030(2)					
O(102)	0.072(3)					
O(103)	0.074(3)					
O(104)	0.088(4)					
O(105)	0.084(4)					
O(106)	0.097(4)					
O(107)	0.151(6)					

Table AII-1. Positional parameters and equivalent isotropic thermal parameters (\AA^2) for $[\text{Cr}_2(\text{OH})_2(\text{HCOO})(\text{bispicam})_2](\text{ClO}_4)_3 \cdot 0.5\text{H}_2\text{O}$ (**D-1**).

Atom	x / a	y / b	z / c	B(eq)
Cr(1)	0.22983(4)	0.13098(5)	0.06503(4)	2.29(2)
O(1)	0.2632(3)	0.2500	0.1277(2)	2.7(2)
O(2)	0.2438(3)	0.2500	-0.0011(2)	2.4(2)
O(3)	0.0989(2)	0.1585(2)	0.0769(2)	2.8(1)
N(1)	0.3606(2)	0.0742(3)	0.0538(2)	3.2(2)
N(2)	0.2365(2)	0.0222(3)	0.1456(2)	2.7(2)
N(3)	0.2062(2)	0.0185(3)	-0.0117(2)	2.6(2)
C(1)	0.0619(4)	0.2500	0.0789(3)	2.8(3)
C(2)	0.3953(3)	0.0522(4)	0.1250(3)	3.7(2)
C(3)	0.3223(3)	-0.0005(4)	0.1667(2)	3.3(2)
C(4)	0.3370(4)	-0.0671(5)	0.2242(3)	4.9(3)
C(5)	0.2649(5)	-0.1068(4)	0.2605(3)	5.4(3)
C(6)	0.1785(4)	-0.0853(4)	0.2390(3)	4.8(3)
C(7)	0.1666(3)	-0.0205(4)	0.1814(3)	3.7(2)
C(8)	0.3633(3)	-0.0227(4)	0.0088(3)	3.9(2)
C(9)	0.2800(3)	-0.0337(4)	-0.0356(2)	3.0(2)
C(10)	0.2771(4)	-0.0975(4)	-0.0949(3)	4.4(3)
C(11)	0.1979(4)	-0.1083(4)	-0.1302(3)	5.0(3)
C(12)	0.1206(4)	-0.0578(4)	-0.1049(3)	4.3(3)
C(13)	0.1281(3)	0.0056(4)	-0.0467(3)	3.4(2)
Cl(1)	0.0561(1)	0.2500	0.26699(9)	3.83(8)
O(11)	0.0436(3)	0.2500	0.3406(2)	4.1(3)
O(12)	0.1506(4)	0.2500	0.2509(3)	6.1(3)
O(13)	0.0162(4)	0.1576(5)	0.2382(3)	10.3(4)
Cl(2)	0.4724(1)	0.2500	0.9152(1)	3.86(9)
O(21)	0.4789(3)	0.2500	0.9911(3)	4.2(3)
O(22)	0.5610(4)	0.2500	0.8863(3)	6.6(4)
O(23)	0.4259(3)	0.3436(4)	0.8749(1)	4.4(1)
Cl(3)	0.0234(1)	0.2500	0.9152(1)	3.86(9)
O(31)	0.1185(4)	0.2500	0.8888(3)	5.6(3)
O(32A) ^a	-0.0173(9)	0.2500	0.9372(6)	8.2(3)
O(32B) ^a	0.001(1)	0.2500	0.803(1)	7.7(4)
O(33A) ^a	0.0037(5)	0.3425(6)	0.8356(4)	7.1(2)
O(33B) ^a	-0.0272(8)	0.340(1)	0.9103(6)	7.8(3)
O(51)	0.269(1)	0.2500	0.5695(7)	7.1(3)

^a Population is 0.5.

Table AII-2. Positional parameters and equivalent isotropic thermal parameters (\AA^2) for $[\text{Cr}_2(\text{OH})_2(\text{HCOO})(\text{bispicam})_2](\text{ClO}_4)_3 \cdot 0.5\text{H}_2\text{O}$ (**D-1**)(hydrogen atoms).

Atom	x / a	y / b	z / c	B(eq)
H(1)	0.244(3)	0.2500	0.158(3)	1(1)
H(2)	0.219(3)	0.2500	-0.031(2)	1(1)
H(3)	0.004(4)	0.2500	0.089(3)	3(1)
H(4)	0.409(3)	0.116(4)	0.148(2)	4(1)
H(5)	0.451(3)	0.009(3)	0.123(2)	3(1)
H(6)	0.395(3)	-0.082(3)	0.238(2)	3(1)
H(7)	0.268(3)	-0.145(4)	0.299(3)	5(1)
H(8)	0.120(4)	-0.109(4)	0.261(3)	6(1)
H(9)	0.108(4)	-0.006(5)	0.161(3)	7(1)
H(10)	0.361(3)	-0.078(3)	0.037(2)	3(1)
H(11)	0.421(3)	-0.026(4)	-0.025(2)	5(1)
H(12)	0.331(3)	-0.141(4)	-0.111(3)	6(1)
H(13)	0.196(3)	-0.143(4)	-0.169(2)	4(1)
H(14)	0.073(3)	-0.161(4)	-0.122(2)	4(1)
H(15)	0.084(3)	0.038(4)	-0.024(2)	4(1)
H(16)	0.389(3)	0.123(3)	0.038(2)	3(1)

Table AII-3. Thermal parameters for
[Cr₂(OH)(HCOO)(bispicam)₂](ClO₄)₃·0.5H₂O (**D-1**).

Atom	U ₁₁	U ₂₂	U ₃₃	U ₁₂	U ₁₃	U ₂₃
Cr(1)	0.0258(3)	0.0251(3)	0.0361(3)	-0.0002(3)	0.0025(3)	0.0006(3)
O(1)	0.034(2)	0.034(2)	0.033(2)	0	0.002(2)	0
O(2)	0.027(2)	0.032(2)	0.033(2)	0	0.001(2)	0
O(3)	0.027(1)	0.032(2)	0.046(2)	-0.001(1)	0.005(1)	-0.002(1)
N(1)	0.031(2)	0.031(2)	0.058(3)	0.000(2)	0.002(2)	0.004(2)
N(2)	0.037(2)	0.029(2)	0.039(2)	-0.002(2)	-0.002(2)	0.002(2)
N(3)	0.031(2)	0.027(2)	0.039(2)	-0.002(2)	0.002(2)	0.001(2)
C(1)	0.026(3)	0.040(4)	0.039(4)	0	0.001(3)	0
C(2)	0.033(2)	0.048(3)	0.061(3)	0.002(2)	-0.013(2)	-0.003(3)
C(3)	0.047(3)	0.035(3)	0.045(3)	0.003(2)	-0.006(2)	-0.003(2)
C(4)	0.074(4)	0.051(4)	0.059(4)	0.010(3)	-0.025(3)	0.006(3)
C(5)	0.106(5)	0.047(3)	0.051(3)	-0.005(4)	-0.010(3)	0.019(3)
C(6)	0.086(4)	0.051(3)	0.046(3)	-0.016(3)	0.001(3)	0.011(3)
C(7)	0.051(3)	0.042(3)	0.049(3)	-0.009(3)	0.002(2)	0.005(3)
C(8)	0.046(3)	0.041(3)	0.060(3)	0.014(2)	0.014(3)	-0.001(3)
C(9)	0.044(3)	0.028(2)	0.041(2)	0.004(2)	0.007(2)	0.002(2)
C(10)	0.071(4)	0.036(3)	0.059(3)	0.009(3)	0.011(3)	-0.009(3)
C(11)	0.093(5)	0.043(3)	0.054(3)	-0.006(3)	-0.001(3)	-0.012(3)
C(12)	0.067(4)	0.038(3)	0.059(3)	-0.013(3)	-0.012(3)	-0.002(3)
C(13)	0.042(3)	0.034(3)	0.055(3)	-0.004(2)	0.002(2)	-0.004(2)
Cl(1)	0.042(1)	0.067(1)	0.036(1)	0	0.0057(8)	0
O(11)	0.047(3)	0.072(4)	0.038(3)	0	-0.001(2)	0
O(12)	0.049(3)	0.119(5)	0.063(4)	0	0.023(3)	0
O(13)	0.119(4)	0.175(5)	0.096(4)	-0.072(4)	0.036(3)	-0.074(4)
Cl(2)	0.056(1)	0.042(1)	0.049(1)	0	0.0060(9)	0
O(21)	0.051(3)	0.063(4)	0.045(3)	0	0.003(3)	0
O(22)	0.075(4)	0.092(5)	0.086(5)	0	0.044(4)	
O(23)	0.109(4)	0.079(3)	0.079(3)	0.036(3)	-0.001(3)	0.019(3)
Cl(3)	0.054(4)	0.076(4)	0.082(4)	0	-0.012(1)	0
O(31)	0.054(4)	0.076(4)	0.082(4)	0	-0.030(3)	0
O(32A)	0.103(4)					
O(32B)	0.097(5)					
O(33A)	0.090(2)					
O(33B)	0.098(4)					
O(51)	0.090(4)					

Acknowledgement

I would like to thank Professor Sumio Kaizaki (Faculty of Science, Osaka University) for his guidance in the present work, and to Professors Yoshihiko Kushi and Shinichiro Suzuki (Faculty of Science, Osaka University) for their helpful advise.

Special thanks are due to Drs. Wasuke Mori and Hirokazu Nakayama (Faculty of Science, Osaka University) for constructing a Faraday apparatus for the magnetic susceptibility measurements, to Dr. Akira Fuyuhiko (Faculty of Science, Osaka University) for his kindly instruction in X-ray crystallography, to Dr. Norio Koine (Faculty of Engineering, Ehime University) for his valuable suggestions about deuteration of H_3nta and informing of the unpublished results of his X-ray analysis of $\text{Cs}_2[\text{Cr}_2(\text{nta})_2(\text{OH})_2] \cdot 6\text{H}_2\text{O}$, to Drs. Hiroo Kuma and Tatsuya Kawamoto (Faculty of Science, Osaka University) for their kindly instruction in X-ray crystallography and to Dr. Yuriko Abe (Faculty of Science, Nara Women's University) for her valuable discussions about kinetics.

I am grateful to the members of Kaizaki Laboratory for their helpful advise and discussions.

I wish thank to my parents for their encouragement and to Miss. Yukiko Terasaki (Toyama National College of Maritime Technology) for her encouragement and collaboration throughout this work.